"VIBRATIONAL ANALYSIS OF ROTOR BLADES OF COMPLEX SHAPES"

by

S K Subramanian BE(Mech), M.Phil(Eng), C.Eng, M.I.Mech.E, D.S.S.

Thesis submitted for the degree of

DOCTOR OF PHILOSOPHY

of

THE CITY UNIVERSITY

Department of Aeronautical Engineering

THE CITY UNIVERSITY

LONDON EC1

November 1977

CONTENTS

LIST OF TABLES

LIST OF FIGURES

Figure No.	Description
18	Mode shapes of a straight rectangular cross section blade. Torsional and longitudinal modes - Third and Fourth modes.
19	Mode shapes of a straight rectangular cross section blade. Torsional and longitudinal modes - Fifth mode.
20	Mode shapes of a blade with s.c offset from c.g in y axis only. Flapping modes - Torsional coupling negligible. First and Second modes.
21	Mode shapes of a blade with s.c offset from c.g in y axis only - Third and Fourth modes - coupled flapping-torsion.
22	Mode shapes of a blade with s.c offset from c.g in y axis only. Fifth mode - coupled flapping-torsion.
23	Mode shapes of a blade with s.c offset from c.g. Sixth mode. Coupled Flapping-Drag-torsion.
24	Frequencies of pretwisted uniform rectangular blades.
25	Mode shapes of a pretwisted uniform blade. First and Second modes - coupled flapping-drag.
26	Mode shapes of a pretwisted uniform blade. Third and Fourth modes - coupled flapping-drag.
27	Mode shapes of a pretwisted uniform blade. Fifth mode, coupled flapping-drag.
28	Mode shapes of a sweep back blade. First mode - coupled Flapping-torsion. Second mode - coupled Drag-longitudinal.
29	Mode shapes of a sweep back blade. Third mode - coupled flapping-torsion. Fourth mode - coupled flapping-torsion.
30	Mode shapes of a sweep back blade. Fifth mode - coupled drag longitudinal.
31	Mode shapes of a zig-zag blade. First and Second modes - coupled flapping-drag-torsion-longitudinal.
32	Mode shapes of a zig-zag blade. Third and Fourth modes - coupled flapping-drag-torsion-longitudinal.
33	Mode shapes of a zig-zag blade. Fifth mode - coupled flapping-drag-torsion-longitudinal.
34	Frequencies of pretwisted rectangular blades. First and Second coupled modes.

Figure No.	Description
35	Frequencies of pretwisted rectangular blades. Third and Fourth coupled modes.
36	Frequencies of pretwisted rectangular blades. Fifth coupled mode.
37	Frequencies of pretwisted aerofoil blades; First coupled modes.
38	Frequencies of pretwisted aerofoil blades; Second coupled modes.
39	Frequencies of pretwisted aerofoil blades; Third coupled modes.
40	Frequencies of pretwisted aerofoil blades; Fourth coupled modes.
41	Frequencies of pretwisted aerofoil blades; Fifth coupled modes.
42	Mode shapes of pretwisted aerofoil blade; $e_y = e_z = B1 = B2 = B3 = o$. First and Second coupled modes.
43	Mode shapes of pretwisted aerofoil blade; $e_y = e_z = B1 = B2 = B3 = o$. Third and fourth coupled modes.
44	Mode shapes of pretwisted aerofoil blade; $e_y = e_z = B1 = B2 = B3 = o$. Fifth coupled modes.
45	Mode shapes of pretwisted aerofoil blade; e_y & e_z included but $B1 = B2 = B3 = o$. First and Second coupled modes.
46	Mode shapes of pretwisted aerofoil blade; e_y & e_z included but $B1 = B2 = B3 = o$. Third and Fourth coupled modes.
47	Mode shapes of pretwisted aerofoil blade; e_y & e_z included but $B1 = B2 = B3 = o$. Fifth coupled mode.
48	Mode shapes of pretwisted aerofoil blade; e_y, e_z, B1, B2, B3 included; First and Second coupled modes.
49	Mode shapes of pretwisted aerofoil blade; e_y, e_z, B1, B2, B3 included; Third and Fourth coupled modes.
50	Mode shapes of pretwisted aerofoil blade; e_y, e_z, B1, B2, B3 included; Fifth coupled mode.

Figure No.	Description
51	Mode shapes of pretwisted aerofoil blade - 30° pretwist e_y, e_z, B1, B2, B3 included; First and Second coupled mode.
52	Mode shapes of pretwisted aerofoil blade - 30° pretwist e_y, e_z, B1, B2, B3 include; Third and Fourth coupled modes.
53	Mode shapes of pretwisted aerofoil blade - 30° pretwist e_y, e_z, B1, B2, B3 included; Fifth coupled mode.
54	Mode shapes of pretwisted aero foil blade - 45° pretwist e_y, e_z, B1, B2, B3 included; First and Second coupled modes.
55	Mode shapes of pretwisted aerofoil blade - 45° pretwist e_y, e_z, B1,B2,B3 included; Third and Fourth coupled modes.
56	Mode shapes of pretwisted aerofoil blade - 45° pretwist e_y, e_z, B1, B2, B3 included; Fifth coupled modes.
57	Mode shapes of pretwisted aerofoil blade -90° pretwist e_y, e_z, B1, B2, B3 included. First and Second coupled modes.
58	Mode shapes of pretwisted aerofoil blade - 90° pretwist e_y, e_z, B1, B2, B3 included. Third and Fourth coupled modes.
59	Mode shapes of pretwisted aerofoil blade - 90° pretwist e_y, e_z, B1, B2, B3 included, Fifth coupled mode.
60	Frequencies of rotating blades; First modes.
61	Frequencies of rotating blades; Second modes.
62	Frequencies of rotating blades; Third modes.
63	Frequencies of rotating blades; Fourth modes.
64	Frequencies of rotating blades; Fifth modes.
65	Mode shapes of rotating blades flapping modes. First and Second modes.
66	Mode shapes of rotating blades, flapping modes. Third and Fourth modes.
67	Mode shapes of rotating blades, flapping modes. Fifth modes.
68	Mode shapes of rotating blades, drag modes. First and Second modes.
69	Mode shapes of rotating blades, drag modes. Third and Fourth modes.

Figure No.	Description
70	Mode shapes of rotating blades, drag modes. Fifth modes.
71	Mode shapes of rotating blades; torsional and longitudinal modes; First and Second modes.
72	Mode shapes of rotating blades; torsional and longitudinal modes; Third and Fourth modes.
73	Mode shapes of rotating blades; torsional and longitudinal modes; Fifth modes.
74	Frequencies of Montoya's rotating blades.
75.	Comparison of a bending mode shape of WILDE's rotating blade.
76	Mode shapes of a rectangular blade - flapping and drag modes. 20 element idealisation - First and Second modes.
77	Mode shapes of a rectangular blade - flapping and drag modes. 20 element idealisation - Third and Fourth modes.
78	Modes shapes of a rectangular blade - flapping and drag modes. 20 element idealisation - Fifth modes.

Figures in Appendices

A1	Global set of axes and local member axes.
A2	Representation of nodes and elements.
A3	Torsional displacement of a sweep back element.
A4	Inertia forces caused on element J-1 and J due to displacements at node J.
A5	Moments applied to inboard section by inertia forces on the element.
A6	Centrifugal loads in an element X direction.
A7	Centrifugal forces in X direction of an element J in X direction.
A8	Centrifugal forces in Y direction of an element J.

*

ACKNOWLEDGEMENTS

The author expresses his thanks to Dr R. F. Williams for his valuable guidance and useful discussion on the work and helpful suggestions in preparing this thesis. The author also wishes to express his thanks to [redacted], Head of the Aeronautics Department for making this work possible. Facilities were provided by the Aeronautics Department and the Computer Unit of the City University. Thanks are also due to [redacted] for arranging time off adjustment from work.

DECLARATION

The author hereby declares that he grants powers to the Librarian of The City University to allow this thesis to be copied in whole or in part without further reference to the author. This permisson covers only single copies made for study purposes, subject to normal conditions of acknowledgement.

Signed .....

ABSTRACT

The seriousness of the rotor vibration problem demands a reasonably accurate knowledge of natural frequencies and their mode shapes at the design stage. This thesis is concerned with the vibrational characteristics of rotor blades of complex geometrical configurations. A discrete element method is developed to study the vibrational characteristics of both rotating and non-rotating rotor blades, which includes complexities such as pretwist angle, shear centre being off-set from centroid, variable mass densities and abrupt changes in blade geometry like sweep back.

The blade is idealised into a number of discrete elements and the theory is developed along the engineering beam theory. Both flapping loads and centrifugal loads are taken into consideration. The unit load method is used in developing the flexibility matrix. The loads are assembled to form an eigenvalue problem. A programme called VTRI was written in Fortran IV language and this programme makes use of the library subroutines for establishing the eigenvalues and eigen-vectors of the dynamic matrix. On the University ICL 1905 computer the programme uses 46K of core storage. A maximum run time of 3 minutes and 34 seconds was needed for a ten element idealisation.

In total 62 different cases were run on the computer to include as many variations as possible and the natural modes of vibration and the mode shapes established. Comparison with known exact solutions and other investigators' results, where available, shows the accuracy to be good, especially for the lower modes. A considerable increase in accuracy of results has been achieved when the number of elements was increased to 20. The accuracy of the technique with respect to frequency and mode shapes and the results obtained have been encouraging. A few concluding remarks have been presented and certain suggestions were indicated for future work.

LIST OF SYMBOLS

a_i	Points located by X, Y, Z co-ordinates where i = 1, 2, ... n
a_{iX}	X co-ordinates of points a
a_{iY}	Y co-ordinates of points a
a_{iZ}	Z co-ordinates of points a
A	Area of cross section
$\bar{A}$	Matrix
$\bar{A}_1$	Matrix
b	Arbitrary point located by b (X, Y, Z)
B1	Higher moment of area 1
B2	Higher moment of area 2
B3	Higher moment of area 3
$\bar{B}$	Matrix
$\bar{B}_1$	Matrix
c.s.	Centre of shear, shear centre (s.c) also referred to as centre of flexure and flexural centre.
c.g.	centre of gravity, centroid.
C_1	Sectional constant associated with higher moments of area and pretwist angle.
C_2	Sectional constant associated with higher moments of area and pretwist angle.
C_3	Sectional constant associated with higher moments of area and pretwist angle.
$\bar{C}_1$	Matrix
$\bar{C}$	Matrix
$\bar{D}$	Matrix
e_y	Shear centre co-ordinate in y axis with reference to c.g.
e_z	Shear centre co-ordinate in z axis with reference to c.g.
$\bar{e}$	Strain matrix.
E	Young's Modulus.
$\bar{E}$	Matrix.
$\bar{F}$	Flexibility matrix.
$F_{1,1} \ldots F_{n,n}$	Elements of flexibility matrix.
G	Rigidity modulus.

$\bar{i}$	Unit vector, local axis.
I	Integer variable.
$\bar{I}$, $\underline{I}$	Unit vector, overall axis.
$\bar{\bar{I}}$	Identity matrix.
I_P	Polar moment of inertia, Pitching inertia.
I_y	Second moment of area about y axis.
I_z	Second moment of area about z axis.
$\bar{j}$	Unit vector, local axis.
J	Torsional stiffness.
J, JJ, J-1, JJ-1, J + 1, JJ + 1	Integer variables representing the elements, nodal positions.
$\bar{J}$, $\underline{J}$	Unit vector, overall axis.
J_A	Additional torsional stiffness due to pretwist.
$\bar{k}$	Unit vector, local axis.
K	Integer variable.
$\bar{K}$, $\underline{K}$	Unit vector, overall axis.
l_x, l_y, l_z	Direction cosines of local x, y, z axes with reference to X axis
l_{y1}, l_{z1}	Direction cosines of intermediate axes y_1 and z_1.
$l_{x(J)}$, $l_{x(J-1)}$	Direction cosines of elements J and J-1.
L, L_r, L_n, L_{AB}	Lengths
m	Array size, array suffix.
m_x, m_y, m_z	Moments about local axes.
m'_x, m'_y, m'_z	Moments about local axes.
m_x, m_y, m_z	Direction cosines of local x, y, z axes with reference to overall Y axis.
m_{y1}, m_{z1}	Direction cosines of intermediate axes.
m_{xJ}, m_{xJ-1}	Direction cosines of elements J and J-1.
m_{xv}	Unit moment about the local x axis.
M	Integer variable.
M_i	Moments.
M_x, M_y, M_z	Moments about local x, y, z axes.
My_1, Mz_1 M_{y1} M_{z1}	Moments about y, z axes, tip end.
My_2, Mz_2 M_{y2} M_{z2}	Moments about y, z axes, root end.
M_{svA}, M_{sv}, M_{xsv}, M_{ssv}	St Venant's stresses.

M_{xA}, M_{yA}, M_{zA}	Applied moments about x, y, z axes.
M_{xv}, M_{yv}, M_{zv}	Virtual or unit moments about x, y, z axes.
M_y^*, M_z^*	Moments about y and z axes without considering pretwist effect.
M_X, M_Y, M_Z	Moments about X, Y, Z axes.
M_{XJ}, M_{XJ+1}	Moments about X axis referred to elements J and J +1.
M_{YJ}, M_{YJ+1}	Moments about Y axis referred to elements J and J +1.
M_{ZJ}, M_{ZJ+1}	Moments about Z axis referred to elements J and J +1.
M_{iX}, M_{iY}, M_{iZ}	Moments about X, Y, Z axes.
$M_{XJJ}, M_{YJJ}, M_{ZJJ}$	Moments about X, Y, Z axes due to centrifugal loads of element JJ.
n	Array size, array suffix.
n_x, n_y, n_z	Direction cosines of local x, y, z axes with reference to Z axis.
n_{y1}, n_{z1}	Direction cosines of intermediate axes.
n_{xJ}, n_{xJ-1}	Direction cosines of elements J and J-1.
N	Integer variable.
N	Number of elements.
p_x', p_y', p_z'	Local axes loads in x, y, z directions.
p_{JJ}	Local axis loads at node JJ.
P_i	Forces at i (i = 1, 2, 3. . . . n).
$P_1, P_2, P_3 \ldots P_n$	System of n forces.
P_x	Tensile load, end load.
P_{x1}, P_{x2} P_{x_1}, P_{y_2}	End loads at positions 1 and 2.
P_{xA}	Applied load in x direction.
P_{xv}	Virtual load in x direction.
P_X, P_Y, P_Z	Forces in X, Y, Z directions.
P_{XJ}, P_{YJ}, P_{ZJ}) $P_{XJ+1}, P_{YJ+1}, P_{ZJ+1}$)	Loads in X, Y, Z directions at nodes J and J +1.
P_{XJJ}, P_{YJJ}	Changes in centrifugal loads in X and Y directions of nodes JJ.
P_{Xv}, P_{Yv}, P_{Zv}	Unit loads in X, Y, Z directions.
$\bar{P}$	Forces matrix.
$\bar{P}_v$	Unit load matrix.
$\bar{P}_J, \bar{P}_{J+1}$	Load matrices of nodes J and J +1.
$\bar{P}_{JJ}$	Load matrix of node JJ.
$\bar{p}_{JJ}, \bar{p}'_{JJ}$	Local axes load matrices.
$\bar{P}_A$	Applied load matrix.
$\bar{P}_{vJJ}$	Unit load matrix of element JJ.

$\bar{P}_{F1}, \bar{P}_{F2}, \bar{P}_{F3}$ ... $\bar{P}_{Fn}, \bar{P}_{F}$	Flapping load matrices.
$\bar{P}_{C1}, \bar{P}_{C2}, \bar{P}_{C3}$ ... $\bar{P}_{Cn}, \bar{P}_{C}$	Centrifugal load matrices.
$\bar{P}_{v1,1}$ .. $\bar{P}_{vnn}$	Unit load matrices.
P_{iX}	Forces at i (i = 1, 2, ...n) in X direction.
P_{iY}	Forces at i (i = 1, 2, ...n) in Y direction.
P_{iZ}	Forces at i (i = 1, 2, ...n) in Z direction.
$\bar{R}$ $\bar{RR}$	Matrices.
$\bar{R}_{1,1}$ $\bar{R}_{12}$ .. $\bar{R}_{nn}$	Matrices.
$\bar{\bar{RR}}_{1,1}$ $\bar{\bar{RR}}_{12}$ .. $\bar{\bar{RR}}_{nn}$	Matrices.
s_y, s_z	Shear loads in y and z directions at shear centre position.
$\bar{T}$	Matrix.
u	Displacements in x direction.
v	Displacements in y direction.
w	Displacement in z direction.
v' w'	Slopes of fibres due to pretwist.
x	Local axis, x co-ordinate.
X	Overall axis, X co-ordinate.
X_1, X_2 etc., X_J, X_{JJ}	Overall axis X co-ordinates.
y	Local axis, y co-ordinate.
Y	Overall axis, Y co-ordinate.
Y_1, Y_2 etc., Y_J, Y_{JJ}	Overall axis Y co-ordinates.
y_1	Intermediate axis.
z	Local axis, z co-ordinate.
Z	Overall axis, Z co-ordinate.
Z_1, Z_2 etc., Z_J, Z_{JJ}	Overall axis Z co-ordinates.
z_1	Intermediate axis.
β	Pretwist angle.
β_1, β_A	Pretwist angle, tip end.
β_2, β_B	Pretwist angle, root end.
β'	Rate of pretwist.
θ_x θ_J θ_{J-1}	Torsional deformation about local x axis.

ϕ_x ϕ_J ϕ_{J-1}	Torsional deformation about local x axis.
$\rho, \rho_x, \rho_J, \rho_{J-1}$	Mass per unit length.
σ	Stress.
$\bar{\sigma}$	Stress matrix.
ω	Frequency.
Ω	Speed of rotation.
$\Delta_1, \Delta_2, \Delta_3, \ldots \Delta_n$	Displacements.
$\bar{\Delta}$	Displacement matrix.
$\Delta_X, \Delta_Y, \Delta_Z$	Displacements in X, Y, Z directions.
$\Delta_{XJ}, \Delta_{YJ}, \Delta_{ZJ}$	Displacements in X, Y, Z directions of node J.
$\Delta_{XJ+1}, \Delta_{YJ+1}, \Delta_{ZJ+1}$	Displacements in X, Y, Z directions of node J + 1.
$\bar{\Delta}_J, \bar{\Delta}_{J+1}, \bar{\Delta}_{JJ}$	Displacement matrices.
$\bar{\Delta}_1, \bar{\Delta}_2, \bar{\Delta}_3, \ldots \bar{\Delta}_n$	Displacement matrices.
λ	Eigenvalue.
λ_k	kth eigenvalue.
α_k, ϕ_k	Eigenvectors.

INTRODUCTION

Helicopter blades are subject to numerous vibration and flutter problems. Turbine and compressor blades fail frequently because of some vibration phenomena. The failure of rotor blades due to fatigue has led to an increased interest in the study of the vibrations of these blades. The seriousness of the rotor vibration problem necessitates a fairly accurate knowledge of the natural frequencies of vibration at the design stage. It is,consequently, desirable that efficient means be available for the estimation of these frequencies. There is, therefore, much interest in the development of deformation theory which is fundamental in the structural and dynamical analysis of these problems.

Two main areas of helicopter rotor dynamical research concern forced response of the blades to time varying loads, and the aeromechanical stability of the aircraft. Both these problem areas show an unusual degree of sensitivity of the analysis to the structural assumptions and indicate that greater attention must be paid to the analysis of the normal modes of the system. Present design trends of high speed aircraft have created a number of difficult fundamental structural problems for the engineers in aeroelasticity and structural dynamics. The chief problem in this category is to predict for a given elastic structure, a comprehensive set of load-deflection relations which can serve as structural basis for dynamic load calculations and theoretical analysis of elastic effects on stability.

Propeller blades have become larger and thinner particularly in connection with aircraft designed for vertical short take-off and landing and as a consequence are more and more susceptible to vibration and flutter problems. Solution of the structural and aeroelastic problems associated with such blades requires understanding of their dynamic behaviour in the very high centrifugal force field. The structural problems of these blades have become more acute in almost every phase of aeronautical engineering application.

Turbines and compressors also face identical problems offering a wide range of challenging research work. Turbine and compressor blade design, like helicopter blade design, covers a large scope of engineering knowledge involving the co-operative efforts of engineers in several scientific fields such as fluid flow, heat transfer, structures, strength of materials and vibration.

In a theoretical study it is customary to consider the rotor blades as cantilever beams. The determination of the theoretical vibrational characteristics of straight arbitrary shaped cantilever beams, and in particular rectangular cross section cantilever beams, has been extensively investigated. In simple cases like rectangular cross section cantilever beams, it is usual to assume that flapwise, chordwise and torsional deformations are mechanically decoupled.

However, the type of blades used in practice have initial pretwist, variable stiffness, variable mass per unit length, centre of shear being off-set from centre of gravity, and sweep back at the tip. The blades are also subject to centrifugal forces, shear deformation, Coriolis forces etc. Although many theories on blade deformation exist, these theories either neglect some of the factors of concern or treat them only approximately.

The determination of natural frequencies of pretwisted cantilever beams has received increasing interest in recent years due to the direct application to aircraft propellers. The comparitively recent development of the gas turbine has necessitated the use of pretwisted blading in the turbo-compressor and the turbine unit. The analysis of a twisted beam poses certain added complications over that of an untwisted beam due to the geometry of the structure. It has also introduced new aerodynamical and structural problems demanding the attention of engineers. When a beam is twisted, vibrations in flapwise and chordwise directions no longer take place independently. They become coupled together and give rise to complex modes and execute simultaneous vibration about both principal axes (bending-bending coupled vibration).

For example, a blade of rectangular cross section without any pretwist has two different flexural rigidities about principal axes. When the blade is twisted the flexural rigidity in one direction increases while the flexural rigidity in the other direction decreases. This results in an increase in the frequency of vibration when the predominating component of the mode shape is in the stiffened direction; and a decrease in the frequency when the predominating component of mode shape is in the weakened direction. Thus the frequencies of the two modes tend to approach each other as the rate of pretwist with length increases.

It should be also remarked that the inclusion of torsional deformation complicates the effects of pretwist and rotation considerably. There may be a sizeable steady state or 'pseudo static' torsional deformation of the rotating blade. This is due to the centrifugal twisting moment which,in the case of a pretwisted blade, tends to

twist the blade negatively; and this is also due to the twisting moment associated with tensile stress in the longitudinal fibres. (This phenomenon is sometimes called the centrifugal untwisting moment). These two effects oppose each other in the normal case. The extent to which one or the other predominates depends primarily upon the amount of pretwist of the blade. As the normal modes of motion and associated natural frequencies of vibration depend on the magnitude of the pretwist angle, the theoretical analysis of pretwisted beams is, therefore, of considerable importance.

Recently the swept back wing and rotor has become popular with aircraft designers. It is generally recognised that in a swept back rotor, the interaction between bending and torsion may greatly affect the modes and frequencies of vibration. The problem is further complicated if pretwist is also present in the swept back structures; and careful examination is, therefore, essential.

Generally, in the case of complicated structures there are three types of coupling that need to be considered:

(a) coupling between bending and torsion;

(b) coupling between bending in two directions;

(c) coupling between bending in two directions and torsion.

The importance of the inclusion of other aspects such as offset of shear centre from centre of gravity, Coriolis forces, shear deformation, variable mass per unit length is well known. It is remarked that the inclusion of these factors complicates the theoretical analysis of natural frequencies and their mode shapes.

The purpose of the present work is to study the vibrational characteristics, by developing a discrete element method which would include both rotating and non-rotating cases of rotor blades and to investigate the effects of pretwist; sweep back; offset of shear centre from centre of gravity; variable stiffness and mass densities per unit length.

A review of previous works and the scope of the present investigation is presented in Section 2. The theoretical anlaysis is carried out in Section 3. This section is subdivided in to eight groups as follows:

(a) general conventions

(b) direction cosines

(c) flexibility matrix

(d) flapping loads

(e) centrifugal loads

(f) unit loads

(g) eigenvalue problem, and

(h) programming.

Section 4 deals with the discussion of results. Several known results were compared with the computed results. Conclusions are presented in Section 5 followed by certain indications for future work in the last section.

REVIEW OF PREVIOUS WORKS AND SCOPE OF PRESENT INVESTIGATION

The seriousness of rotor vibration has led to considerable interest in the analysis of helicopter, turbine and compressor blade vibrational characteristics. Many research scholars concentrated on the geometrical shape of the cross sectional area of the rotor blade, such as rectangular, circular, aerofoil, cubical-oval, etc. Some other authors carried out extensive research work on imposed geometrical conditions such as pretwist, taper, offset shear centre, variable second moment of area, sweep back, etc. Their investigations included one or some of the dynamical load characteristics such as flapping loads, centrifugal loads, Coriolis forces, shear deformation, aerodynamic loads, etc. Different theoretical processes available for a designer, include Rayleigh's method, Rayleigh-Ritz method, Ritz-Galerkin, Holzer, Stodola, Myklestad, Prohl, Finite difference, Finite element, Matrix iteration, Transformation and Numerical methods, amongst others. The choice of a particular method or a combination of different methods, depends upon the load conditions and knowledge and experience of the designer in these methods.

A bibliography is presented, arranged alphabetically by authors. Any references to the authors in the discussions are indicated by the author's name and or serial number in the bibliography.

The effect of pretwist on rotor blade vibration, received by far the most attention of many authors. In the case of a straight rectangular cross section beam, the bending vibrations in the two perpendicular principal planes occur independently as well as an independent torsional vibration. Initial pretwist of a rectangular cross section beam causes the two independent bending vibrations to couple together resulting in a vibration of the bending-bending type, but the torsional vibration remains uncoupled. When a straight beam of asymmetrical aerofoil cross section, is subjected to vibrating movement the motion consists of simultaneous displacements in two perpendicular directions coupled with torsion. This is referred to as bending-bending-torsion vibration and each normal mode consists of simultaneous bending displacements in two perpendicular directions together with torsional movement. The initial pretwist of beams of asymmetrical aerofoil cross section will affect the values of the natural frequencies but the vibration will still be of the bending-bending-torsion type.

Many investigators have worked on the vibrations of pretwisted beams of rectangular cross section, whereas others concentrated on pretwisted beams of aerofoil cross section. Some scholars have done work on the effect of pretwist on tapered beams, and on dynamical effects like shear deformation, Coriolis forces, etc. Bogdanoff and Horner (2) presented an account of how the torsional vibration of rotating bars are influenced by the angular velocity - the amount of this influence being dependent upon the base setting angle, the radius of the base and the pretwist. In this brief note they presented numerical results on the influence of rotation on the first three natural frequencies of a uniform fixed-free bar having different base setting angles and constant pretwist rates. They have also given an approximate formula for the fundamental frequency of such bars and the total pretwist does not exceed 45^{o}. Although this work treated pretwist cases, the main concentration was on the base setting angle and is applicable only to torsional vibration cases, up to 45^{o} pretwist angle.

Carnegie, (6) and (7), developed a static bending theory of pretwisted cantilever blading. This has been done by the application of calculus of variation, equations have been established, fulfilling the requirements for stationary values of potential energy and hence for equilibrium of pretwisted cantilever blades subjected to either single concentrated or uniformly distributed lateral loading. He treated cases where the pretwist is up to 90^{o}. He extended his static bending theory to develop equations for vibrations of pretwisted cantilever blading, the object being mainly to study the effect of pretwist on the natural frequencies. He used two theoretical approaches, the first one involving a direct solution of differential equations of motion and the second one based on the well known Rayleigh's principle. However, he used the second approach to derive the fundamental mode of lateral motion of rectangular and aerofoil cross section cantilever bladings. He also carried out an extensive analysis of the effect of pretwist on torsional stiffness and torsional frequencies. He justified the use of Rayleigh's approach by conducting practical tests on rectangular and aerofoil cross section beams. For the modes of motion where theoretical solutions are provided, reasonable agreement was shown to exist, between the calculated and corresponding measured frequencies. Higher modes of theoretical frequencies on the torsion side have been derived.

While analysing the coupling effects he has included the effects due to offset shear centre although this effect has been shown as negligible. On examining his experimental frequency curves of pretwisted rectangular cross section beams, the

influence of pretwist is well appreciated. The second coupled frequency values reduce with the increase in pretwist. A frequency doubling effect is shown to occur on higher overtones as would be expected in a coupled system. The theoretical and experimental torsional frequencies of rectangular cross section blades has been analysed in some detail and established that the increase in stiffness of a system without alteration of mass raises the frequency of vibration. He also spotted frequency doubling effects on third overtone beyond 60^{o} pretwist angle. He has presented a similar analysis on aerofoil cross section beams and his conclusions were as follows:

(a) the measured fundamental frequencies of transverse vibration of uniform cantilever blades, both rectangular and aerofoil cross section, pretwisted within the range of 0 to 90^{o} show a slight increase of frequency.

(b) the experimentally determined higher overtone lateral frequencies of blades, with both types of cross section, can be considerably affected by pretwist. Certain modes show frequency doubling with the increase of pretwist.

(c) all the measured torsional frequencies, for blades of both cross sections, show an increase with the increase of pretwist.

Carnegie and others (9) developed differential equations of motion for cantilever beam having linear taper, offset shear centre and pretwist. They used a finite difference approach in solving the problem, and compared their theoretical results with experimental results. Although pretwist is also included in this work, their main concentration was on the effects of taper on the vibrational characteristics.

Dawson (10) and (11) carried out research work on the vibrational characteristics of straight and pretwisted cantilever beams of uniform rectangular and aerofoil cross section. He developed a method known as transformation method to solve the equations of motion. In short the method involves the reduction of the coupled higher order differential equations to a set of simultaneous first order equations. A set of simultaneous solutions of these equations is then obtained by Runge-Kutta step by step integration. The process is an iteration type which relies on the repeated assumptions of the value of normal mode frequency. The actual normal mode frequency is eventually determined by extrapolation of the results. He used Rayleigh-Ritz procedure to compare his results. The natural frequencies and mode shapes of vibration were obtained up to fifth mode by both methods. He has also compared his results with experimental results for both straight and pretwisted cases. Although his method has been used by many investigators, prior knowledge of approximate

normal frequency is essential as subsequent iterations are based on the initially assumed frequency.

Diprima and Handleman (12) set up equations of equilibrium for non-rotating and rotating pretwisted rotor blades using vector representation of static equilibrium. They used Rayleigh-Ritz principle to solve the equations using fourth order polynomials as approximations to the dynamic displacement curves. The fundamental frequencies only were obtained for a set of pretwisted beams of various width to thickness ratios with pretwist angle up to 29^{o}. Although they have indicated another simpler method to derive a general condition for numerical analysis, no results were produced to prove the same.

Dunholter (14) considered a uniform rectangular cross section cantilever beam with an initial twist and developed a unique method of calculating the first two natural modes of frequencies. Basically he used Rayleigh's energy method and also calculated the static displacements in the two principal axes directions. Many authors quoted his method for comparing their results. However, this method is valid only for small values of the rate of twist angle.

Houbolt and Brooks (18) developed differential equations of motion for the lateral and torsional deformations of twisted rotating beams for application to helicopter rotor and propeller blades. Although the motion of the blades of a helicopter has been modelled before, their work is well appreciated by many authors. Their work is valuable because, they established a system of linear differential equations of greater accuracy than before, they chose a system of analysis which is easily extended and they indicated and demonstrated how the complex analysis can be verified. Their work formed a basis for many later research scholars. The extention of their theory found its way not only in helicopter rotors, but also in turbine and compressor blades and other types of structures.

They treated the coupled bending in two directions and torsion of a twisted rotating blade where the elastic axes and mass axis are not necessarily coincident. The development was made along the principles of engineering beam theory (EBT) and differential equations of motion have been derived for blades under the action of various loads. They have included Coriolis forces in their analysis but neglected shear deformation. They developed equation for longitudinal strain at any point in terms of displacement and internal elastic moments are established. Subsequently the equilibrium expressions for the moments are derived including the body forces

and applied loadings. They treated several sub cases of the general theory. Although they have indicated two methods of solution, one using Galerkin type procedure and the other Rayleigh-Ritz procedure, they have not produced results to check their work.

Eisakson and Eisley (20) aimed to develop a simple approximate procedure for the rapid estimation of natural frequencies of blade vibration. They considered the effect of twist on the natural frequencies of uniform and tapered non-rotating blades; and also the effect of twist on the natural frequencies of rotating blades. Both cantilevers and articulated blades were considered. Offset of the root support from the axis of rotation is also included in the analysis. The Rayleigh-Southwell procedure for determining the effect of rotation on natural frequencies has been used with respect to twisted rotating blades and found to provide a useful approximation, only in certain cases.

However, they have subsequently developed (21) a Holzer-Myklestad type of procedure, using a matrix formulation, for the determination of the natural frequencies of a pretwisted rotating blade in coupled bending and torsion. Their study is oriented on the effect of centrifugal force coupling in bending and torsional vibrations and non-rotating beams are treated as a special case. They have investigated the effects of Coriolis forces and the non linear effects of large angular displacements, at length. They have used Houbolt and Brooks' (18) analysis as a basis for the development of their work. No comparison is made to prove their theoretical results and mode shapes were presented only for certain cases.

Jarrett and Warner (22) extended the Myklestad's adoption of Holzer method of calculating natural frequencies and mode shapes of systems to the case of a twisted-tapered blade with certain elastic constraints. The details of solution are so arranged that the bulk of the numerical work could be carried out with basic mathematical knowledge. This extension makes possible the evaluation of the effect of rotation of a beam on a radial line, of certain elastic constraints such as the lashing wires and shrouding used on turbine blades, and of coupling between the torsional and flexural vibrations. In this paper, however, the effects of coupling between the torsional and flexural vibrations were not considered. The basic differential equations were solved by the tabular method due to Holzer. They calculated frequencies up to third mode and compared with experimental results.

Mendalson and Gendler (29) developed a method for determining the coupled modes and frequencies of non uniform twisted cantilever beams with a particular interest to study the effect of pretwist on the vibrational frequencies. The method is based on the use of station functions incorporated in which are the advantages of the continuous-function deflections of the Rayleigh-Ritz and Stodola methods together with the advantages of the finite number of degrees of freedom of the influence coefficient method. They compared their results with an exact solution of differential equations of equilibrium of the system. They determined the first three natural frequencies of a rectangular beam of width to thickness ratio 12:1 for pretwist angles in the range of 0 to 60^{o}. Experimental results were obtained for the first two natural frequencies and compared to the theoretical results. The mode shapes of vibration were not, however, presented. Their method has a disadvantage in that the moments are incorrect for finite rates of pretwist.

Montoya (30) developed differential equations of motion of a large turbine blade which has the peculiarity of being highly twisted. He treated the blade as a rod and introduced classic formula for bending and torsional vibrations and considered interaction between the bending and torsional vibrations. His method included certain higher order effects and the equations of motion were solved by a method similar to the transformation method developed by Dawson (10). Natural frequencies were obtained up to seventh mode of vibration for an actual turbine blade of tapered aerofoil cross section and 72 cms long. The theoretical natural frequencies were shown to give satisfactory agreement with experimental results, the maximum error up to fifth mode being 7% at the fifth mode.

In his theory he allowed for offset shear centre, varying cross section and high rate of pretwist. Unfortunately, neither theoretical or experimental results were presented for the mode shapes of vibration which limits the value of the work.

Rosard (39) determined the experimental natural frequencies for beams of width to thickness ratios in the range 4:1 to 12:1 and pretwist angle up to 40^{o}. The results were compared to the theoretical results determined by Myklestad method. Calculated mode shapes were presented for the first three modes of vibration of an 8:1 width to thickness ratio beam with a pretwist angle of 40^{o}. In his experimental analysis, the methods of excitation and vibration detection were not very refined and the accuracy of the experimental results is open to doubt. However, in his analysis he quoted an interesting definition which states "if two vibrating systems having nearly equal natural frequencies are coupled together, the resulting system has one natural frequency below the lower uncoupled frequency and one natural frequency above the higher uncoupled frequency".

In the beam vibration problem, the vibrating systems involved are the second mode vibration in the flexible direction and the first mode vibration in the stiff direction.

Sobey (41) has examined the motion of flexible helicopter blade in torsion-fluxure when rotating about a fixed shaft. The influence of pretwist, shear deformation, rotary inertia (Coriolis), taper and coning has been included. He used Houbolt and Brooks'(18) equations as basis and derived equations for steady coning and the perturbed motion about steady coning.

An alternative presentation in finite element form has been considered, leading to a classical linear algebraic eigenvalue problem. However, he has not presented a solution technique. Although his work includes a number of higher order terms which complicated the equations, it does not seem to be suitable for easy solutions. Moreover, in the absence of any results for comparison, it could be not appreciated very much. Even though his work is a complex one , it can be considered as a useful analysis.

The author of the present investigation, in his previous research work (42) considered the effect of second order terms with particular reference to cubical oval cross section beams. The differential equations of motion allowing for higher order terms were derived based on the works of Houbolt and Brooks (18). The differential equations of motion were solved by transformation method (10). The natural frequencies of vibration up to third mode have been calculated for beams of equivalent width to thickness ratios of 15.7:1 and 7.9:1 and pretwist angles in the range 0 to 90^{o}. The theoretical results both with and without second order terms were compared with the experimental results obtained on sets of machined cubical oval cross section pretwisted beams.

In the WADC technical report (46) a corollary analytic theory has been developed, in order to more fully understand the results of an experimental programme investigating the dynamic behaviour of propeller blades rotating in vacua. The method permits the computation of the natural modes and frequencies of twisted rotating beams and employs a mathematics and symbology easily comprehended by the average vibration engineer.

The factors affecting the vibrational characteristics of asymmetrical cross section beams can be well appreciated by studying the equations of motion which normally contain coupling terms. These coupling terms invariably depend upon the co-ordinates of shear centre relative to the centre of gravity of the cross section

of the blade. Complete solution of equations, therefore, requires a knowledge of shear centre and its co-ordinates. Different terms have been used by different authors such as centre of shear, flexural centre and centre of flexure, to define the shear centre. Also different definitions have been given by different authors.

The question of shear centre has been well analysed in various text books. However, the definition used by Carnegie (8) is well received and is quoted below:

"When a cantilever blade of elastic material is supported rigidly at the root and loaded at the free end with a concentrated load normal to the longitudinal axis, then in general, lateral displacement and twist of normal cross sections relative to one another will occur. Application of the load at one particular point in the free end cross section (considered not to distort) will not cause twist and this point is defined as the shear centre of that cross section. When a blade is subjected to distributed transverse loads, the shear centre may depend on the load distribution, but for a long blade the dependence will not be appreciable".

It is usual to assume that for a uniform cantilever beam the locus of the shear centre is a straight line parallel to the centroidal axis. Some authors considered that the locus of shear centre need not be a straight line but depends on the load conditions and load distribution. This locus is also referred to as the shear centre axis or flexural axis. Many authors have assumed that the shear centre axis and centroidal axis are coincident mainly because the variation in normal frequencies is negligible. However, the mode shapes of these frequencies indicate that coupling takes place between torsional and flexural modes.

In his research works (6) and (7), Carnegie has included the effects of offset between centroid and shear centre and developed a more general equation, although this effect has been shown negligible. He also presented (8) a useful work explaining the experimental determination of the shear centre and torsion centre co-ordinates of an asymmetrical aerofoil cross section.

Carnegie and others (9) have included the offset effect of the shear centre in their paper. Although this paper concentrates on the taper of a cantilever blade, the coupling effects due to the offset distance between shear centre and centroid are well established.

Dawson (10) concluded that the effect upon the natural frequencies and mode shapes, of variation in the value of the shear centre co-ordinates is considerable and also emphasised that the calculation of the natural frequencies and mode shapes of vibration of asymmetrical beams, neglecting coupling with torsion or with inaccurate values of shear centre co-ordinates could result in errors. His work (11) on the vibration of a straight asymmetrical aerofoil section blade also includes the effect

of shear centre offset.

Duncan, Ellis and Scruton (15) gave a similar definition to that of Carnegie (8) for shear centre and argued that in an ideal case of rigid cantilever the shear centre and torsion centre must coincide. If transverse loads are applied to a beam which has an asymmetric cross section then flexure will occur followed by torsion. Long ago this torsional problem was assumed to be covered by the theory of St Venant which predicted the shear stress distribution and the angle of twist of a beam under torsion. The assumptions were that the torque along the beam was constant i.e. equal and opposite couples applied at each end; that these couples were also the resultants of shear stresses distribut ed over every cross section of the beam, and that the end sections are free to warp. Analysis based on this theory is known as St Venant's torsion. Duncan and others (15) derived a formula for shear centre of a blade with one axis of symmetry (cubical oval), based on St Venant's theory. The accuracy of the above theory is verified by the authors (15) by experimentally determining the co-ordinates of shear centre of cubical oval cross section.

In their work Houbolt and Brooks (18) started in their analysis with the assumption that centroidal axis and shear centre axis are not coincident. Their theory contributed much towards the coupling effect due to the offset between centroid and shear centre.

Eisakson and Eisley (20) and (21) also included the offset effect of shear centre in their semi-matrix approach and used a Holzer-Myklestad type of procedure for solving.

Montoya (30) has also studied the effect of shear centre offset from c.g and compared his theoretical results with the experimental ones. D. Morrison (31) tried to prove logically that shear centre and torsion centre are one and the same. He argued that for a rational calculation of coupled flexural and torsional vibration of blades, it is necessary to define a point, characteristic of each blade section such that a pure twisting couple applied to the blade will cause relative twisting about the defined point (the torsion centre). By reciprocal theorem, it can be argued that the application of a shear load with resultant passing through this point will give no twisting of the blade and the point is, therefore, also the shear centre.

Osgood (35) discussed the relevance of Poisson's ratio in determining the co-ordinates of shear centre, at length and produced a unique definition for shear

centre for any cross section. His definition is as follows:

"shear centre may be defined as that point of the cross section (x_F, y_F) through which the load must act in order that no twist shall occur along the line $x = x_F$, $y = y_F$".

Sobey (41) and the author (of the present investigation) in his previous work (42) have also analysed the effect of shear centre offset.

Many authors have tried to establish approximate methods of rotating blades. Although no exact theory is available most of these works contribute in one way or another towards better approach of a rotating blade.

Bogdanoff and Horner (2) in their brief note presented numerical results on the influence of rotation on the first three natural frequencies of a uniform fixed-free bar and constant pretwist rates. However, their work is limited to torsional vibration only.

Houbolt and Brooks (18) presented a useful analysis wherein centrifugal force coupling is discussed at length, which formed a useful basis for many authors; (20), (21), (41), etc. Jarrett and Warner (22) used Holzer-Myklestad type of calculating natural frequencies and mode shapes of rotating, twisted tapered beams. However, they did not consider the effects of coupling between the torsional and flexural vibrations.

Montoya (30) developed a classical analysis which includes centrifugal force components amongst other higher order terms. He analysed the effect of centrifugal force, on a specially designed apparatus. Although he has not produced any results for comparison he has presented the variation of first two normal frequencies with the speed of rotation, in the form of graph. However, no mode shapes were presented which limits the value of the work.

Niblett (33) calculated the lower natural frequencies of a simple rotating beam using arbitrary modes and established that the frequencies can be obtained accurately using comparitively few functions. He used two methods: one based on Lagrange and Galerkin involving arbitrary modes which he thought is not accurate enough; and the other based on Stodolas method. He compared his results with those for a non-rotating beam and a rotating chain. However, his analysis has limitations, because he considered only a case of simple beam of uniform mass and rigidity.

Ormiston and Hodges (34) analysed the stability characteristics of rotor blade flap-lag oscillations in the hovering flight conditions. Their study is focused on the effects

of pre-cone, variable elastic coupling, and the aerodynamics of induced flow. Together with an improved perturbation analysis for deriving the equations, these factors are shown to significantly influence the flap-lag stability characteristics of hingeless rotor blades. In order to validate the approximate rigid blade equations, elastic blade model equations are presented together with comparitive solutions.

Prohl (37) presented a method for calculating vibration frequency and stresses of a banded group of turbine blades. His method is an extension of Myklestad's method. His contention is that blades should be considered in groups rather than as individual cantilevers. He has also included a procedure for evaluating vibration amplitude and stress at resonance.

Shulman (40) considered the problem of stability of the transient motion in the flapping plane of a flexible helicopter rotor blade in forward flight. The formulation of the problem considers two degrees of freedom, rigid flapping and elastic bending. A new method of determining the transient stability of the motion was developed, using the concept of stability number. It was shown that the results obtained by inclusion of the elastic degree of freedom agree with experimental results to a much larger extent than was achieved by analysis neglecting blade flexibility.

Sobey (41) has examined the motion of flexible helicopter blade in torsion-flexure when rotating about a fixed shaft and included many aspects such as coriolis forces, plan form variation, conning, etc., in his analysis. However, no results are shown to appreciate his work.

WADC technical report (46) investigates the dynamical behaviour of propeller blades in vacua. A complete derivation of the method is given and some numerical results were presented for cases where experimental comparison can be made. A high degree of accuracy is indicated.

Weaver and Prohl (47) considered the design of short and medium-height steam turbine buckets, with reference to the possibility of resonant vibration at the frequency of passing nozzles. Particular attention has been given to the design problems involved in marine applications. Calculated results were pre sented and discussed with relation to their influence on blade design.

Some authors have considered the relevance of taper in a blade, variable mass

density and variable second moment of area of cross section to the vibrational characteristics. Carnegie and others (9) derived general equations of dynamic motion for rectangular cross section blades with pretwist and taper. From these equations, frequencies and mode shapes for various degrees of taper and pretwist over a range of 0 to 90^{o} have been calculated using finite difference approach. They also described a series of experimental investigations on the vibrations of tapered blades with and without pretwist. Myklestad (32) produced a simple tabular method of calculating deflections and influence coefficients of beams. In his later works he extended his method to include vibrational problems of complex structures. His method of finding deflection curves and influence coefficients can be easily applied to cantilever beams and to simple beams with or without overhangs. His method assumes that the beam itself is weightless and carries a finite number of concentrated forces. Although his method is somewhat tedious, owing to the acceptability many investigators used his approach. Myklestad's tabular method is perhaps the most successful method of determining the natural frequencies of non uniform beams. The method is used successfully in the vibration analysis of airplane wings, fuselages, bridges, critical speeds of shafts, and so forth. The uniqueness of the method lies in the fact that the shape of the vibration curve need not be assumed and higher modes of vibration are obtained readily. The stiffness coefficients for each section of the beam are determined from the actual stiffness curve of the beam by area moment principle. The geometric and equilibrium equations are then transformed to a tabular computational scheme. The tedious calculations in his method can be easily overcome by matrix methods.

Some authors have included (22), (26), (30), (41), (45) the study of non uniform beams in their investigations. Some investigators considered the effect of Coriolis forces otherwise known as 'secondary inertia' forces associated with the combined vibrational and rotational motion which introduces a phase difference between the bending and torsional vibration. Although the effect is considered negligible, inclusion of this force in the investigations improves the scope. Houbolt and Brooks (18), Dawson (10), Montoya (30) and Eisakson and Eisley (21) have analysed this effect.

Eisakson and Eisley (21) investigated the effects of Coriolis forces and other non linear effects at length. They constructed a simple model and produced numerical results to indicate that the Coriolis forces may introduce substantial phase differences between bending and torsional vibration.

Another effect which is usually omitted is the shear deformation. This is not very important in the cases of long beams, but should not be ignored for the shorter and stubby beams. In practice, most of the blades considered for analysis are thinner and longer.

The papers presented by Argyris (1), Doolin (13) and Hopkin (17) are of general nature. Argyris reviewed critically on the analysis of complex elastic structures and stressed upon the importance of matrix methods. His general survey included some important papers on matrix analysis. Doolin's paper (13) is on the application of matrix methods to co-ordinate transformations occurring in system studies involving large motions of aircraft. Although his paper appears to be complicated, it serves a very good purpose in showing the method and advantages of matrix algebra in setting up the geometrical aspects of problems of airplane motion. Hopkin's (17) work in five parts is a very useful general guide for designers in the aerodynamics field. He produced a scheme of notation and nomenclature for aircraft dynamics and associated aerodynamics.

Of late the discontinuities and sweep back are gaining some importance amongst investigators. The analysis of these cases mainly involves estimating the appropriate influence coefficients.

Levy (25) outlined a general method for computing influence coefficients using Castiglano's theorem, together with a stress analysis of the airplane structure based primarily on equilibrium conditions. It has been shown that, this method is particularly suited to wings having discontinuities, cut-outs and sweep back. A method is also suggested for the use of influence coefficients in computing by iteration, the normal modes of vibration of an airplance as a free body in either symmetric or anti-symmetric motion. Influence coefficients were computed for a sweep back of 37° with a large cut-out. However, no results of normal modes of vibration are given.

Targoff (43) developed the associated matrix of the bending vibration of beam. This is combined with the torsional matrix to obtain an associated matrix of the coupled vibration. By continued multiplications of the associated matrices of the successive beam sections a final matrix equation can be obtained relating the boundary conditions on both ends of the vibrating beam. His approach could be successfully used for beams with sweep back and discontinuities.

Zahorski (50) obtained the frequencies and modes of free vibrations, coupled in bending and twisting of a free-free, swept back, uniform beam, from the differential equations of motion. The modes of vibration of a non uniform, swept back wing were then determined by Ritz method. The discussion of the methods and various practical aspects of the analysis are presented from an engineering rather than a mathematical point of view.

Leckie and Lindberg (24) investigated the errors involved in using certain lumped parameter methods for the solution of beam frequencies. They concluded that the existing methods are not consistent for all boundary conditions. They also formulated a new dynamic stiffness matrix, which they claim to give consistantly good results even for a few elements.

Number of text books are available on general elastic and structural analysis, to name a few, (3), (16), (23) and (44). Similarly scores of books are available on matrix methods. Some of them are given in the bibliography, (27), (28), (36), (38).

In spite of the wide use of helicopters, the study of helicopter dynamics and aerodynamics has always occupied a lower place. Only a few text books are available on the helicopter study. This has been overcome by a recent publication by Bramwell (4) namely "Helicopter Dynamics", which includes most recent developments and will be useful not only to students but also to research establishments.

Wilde (48) derived expressions for determining the blade mode shapes and frequencies by applying Rayleigh's principle. He used a technique that the behaviour of a rotating blade approaches that of a flexible chain in the cases of small stiffness, so that the chain's motion can be exactly expressed by Legendre's differential equation. He has also indicated a method to include the effect of an offset flapping hinge and presented specimen calculations. His method converges rapidly and is ideal for rotor blades with constant mass and stiffness distribution.

Williams (49) developed a discrete element type of analysis, for a rotating beam. He represented the actual structure by an idealised model having limited allowable distributions of stress and strain, and established the bending modes of vibration of rotating and non rotating beams. He initially restricted the bending moments to vary linearly between selected nodal positions. Subsequently, to improve the accuracy of solution a more sophisticated stress and deformation pattern has been adopted. This has improved the accuracy significantly.

The frequencies and normal mode shapes of the beam in free vibrations have been obtained by using eigen value subroutines, similar to the library subroutines used in the present investigation. He has used the unit load method to establish the flexibility matrix and the bending deformation. He also considered variations in his theory to include whether a beam is a built in rotor, hinged rotor, vibrating beam or a chain. He compared his theoretical results with those of Niblett (33) and with standard exact solutions where possible.

The convergence and accuracy of his method is very encouraging, especially with regard to the internal loading distribution in the beam, and the basic technique has been adopted for the present work. In (49) the method was limited in its application to include only bending effects for untwisted, straight beams with a principal axis in the plane of rotation. The present work has extended the field of application to the more general case to include the effects of pretwist, shear centre position being offset from centroid, sweep back, variable mass densities, etc.

The object of the present work is to study the vibrational characteristics of both non rotating and rotating rotor blades of different geometrical configurations. A rotor blade is idealised into a number of discrete elements and each discrete element is assumed to have a uniform section so that the variations in the mass distribution and bending stiffness could be approximated by step functions in the analytical model. The displaced shape of the blade is defined in terms of the displacements at the tip ends of the defined element lengths. The theory is developed along the engineering beam theory (EBT) taking into consideration both flapping loads and centrifugal loads.

Unit load method is used to derive the flexibility matrix. The loads are assembled to form an eigenvalue problem, and standard library subroutines are used to solve the eigenvalue problem.

The theory is flexible in the sense so many geometrical configurations are built into it, such as pretwist, shear centre being offset from centroid, variable cross section, variable mass densities, sweep back, and the theory can be easily extended to include Coriolis forces, shear deformation, etc.

Many investigators have omitted the Coriolis forces as their effect is considered negligible. In the present work, also, these forces are omitted. In general, the effects of shear deformation are negligible in comparison with those of bending

deformation. For example, it can be shown for a rectangular section cantilever beam of depth d and length l, the tip deflection produced by a load at the tip is proportional to l/d due to shear and it is proportional to $(l/d)^3$ due to bending. For a very short deep beam with depth equal to length (l/d = 1) the ratio of shear deflection to bending deflection is 3/4. For a longer beam (say, l/d = 10) the ratio of shear deflection to bending deflection is reduced to 3/400. Since, most beams used in practice are long in comparison to their depth, the shear effects may be neglected with little loss in accuracy. In the present work also the shear deformation is neglected, but could be easily included if necessary.

The conventional three deformations are included namely two deformations along the two principal axes directions and the torsional deformation. Although it is customary to exclude the deformation along the longitudinal axis, this has been included in the present analysis (this is also some times called a pogo mode of vibration).

Many parameters discussed in this section have been studied by different authors using different approaches, but not all the effects being included in a single research work. The nearest could be that of Houbolt and Brooks (18) by a differential equation approach (but without results to check). In the present investigation, an attempt has been made to include as many parameters as possible. Although the theory developed in this work is for helicopter blades, this can be used for turbine and compressor blades also.

The method was checked initially with simple calculated results and then geometrical complexities were analysed using the theoretical and practical results of different authors, (6), (30), (49). A number of variations are considered to check the results from different view points. (Section 4). The computed results are presented up to fifth mode. A selected number of mode shape curves is also presented. (Section 4).

THEORETICAL CONSIDERATIONS

In continuum structures such as helicopter blades, aircraft wings and bodies, turbine blades etc., the main design problem lies in the analysis of the forces. Structural problems encountered in engineering design tend to be inherently complex in nature. A real structure generally consists of an assemblage of many parts. Geometry of individual components, as well as geometry of the overall structure, is usually non uniform and otherwise irregular. As a result, the true structure must generally be replaced by an idealised approximation, or model, suitable for mathematical analysis. Many structural systems may be quite adequately represented by models which can be solved by application of the equations of static equilibrium.

The use of matrices allows a systematization and simplification of the calculations almost impossible under any other scheme. Matrix methods are based on the concept of replacing the actual continuous structure by a mathematical model made up from structural elements of finite size (also referred to as discrete elements) having known elastic and inertial properties that can be expressed in matrix form. The matrices representing these properties are considered as building blocks, which when fitted together according to a set of rules derived from the theory of elasticity, provide the static and dynamic properties of the actual structural system. The properties of each element are calculated, using the theory of continuous elastic media while the analysis of the entire structure is carried out for the assembly of the individual structural elements.

Thus once the initial matrices are assembled the subsequent operations involve merely elementary matrix algebra. As matrix theory will form the basic frame of this research work, a collection of matrix expressions and operations is presented in Appendix 2. What is more important, however, is that matrix formulation is the ideal 'language' for the electronic digital computer and represents the most powerful design tool in structural engineering.

Various methods of matrix structural analysis can be grouped into two basic methods namely flexibility or virtual force method and stiffness or virtual displacement method. The flexibility method is chosen for the current work. In general, the flexibility method follows the order of flow mentioned hereunder.

(a) Assess the degree of static indeterminacy of the structure.
(b) Choose the required number of unknown forces and set them to zero. This makes the structure statically determinate.
(c) Calculate the displacements of the statically determinate structure due to applied loads. Assess the errors in compatability and apply the unknown forces one at a time and find the displacements.
(d) Set up equations of compatability in terms of the unknowns and solve them. The force distribution for the entire structure can then be found by application of statics.
(e) Back substitute for displacements if necessary.

Generally the above process will require the influence or the flexibility characteristics of the structure; that is, its displacements due to virtual or unit applied loads. As the unit load theorem is widely used in the current work, an account on this theorem is presented in Appendix 3. The theory flows naturally from the very simple matrix of the unit load theorem to an engineering system consisting of an assembly of elements. The matrix formulation of structural analysis by the flexibility method starts by setting up four matrices. They are:

(i) a rectangular matrix, the elements of which are stresses, statically equivalent to unit external forces in the components of the system.
(ii) a rectangular matrix, the elements of which are the stresses in the components per unit static redundancies and zero external forces.
(iii) a square matrix, the elements of which are the flexibilities of the unassembled components for the prescribed pattern of stresses.
In dynamic problems with a discrete mass distribution there is a square mass matrix, the elements of which may themselves be submatrices.
(iv) a column matrix of the prescribed displacement.

The theoretical analysis is carried out in the following steps.

(a) General conventions explaining the definitions, assumptions and idealisation.
(b) Establishing the direction cosines between overall and local axes.
(c) Derivation of flexibility matrix.
(d) Establishing the flapping loads.
(e) Establishing the centrifugal loads.
(f) Establishing the unit loads.
(g) Forming the eigenvalue problem, and
(h) Programming.

3.1 GENERAL CONVENTIONS

To start a discussion on force and displacement systems in the form of matrix presentation, it is necessary to define the co-ordinate systems in which they may be defined. Two types of rectangular cartesian co-ordinate systems are used mainly:

(a) member or local axes co-ordinates (x, y, z) oriented along a member, and

(b) global or overall axes co-ordinates (X, Y, Z) which are fixed with regard to a specified origin and axis system for the entire structure.

In component notation a right handed co-ordinate convention is used in either case, and these are presented diagramatically in Figure 1. The words 'loads' (forces) and 'displacements' are used in a generalised sense to represent not only linear forces and displacements, but also moments and rotational displacements. Loads which are specified in local co-ordinates will be denoted by suffices of lower case type, while the loads in global co-ordinates will be written using suffices in upper case characters. Vector and matrix notation are used to represent forces and moments and these are done by a bar (-) above the characters.

3.1.1 Definitions

Some of the basic definitions which are considered essential are presented here.

(a) The shear force at any section is taken positive if the tip end tends to slide upwards relative to the root end.

(b) Usually positive bending moment gives tensile stress in the positive quadrant of the axes.

(c) The pretwist angle is defined by giving the direction of the local y axis (major principal axis of the cross section). The angle of pretwist is measured in the plane of the cross section between the local y axis and the line of intersection of the XY plane with the plane of the cross section.

(d) Location of the local y axis:

(i) Reference direction y_1.
A reference line will be defined by the intersection of the plane of the cross section with the XY plane. The vector y_1 will lie along this line and have a positive component in the Y axis direction.

(ii) The local y axis will be formed by rotating the y_1 vector about the local x axis through an angle of β in the positive right hand sense.
Note: to cover exceptional conditions such as the local x axis of a section lying in the Z axis direction alternative definitions are used. (See Section 3.2).

(e) Positive directions are selected for the line through the shear centres and for the angle of twist such that the rate of twist $\frac{d\beta}{dx}$ (β') remains positive.

Other definitions, if any, may be included while considering the individual sections.

3.1.2 Assumptions

The theory is developed on the basis that internal and external forces are in equilibrium and along the principles of engineering beam theory and the following assumptions apply:

(i) a linear relationship exists between applied loads and resulting displacements of the structure so that the principle of superposition is valid.

(ii) the material of the structure obeys Hook's law i.e. stress is proportional to strain and must not be stressed beyond its elastic limit.

(iii) St Venant's principle applies. This is a reasonable assumption as long as the beam is not too short and deep.

(iv) the maximum cross sectional dimension (e.g. chord) is small in comparison to the length of the blade.

(v) the equations of equilibrium are developed using the geometry of the undeflected structural model assuming that the change in geometry due to imposed deformation is negligible while considering flapping loads only. However while considering the centrifugal loads the imposed deformation is also taken into account.

(vi) initially plane sections remain plane.(applicable for end load stress only)

(vii) the Coriolis forces, so called 'secondary inertia forces' associated with the combined vibrational and rotational motion introduce a phase difference between bending and torsion al vibration. However, effects due to Coriolis forces are assumed small and not included.

(viii) shear deformations other than St Venant's torsion are neglected. This is a reasonable assumption except for short deep beams.

Other assumptions, if any, may be included while considering the individual sections.

3.1.3 Idealisation of the structure

The idealised blade will consist of a number of discretelengths. Each discrete element is assumed to have a uniform section so that the variation of bending stiffness and mass distribution in the actual blade will be approximated by step functions in the analytical model. While idealising the structure the local x axis is assumed to lie along the locus of shear centres and local y and z axes directions are taken as the principal axes directions.

The displaced shape of the blade will be defined in terms of the displacements at the tip ends of the defined element lengths. The number of such displacements defines the degrees of freedom. Three lateral displacements and a torsional displacement are chosen to represent the displacements.

In actual practice, a rotor blade may have some or all of the following characteristics:

(a) pretwist of blade which couples the two bending modes of vibration.

(b) asymmetry of cross section and offset shear centre location with reference to centre of gravity, which couples bending and torsion modes.

(c) variable cross section which alters the natural frequencies, from those of uniform cross section.

(d) centrifugal loads which stiffen the blade.

(e) sweep back of blade which couples torsion, bending and longitudinal modes.

(f) steps, abrupt changes, and variable mass densities from one element to another.

Allowance has been made to include all the above aspects in the present work.

The conditions of overall equilibrium of a structure are:

(a) the vector sum of the forces acting on the structure must be zero.

(b) the vector sum of the moments about any arbitrary point of the forces, and moments acting on the structure must be zero.

If the forces are P_i ($i = 1, 2, 3\ldots$) acting at point a_i (X, Y, Z) ($i = 1, 2, 3\ldots$) and the moments are M_i ($i = 1, 2, 3\ldots$) and the moments are taken about an arbitrary point b (X, Y, Z) then the following conditions apply:

$$\Sigma \bar{P}_i = o \quad \ldots\ldots (1)$$

$$\Sigma(\bar{a}_i - b)\, \bar{P}_i + \Sigma \bar{M}_i = o \quad \ldots\ldots (2)$$

In component notation each of these single conditions becomes three conditions in X, Y, Z directions as follows:

$$\Sigma\, \bar{P}_{iX} = o \quad \ldots\ldots (3)$$

$$\Sigma\, \bar{P}_{iY} = o \quad \ldots\ldots (4)$$

$$\Sigma\, \bar{P}_{iZ} = o \quad \ldots\ldots (5)$$

$$\Sigma\{\bar{P}_{iZ}(\bar{a}_{iY} - b_Y) - \bar{P}_{iY}(\bar{a}_{iZ} - b_Z)\} + \Sigma \bar{M}_{iX} = o \quad \ldots\ldots (6)$$

$$\Sigma\{\bar{P}_{iX}(\bar{a}_{iZ} - b_Z) - \bar{P}_{iZ}(\bar{a}_{iX} - b_X)\} + \Sigma \bar{M}_{iY} = o \quad \ldots\ldots (7)$$

$$\Sigma\{\bar{P}_{iY}(\bar{a}_{iX} - b_X) - \bar{P}_{iX}(\bar{a}_{iY} - b_Y)\} + \Sigma \bar{M}_{iZ} = o \quad \ldots\ldots (8)$$

3.2 DIRECTION COSINES

The two systems of axes are defined in Section 3.1. The nodal points are located with reference to global axes whereas many geometrical properties are defined with reference to local axes. The built-in pretwist angle is defined in Section 3.1.1. It is essential that calculations are carried out with reference to one system of axes. The nodal points, loads and moments have to be resolved with reference to either one system. In order to carry out this, the direction cosines between two co-ordinate axes systems must be established. The two systems are presented in Figure 1 and 2a. The properties of the direction cosines between two orthogonal sets of axes are presented in Appendix 1. The direction cosines of the two orthogonal axes systems may be defined as follows:

$$\begin{array}{c} \\ x \\ y \\ z \end{array} \begin{array}{c} \begin{array}{ccc} X & Y & Z \end{array} \\ \begin{bmatrix} l_x & m_x & n_x \\ l_y & m_y & n_y \\ l_z & m_z & n_z \end{bmatrix} \end{array} \quad \ldots\ldots\ldots\ldots\ldots\ldots (9)$$

However, because of the additional constraint imposed on a pretwisted structure, it is essential to establish the direction cosines including this effect. This is done by choosing an intermediate axes system x, y_1, z_1 such that local y_1 will lie in the plane of the cross section and also in the X Y plane. The directions of the local (x, y, z) axes are then determined by rotating the intermediate axes about the local x axis through angle β in the positive sense.

Defining the direction cosines of the intermediate axes for a general case as

	X	Y	Z
x	l_x	m_x	n_x
y	l_{y1}	m_{y1}	n_{y1}
z	l_{z1}	m_{z1}	n_{z1}

$\ldots\ldots\ldots\ldots\ldots\ldots (10)$

If two nodal points at element ends say A and B are located by the co-ordinates X_1, Y_1, Z_1 and X_2, Y_2, Z_2 then the length AB is given by

$$L_{AB} = \left[(X_1 - X_2)^2 + (Y_1 - Y_2)^2 + (Z_1 - Z_2)^2 \right]^{\frac{1}{2}} \quad \ldots\ldots\ldots\ldots\ldots (11)$$

and

$$\left.\begin{aligned} l_x &= (X_1 - X_2)/L_{AB} \\ m_x &= (Y_1 - Y_2)/L_{AB} \\ n_x &= (Z_1 - Z_2)/L_{AB} \end{aligned}\right\} \quad \ldots\ldots\ldots\ldots\ldots\ldots\ldots\ldots\ldots\ldots\ldots\ldots (12)$$

The reference direction y_1 is given by

$$l_x l_{y1} + m_x m_{y1} + n_x n_{y1} = o \quad \ldots\ldots (13)$$

$$l_{y1}^2 + m_{y1}^2 + n_{y1}^2 = 1 \quad \ldots\ldots (14)$$

Please see Appendix 1 also for orthogonal conditions.

By definition $n_{y1} = 0$ (in X Y plane) and $m_{y1} > o$

Equations (13) and (14) reduce to

$$\left.\begin{aligned} l_x l_{y1} + m_x m_{y1} &= o \\ l_{y1}^2 + m_{y1}^2 &= 1 \end{aligned}\right\} \quad \ldots\ldots (15)$$

From the above equations

$$m_{y1} = - l_x l_{y1} / m_x$$

$$l_{y1}^2 + l_x^2 l_{y1}^2 / m_x^2 = 1$$

$$l_{y1}^2 \quad (1 + l_x^2 / m_x^2) = 1$$

This yields

$$\left.\begin{aligned} l_{y1} &= \pm m_x / (l_x^2 + m_x^2)^{\frac{1}{2}} \\ \text{and} \\ m_{y1} &= \pm l_x / (l_x^2 + m_x^2)^{\frac{1}{2}} \end{aligned}\right\} \quad \ldots\ldots (16)$$

Sign will be decided by $m_{y1} > o$. In most foreseeable cases l_x will be $> o$ giving

$$\left.\begin{aligned} l_{y1} &= -m_x / (l_x^2 + m_x^2)^{\frac{1}{2}} \\ m_{y1} &= l_x / (l_x^2 + m_x^2)^{\frac{1}{2}} \end{aligned}\right\} \quad \ldots\ldots (17)$$

Direction of local z_1 is orthogonal to x and y_1 giving

$$l_{z1} \underline{I} + m_{z1} \underline{J} + n_{z1} \underline{K} = \begin{vmatrix} \underline{I} & \underline{J} & \underline{K} \\ l_x & m_x & n_x \\ \dfrac{-m_x}{(l_x^2 + m_x^2)^{\frac{1}{2}}} & \dfrac{l_x}{(l_x^2 + m_x^2)^{\frac{1}{2}}} & o \end{vmatrix} \quad \ldots\ldots (18)$$

Expanding equation 18 and solving, yield the following results

$$l_{z1} = -n_x l_x / (l_x^2 + m_x^2)^{\frac{1}{2}}$$

$$m_{z1} = -n_x m_x / (l_x^2 + m_x^2)^{\frac{1}{2}}$$

$$n_{z1} = (l_x^2 + m_x^2)^{\frac{1}{2}}$$

A set of direction cosines for the intermediate axes as a general case may, therefore, be presented as follows:

$$\begin{array}{c|ccc} & X & Y & Z \\ x & l_x & m_x & n_x \\ y_1 & \dfrac{-m_x}{(l_x^2+m_x^2)^{\frac{1}{2}}} & \dfrac{l_x}{(l_x^2+m_x^2)^{\frac{1}{2}}} & o \\ z_1 & \dfrac{-n_x l_x}{(l_x^2+m_x^2)^{\frac{1}{2}}} & \dfrac{-n_x m_x}{(l_x^2+m_x^2)^{\frac{1}{2}}} & (l_x^2+m_x^2)^{\frac{1}{2}} \end{array} \quad \ldots\ldots(19)$$

This general transformation is acceptable for values of n_x less than Unity. There will be always difficulty with the singular case when n_x approaches Unity. From the computational point of view this could be stated as a limiting case for values of

$$(l_x^2 + m_x^2)^{\frac{1}{2}} \leq 10^{-7} \qquad \ldots\ldots\ldots\ldots\ldots(20)$$

To allow for the possibility of an exceptional condition such as the local x axis lying in the Z axis direction ($n_x = 1$) alternative directions are chosen. For the limiting case the transformation is

$$\begin{bmatrix} \underline{i} \\ \underline{j} \\ \underline{k} \end{bmatrix} = \begin{bmatrix} 0 & 0 & 1 \\ 0 & 1 & 0 \\ -1 & 0 & 0 \end{bmatrix} \begin{bmatrix} \underline{I} \\ \underline{J} \\ \underline{K} \end{bmatrix} \qquad \ldots\ldots\ldots\ldots\ldots(21)$$

The best way of getting at this is to follow through a sequence of local axes transformations at each of the nodes upto that node at which difficulty arises and adopt the above transformation for the limiting case.

A set of direction cosines for the present case may be written as follows:

$$\begin{array}{c} \\ x \\ y \\ z \end{array} \begin{array}{c} \begin{array}{ccc} X & Y & Z \end{array} \\ \begin{bmatrix} 0 & 0 & 1 \\ 0 & 1 & 0 \\ -1 & 0 & 0 \end{bmatrix} \end{array} \quad \ldots(22)$$

The direction cosine subroutine is programmed in such a way that a print out will show that an exceptional case has occured and alternative direction cosines are used.

On establishing the choice of the direction cosines of the intermediate axes, the actual direction cosines are calculated by a suitable transformation matrix. This is done by rotating the intermediate axes about the local x axis through angle ß in the positive sense. This rotation is represented in Figure 2.b. The transformation matrix is given by

$$\begin{bmatrix} 1 & o & o \\ o & \cos\beta & \sin\beta \\ o & -\sin\beta & \cos\beta \end{bmatrix} \quad \ldots\ldots\ldots\ldots\ldots\ldots(23)$$

then

$$\begin{bmatrix} l_x & m_x & n_x \\ l_y & m_y & n_y \\ l_z & m_z & n_z \end{bmatrix} = \begin{bmatrix} 1 & o & o \\ o & \cos\beta & \sin\beta \\ o & -\sin\beta & \cos\beta \end{bmatrix} \begin{bmatrix} l_x & m_x & n_x \\ l_{y1} & m_{y1} & n_{y1} \\ l_{z1} & m_{z1} & n_{z1} \end{bmatrix} \quad \ldots\ldots\ldots\ldots\ldots\ldots(24)$$

or

$$\overline{C} = \overline{T}\ \overline{C}_1 \quad \ldots\ldots\ldots\ldots\ldots\ldots(25)$$

Thus the direction cosines between overall axes and local axes of any blade section are established. When the pretwist is absent the $\overline{T}$ matrix will become a unit matrix.

3.2.1 Programming logic of Direction Cosines

The direction cosines established are used frequently in the calculations and hence these are programmed profitably as a subroutine called 'COSN'. A call of this subroutine (CALL COSN(I)) yields the required direction cosines of the member considered (I). This subroutine is not only used to transfer co-ordinates from one system of axes to another, but also used to transfer forces and moments from one axes system to another. A logic of operation of this subroutine is presented in Figure (3). While programming the matrices referred to in 3.2 ($\bar{C}$, $\bar{T}$, $\bar{C}_1$) are given the following names:

Direction cosine matrix $[\bar{C}]$ = $[\overline{DRMT}]$

Pre multiplying matrix $[\bar{T}]$ = $[\overline{DM}]$

Direction cosines without pretwist effect $[\bar{C}_1]$ = $[\overline{DC}]$

3.3 DERIVATION OF FLEXIBILITY MATRIX

The fundamental consideration in the matrix force method of analysis is the determination of the flexibility properties of the structural elements. The flexibility properties are determined by applying the unit load theorem. If an elastic element is subject to a set of n forces

$$\bar{P} = [P_1, P_2, P_3 \ldots\ldots\ldots P_n] \qquad \ldots\ldots (26)$$

and the corresponding displacements are denoted by

$$\bar{\Delta} = [\Delta_1, \Delta_2, \Delta_3 \ldots\ldots\ldots \Delta_n] \qquad \ldots\ldots (27)$$

then

$$\bar{\Delta} = \bar{F}\bar{P} \qquad \ldots\ldots (28)$$

where $\bar{F}$ is known as matrix of deflection influence coefficients otherwise called as flexibility matrix. According to the unit load theorem

$$\bar{P}_v^T \bar{\Delta} = \int_V \bar{\sigma}^T \bar{e}\, dv \qquad \ldots\ldots (29)$$

where $\bar{P}_v$ represents applied unit load matrix, $\bar{\sigma}$ represents the matrix of statically equivalent stresses due to unit loads and $\bar{e}$ is the exact strain matrix due to applied forces $\bar{F}$. For a linear system

$$\bar{e} = \bar{E}\bar{P} \qquad \ldots\ldots (30)$$

where $\bar{E}$ represents the stress distribution factors.

Applying equation (30) in (29)

$$\bar{\Delta} = \int_v \bar{\sigma}^T \bar{E} \bar{P} \, dv \qquad \ldots\ldots\ldots(31)$$

or

$$\bar{\Delta} = \bar{F} \quad \bar{P} \qquad \ldots\ldots\ldots(32)$$

where $\bar{F} = \int \bar{\sigma}^T \bar{E} \, dv$ represents the flexibility matrix.

The flexibility matrix is derived with reference to the local body axes dimensions for a discrete element of uniform section under a constant rate of pretwist $\frac{d\beta}{dx}$ (β') The general conventions explained in 3.1 are applicable. In addition, the following definitions and assumptions also apply:

(a) shear centre is offset fromthe centre of gravity of the cross sectional area. e_y and e_z are co-ordinate positions of the c.g referred to local axis through the shear centre. (Figure 4).

(b) P_x is the end load positive tensile (away from the section). EBT will yield x wise end load stress σ_x . This is caused by applied end load P_x and applied bending moment M_y and M_z (about c.g). Positive M_y and M_z will give positive tension in the positive quadrant. Positive M_x twists the section nose up at tip end.

(c) The moments and end loads will vary linearly along the section so that the distribution will be defined by giving values at the two ends. Displacements are assumed small so that small displacement theory could be used.

(d) The resisting torque includes St Venant's type of torsional term which is the same as would develop if the beam were initially untwisted.

(e) St Venant's shear distribution will balance the applied torque M_x. This applied torque is about the shear centre.

(f) The torque distribution resulting from the end load distribution and from the pretwist of the blade will be balanced by St Venant's stresses to give a zero resultant torque on the section. This approximation has been used by many scholars.

(g) y and z directions are taken as principal axes directions.

(h) P_{x1}, M_{x1}, M_{y1}, and M_{z1} are the loads at the tip end of an element and P_{x2}, M_{x2}, M_{y2}, M_{z2} are the loads at the root end of an element (referred to principal axes at end 1).

A typical blade element is shown in Figure (5a) indicating the loads. The end loads P_{x1} and P_{x2} are through the c.g positions and x wise moments are about the shear centre.However, the bending moments M_{y1}, M_{y2}, M_{z1} and M_{z2} are about the c.g positions. A general stress formula due to end load and applied bending moments is given by

$$\sigma_x = P_x / A + M_y .z / I_y + M_z .y / I_z \qquad \ldots\ldots\ldots(33)$$

where A is the cross sectional area and I_y and I_z are the principal second moments of area; and y and z are measured from the c.g position. As y and z are to be measured from shear centre position the stress formula is modified as follows:

$$\sigma_x = \frac{P_x}{A} + \frac{M_y (z - e_z)}{I_y} + \frac{M_z (y - e_y)}{I_z} \quad \ldots\ldots\ldots(34)$$

The directions of end load fibres due to pretwist are presented in Figures (5b) and (5c.) The slopes of the fibres are given by $\frac{dv}{dx}$ and $\frac{dw}{dx}$ and the rate of pretwist is given by $\frac{d\beta}{dx} = (\beta')$. From the Figures (5b) and (5c)

$$v = -z\, d\beta \quad \ldots\ldots\ldots(35)$$

$$w = y\, d\beta \quad \ldots\ldots\ldots(36)$$

$$v' = -z\, d\beta/dx \quad \ldots\ldots\ldots(37)$$

$$w' = y\, d\beta/dx \quad \ldots\ldots\ldots(38)$$

Therefore, the two slopes are given by:

$$\frac{dv}{dx} = -z\beta' \quad \text{and} \quad \frac{dw}{dx} = y\beta' \quad \ldots\ldots\ldots(39)$$

Assuming that shear loads S_y and S_z act at c.s positions and considering a small elemental area $d_y d_z$ the shear component of end load along fibre direction is given by:

$$ds_y = -\sigma_x \frac{dv}{dx}\, dydz \quad \ldots\ldots\ldots(40)$$

and

$$ds_z = -\sigma_x \frac{dw}{dx}\, dydz \quad \ldots\ldots\ldots(41)$$

$$dM_x = -ds_y \cdot z + ds_z \cdot y \quad \ldots\ldots\ldots(42)$$

For the element to be in equilibrium, St Venant's assumptions mentioned in (f) must apply and compensating St Venants type of shear flows to give a zero overall torque the following relationship is established:

$$M_{x_{sv}} + \int_y \int_z dM_x = 0 \quad \ldots\ldots\ldots(43)$$

or

$$M_{x_{sv}} = -\int_y \int_z dM_x$$

Substituting the value of dM_x from (42) in (43)

$$M_{xsv} = \iint_{y\,z} - \left\{ -ds_y \cdot z + ds_z \cdot y \right\} \quad \text{.....(44)}$$

or $$= \iint_{y\,z} ds_y \cdot z - ds_z \cdot y$$

Substituting the values of ds_y, ds_z, $\frac{dv}{dx}$, $\frac{dw}{dx}$ and σ_x from equations (40), (41), (39) and (34), equation (44) can be written as:

$$\begin{aligned} M_{xsv} &= \int_y \int_z \left\{ P_x/A + \frac{1}{I_y} M_y (z - e_z) + M_z/I_z (y - e_y) \right\} z^2 \beta' \, dy \, dz \\ &\quad - \int_y \int_z (-) \left\{ P_x/A + \frac{1}{I_z} M_y (z - e_z) + \frac{1}{I_z} M_z (y - e_y) \right\} y^2 \beta' \, dy \, dz \\ &= \iint \beta' (y^2 + z^2) \left\{ P_x/A + \frac{1}{I_y} M_y (z - e_z) + \frac{1}{I_z} M_z (Y - e_y) \right\} dy \, dz \\ &= \iint \beta' (y^2 + z^2) \frac{P_x}{A} \, dy \, dz \\ &\quad + \iint \beta' (y^2 + z^2)(z - e_z) \frac{1}{I_y} M_y \, dy dz \\ &\quad + \iint \beta' (y^2 + z^2)(y - e_y) \frac{1}{I_z} M_z \, dy dz \quad \text{.....(45)} \end{aligned}$$

Moments of higher order are defined as follows

$$B1 = \iint (y^2 + z^2) \, dydz \quad \text{.....(46)}$$

$$B2 = \iint (y^2 + z^2) \, y \, dydz \quad \text{.....(47)}$$

$$B3 = \iint (y^2 + z^2) \, z \, dydz \quad \text{.....(48)}$$

Substituting the values of (46) - (48) in (45)

$$M_{xsv} = P_x/A \cdot B1 \beta' + M_y/I_y \cdot (\beta' B3 - e_z \beta' B1) + \frac{M_z}{I_z} (\beta' B2 - e_y B1 \beta'). \quad (49)$$

i.e.

$$M_{xsv} = \frac{B1 \, \beta'}{A} P_x + \beta' \frac{(B3 - e_z B1) M_y}{I_y} + \beta' \frac{(B2 - e_y B1) M_z}{I_z} \quad \text{....(50)}$$

Letting $C_1 = \frac{B1 \beta'}{A}$, $C_2 = \beta' \frac{(B3 - e_z B1)}{I_y}$ and $C_3 = \beta' \frac{(B2 - e_y B1)}{I_z}$

equation (50) takes a simple form

$$M_{xsv} = C_1 P_x + C_2 M_y + C_3 M_z \quad \text{.....(51)}$$

The total torque on the section which includes St Venant's terms is as follows

$$M_{sv} = M_x + C_1 P_x + C_2 M_y + C_3 M_z \quad \text{.....(52)}$$

where M_x is the applied torque.

The degrees of freedom chosen for applied loads (end load, torque and two bending moments) allow to choose the applied loads as an 8 x 1 column matrix as follows:

$$\bar{P} = \begin{vmatrix} P_{x1} \\ P_{x2} \\ M_{x1} \\ M_{x2} \\ M_{y1} \\ M_{y2} \\ M_{z1} \\ M_{z2} \end{vmatrix}$$

Note:

suffix 1 represents loads at tip end of an element and suffix 2 represents loads at root end of an element

.....(53)

Letting $\bar{P}_v$ = virtual load or unit load matrix, $\bar{F}$ = flexibility matrix and $\bar{\Delta}_A$ = displacement matrix due to applied loads and applying unit load theorem

$$\bar{P}_v^T \bar{\Delta}_A = \int \bar{P}_v^T \bar{F} \bar{P}_A \qquad \text{.....(54)}$$

or $$\bar{P}_v^T \bar{\Delta}_A = \int \bar{\sigma}_v^T \epsilon_A \, dv$$

where $\bar{F}$ is an 8 x 8 matrix

$$\bar{P}_v^T \bar{\Delta}_A = \int_0^L \frac{P_{xA} P_{xv}}{EA} dx + \int_0^L \frac{M_{yA} M_{yv}}{EI_y} dx + \int_0^L \frac{M_{zA} M_{zv}}{EI_z} dx + \int \frac{M_{svA} M_{svv}}{GJ} dx \qquad \text{.....(55)}$$

In equation (55) the suffices v represent virtual or unit loads and suffices A represent applied loads and J is the torsional constant of the cross section. It is to be noted that the above equation also ignores temperature effects and shear deformations.

The internal forces acting on the cross section at a distance x_r from the tip end are worked out by linear interpolation. These are given as follows:

$$P_x = P_{x1} + (P_{x2} - P_{x1}) \frac{x_r}{L_r} \qquad \text{.....(56)}$$

$$M_x = M_{x1} + (M_{x2} - M_{x1}) \frac{x_r}{L_r} \qquad \text{.....(57)}$$

$$M_y^* = M_{y1} + (M_{y2} - M_{y1}) x_r / L_r \qquad \text{.....(58)}$$

$$M_z^* = M_{z1} + (M_{z2} - M_{z1}) x_r / L_r \qquad \text{.....(59)}$$

The moments M_y^* and M_z^* do not account for the effects due to pretwist and they refer to tip end reference axes moments. Using small angle approximations $\cos\beta x_r = 1 - \beta^2/2\,(x_r/L_r)^2$ and $\sin\beta x_r = \beta x_r / L_r$, the moments M_y and M_z are calculated as

$$M_y = M_y^* + \beta \frac{x_r}{L_r} M_z^* - \frac{\beta^2 x_r^2}{2L_r^2} M_y^* \quad \ldots\ldots\ldots(60)$$

$$M_z = M_z^* - \beta \frac{x_r}{L_r} M_y^* - \frac{\beta^2 x_r^2}{2L_r^2} M_z^* \quad \ldots\ldots\ldots(61)$$

Substituting the values of M_y^* and M_z^* from (58) and (59) in (60) and (61) the internal forces acting on the cross section at a distance of x_r from the tip end are given by:

$$P_x = P_{x1} + (P_{x2} - P_{x1}) \frac{x_r}{L_r} \quad \ldots\ldots\ldots(62)$$

$$M_x = M_{x1} + (M_{x2} - M_{x1}) \frac{x_r}{L_r} \quad \ldots\ldots\ldots(63)$$

$$M_y = M_{y1} + (M_{y2} - M_{y1}) \frac{x_r}{L_r} + \frac{\beta x_r}{L_r} \left\{ M_{z1} + (M_{z2} - M_{z1}) \frac{x_r}{L_r} \right\} - \frac{\beta^2 x_r^2}{2L_r^2} \left\{ M_{y1} + (M_{y2} - M_{y1}) \frac{x_r}{L_r} \right\} \quad \ldots\ldots\ldots(64)$$

$$M_z = M_{z1} + (M_{z2} - M_{z1}) \frac{x_r}{L_r} - \frac{\beta x_r}{L_r} \left\{ M_{y1} + (M_{y2} - M_{y1}) \frac{x_r}{L_r} \right\} - \frac{\beta^2 x_r^2}{2L_r^2} \left\{ M_{z1} + (M_{z2} - M_{z1}) \frac{x_r}{L_r} \right\} \quad \ldots\ldots\ldots(65)$$

According to equation (52)

$$M_{sv} = M_x + C_1 P_x + C_2 M_y + C_3 M_z \quad \ldots\ldots\ldots(66)$$

Substituting the values of Mx , P_x , M_y and M_z from (62)-(65) in (66)

$$\begin{aligned} M_{sv} = {} & M_{x1} + (M_{x2} - M_{x1}) x_r / L_r + C_1 \left\{ P_{x1} + (P_{x2} - P_{x1}) \frac{x_r}{L_r} \right\} \\ & + C_2 \left\{ \left[M_{y1} + (M_{y2} - M_{y1}) \frac{x_r}{L_r} \right] + \frac{\beta x_r}{L_r} \left[M_{z1} + (M_{z2} - M_{z1}) \frac{x_r}{L_r} \right] \right. \\ & \left. - \frac{\beta^2 x_r^2}{2L_r^2} \left[M_{y1} + (M_{y2} - M_{y1}) \frac{x_r}{L_r} \right] \right\} \\ & + C_3 \left\{ \left[M_{z1} + (M_{z2} - M_{z1}) \frac{x_r}{L_r} \right] - \frac{\beta x_r}{L_r} \left[M_{y1} + (M_{y2} - M_{y1}) \frac{x_r}{L_r} \right] \right. \\ & \left. - \frac{\beta^2 x_r^2}{2L_r^2} \left[M_{z1} + (M_{z2} - M_{z1}) \frac{x_r}{L_r} \right] \right\} \quad \ldots\ldots\ldots(67) \end{aligned}$$

The elements of flexibility matrix $\overline{F}$ are derived by integrating the equation (55) (the values of P_x , M_y , M_z and M_x from (62) - (67)). Evaluation of these integrals are presented in Appendix 4. The elements are properly arranged to form an 8x8 matrix when these are referred to the elements of $\bar{\Delta}_A$ matrix as follows:

$$\overline{F} = \begin{bmatrix} F_{1,1} & F_{1,2} & F_{1,3} & F_{1,4} & F_{1,5} & F_{1,6} & F_{1,7} & F_{1,8} \\ F_{2,1} & F_{2,2} & F_{2,3} & F_{2,4} & F_{2,5} & F_{2,6} & F_{2,7} & F_{2,8} \\ F_{3,1} & F_{3,2} & F_{3,3} & F_{3,4} & F_{3,5} & F_{3,6} & F_{3,7} & F_{3,8} \\ F_{4,1} & F_{4,2} & F_{4,3} & F_{4,4} & F_{4,5} & F_{4,6} & F_{4,7} & F_{4,8} \\ F_{5,1} & F_{5,2} & F_{5,3} & F_{5,4} & F_{5,5} & F_{5,6} & F_{5,7} & F_{5,8} \\ F_{6,1} & F_{6,2} & F_{6,3} & F_{6,4} & F_{6,5} & F_{6,6} & F_{6,7} & F_{6,8} \\ F_{7,1} & F_{7,2} & F_{7,3} & F_{7,4} & F_{7,5} & F_{7,6} & F_{7,7} & F_{7,8} \\ F_{8,1} & F_{8,2} & F_{8,3} & F_{8,4} & F_{8,5} & F_{8,6} & F_{8,7} & F_{8,8} \end{bmatrix} \quad \ldots\ldots\ldots\ldots (68)$$

where

$$F_{1,1} = F_{2,2} = \frac{L}{3EA} + \frac{C_1^2 L}{3GJ} \quad \ldots\ldots\ldots\ldots (69)$$

$$F_{1,2} = F_{2,1} = \frac{L}{6EA} + \frac{C_1^2 L}{6GJ} \quad \ldots\ldots\ldots\ldots (70)$$

$$F_{1,3} = F_{3,1} = F_{2,4} = F_{4,2} = \frac{C_1 L}{3GJ} \quad \ldots\ldots\ldots\ldots (71)$$

$$F_{1,4} = F_{4,1} = F_{2,4} = F_{4,2} = \frac{C_1 L}{6GJ} \quad \ldots\ldots\ldots\ldots (72)$$

$$F_{1,5} = F_{5,1} = \frac{C_1 C_2 L}{3GJ} - \frac{C_1 C_2 \beta^2 L}{60GJ} - \frac{C_1 C_3 \beta L}{12GJ} \quad \ldots\ldots\ldots\ldots (73)$$

$$F_{1,6} = F_{6,1} = F_{2,5} = F_{5,2} = \frac{C_1 C_2 L}{6GJ} - \frac{C_1 C_2 \beta^2 L}{40GJ} - \frac{C_1 C_3 \beta L}{12GJ} \quad \ldots\ldots\ldots\ldots (74)$$

$$F_{1,7} = F_{7,1} = \frac{C_1 C_2 \beta L}{12GJ} + \frac{C_1 C_3 L}{3GJ} - \frac{C_1 C_3 \beta^2 L}{60GJ} \quad \ldots\ldots\ldots\ldots (75)$$

$$F_{1,8} = F_{8,1} = F_{2,7} = F_{7,2} = \frac{C_1 C_2 \beta L}{12GJ} + \frac{C_1 C_3 L}{6GJ} - \frac{C_1 C_3 \beta^2 L}{40GJ} \quad \ldots\ldots\ldots\ldots (76)$$

$$F_{2,6} = F_{6,2} = \frac{C_1 C_2 L}{3GJ} - \frac{C_1 C_2 \beta^2 L}{10GJ} - \frac{C_1 C_3 \beta L}{4GJ} \quad \ldots\ldots\ldots\ldots (77)$$

$$F_{2,8} = F_{8,2} = \frac{C_1 C_2 \beta L}{4GJ} + \frac{C_1 C_3 L}{3GJ} - \frac{C_1 C_3 \beta^2 L}{10GJ} \quad \ldots\ldots\ldots\ldots (78)$$

$$F_{3,3} = F_{4,4} = \frac{L}{3GJ} \quad \ldots\ldots\ldots\ldots (79)$$

$$F_{34}=F_{43} = \frac{L}{6GJ} \qquad \text{.....(80)}$$

$$F_{35}=F_{53} = \frac{C_2 L}{3GJ} - \frac{C_2^2\beta L}{60GJ} - \frac{C_3\beta L}{12GJ} \qquad \text{.....(81)}$$

$$F_{36}=F_{63}=F_{45}=F_{54} = \frac{C_2 L}{6GJ} - \frac{C_2^2\beta L}{40GJ} - \frac{C_3\beta L}{12GJ} \qquad \text{.....(82)}$$

$$F_{37}=F_{73} = \frac{C_2\beta L}{12GJ} + \frac{C_3 L}{3GJ} - \frac{C_3\beta^2 L}{60GJ} \qquad \text{.....(83)}$$

$$F_{38}=F_{83}=F_{47}=F_{74} = \frac{C_2\beta L}{12GJ} + \frac{C_3 L}{6GJ} - \frac{C_3\beta^2 L}{40GJ} \qquad \text{.....(84)}$$

$$F_{46}=F_{64} = \frac{C_2 L}{3GJ} - \frac{C_2^2\beta L}{10GJ} - \frac{C_3\beta L}{4GJ} \qquad \text{.....(85)}$$

$$F_{48}=F_{84} = \frac{C_2\beta L}{4GJ} + \frac{C_3 L}{3GJ} - \frac{C_3\beta^2 L}{10GJ} \qquad \text{.....(86)}$$

$$F_{55} = \frac{LC_2^2}{3GJ} - \frac{C_2^2\beta^2 L}{30GJ} - \frac{C_2 C_3\beta L}{6GJ} + \frac{L}{3EI_y} + \frac{C_3^2\beta^2 L}{30GJ} + \left(\frac{1}{I_z}-\frac{1}{I_y}\right)\frac{\beta^2 L}{30E} \qquad \text{.....(87)}$$

$$F_{56}=F_{65} = \frac{LC_2^2}{6GJ} - \frac{C_2^2\beta^2 L}{20GJ} - \frac{C_2 C_3\beta L}{6GJ} + \frac{L}{6EI_y} + \frac{C_3^2\beta^2 L}{20GJ} + \left(\frac{1}{I_z}-\frac{1}{I_y}\right)\frac{\beta^2 L}{20E} \qquad \text{.....(88)}$$

$$F_{57}=F_{75} = \frac{C_2^2\beta L}{12GJ} - \frac{C_3^2\beta L}{12GJ} + \frac{C_2 C_3 L}{3GJ} - \frac{C_2 C_3^2\beta L}{15GJ} + \left(\frac{1}{I_y}-\frac{1}{I_z}\right)\frac{\beta L}{12E} \qquad \text{.....(89)}$$

$$F_{58}=F_{85}=F_{67}=F_{76} = \frac{C_2^2\beta L}{12GJ} - \frac{C_3^2\beta L}{12GJ} + \frac{C_2 C_3 L\beta}{6GJ} - \frac{C_2 C_3^2\beta L}{10GJ} + \left(\frac{1}{I_y}-\frac{1}{I_z}\right)\frac{\beta L}{12E} \qquad \text{.....(90)}$$

$$F_{66} = \frac{LC_2^2}{3GJ} - \frac{C_2^2\beta L}{5GJ} - \frac{C_2 C_3\beta L}{2GJ} + \frac{L}{3EI_y} + \frac{C_3^2\beta^2 L}{5GJ} + \left(\frac{1}{I_z}-\frac{1}{I_y}\right)\frac{\beta^2 L}{5E} \qquad \text{.....(91)}$$

$$F_{68}=F_{86} = \frac{C_2^2\beta L}{4GJ} - \frac{C_3^2\beta L}{4GJ} + \frac{C_2 C_3 L}{3GJ} - \frac{C_2 C_3^2 L}{2.5GJ} + \left(\frac{1}{I_y}-\frac{1}{I_z}\right)\frac{\beta L}{4E} \qquad \text{.....(92)}$$

$$F_{7,7} = \frac{C_2 C_3 \beta L}{6GJ} + \frac{C_2^2 \beta L}{30GJ} + \frac{C_3^2 L}{3GJ} - \frac{C_3^2 \beta^2 L}{30GJ} + \frac{L}{3EI_z} + \left(\frac{1}{I_y} - \frac{1}{I_z}\right) \frac{\beta^2 L}{30E} \quad \ldots\ldots\ldots\ldots (93)$$

$$F_{7,8} = F_{8,7} = \frac{C_2 C_3 \beta L}{6GJ} + \frac{C_2^2 \beta L}{20GJ} + \frac{C_3^2 L}{6GJ} - \frac{C_3^2 \beta^2 L}{20GJ} + \frac{L}{6I_z E} + \left(\frac{1}{I_y} - \frac{1}{I_z}\right) \frac{\beta^2 L}{20E} \quad \ldots\ldots\ldots\ldots (94)$$

$$F_{8,8} = \frac{C_2 C_3 \beta L}{2GJ} + \frac{C_2^2 \beta L}{5GJ} + \frac{C_3^2 L}{3GJ} - \frac{C_3^2 \beta^2 L}{5GJ} + \frac{L}{3EI_z} + \left(\frac{1}{I_y} - \frac{1}{I_z}\right) \frac{\beta^2 L}{5E} \quad \ldots\ldots\ldots\ldots (95)$$

Thus the flexibility matrix is formed.

3.3.1 Programming logic of Flexibility Matrix

As the flexibility matrix is widely used in the present work, it is programmed as a subroutine called FLEX (I) where the integer I represents the element considered. A call of this subroutine gives the required elements in a flexibility matrix. The matrix $\overline{F}$ considered in Section 3.3 is referred as FXMT in the subroutine FLEX. As the matrix is symmetric only upper triangle elements are initially formed and the lower triangle elements are fixed by suitable transformation. A logic of operation of this subroutine is presented in Figure 6.

3.3.2 Increase in torsional rigidity due to pretwist

When a blade of thin walled section is pretwisted the torsional stiffness will increase. This has been proved by previous investigators. The increase in torsional rigidity is due to the change in length of fibres away from the axis of twist leading to longitudinal stresses (assuming that plane sections remain plane). These stresses resist torque and reduce the Saint Venant's rotation. In reference (6) a formula for increased torsional rigidity has been derived for rectangular blades. Although a straight forward version for aerofoil section is not made, an equivalent breadth/ depth ratio approximation is used in the above formula to give the following increased torsional rigidity

$$GJ_A = GJ \left\{ 1 + I_z^2 \beta'^2 / I_y \, .2A \right\} \quad \ldots\ldots\ldots\ldots (96)$$

This increased torsional rigidity is included in the subroutine FLEX.

3.4 ANALYSIS OF FLAPPING LOADS.

For a rotating blade the forces due to small amplitude flapping vibration consist of two components:

(a) Flapping loads or inertia forces and

(b) Centrifugal loads or rotary forces.

The term 'flapping ' in this section is used in a general sense to denote the vibrational effects in the absence of a centrifugal force field. This term is used elsewhere to refer the displacements in Z axis direction.(The term 'drag' is used to indicate the displacements in Y axis direction) The current section deals with the flapping loads.

Centrifugal loads are considered in section 3.5

For inertia calculations the blade is idealized into a number of elements and the assumption is made that the mass is located along the centroidal axis. One is reminded that the flapping loads are considered with reference to global axis directions at c.g positions and the flexibility matrix derived in the section 3.5 is with reference to local axes directions.(locus of s.c positions is one of the reference axes) It is therefore,essencial that the flapping loads are also converted to local axes directions. This involves a number of transformations as follows: (a) Establish the flapping loads due to the arbitrary nodal displacements (say node J),(Global axes directions at c.g). (b) Transfer the loads established above to the position where the actual analysis is being considered(say node JJ). (c) Transform these loads into local axes directions by applying direction cosines. (d) Transfer the loads to s.c position. (e) Add the loads into an 8 x 5 matrix.

Six conventional loads are considered which are defined as follows:

P_X = force in X direction
P_Y = force in Y direction
P_Z = force in Z direction
M_X = bending moment about X direction
M_Y = bending moment about Y direction
M_Z = bending moment about Z direction

The distorsion of the blade is described in terms of lateral and twisting deformations as follows:

Δ_X = displacement in X direction
Δ_Y = displacement in Y direction
Δ_Z = displacement in Z direction
θ_x = torsional or twisting deformation about local x axis.

Note:

Although four degrees of freedom in the displacements are sufficient to establish the conventional loads, an additional degree of freedom in the twisting deformation is introduced in the current analysis. This is to study the variation in the vibrational characteristics due to change in direction of the blade centroidal axis (e.g sweep back)from one element to another element. This additional deformation ϕ is used on the inboard end of a node, whereas θ is used on the outboard end of

the same node. In practice θ and ϕ are one and the same if the change in the direction of the centroidal axis is absent.

The number of nodal points chosen decides the number of degrees of freedom in displacement and hence the number of modes of vibration. A simple harmonic vibration with a frequency ω is assumed. The forces acting on an element JJ are calculated by adding the effects of loads due to displacements at all nodes J on the tip side of node J. The node J is varied from 1 to JJ i.e. from tip end to root end, and while moving from one node to another the total loads are accumulated. The JJ and J notations are also explained in Figure 8.

When the displacements at J are considered, there are two systems of loads due to these displacements. They are:

(a) Global axes forces at J due to displacements at J causing inertia forces on element J-1 and

(b) Global axes forces at J + 1 due to displacements at J causing inertia forces on elementJ.

A diagrammatic representation of the displaced shape (in one of the axes directions) for inertia calculations is presented in Figure 7. The derivation of the forces is presented in Appendix 5. A three-dimensional view of an element with the representation of forces and moments is also shown in Figure 1.

The global axes forces at any nodal point consists of three forces and three moments.

The loads and moments at ends J and J + 1 are derived in Appendix 5 and are as follows:

$$P_{XJ} = \frac{\rho_{J-1}\omega^2 L_{J-1}}{2} \Delta_{X_J} \qquad \ldots\ldots(97)$$

$$P_{YJ} = \frac{\rho_{J-1}\omega^2 L_{J-1}}{2} \Delta_{Y_J} \qquad \ldots\ldots(98)$$

$$P_{ZJ} = \frac{\rho_{J-1}\omega^2 L_{J-1}}{2} \Delta_{Z_J} \qquad \ldots\ldots(99)$$

$$M_{XJ} = -\frac{\rho_{J-1}\omega^2 L_{J-1}^2}{6}(Z_{J-1}-Z_J)\Delta_{Y_J} + \frac{\rho_{J-1}\omega^2 L_{J-1}}{6}(Y_{J-1}-Y_J)\Delta_{Z_J} + \frac{\omega^2 I_P L_{J-1} I_{x(J-1)}}{2}\phi_{J-1} \qquad \ldots\ldots(100)$$

$$M_{YJ} = \frac{\rho_{J-1}\omega^2 L_{J-1}}{6}(Z_{J-1} - Z_J)\Delta X_J - \frac{\rho_{J-1}\omega^2 L_{J-1}}{6}(X_{J-1} - X_J)\Delta Z_J + \frac{\omega^2 I_P L_{J-1} m_{x(J-1)}}{2}\phi_{J-1} \quad \ldots\ldots(101)$$

$$M_{ZJ} = -\frac{\rho_{J-1}\omega^2 L_{J-1}}{6}(Y_{J-1} - Y_J)\Delta X_J + \frac{\rho_{J-1}\omega^2 L_{J-1}}{6}(X_{J-1} - X_J)\Delta Y_J + \frac{\omega^2 I_P L_{J-1} n_{x(J-1)}}{2}\phi_{J-1} \quad \ldots\ldots(102)$$

$$P_{XJ+1} = \rho_J \omega^2 L_J \Delta X_J / 2 \quad \ldots\ldots(103)$$

$$P_{YJ+1} = \rho_J \omega^2 L_J \Delta Y_J / 2 \quad \ldots\ldots(104)$$

$$P_{ZJ+1} = \rho_J \omega^2 L_J \Delta Z_J / 2 \quad \ldots\ldots(105)$$

$$M_{XJ+1} = -\frac{\rho_J \omega^2 L_J}{3}(Z_J - Z_{J+1})\Delta Y_J + \frac{\rho_J \omega^2 L_J}{3}(Y_J - Y_{J+1})\Delta Z_J + \frac{\omega^2 I_P L_J l_{xJ}\theta_J}{2} \quad \ldots\ldots(106)$$

$$M_{YJ+1} = \frac{\rho_J \omega^2 L_J}{3}(Z_J - Z_{J+1})\Delta X_J - \frac{\rho_J \omega^2 L_J}{3}(X_J - X_{J+1})\Delta Z_J + \frac{\omega^2 I_P L_J m_{xJ}\theta_J}{2} \quad \ldots\ldots(107)$$

$$M_{ZJ+1} = -\frac{\rho_J \omega^2 L_J}{3}(Y_J - Y_{J+1})\Delta X_J + \frac{\rho_J \omega^2 L_J}{3}(X_J - X_{J+1})\Delta Y_J + \frac{\omega^2 I_P L_J n_{xJ}\theta_J}{2} \quad \ldots\ldots(108)$$

It has to be noted that torsional moments about x have been resolved into X, Y, Z directions. ϕ_{J-1} and θ_J are defined in the beginning of 3.4.

Equations (97)-(108) can be written in matrix form as follows:

$$\begin{bmatrix} P_{XJ} \\ P_{YJ} \\ P_{ZJ} \\ M_{XJ} \\ M_{YJ} \\ M_{ZJ} \end{bmatrix} = \frac{\omega^2 L_{J-1}}{2} \begin{bmatrix} \rho_{J-1} & 0 & 0 & 0 & 0 \\ 0 & \rho_{J-1} & 0 & 0 & 0 \\ 0 & 0 & \rho_{J-1} & 0 & 0 \\ 0 & -\rho_{J-1}(Z_{J-1}-Z_J)/3 & \rho_{J-1}(Y_{J-1}-Y_J)/3 & 0 & I_P l_{x(J-1)} \\ \rho_{J-1}(Z_{J-1}-Z_J)/3 & 0 & -\rho_{J-1}(X_{J-1}-X_J)/3 & 0 & I_P m_{x(J-1)} \\ \rho_{J-1}(Y_{J-1}-Y_J)/3 & \rho_{J-1}(X_{J-1}-X_J)/3 & 0 & 0 & I_P n_{x(J-1)} \end{bmatrix} \begin{bmatrix} \Delta X_J \\ \Delta Y_J \\ \Delta Z_J \\ \theta_J \\ \phi_{J-1} \end{bmatrix} \quad \ldots\ldots(109)$$

$$\begin{bmatrix} P_{XJ+1} \\ P_{YJ+1} \\ P_{ZJ+1} \\ M_{XJ+1} \\ M_{YJ+1} \\ M_{ZJ+1} \end{bmatrix} = \frac{\omega^2 L_J}{2} \begin{bmatrix} \rho_J & 0 & 0 & 0 & 0 \\ 0 & \rho_J & 0 & 0 & 0 \\ 0 & 0 & \rho_J & 0 & 0 \\ 0 & -\frac{2}{3}\rho_J(Z_J - Z_{J+1}) & \frac{2}{3}\rho_J(Y_J - Y_{J+1}) & I_{P^l}{}_{xJ} & 0 \\ \frac{2}{3}\rho_J(Z_J - Z_{J+1}) & 0 & -\frac{2}{3}\rho_J(X_J - X_{J+1}) & I_{P^m}{}_{xJ} & 0 \\ -\frac{2}{3}\rho_J(Y_J - Y_{J+1}) & \frac{2}{3}\rho_J(X_J - X_{J+1}) & 0 & I_{P^n}{}_{xJ} & 0 \end{bmatrix} \begin{bmatrix} \Delta X_J \\ \Delta Y_J \\ \Delta Z_J \\ \Theta_J \\ \phi_{J-1} \end{bmatrix} \quad \ldots\ldots(110)$$

Or

$$\overline{P}_J = \omega^2 \overline{A}\ \overline{\Delta}_J \quad \ldots\ldots(111)$$

$$\overline{P}_{J+1} = \omega^2 \overline{B}\ \overline{\Delta}_J \quad \ldots\ldots(112)$$

Further treatment of these loads are carried out as follows: firstly (111) and (112) are combined and the effect transfered to a node where distorsions are desired. Secondly, these transfered loads are resolved into local body axes directions and subsequently transfered to shear centre position.

3.4.1 Operational logic of $\overline{A}$ & $\overline{B}$

The matrices mentioned in (111) and (112) namely $\overline{A}$ and $\overline{B}$ are programmed as two subroutines called FLAP (I, K) and FLAB (I, K). A flow of logics of these subroutines is presented in Figure 9. A call of either one of these subroutines would produce a 6 x 5 matrix consisting of flapping loads. In the above subroutines, I and K are the controlling parameters to indicate the nodal position and to control the call of subroutines(either FLAP or FLAB to be called). It is programmed to select FLAP subroutine for K=1 and FLAB subroutine for K=2.

3.4.2 Transformation of Loads

The loads established by $\overline{A}$ and $\overline{B}$ are applied forces due to distorsions at out board end of element J (at node J). When the deflection analysis is carried out at node JJ, global forces and moments at an inboard end of element JJ (node JJ) due to forces applied at outboard end of element J, have to be established. This is done by premultiplying the loads $\overline{P}_J$ by a transformation matrix, and the transformation matrix is programmed as a subroutine called TRAN (I, II).

The global forces at JJ (inboard) are given by:

$$\begin{bmatrix} P_X \\ P_Y \\ P_Z \\ M_X \\ M_Y \\ M_Z \end{bmatrix}_{JJ} = \begin{bmatrix} 1 & 0 & 0 & 0 & 0 & 0 \\ 0 & 1 & 0 & 0 & 0 & 0 \\ 0 & 0 & 1 & 0 & 0 & 0 \\ 0 & -(Z_J - Z_{JJ}) & (Y_J - Y_{JJ}) & 1 & 0 & 0 \\ (Z_J - Z_{JJ}) & 0 & -(X_J - X_{JJ}) & 0 & 1 & 0 \\ -(Y_J - Y_{JJ}) & (X_J - X_{JJ}) & 0 & 0 & 0 & 1 \end{bmatrix} \begin{bmatrix} P_X \\ P_Y \\ P_Z \\ M_X \\ M_Y \\ M_Z \end{bmatrix}_{J} \quad \ldots\ldots\ldots(113)$$

Or $$\overline{P_{JJ}} = \overline{TRA}\ \overline{P}_J \quad \ldots\ldots\ldots(114)$$

Where $\overline{TRA}$ represents the above 6 x 6 transformation matrix. It has to be noted that when J is equal to JJ the transformation matrix becomes a unit matrix and hence $\overline{P_{JJ}} = \overline{P_J}$. Care has also been taken in programming to account for the value of J greater than JJ. On such cases $\overline{P_{JJ}} =$ o.

Transforming both loads due to $\overline{A}$ and $\overline{B}$ mentioned earlier on

$$\overline{P_{JJ}} = \overline{TRA}\ \overline{P_J} + \overline{TRA}\ \overline{P_{J+1}} \quad \ldots\ldots\ldots(115)$$

or

$$\overline{P_{JJ}} = \omega^2\ \overline{TRA}\ \overline{A}\ \overline{\Delta}_J + \omega^2\ \overline{TRA}\ \overline{B}\ \overline{\Delta}_J \quad \ldots\ldots\ldots(116)$$

3.4.3 Resolution of Loads to Local Axes Directions

The loads depicted in 3.4.2 are in global axes directions and have to be resolved to local axes directions. This is done by applying direction cosines as follows:

$$\begin{bmatrix} p'_x \\ p'_y \\ p'_z \\ m'_x \\ m'_y \\ m'_z \end{bmatrix}_{JJ} = \begin{bmatrix} l_x & m_x & n_x & o & o & o \\ l_y & m_y & n_y & o & o & o \\ l_z & m_z & n_z & o & o & o \\ o & o & o & l_x & m_x & n_x \\ o & o & o & l_y & m_y & n_y \\ o & o & o & l_z & m_z & n_z \end{bmatrix} \begin{bmatrix} P_X \\ P_Y \\ P_Z \\ M_X \\ M_Y \\ M_Z \end{bmatrix}_{JJ} \quad \ldots\ldots\ldots(117)$$

or $$\overline{P'_{JJ}} = \overline{EC}\ \overline{P_{JJ}} \quad \ldots\ldots\ldots(118)$$

The 6 x 6 matrix $\overline{EC}$ is programmed as a subroutine called RESL (JJ) where JJ is the controlling index. The appropriate values of l_x, m_x, n_x etc., are taken from the direction cosine subroutine COSN (I).

Substituting the values of $\overline{P}_{JJ}$ from (116) in (118) the value for $\overline{p'_{JJ}}$ can be written as

$$\overline{p'_{JJ}} = \omega^2 \overline{EC}\ \overline{TRA}\ \overline{A}\ \overline{\Delta}_J + \omega^2 \overline{EC}\ \overline{TRA}\ \overline{B}\ \overline{\Delta}_J \quad \ldots\ldots\ldots(119)$$

3.4.4 Transfer of Loads to Shear Centre Position

The loads formed in Section 3.4.3 are with reference to centre of gravity. However, further calculations and in fact the flexibility matrix are with reference to shear centre position. Moreover only end load and three moments are required for further operation in line with the requirements of flexibility matrix. The transfer is carried out as follows:

$$\begin{bmatrix} p_x \\ m_x \\ m_y \\ m_z \end{bmatrix}_{JJ} = \begin{bmatrix} 1 & 0 & 0 & 0 & 0 & 0 \\ 0 & e_z & -e_y & 1 & 0 & 0 \\ 0 & 0 & 0 & 0 & 1 & 0 \\ 0 & 0 & 0 & 0 & 0 & -1 \end{bmatrix} \begin{bmatrix} p'_x \\ p'_y \\ p'_z \\ m'_x \\ m'_y \\ m'_z \end{bmatrix}_{JJ} \quad \ldots\ldots(120)$$

or $$\overline{P_{JJ}} = \overline{STR}\ \overline{p'_{JJ}} \quad \ldots\ldots(121)$$

In equation (120) e_z and e_y refer to the co-ordinates of c.g with reference to c.s. and a negative sign is introduced at element 4, 6 to adopt structural moments (positive tension in positive quadrant). This matrix $\overline{STR}$ is programmed as a subroutine called STRU (JJ). A call of this subroutine provides the necessary transfer matrix STR (4 x 6). Substituting the value of $\overline{p'_{JJ}}$ from equation (119) in (121)

$$\overline{P}_{JJ} = \omega^2 \overline{STR}\ \overline{EC}\ \overline{TRA}\ \overline{A}\ \overline{\Delta}_J + \omega^2 \overline{STR}\ \overline{EC}\ \overline{TRA}\ \overline{B}\ \overline{\Delta}_J \ldots(122)$$

3.4.5 Assembly of Loads

The loads in (122) are assembled into an 8 x 5 matrix depending on which end of the element JJ is under consideration. This matrix is called $\overline{R}$ matrix and is programmed as a subroutine called ASMB (JJ, K). Loads are also added in turn from tip end to root end. The assembly logic is better presented in Figure 10. A call of the subroutine ASMB adds the current loads into the previous appropriate elements in the matrix $\overline{R}$ (8 x 5).

3.5 ANALYSIS OF CENTRIFUGAL LOADS

The centrifugal loads are concerned only with a line distribution of mass idealised as concentrated along the centroidal axis of the section.

The conventions adopted in Section 3.1 apply. Overall Z axis direction is chosen as the axis of rotation. There will be two centrifugal force components in X and Y directions and there will not be any component in Z axis, this axis being the rotational axis. However, the moment contributions will be about all the three axes directions. The blade is assumed to rotate at an angular frequency of Ω.

The five loads considered are defined as follows:

P_X = force in X direction.

P_Y = force in Y direction.

M_X = bending moment about X axis.

M_Y = bending moment about Y axis.

M_Z = bending moment about Z axis.

The deformations of the blade are described in terms of displacements defined as follows:

Δ_X = displacement in X direction.

Δ_Y = displacement in Y direction.

Δ_Z = displacement in Z direction.

In order to make matrix operations conformable, two dummy variables are introduced. The column vectors associated with these two variables would be given zero values.

The centrifugal loads and moments at the root end, node J + 1, of element J due to the centrifugal loading of that element alone are derived in Appendix 6. The loads and moments as derived, of an element J (Appendix 6) are as follows:

$$P_{XJ+1} = \frac{\rho_J \Omega^2}{2} L_J \left(X_J + \Delta X_J + X_{J+1} + \Delta X_{J+1} \right) \quad \ldots\ldots\ldots (123)$$

$$P_{YJ+1} = \frac{\rho_J \Omega^2}{2} L_J \left(Y_J + \Delta Y_J + Y_{J+1} + \Delta Y_{J+1} \right) \quad \ldots\ldots\ldots (124)$$

$$M_{XJ+1} = \frac{-\rho_J \Omega^2}{2} L_J \left[\left(Y_J + \Delta Y_J \right) \frac{2}{3} \left(Z_J - Z_{J+1} \right) + \left(Y_{J+1} + \Delta Y_{J+1} \right) \frac{1}{3} \left(Z_J - Z_{J+1} \right) \right] \quad \ldots\ldots\ldots (125)$$

$$M_{YJ+1} = \frac{\rho_J \Omega^2}{2} L_J \left[\left(X_J + \Delta X_J \right) \frac{2}{3} \left(Z_J - Z_{J+1} \right) + \left(X_{J+1} + \Delta X_{J+1} \right) \frac{1}{3} \left(Z_J - Z_{J+1} \right) \right] \quad \ldots\ldots\ldots (126)$$

$$M_{ZJ+1} = \frac{-\rho_J \Omega^2 L_J}{2}\left[(X_J+\Delta X_J)\frac{2}{3}(Y_J-Y_{J+1}) + (X_{J+1}+\Delta X_{J+1})\frac{1}{3}(Y_J-Y_{J+1})\right] + \frac{\rho_J \Omega^2 L_J}{2}\left[(Y_J+\Delta Y_J)\frac{2}{3}(X_J-X_{J+1}) + (Y_{J+1}+\Delta Y_{J+1})\times\frac{1}{3}(X_J-X_{J+1})\right] \quad \ldots\ldots\ldots(127)$$

However, as a general case (as explained in Section 3.4) J and JJ are used to define the nodal points, where JJ represents the node at which distortions are calculated and J represents the node from which distortions are derived. When an element J is considered as opposed to node J, then J is treated as the outboard end or tip end and J + 1 is treated as the root end or inboard end. The same consideration applies to JJ also.

In the case of flapping loads the load vectors $\overline{P_J}$ and $\overline{P_{J+1}}$ were transformed by premultiplying by a transformation vector $\overline{TRA}$, to establish the loads at JJ. However, in the case of centrifugal loads a straightforward transformation is not applicable. This is because of the fact that the change of internal forces on element JJ due to the centrifugal forces on element J is somewhat different from the flapping case. The loads at JJ are established as follows.

3.5.1 Establishing Centrifugal Loads at JJ

There are two effects to be considered in establishing the change of internal forces at JJ and they are as follows:

(a) change of centrifugal force with unchanged moment arms.

(b) change of moment arms with unchanged centrifugal force.

These changes are associated with displacements $\overline{\Delta}_J$, $\overline{\Delta}_{JJ}$ and $\overline{\Delta}_{J+1}$, each vector representing X, Y, Z, θ and ϕ deflections. (Note that θ and ϕ are dummy deflections as explained earlier on).

(a) change of centrifugal force:

It is obvious from equations (123) and (124) that changes in centrifugal forces are due to distortions and are as follows:

$$P_{XJJ} = \frac{\rho_J \Omega^2 L_J}{2}(\Delta X_J + \Delta X_{J+1}) \quad \ldots\ldots\ldots(128)$$

$$P_{YJJ} = \frac{\rho_J \Omega^2 L_J}{2}(\Delta Y_J + \Delta Y_{J+1}) \quad \ldots\ldots\ldots(129)$$

The moments associated with the above forces are as follows:

$$M_{XJJ} = \frac{-\rho_J \Omega^2 L_J}{2}\left[\Delta Y_J\frac{2}{3}(Z_J-Z_{J+1}) + \Delta Y_{J+1}\frac{1}{3}(Z_J-Z_{J+1}) + (\Delta Y_J+\Delta Y_{J+1})(Z_{J+1}-Z_{JJ})\right] \quad \ldots\ldots\ldots(130)$$

$$M_{YJJ} = \frac{\rho_J \Omega^2 L_J}{2}\left[\Delta X_J \frac{2}{3}(Z_J - Z_{J+1}) + \Delta X_{J+1}\frac{1}{3}(Z_J - Z_{J+1}) + (\Delta X_J + \Delta X_{J+1})(Z_{J+1} - Z_{JJ})\right] \quad \ldots\ldots\ldots(131)$$

$$M_{ZJJ} = -\frac{\rho_J \Omega^2 L_J}{2}\left[\Delta X_J \frac{2}{3}(Y_J - Y_{J+1}) + \Delta X_{J+1}\frac{1}{3}(Y_J - Y_{J+1}) + (\Delta X_J + \Delta X_{J+1})(Y_{J+1} - Y_{JJ})\right]$$
$$+\frac{\rho_J \Omega^2 L_J}{2}\left[\Delta Y_J \frac{2}{3}(X_J - X_{J+1}) + \Delta Y_{J+1}\frac{1}{3}(X_J - X_{J+1}) + (\Delta Y_J + \Delta Y_{J+1})(X_{J+1} - X_{JJ})\right] \quad \ldots\ldots\ldots(132)$$

Additional moment arm terms containing JJ co-ordinates are introduced to add the moment effects at JJ due to changes in centrifugal forces.

(b) change of moment arms:

Three moment arms are assumed to undergo deformations and the effective changes in each direction are given by:

$$\Delta X_J - \Delta X_{J+1},\ \Delta Y_J - \Delta Y_{J+1} \text{ and } \Delta Z_J - \Delta Z_{J+1}$$

These changes in moment arms are multiplied by the unchanged centrifugal forces to give the additional moments desired. Three additional moment arms $\Delta X_{J+1} - \Delta X_{JJ}$, $\Delta Y_{J+1} - \Delta Y_{JJ}$, and $\Delta Z_{J+1} - \Delta Z_{JJ}$ are also introduced in line with Section 3.5.1 (a).

The additional moments due to changes in moment arms are as follows:

$$M_{XJJ} = -\frac{\rho_J \Omega^2 L_J}{2}\left[\frac{2}{3}Y_J(\Delta Z_J - \Delta Z_{J+1}) + \frac{1}{3}Y_{J+1}(\Delta Z_J - \Delta Z_{J+1}) + (Y_J + Y_{J+1})(\Delta Z_J - \Delta Z_{JJ})\right] \quad \ldots\ldots\ldots(133)$$

$$M_{YJJ} = \frac{\rho_J \Omega^2 L_J}{2}\left[\frac{2}{3}X_J(\Delta Z_J - \Delta Z_{J+1}) + \frac{1}{3}X_{J+1}(\Delta Z_J - \Delta Z_{J+1}) + (X_J + X_{J+1})(\Delta Z_{J+1} - \Delta Z_{JJ})\right] \quad \ldots\ldots\ldots(134)$$

$$M_{ZJJ} = -\frac{\rho_J \Omega^2 L_J}{2}\left[\frac{2}{3}X_J(\Delta Y_J - \Delta Y_{J+1}) + \frac{1}{3}X_{J+1}(\Delta Y_J - \Delta Y_{J+1}) + (X_J + X_{J+1})(\Delta Y_{J+1} - \Delta Y_{JJ})\right]$$
$$+\frac{\rho_J \Omega^2 L_J}{2}\left[\frac{2}{3}Y_J(\Delta X_J - \Delta X_{J+1}) + \frac{1}{3}Y_{J+1}(\Delta X_J - \Delta X_{J+1}) + (Y_J + Y_{J+1})(\Delta X_{J+1} - \Delta X_{JJ})\right] \quad \ldots\ldots\ldots(135)$$

The loads considered above (3.5.1 (a) and (b) are added to get the combined effect and are as follows:

$$P_{XJJ} = \frac{\rho_J \Omega^2 L_J}{2}(\Delta X_J + \Delta X_{J+1}) \quad \ldots\ldots\ldots(136)$$

$$P_{YJJ} = \frac{\rho_J \Omega^2 L_J}{2}(\Delta Y_J + \Delta Y_{J+1}) \quad \ldots\ldots\ldots(137)$$

$$M_{XJJ} = -\frac{\rho_J \Omega^2 L_J}{2}\left[\frac{2}{3}(Z_J-Z_{J+1})\Delta Y_J + \frac{1}{3}(Z_J-Z_{J+1})\Delta Y_{J+1} + (\Delta Y_J+\Delta Y_{J+1})(Z_{J+1}-Z_{JJ}) + \frac{2Y_J}{3}(\Delta Z_J-\Delta Z_{J+1}) + \frac{1}{3}Y_{J+1}(\Delta Z_J-\Delta Z_{J+1}) + (Y_J+Y_{J+1})(\Delta Z_{J+1}-\Delta Z_{JJ})\right] \quad \ldots\ldots(138)$$

$$M_{YJJ} = \frac{\rho_J \Omega^2 L_J}{2}\left[\frac{2}{3}(Z_J-Z_{J+1})\Delta X_J + \frac{1}{3}(Z_J-Z_{J+1})\Delta X_{J+1} + (\Delta X_J+\Delta X_{J+1})(Z_{J+1}-Z_{JJ}) + \frac{2X_J}{3}(\Delta Z_J-\Delta Z_{J+1}) + \frac{1X_{J+1}}{3}(\Delta Z_J-\Delta Z_{J+1}) + (X_J+X_{J+1})(\Delta Z_{J+1}-\Delta Z_{JJ})\right] \quad \ldots\ldots\ldots(139)$$

$$M_{ZJJ} = -\frac{\rho_J \Omega^2 L_J}{2}\left[\frac{2}{3}(Y_J-Y_{J+1})\Delta X_J + \frac{1}{3}(Y_J-Y_{J+1})\Delta X_{J+1} + (\Delta X_J+\Delta X_{J+1})(Y_{J+1}-Y_{JJ}) + \frac{2X_J}{3}(\Delta Y_J-\Delta Y_{J+1}) + \frac{1X_{J+1}}{3}(\Delta Y_J-\Delta Y_{J+1}) + (X_J+X_{J+1})(\Delta Y_{J+1}-\Delta Y_{JJ})\right] + \frac{\rho_J \Omega^2 L_J}{2}\left[\frac{2}{3}(X_J-X_{J+1})\Delta Y_J + \frac{1}{3}(X_J-X_{J+1})\Delta Y_{J+1} + (\Delta Y_J+\Delta Y_{J+1}) + \frac{2Y_J}{3}(\Delta X_J-\Delta X_{J+1}) + \frac{1Y_{J+1}}{3}(\Delta X_J-\Delta X_{J+1}) + (Y_J+Y_{J+1})(\Delta X_{J+1}-\Delta X_{JJ})\right] \quad \ldots\ldots(140)$$

The loads represented in equations (136) - (140) are better presented in matrix form as follows:

$$\begin{bmatrix} P_{XJJ} \\ P_{YJJ} \\ M_{XJJ} \\ M_{YJJ} \\ M_{ZJJ} \end{bmatrix} = \frac{\rho_J \Omega^2 L_J}{2} \begin{bmatrix} 1 & 0 & 0 \\ 0 & 1 & 0 \\ 0 & -\frac{2}{3}(Z_J-Z_{J+1})-(Z_{J+1}-Z_{JJ}) & -\frac{2Y_J}{3}-\frac{1Y_{J+1}}{3} \\ \frac{2}{3}(Z_J-Z_{J+1})+(Z_{J+1}-Z_{JJ}) & 0 & \frac{2X_J}{3}+\frac{1X_{J+1}}{3} \\ \begin{cases}\frac{2}{3}(Y_J-Y_{J+1}) \\ -(Y_{J+1}-Y_{JJ}) \\ +\frac{2Y_J}{3}+\frac{1Y_{J+1}}{3}\end{cases} & \begin{cases}-\frac{2X_J}{3}-\frac{1X_{J+1}}{3} \\ +\frac{2}{3}(X_J-X_{J+1}) \\ +(X_{J+1}-X_{JJ})\end{cases} & 0 \end{bmatrix} \begin{bmatrix} \Delta X_J \\ \Delta Y_J \\ \Delta Z_J \end{bmatrix}$$

$$+ \frac{\rho_J \Omega^2 L_J}{2} \begin{bmatrix} 1 & 0 & 0 \\ 0 & 1 & 0 \\ 0 & -\frac{1}{3}(Z_J-Z_{JJ})-(Z_{J+1}-Z_{JJ}) & \frac{2Y_J}{3}+\frac{1Y_{J+1}}{3}+Y_J+Y_{J+1} \\ \frac{1}{3}(Z_J-Z_{J+1})+(Z_{J+1}-Z_{JJ}) & 0 & -\frac{2X_J}{3}-\frac{1X_{J+1}}{3}+X_J+X_{J+1} \\ \begin{cases}-\frac{1}{3}(Y_J-Y_{J+1})-(Y_{J+1}-Y_{JJ}) \\ -\frac{2Y_J}{3}-\frac{1Y_{J+1}}{3}+Y_J+Y_{J+1}\end{cases} & \begin{cases}\frac{2X_J}{3}+\frac{1X_{J+1}}{3}-(X_J+X_{J+1}) \\ +\frac{1}{3}(X_J-X_{J+1})+(X_{J+1}-X_{JJ})\end{cases} & 0 \end{bmatrix} \begin{bmatrix} \Delta X_{J+1} \\ \Delta Y_{J+1} \\ \Delta Z_{J+1} \end{bmatrix}$$

$$+\frac{\rho_J \Omega^2 L_J}{2}\begin{bmatrix} 0 & 0 & 0 \\ 0 & 0 & 0 \\ 0 & 0 & (Y_J+Y_{J+1}) \\ 0 & 0 & -(X_J+X_{J+1}) \\ -(Y_J+Y_{J+1}) & (X_J+X_{J+1}) & 0 \end{bmatrix}\begin{bmatrix} \Delta X_{JJ} \\ \Delta Y_{JJ} \\ \Delta Z_{JJ} \end{bmatrix}$$

.....(141)

The above equation reduces to:

$$\begin{bmatrix} P_{XJJ} \\ P_{YJJ} \\ M_{XJJ} \\ M_{YJJ} \\ M_{ZJJ} \end{bmatrix} = \frac{\rho_J \Omega^2 L_J}{2}\begin{bmatrix} 1 & 0 & 0 \\ 0 & 1 & 0 \\ 0 & -\frac{2Z}{3}_J-\frac{1Z}{3}_{J+1}+Z_{JJ} & -\frac{2Y}{3}_J-\frac{1Y}{3}_{J+1} \\ \frac{2Z}{3}_J+\frac{1Z}{3}_{J+1}-Z_{JJ} & 0 & \frac{2X}{3}_J+\frac{1X}{3}_{J+1} \\ Y_{JJ} & -X_{JJ} & 0 \end{bmatrix}\begin{bmatrix} \Delta X_J \\ \Delta Y_J \\ \Delta Z_J \end{bmatrix}$$

$$+\frac{\rho_J \Omega^2 L_J}{2}\begin{bmatrix} 1 & 0 & 0 \\ 0 & 1 & 0 \\ 0 & -\frac{1Z}{3}_J-\frac{2Z}{3}_{J+1}+Z_{JJ} & -\frac{1Y}{3}_J-\frac{2Y}{3}_{J+1} \\ \frac{1Z}{3}_J+\frac{2Z}{3}_{J+1}-Z_{JJ} & 0 & \frac{1X}{3}_J+\frac{2X}{3}_{J+1} \\ Y_{JJ} & -X_{JJ} & 0 \end{bmatrix}\begin{bmatrix} \Delta X_{J+1} \\ \Delta Y_{J+1} \\ \Delta Z_{J+1} \end{bmatrix}$$

$$+\frac{\rho_J \Omega^2 L_J}{2}\begin{bmatrix} 0 & 0 & 0 \\ 0 & 0 & 0 \\ 0 & 0 & (Y_J+Y_{J+1}) \\ 0 & 0 & -(X_J+X_{J+1}) \\ -(Y_J+Y_{J+1}) & (X_J+X_{J+1}) & 0 \end{bmatrix}\begin{bmatrix} \Delta X_{JJ} \\ \Delta Y_{JJ} \\ \Delta Z_{JJ} \end{bmatrix}$$

.....(142)

Forces at end JJ + 1 of the member JJ (root end of the member JJ) are obtained by substituting JJ + 1 for JJ in equation (142). When member J coincides with member JJ then only substitution for end JJ + 1 is applicable. However, this equation has to be modified to account for the dummy distortions θ and ϕ. It is reminded that these are introduced just for compatibility and no physical

change is done to the equation. Allowing for the above distortions, equation (142) can be written as follows :

$$\begin{bmatrix} P_{XJJ} \\ P_{YJJ} \\ M_{XJJ} \\ M_{YJJ} \\ M_{ZJJ} \end{bmatrix} = \frac{\rho_J \Omega^2 L_J}{2} \begin{bmatrix} 1 & o & o & o & o \\ o & 1 & o & o & o \\ o & -\frac{2Z_J}{3}-\frac{1Z_{J+1}}{3}+Z_{JJ} & -\frac{2Y_J}{3}-\frac{1Y_{J+1}}{3} & o & o \\ \frac{2Z_J}{3}+\frac{1Z_{J+1}}{3}-Z_{JJ} & o & \frac{2X_J}{3}+\frac{1X_{J+1}}{3} & o & o \\ Y_{JJ} & -X_{JJ} & o & o & o \end{bmatrix} \begin{bmatrix} \Delta X_J \\ \Delta Y_J \\ \Delta Z_J \\ \theta \\ \phi \end{bmatrix}$$

$$+ \frac{\rho_J \Omega^2 L_J}{2} \begin{bmatrix} 1 & o & o & o & o \\ o & 1 & o & o & o \\ o & -\frac{1Z_J}{3}-\frac{2Z_{J+1}}{3}+Z_{JJ} & -\frac{1Y_J}{3}-\frac{2Y_{J+1}}{3} & o & o \\ \frac{1Z_J}{3}+\frac{2Z_{J+1}}{3}-Z_{JJ} & o & \frac{1X_J}{3}+\frac{2X_{J+1}}{3} & o & o \\ Y_{JJ} & -X_{JJ} & o & o & o \end{bmatrix} \begin{bmatrix} \Delta X_{J+1} \\ \Delta Y_{J+1} \\ \Delta Z_{J+1} \\ \theta \\ \phi \end{bmatrix}$$

$$+ \frac{\rho_J \Omega^2 L_J}{2} \begin{bmatrix} o & o & o & o & o \\ o & o & o & o & o \\ o & o & (Y_J+Y_{J+1}) & o & o \\ o & o & -(X_J+X_{J+1}) & o & o \\ -(Y_J+Y_{J+1}) & (X_J+X_{J+1}) & o & o & o \end{bmatrix} \begin{bmatrix} \Delta X_{JJ} \\ \Delta Y_{JJ} \\ \Delta Z_{JJ} \\ \theta \\ \phi \end{bmatrix} \quad \ldots\ldots\ldots(143)$$

or

$$\bar{P}_{JJ} = \bar{A}_1 \bar{\Delta}_J + \bar{B}_1 \bar{\Delta}_{J+1} + \bar{C}_1 \bar{\Delta}_{JJ} \quad \ldots\ldots\ldots(144)$$

When the loads at root end of element JJ are required JJ is replaced by JJ + 1 in the above equation. This involves not only replacing distortion vector $\bar{\Delta}_{JJ}$ by $\bar{\Delta}_{JJ+1}$, but also changing moment arms consisting of JJ terms to JJ + 1, where applicable.

In the equation (144), vectors $\bar{A}_1$, $\bar{B}_1$ and $\bar{C}_1$ are 5 x 5 matrices and it is reminded that there is no centrifugal force in overall Z direction. However, the load vector $\bar{P}_{JJ}$ has to be resolved to local axes directions and subsequently transferred to shear centre position. To make these operations possible the matrices $\bar{A}_1$, $\bar{B}_1$ and $\bar{C}_1$ have to be of size 6 x 5 and, therefore, a dummy row is introduced in each of those matrices as Z direction loads.

3.5.2 Logic of Operation of $\overline{P}_{JJ}$

The matrices $\overline{A}_1$, $\overline{B}_1$ and $\overline{C}_1$ are programmed as subroutines called CENT (JJ, J), CENF (JJ, J) and CEJJ (JJ, J) respectively where JJ and J represent control indices, JJ being the element where deflections are analysed and J being the element where contributions are derived from. A substitution of JJ + 1 or J + 1 instead of JJ or J would decide the loads at root ends of element JJ or J. A call of any one of the above subroutines would produce a 6 x 5 matrix. A flow of logic of these subroutines is presented in Figure 11.

3.5.3 Resolution of Loads to Local Axes Directions

The loads depicted in 3.5.1 are in global axes directions and have to be resolved to local axes directions. This is done by applying direction cosines as follows:

$$\begin{bmatrix} p'_x \\ p'_y \\ p'_z \\ m'_x \\ m'_y \\ m'_z \end{bmatrix}_{JJ} = \begin{bmatrix} l_x & m_x & n_x & o & o & o \\ l_y & m_y & n_y & o & o & o \\ l_z & m_z & n_z & o & o & o \\ o & o & o & l_x & m_x & n_x \\ o & o & o & l_y & m_y & n_y \\ o & o & o & l_z & m_z & n_z \end{bmatrix} \begin{bmatrix} P_X \\ P_Y \\ P_Z \\ M_X \\ M_Y \\ M_Z \end{bmatrix}_{JJ}$$

or $$\overline{p'}_{JJ} = \overline{EC}\ \overline{P}_{JJ} \qquad \text{.....(146)}$$

As referred in Section 3.4.3, the 6 x 6 matrix $\overline{EC}$ is programmed as a subroutine (RESL). Substituting the values of $\overline{P}_{JJ}$ from (144) in equation (146).

$$\overline{p'}_{JJ} = \Omega^2\ \overline{EC}\ \overline{A}_1\ \overline{\Delta}_J + \overline{EC}\ \overline{B}_1 \overline{\Delta}_{J+1} + \overline{EC}\ \overline{C}_1\ \overline{\Delta}_{JJ} \qquad \text{.....(147)}$$

The loads at root end of element JJ are computed by substituting JJ + 1 in the place of JJ in equation (147).

3.5.4 Transfer of Loads to Shear Centre Position

The loads calculated in 3.5.3 have to be transferred to shear centre position. This is done by premultiplying the equation (147) by the transformation matrix referred in 3.4.4. Bearing in mind only end load p_x and three moments are required at each end of an element, the transformation is carried out as follows:

$$\begin{bmatrix} p_x \\ m_x \\ m_y \\ m_z \end{bmatrix}_{JJ} = \begin{bmatrix} 1 & o & o & o & o & o \\ o & e_z & -e_y & 1 & o & o \\ o & o & o & o & 1 & o \\ o & o & o & o & o & -1 \end{bmatrix} \begin{bmatrix} p'_x \\ p'_y \\ p'_z \\ m'_x \\ m'_y \\ m'_z \end{bmatrix}_{JJ} \quad \ldots\ldots\ldots(148)$$

or $$\bar{p}_{JJ} = \overline{STR}\ \bar{p}'_{JJ} \quad \ldots\ldots\ldots(149)$$

e_z and e_y represent the co-ordinate position of centre of gravity with reference to shear centre position. As explained in 3.4.4 (-1) is introduced in the matrix STR at element 4, 6 to adopt structural moments. The matrix $\overline{STR}$ is programmed as subroutine STRU.

Substituting the values of $\bar{p}'_{JJ}$ from equation (147) in (149)

$$\bar{p}_{JJ} = \Omega^2\left[\overline{STR}\ \overline{EC}\ \bar{A}_1\bar{\Delta}_J + \overline{STR}\ \overline{EC}\ \bar{B}_1\bar{\Delta}_{J+1} + \overline{STR}\ \overline{EC}\ \bar{C}_1\bar{\Delta}_{JJ}\right] \quad \ldots\ldots(150)$$

3.5.5 Assembly of Loads

The loads calculated in (149) are assembled into a 8 x 5 matrix $\bar{R}$ depending on which side of the element JJ is under consideration; i.e. if tip end of the element is considered then the loads are assembled in rows 1, 3, 5 and 7 and if the root end of the element is considered then the loads are assembled in rows 2, 4, 6 and 8. The subroutine ASMB is used to carry out this operation. The matrix $\bar{R}$ is renamed as $\overline{RR}$ to differentiate from flapping loads. ($\bar{R}$ represents assembled flapping loads and $\overline{RR}$ represents assembled centrifugal loads).

3.6 ANALYSIS OF UNIT LOADS

The deformation of the structure will be evaluated using the unit load method formula.

$$\bar{P}_v^T\bar{\Delta} = \int \bar{P}_v^T\ \overline{F}\ \bar{P}_A \quad \ldots\ldots\ldots(151)$$

Where $\bar{\Delta}$ represents the deformation vector, $\overline{F}$ represents the flexibility matrix, $\bar{P}_A$ represents the applied load matrix and $\bar{P}_v$ represents the unit load matrix. Section 3.3 deals with the derivation of flexibility matrix and Sections 3.4 and 3.5 deal with matrix $\bar{P}_A$ (flapping loads and centrifugal loads). It is, therefore, necessary to evaluate unit loads, matrix $\bar{P}_v$. The sign conventions as used for flapping loads are applicable here also.

Unit loads are placed on the structure in global axes directions at c.g. positions. The calculated bending moments about global axes directions are then transferred to local axes directions.

Four conventional loads are considered as follows:

P_{Xv} = unit or virtual load in X direction.

P_{Yv} = unit or virtual load in Y direction.

P_{Zv} = unit or virtual load in Z direction.

m_{xv} = unit or virtual moment about the local x axis direction.

These four unit loads are chosen in line with the four degrees of freedom in displacements namely $\Delta_X, \Delta_Y, \Delta_Z$, and θ. However, an additional torsional displacement degree of freedom (ϕ) has been introduced to consider blades having a kinked centroidal axis.

It is, therefore, necessary to introduce an additional unit moment also and m_{xv} the virtual moment in local axis is divided into two components as $m_{x\theta v}$ and $m_{x\phi v}$. As these moments are in local axis direction they are resolved to global axes directions and the unit load matrix is defined as follows:

$$\begin{bmatrix} P_{Xv} \\ P_{Yv} \\ P_{Zv} \\ M_{Xv} \\ M_{Yv} \\ M_{Zv} \end{bmatrix} = \begin{bmatrix} 1 & o & o & o & o \\ o & 1 & o & o & o \\ o & o & 1 & o & o \\ o & o & o & l_{x\theta} & l_{x\phi} \\ o & o & o & m_{x\theta} & m_{x\phi} \\ o & o & o & n_{x\theta} & n_{x\phi} \end{bmatrix} \quad \ldots\ldots\ldots(152)$$

or $\overline{P_v} = \overline{BAB}$ $\ldots\ldots\ldots(153)$

The direction cosines used in columns 4 and 5 of matrix $\overline{BAB}$ are decided by the choice of $m_{x\theta}$ or $m_{x\phi}$. As in the cases of flapping loads (3.5) as a general case J and JJ are used to define the nodal points where JJ represents the node at which distortions are calculated and J represents the node at which distortions are derived from.

The unit loads are applied at node J and their effects at node JJ are established by premultiplying the unit loads by the transformation matrix in the same manner described in 3.4.2., and resolution of these loads to local axis and shifting to shear centre position follows exactly in the same fashion described in 3.4.3 and

3.4.4. The unit loads thus established are

$$\overline{P}_{vJJ} = \overline{\overline{STR}}\ \overline{EC}\ \overline{TRA}\ \overline{BAB} \quad \ldots\ldots\ldots(154)$$

where $\overline{\overline{STR}}$, $\overline{EC}$ and $\overline{TRA}$ represent the vectors transforming to shear centre position, resolving to local axis and transferring to JJ position respectively. The loads calculated in (154) are assembled into an 8 x 5, $\overline{R}$ matrix as explained in 3.4.5.

3.7 EIGEN VALUE PROBLEM

The flapping and centrifugal loads are derived in 3.4 and 3.5 respectively and are finally assembled in the form of 8 x 5 matrices ($\overline{R}$ and $\overline{RR}$). In forming the total loads on the structure in either case an element JJ is considered where deformation occurs, another element J is considered where the loads are applied and their effect on JJ is analysed. A blade is divided into N elements. Whilst JJ is considered from tip end to root end (1 to N), J is considered from tip end to JJ (1 to JJ + 1, plus 1 is to account for either side of an element. However, when the last element is considered JJ+1 is ignored as only N deflections at tip ends are required).

When element no.1 is analysed (JJ) loads at position 1 and 2 (J = JJ and J = JJ +1) are calculated and loads are assembled into 8 x 5 matrices ($\overline{R}$ if flapping and $\overline{RR}$ if centrifugal). When element no.2 is analysed loads at position 1, 2, and 3 are calculated. Similarly when element no.3 is considered loads at 1, 2, 3 and 4 are considered. In general, when element n is considered loads at 1 to n + 1 are calculated. Thus the total load matrix would be a lower triangle matrix of size 80 x 50, for a ten element idealisation.

Similarly the unit load matrix would be a lower triangle matrix of size 80 x 50 and when it is transposed the same would be an upper triangle matrix of size 50 x 80. On the other hand, the flexibility matrix would be a diagonal matrix of size 80 x 80.

The flapping loads and centrifugal loads as derived in 3.4 and 3.5 are as follows:

$$\overline{P}_F = \overline{R}\,\omega^2\,\overline{\Delta} \quad \ldots\ldots\ldots(155)$$

$$\overline{P}_C = \overline{RR}\,\Omega^2\,\overline{\Delta} \quad \ldots\ldots\ldots(156)$$

where

$$\overline{P}_{F1} = \overline{R}_{1,1}\omega^2\overline{\Delta}_1 + \overline{R}_{1,2}\omega^2\overline{\Delta}_2$$

$$\overline{P}_{F2} = \overline{R}_{2,1}\omega^2\overline{\Delta}_1 + \overline{R}_{2,2}\omega^2\overline{\Delta}_2 + \overline{R}_{2,3}\omega^2\overline{\Delta}_3$$

$$\bar{P}_{F3} = \bar{R}_{3,1}\omega^2\bar{\Delta}_1 + \bar{R}_{3,2}\omega^2\bar{\Delta}_2 + \bar{R}_{3,3}\omega^2\bar{\Delta}_3 + \bar{R}_{3,4}\omega^2\bar{\Delta}_4$$

$$\bar{P}_{Fn} = \bar{R}_{n,1}\omega^2\bar{\Delta}_1 + \bar{R}_{n,2}\omega^2\bar{\Delta}_2 + \cdots\cdots \bar{R}_{nn}\omega^2\bar{\Delta}_n + \bar{R}_{nn+1}\omega^2\bar{\Delta}_{n+1}$$

similarly

$$\bar{P}_{C1} = \overline{RR}_{1,1}\Omega^2\bar{\Delta}_1 + \overline{RR}_{1,2}\Omega^2\bar{\Delta}_2$$

$$\bar{P}_{C2} = \overline{RR}_{2,1}\Omega^2\bar{\Delta}_1 + \overline{RR}_{2,2}\Omega^2\bar{\Delta}_2 + \overline{RR}_{2,3}\Omega^2\bar{\Delta}_3$$

$$\bar{P}_{C3} = \overline{RR}_{3,1}\Omega^2\bar{\Delta}_1 + \overline{RR}_{3,2}\Omega^2\bar{\Delta}_2 + \overline{RR}_{3,3}\Omega^2\bar{\Delta}_3 + \overline{RR}_{3,4}\Omega^2\bar{\Delta}_4$$

$$\bar{P}_{Cn} = \overline{RR}_{n,1}\Omega^2\bar{\Delta}_1 + \overline{RR}_{n,2}\Omega^2\bar{\Delta}_2 + \cdots + \overline{RR}_{nn}\Omega^2\Delta_n + \overline{RR}_{nn+1}\Omega^2\bar{\Delta}_{n+1}$$

Total load $= \bar{P}_F + \bar{P}_C$

$$= \bar{R}\omega^2\bar{\Delta} + \overline{RR}\Omega^2\bar{\Delta}$$

$$\bar{P}_A = \left[\bar{R}\omega^2 + \overline{RR}\Omega^2\right]\bar{\Delta} \qquad \text{.....(157)}$$

By applying unit loads

$$\bar{\Delta} = \bar{P}_v^T \bar{F} \bar{P}_A \qquad \text{.....(158)}$$

Substituting $\bar{P}_A$ from (157)

$$\bar{\Delta} = \bar{R}_v^T \bar{F}\left[\bar{R}\omega^2 + \overline{RR}\Omega^2\right]\bar{\Delta} \qquad \text{.....(159)}$$

or

$$\bar{\Delta} = \left[\bar{C}\omega^2 + \bar{D}\Omega^2\right]\bar{\Delta} \qquad \text{.....(160)}$$

This represents an eigenvalue problem. Rearranging equation (160)

$$\left[\bar{I} - \bar{D}\Omega^2\right]\bar{\Delta} = \bar{C}\omega^2\bar{\Delta} \qquad \text{.....(161)}$$

$$\bar{\Delta} = \left[\bar{I} - \bar{D}\Omega^2\right]^{-1}\bar{C}\omega^2\bar{\Delta} \qquad \text{.....(162)}$$

In equations (161) and (162) $\bar{I}$ represents the identity matrix. Equation (162) could be rearranged as follows:

$$\left[\bar{I} - (\bar{I} - \bar{D}\Omega^2)^{-1}\bar{C}\omega^2\right]\bar{\Delta} = 0 \qquad \text{.....(163)}$$

$$\left[\frac{I}{\omega^2} - (\bar{I} - \bar{D}\Omega^2)^{-1}\bar{C}\right]\bar{\Delta} = 0 \qquad \text{.....(164)}$$

By solving the above equation the frequencies of vibration and the mode shapes are established. Standard library routines are used to solve the equation. This is explained in Section 3.8. It is essential to analyse the formation of $\bar{C}$ matrix and $\bar{D}$ matrix in the current section as they form the essential part of the eigenvalue problem.

3.7.1 Formation of $\bar{C}$ Matrix

The $\bar{C}$ matrix and $\bar{D}$ matrix referred to in equation (163) are of size 50 x 50. The matrix $\bar{C}$ is the outcome of the product $\bar{P}_v^T$ x $\bar{F}$ x $\bar{R}$ (50 x 80, 80 x 80, 80 x 50).

This could be diagrammatically represented as in Figure 12a. In order to avoid unnecessary storage of $\bar{P}_v^T$, $\bar{F}$ and $\bar{R}$, the assembly of $\bar{C}$ matrix is carried out as follows. The first column in the $\bar{P}_v^T$ matrix, the first element in the $\bar{F}$ matrix and first row in the $\bar{R}$ matrix are multiplied. As $\bar{P}_v^T$ and $\bar{R}$ are upper and lower triangle matrices and $\bar{F}$ is a diagonal matrix the multiplication is limited to one set as shown in Figure 12b. The outcome of this multiplication is a 5 x 5 matrix and this will be stored in the first 5 x 5 position of $\bar{C}$ matrix as shown in Figure 12c.

The next set of calculations would be the product of second column of the $\bar{P}_v^T$ matrix (10 x 5), second diagonal $\bar{F}$ matrix (5 x 5) and the second row of $\bar{R}$ matrix (5 x 10). This is diagrammatically presented in Figure 12 d. The outcome of this product is a 10 x 10 matrix. This product is superimposed on the previously stored 5 x 5 matrix. On superimposition the net result becomes a 10 x 10 matrix. Similarly, on subsequent superimpositions, the $\bar{C}$ matrix would develop as 15 x 15, 20 x 20, 25 x 25,..... until it finally reaches 50 x 50 on the final calculations. This development process is presented in Figure 12e and analytically represented as follows:

J	1	2	3	4.....10
1	$\sum_{i=1}^{n} \bar{P}^T_{v1,i}\, \bar{F}_{i,i}\, \bar{R}_{i,1}$	$\sum_{i=1}^{n} \bar{P}^T_{v1,i}\, \bar{F}_{i,i}\, \bar{R}_{i,2}$	$\sum_{i=2}^{n} \bar{P}^T_{v1,i}\, \bar{F}_{i,i}\, \bar{R}_{i,3}$	.....
2	$\sum_{i=2}^{n} \bar{P}^T_{v2,i}\, \bar{F}_{i,i}\, \bar{R}_{i,1}$	$\sum_{i=2}^{n} \bar{P}^T_{v2,i}\, \bar{F}_{i,i}\, \bar{R}_{i,2}$	$\sum_{i=2}^{n} \bar{P}^T_{v2,i}\, \bar{F}_{i,i}\, \bar{R}_{i,3}$	.....
JJ				
3	$\sum_{i=3}^{n} \bar{P}^T_{v3,i}\, \bar{F}_{i,i}\, \bar{R}_{i,1}$	$\sum_{i=3}^{n} \bar{P}^T_{v3,i}\, \bar{F}_{i,i}\, \bar{R}_{i,3}$	$\sum_{i=3}^{n} \bar{P}^T_{v3,i}\, \bar{F}_{i,i}\, \bar{R}_{i,3}$	.....
4	.	.	.	.....
	.	.	.	.....
	.	.	.	.....
	.			
10	.	.	.	.....

where $\bar{R}_v^T$ is the unit load matrix (5 x 8), $\bar{F}$ is the flexibility matrix (8 x 8) and $\bar{R}$ is the applied load matrix (8 x 5).

The $\bar{C}$ matrix thus established is named as EIGA in programming stage naturally of size 50 x 50.

3.7.2 Formation of $\overline{D}$ Matrix

The formation of $\overline{D}$ matrix follows exactly the same logic as the formation of $\overline{C}$ matrix except $\overline{RR}$ matrix is used in the place of $\overline{R}$ matrix. It is reminded that $\overline{RR}$ is associated with centrifugal loads and $\overline{R}$ is associated with flapping loads. The $\overline{D}$ matrix is also of size 50 x 50 and this is referred as $\overline{EIGB}$ in programming.

3.8 PROGRAMMING TECHNIQUE

The programme is written in FORTRAN - IV language for the ICL 1905 computer. MAXIMOP multi-access system is used which facilitates a large number of users to converse directly with the computer through terminals. No use has been made of magnetic disc or tape storage. The programme has been developed for a 10 element idealisation although this could be extended up to 25 element idealisation yielding higher accuracy in results. As the computer milling time and core storage are directly proportional to the square of the number of elements, the choice is limited to 10 elements, with acceptable accuracy. However, one case of 20 element idealisation has been run which indicated higher accuracy.

3.8.1 Subroutines

The following subroutines have been developed in order to increase the efficiency of programming.

(1) COSN (I) - This subroutine evaluates the direction cosines of element I - outcome DRMT (3 x 3).

(2) FLEX (I) - This subroutine evaluates the flexibility matrix of element I - outcome FXMT (8 x 8).

(3) MULT - This subroutine calculates two conformable matrices and stores in a third matrix.

(4) FLAP - This subroutine evaluates global axes forces at J due to displacements at J (inertia forces on element J-1).

(5) FLAB - This subroutine evaluates global axes forces at J + 1 due to displacements at J (inertia forces on element J).

(6) TRAN (I, II) - This subroutine transforms the loads at node I, to node II - outcome TRA (6 x 6).

(7) RESL (II) - This subroutine resolves global axes vectors to local axes vectors.

(8) STRU (II) - This subroutine shifts the loads at c.g. position to shear centre position.

(9) ASMB (II, K) - This subroutine assembles loads in $\overline{R}$ (8 x 5) matrix in rows 1, 3, 5, 7 when K = o and assembles loads in rows 2, 4, 6, 8 when

K = 1. On subsequent calls, the previous values are added to the current values to the respective elements.

(10) CENT (JJ, J) - This subroutine evaluates centrifugal loads at JJ due to deflections at J.

(11) CENF (JJ, J) - This subroutine evaluates centrifugal loads at JJ due to deflections at J + 1.

(12) CEJJ (JJ) - This subroutine evaluates centrifugal loads at JJ due to deflections at JJ.

Individual logic of operation of the subroutines, COSN, FLEX, FLAP, FLAB, ASMB, and a combined operation logic of CENT, CENF and CEJJ are presented in Sections 3.2 to 3.5. The logics of the subroutines MULT, TRAN, RESL and STRU are not presented as they are considered simple and self-explanatory.

These subroutines have been developed as modular programmes individually using MAXIMOP facilities. Hypothetical values were fed in as input data and results were checked by hand calculations. These check results are not presented here as these are used just to verify that the subroutines evaluate correctly. However, these modular programmes were checked by the author using several input data.

3.8.2 Library Subroutines

The following library subroutines have been used for the process of establishing the eigenvalues and eigenvectors:

(1) FPMGESSOL

(2) FPDIRHESSE

(3) FPQRHESSE

(4) FPQRVS and

(5) FPBACK

3.8.2.1 FPMGESSOL

This library subroutine solves a set of simultaneous linear equations of the form $\bar{A}X = \bar{B}$ using a Gaussian elimination method where $\bar{A}$ is an (m x m) matrix and $\bar{B}$ is an (m x n) matrix. The call statement is CALL FPMGESSOL (M, N, E, A(1), B(1), W(1), DET, IRANK, NRR) where M, N, IRANK and NRR are integer variables, E and DET are Real variables and A, B and W are one-dimensional Real arrays of lengths mm, mn and (m + 3) /4 respectively. The solution is left in array $\bar{B}$. Essentially, the equation $\bar{A}X = \bar{B}$ is treated in the form $X = \bar{A}^{-1}\bar{B}$ and the solved result is left in array $\bar{B}$. This subroutine is profitably used to invert $(\bar{I} - D\Omega^2)^{-1}\bar{C}$ referred to in equation (163). ($\bar{C}$ and $\bar{D}$ are termed as EIGA and EIGB in programming).

3.8.2.2 FPDIRHESSE

This library subroutine reduces a real matrix to upper Hessenberg form. The subroutine, given an (m x m) real matrix $\bar{A}$ calculates the (m x m) matrices N, H and P where N is a lower triangle matrix and has a diagonal of 1's and has its first column vector =

$$\begin{bmatrix} 1 \\ o \\ o \\ o \\ \\ o \end{bmatrix}$$

H is of upper Hessenberg form and P is a permutation matrix. The arrays N and H are formed by using a Gauss-like method of direct reduction with pivoting.
The call statement is CALL FPDIRHESSE (M, A(1), INT(1)) where M is an integer variable, A is a one-dimensional Real array of length m^2 and INT is an integer array of length at least M - 2. In the present case the following values are set M = m, the order of the matrix A (m^2 = elements)

$$A(k) = a_{ij} \text{ where } k = i + m\,(j-1)(i, j = 1.....m).$$

3.8.2.3 FPQRHESSE

This library subroutine computes the eigenvalues of a Hessenberg matrix by the QR method, and is taken from a well tested Algol procedure. The eigenvalues are computed by the QR algorithm method which is basically an algorithm which is enhanced by a technique of double shifting and the detection of small elements and pairs of small elements on the subdiagonal of a conveying array. The subroutines find eigenvalues

$\lambda_k = x_k + i\,Y_k$ (k = 1, ...n) of an n x n upper Hessenberg matrix.
The call statement is CALL FPQRHESSE (M, A(1), ITS(1), X(1), Y(1) AA(1), IVS). where M and IVS are integer variables, A and AA are one-dimensional Real arrays of length n^2, ITS is an integer array of length at least n and X and Y are Real arrays of length at least n.

M is set a value n, the order of the matrix (noting n^2 elements) A (k) = h_{ij} where k = i + n (j-1) (i, j = 1....n) of which only those with subscripts $i \leq j+1$ are relevant since the matrix is assumed to be of Hessenberg form. If IVS = o then AA must not be equivalent to A and the Hessenberg matrix in A will be preserved to find eigen-vectors. If IVS $\neq$ o then AA must be equivalent to A and the Hessenberg matrix in

A will be lost. Upon termination of FPQRHESSE X(k) = x_k and Y (k) = y_k are obtained where $x_k + i y_k = \lambda_k$ the kth eigenvalue.

3.8.2.4 FPQRVS

This library subroutine finds the eigenvectors of an (n x n) Hessenberg matrix $A = (a_{ij})$ (i, j = 1.....n) whose eigenvalues are known. $\lambda_k = x_k + iy_k$ (k=1....n). The vectors are found by the method of "inverse iteration" which may be defined by

$v_{s+1} = (A - p\,I)^{-1} u_s$, $u_{s+1} = v_{s+1} / \max(v_{s+1})$ where p is an approximation to an eigenvalue of A. The matrix (A- pI) is decomposed triangularly into the product LU using partial pivoting, and then solve the equations $P(A-p\,I)\bar{x} = \bar{b}$ where P is a computation matrix, obtained by solving $L\bar{y} = P^T \bar{b}$; $U\bar{x} = \bar{y}$.

The call statement is CALL FPQRVS (M, A(1), AA(1), X(1), Y(1), T(1) where M is an integer variable; A and AA are one-dimensional Real arrays of length n^2; X and Y are one-dimensional Real arrays of length n and T is a one-dimensional Real array of length $n^2 + 7$ n. M is set a value of n, the order of the matrix (noting n^2 elements) A(k) = a_{ij} where k = i + n (j-1) (i, j=1.....n) of which only those with subscripts satisfying i $\leq$ j+1 are relevant, since the matrix is assumed to be of Hessenberg form. Upon termination of FPQVRS the eigenvectors of the (n x n) matrix A are recorded in the (n x n) array AA.

3.8.2.5 FPBACK

This library subroutine computes the eigenvectors of the original Real matrix mentioned in FPDIRHESSE, given the results of the subroutines FPDIRHESSE, FPQRHESSE and FPQRVS. Knowing the vectors α_k (k=1....n) satisfying the equations $H\alpha_k = \lambda_k \alpha_k$ the eigenvector ϕ_k is found which satisfied $A\phi_k = \lambda_k \phi_k$ The call statement is CALL FPBACK (M, A(1), AA(1), Y(1), INT(1)) where M is an integer variable, A and AA are one-dimensional Real arrays of length n^2, Y is a one-dimensional Real array of length n and INT is a one-dimensional integer array of length n-2. M is set a value of n, the order of the matrix, the Real array A is set at n^2 and the integer array INT is given a value of n-2. The eigenvectors of the original Real matrix are recorded in the (n x n) array AA.

3.8.3 Input Data Files

The main programme is run by using many DATA files. The use of DATA files allows a good degree of freedom of varying different parameters. Each data file would be of the following form:

FILE NAME

N (number of elements)

E, G, Ω

A1, IY_1, IZ_1, J_1, $B1_1$, $B2_1$, $B3_1$, EY_1, EZ_1, ρ_1, IP_1

A2, IY_2, IZ_2, J_2, $B1_2$, $B2_2$, $B3_2$, EY_2, EZ_2, ρ_2, IP_2

A3, IY_3, IZ_3, J_3, $B1_3$, $B2_3$, $B3_3$, EY_3, EZ_3, ρ_3, IP_3

A_N, IY_N, IZ_N, J_N, $B1_N$, $B2_N$, $B3_N$, EY_N, EZ_N, ρ_N, IP_N

X_1, Y_1, Z_1, β_{A1}, β_{B1}

X_2, Y_2, Z_2, β_{A2} β_{B2}

X_3, Y_3, Z_3, β_{A3}, β_{B3}

X_{N+1}, Y_{N+1}, Z_{N+1}, β_{AN+1}, β_{BN+1}

where the following explanations apply.

N = Number of elements, integer

E = Youngs modulus, G = Modulus of rigidity, Ω = Rotational speed.

A = Sectional areas.

IY = Second moment of area about Y axis.

IZ = Second moment of area about Z axis.

J = Torsional rigidity.

B1 = Higher moment of area 1.

B2 = Higher moment of area 2.

B3 = Higher moment of area 3.

EY, EZ = Shear centre offset co-ordinates.

ρ = Mass per unit length.

IP = Pitching inertias.

X = c.g. position in X direction.

Y = c.g. position in Y direction.

Z = c.g. position in Z direction.

β_A = Angle of inclination (pretwist) of y axis with the line of intersection of the plane of cross section with XY plane, tip end

β_B = Angle of inclination (pretwist) of y axis with the line of intersection of the plane of cross section with XY plane, root end.

Various data files have been formed to deal with different blades and variations in the geometrical phenomena.

3.8.4 Programme VTRI

The main programme is written in FORTRAN - IV and is named as VTRI. This programme is suitable for 10 and 20 element idealisations. The programme may be divided into main blocks as follows:

(1) Dimensioning the arrays and declaration of common storage.

(2) Read input data from DATA file.

(3) Set all arrays to zero.

(4) Write all input data.

(5) Start main calculations.

(5.1) JJ block

(a) form direction cosines

(b) form flexibility matrix

(c) form resolution matrix

(d) form transfer matrix

(5.1.1) JS block. Calculation of unit loads.

(5.1.2) J block.

(a) calculate centrifugal loads.

(b) calculate flapping loads.

(5.1.3) Re-set unit loads.

(5.1.4) Form $\bar{C}$ ($\overline{EIGA}$) matrix

(5.1.5) Form $\bar{D}$ ($\overline{EIGB}$) matrix.

(6) Set values of $\bar{C}$ and $\bar{D}$ suitable for calling library routines.

(7) Use library subroutines.

(8) Print frequencies and mode shapes.

(9) Subroutines.

A complete logic of the programme is presented in Appendix 9 which forms the basis of programming. An output of the programme listing is presented in Appendix 7. The programme uses 46K of core storage. A run time of (maximum) 3 minutes and 34 seconds was needed for a 10 element idealisation. The main features of this programme are the inclusions of pretwist angle, offset shear centre position from c.g. position, abrupt blade geometry changes such as sweep back, increase in torsional rigidity due to pretwist, allowance for changes in sectional elements such as taper and steps. Other factors such as Coriolis forces, shear deformations, coning,

etc., which are neglected in this work could be easily accommodated if necessary. Increase in accuracy can be obtained by increasing the number of elements. Further accuracy could be obtained by introducing an assumption that each discrete blade length deflects into a circular arc and that the blade bending moments in each short blade varies cubically.

3.8.5 Use of MAXIMOP Facility

The multi access system known as MAXIMOP via terminals can process many jobs simultaneously. The type of applications most suitable for MAXIMOP are those in which there is a lot of need for communication between the user and the computer. Applications where less communication is necessary (production run of large tested programmes) are most suited to GEORGE runs. Use is made of MAXIMOP facilities to test the subroutines as modular programmes and other minor programmes. Due to limitations on the usage of MAXIMOP (core size, efficiency), terminal output is not possible and the production runs were carried out as GEORGE jobs, but still using MAXIMOP to request GEORGE runs. This special request facility is called GEO2. A typical GEO2 request is presented in Appendix 8.

RESULTS AND DISCUSSION

In total 62 different cases were run to include as many variations as possible. These cases are in fact the variations of the major blade groups presented in Tables 3-9. The variations considered for analysis and the blade codes as in DATA files are presented in Table 2. While presenting the results in tabular form and in graphical form, these blades are also referred to by their data file codes.

In the initial stages the individual subroutines were checked with numerical values and subsequently adopted in the main programme, VTRI. The programme uses 46K of core storage and a run time (maximum) of 3 minutes and 34 seconds was needed for computation. An output of the programme listing is presented in Appendix 7. To show the output of results, a standard output print is presented in Appendix 10 for reference. The term '% error' referred in this chapter is used to indicate the % difference from one method to another. In certain cases the term 'coupled' is used to represent simultaneous displacements in different directions. The validity of the method is better appreciated by comparing initially the standard cases where classical solutions are possible. The computed results are compared to the known results in most of the cases although this comparison was not possible in certain cases. When the analytical solutions are not available for cases such as sweep back blades, the argument lies on the strength of the other known cases.

Subsequently, the cases where analytical and in certain cases where experimental results are known, have been considered and the results analysed. A selection of rotating blades was also considered and results compared. This section is subdivided into four groups as follows:

(a) standard cases where classical solutions are possible;

(b) cases where no comparative results are presented;

(c) cases where analytical and (in certain cases) practical results are available; and

(d) rotating blades where results are available for comparison.

4.1 STANDARD CASES

A straight rectangular uniform blade as in Table 3, laid in overall X axis is considered as a standard check case. The computed results and exact analytical

solutions are presented up to fifth mode in Tables 10-13, the exact analytical solutions being obtained using classical formulae. The accu racy of the method is considered to be very good for the first normal mode frequencies. The % errors of the first normal mode frequencies are, flap bending mode 0.054%, drag bending mode 0.075%, torsional 0.205% and longitudinal 0.206%. The accuracy of the second mode frequencies are reasonable the % errors being: flap bending 1.075%, drag bending 1.079%, torsional 1.857% and longitudinal 1.857%. The third mode frequencies can be considered satisfactory, the % errors being flap bending 3.596%, drag bending 3.596%, torsional 5.194% and longitudinal 5.194%. The percentage errors on the fourth and fifth modes are in the increasing trend as can be seen in Tables 10-13. The decreasing accuracy obtained for the higher modes is due to the increasing effect of the constraints on deflected shape imposed by the finite number of degrees of freedom in the analysis.

The same blade parameters were used and the case has been run as a 20 element idealised blade. The computed results, results obtained by 10 element idealisation and the exact analytical solutions are presented in Tables 53-56. The accuracy of the method increased considerably. The % errors of the first normal mode frequencies are, flap bending mode 0.00701%, drag bending mode 0.00682%, torsional 0.0514% and longitudinal 0.0514%. The % errors of the second mode frequencies are also reduced considerably, the errors being, flap bending 0.279%, drag bending 0.278%, torsional 0.463% and longitudinal 0.463%. Similar decrease in errors results on higher modes also as could be referred to in Tables 53-56. It is, therefore, concluded that accuracy of the results could be increased if necessary by increasing the number of elements.

This has also been demonstrated by Williams (49). In his work on a case of 10 element idealisation the % errors were as follows: first mode 0.036%, second mode 0.363%, third mode 1.501%, fourth mode 4.07% and fifth mode 8.567%. But these errors have been reduced to a remarkably low percentage level when he adopted 25 element idealisation; the percentage errors being, first mode 0.00076%, second mode 0.0101%, third mode 0.0434%, fourth mode 0.126% and fifth mode 0.290%. It is apparent that the accuracy increases with the increase of number of elements.

However, running of all the cases on 20 element idealisation is not pursued. In practice, the consideration of lower modes is more important than the higher modes and hence it can be concluded that the present method is acceptable especially for

the lower modes. An error analysis is presented in graphical form in Figure 13 for the cases of 10 element idealisation and 20 element idealisation. The percentage errors increase in the form of exponential type with the increase of mode numbers. In the case of 20 element idealisation, however, the curves are flatter, as expected.

The mode shape curves are presented in Figures 14-19. The flapping and drag bending mode shapes are coincident for all modes. The flap bending mode shapes depicted by Williams' (49) method, for the present case by 25 element idealisation are also plotted. The mode shapes compare reasonably well with those of Williams'. No attempt is made to compare the mode shapes obtained by the present 20 element method for flapping and drag bending cases, as the shapes are too close to be identified. However, the mode shapes obtained for these cases are presented in Figures 76-78.

The torsional mode shapes are coincident with those of longitudinal modes for all modes, which follows in the same fashion like flap bending and drag bending modes shapes. The mode shapes obtained by both 10 element and 20 element idealisation for torsional and longitudinal modes are presented in Figures 17-19 and the agreement is considered to be very reasonable.

The frequency ratios, of a straight rectangular blade, between flap bending and drag bending should be in the ratio of $(I_z / I_y)^{\frac{1}{2}}$, which incidently checks all right for all modes.

Another check is made by placing the blade positioned at equal angles to all three global axes as presented in table 4 (blade 2) and also as represented in figure 5d. In the figure the triangle ABC represents the plane of cross section. Displacements in flap bending modes would give rise to displacements in local z direction which has components in global X,Y,Z directions. The displacements in drag bending modes would give rise to displacements in local y directions which has components in global X and Y directions only. The displacements in the longitudinal mode would give displacements in local x axis directions which has components in global X,Y,Z directions. The results computed for this blade are presented in Table 14. All the displacement patterns explained above agreed with the results obtained. It can be seen that there is practically no change in the frequency values. It is interesting to note that the torsional mode shapes are independent irrespective of the inclination of the plane of cross-section. No attempt is made to present the mode shapes as the aim was mainly to check that frequencies are unchanged although the displacements in X,Y,Z directions do.

A case where classical solutions were calculated and run on Williams' programme is also run on the present programme. The blade in question is blade no.3. This blade is similar to blade no.1 but with different mass density and Youngs' modulus. The results obtained by the present method, solutions by classical method and solutions by Williams are presented in Table 15. (Williams' results are for flap bending mode frequencies only). The % errors when compared to Williams' results were, first flap bending mode 0.024%, second flap bending mode 1.328%, third flap bending mode 4.005%, fourth bending mode 7.979 % and fifth bending mode 12.917%. The percentage errors when compared to classical results were as follows for flapping and drag bending modes: first modes 0.062%, 0.061%; second modes 1.078%; third modes 3.596%; fourth modes 7.428% and fifth modes 12.149%. The percentage errors for torsional and longitudinal modes are the same for all identical modes which are as follows: first mode 0.206%;second mode 1.857%; third mode 5.194%; fourth mode 10.284% and fifth mode 17.239%. These errors are of the same order as in blade no.1. The arguments presented for blade no.1 are applicable for the present case also.

A blade with shear centre being offset from centroid in one axis only is considered. This is the blade no.4 with $e_y = 1.0$ inch and $e_z = 0$. Two methods were used to compare the results; Carnegies (6) method and Williams' method, (not in reference 49). Comparison of results is better made by reference to Table 16. The drag bending mode frequencies are not presented as they were independent (uncoupled) modes, and the main interest is to study the coupling effects. Although all the flapping modes are coupled with torsional modes the amount of torsional coupling in the first three modes are negligible. The calculated frequencies up to 7th mode are presented, the fifth mode being predominantly torsional. The percentage errors are in the same order of blades nos. 1 and 3 and can be referred to in Table 16. The mode shapes up to fifth mode are presented in Figures 20-22. The fourth and fifth mode shapes show the torsional coupling which is considerable. The fifth mode is that of fourth mode type of flapping coupled with first mode type of torsional mode shapes. The percentage error of the fifth mode is only 1.32% which is rather low for the mode number. But it has to be appreciated that this frequency originally would have been the first torsional mode in its uncoupled form.

The blades nos. 5 and 6 have been considered to study the variations in frequencies due to offset shear centre from c.g in y and z directions. e_y and e_z values for blade no.5 being 0.1" and the same for blade no.6 being 1". The frequencies up to

fifth modes also of corresponding flap, drag and torsional modes in their original uncoupled forms) are presented in Table 17. The frequency values are virtually unchanged due to a very small offset considered in blade no.5, (comparing to blade no.1). On the examination of mode shapes although coupling is present, the coupling is negligible in smaller modes; in fact, only in the sixth mode any form of appreciable coupling has been noticed. The frequency values of blade no.6 show a slight variation. These changes are presented in Table 17. Once again only in the sixth mode any form of appreciable coupling has been noticed. Just to show the type of coupling the mode shape of this sixth mode is presented in Figure 23. (The earlier mode shapes were not presented due to the negligible coupling). This mode is of flapping-drag-torsional coupled form. The form of coupling is that of first mode type of torsion, third mode type of flap bending and fourth mode type of drag bending mode shapes. It can be concluded that the offset between shear centre and centroid introduces coupled form of frequencies any appreciable coupling being in the higher modes.

For a straight uniform rectangular blade, independent vibrations occur in flap and drag bending directions. With pretwist these vibrations couple together to give complex modes which are best identified by ascending order of frequency. To consider the effect of pretwist a set of blades is considered; blade nos.7 to 12 and 1. The pretwist angle range being 0^{o} to 90^{o} and the variations in pretwist angles were as follows: blade no.1 - 0^{o} pretwist, blade no.7 - 0.2 radian (11.46^{o}), blade no.8 - 0.4 radian (22.92^{o}), blade no.9 - 0.6 radian (34.38^{o}), blade no.10 - 0.8 radian (45.84^{o}), blade no.11 - 1 radian (57.30^{o}) and blade no.12 - 1.51 radian (90^{o}). The coupled mode frequencies computed for these cases are presented in Tables 18 and 19. Carnegies theoretical analysis (6) is used to calculate the first coupled mode frequencies for the above range of pretwist angles. Comparison of results is better made by reference to Table 18. Agreement between the computed results and the results obtained by Carnegies method is very good. The percentage errors being 0.062%, 0.121%, 0.092%, 0.151%, 0.238%, 0.353% and 0.852% for pretwist angles of 0^{o}, 11.46^{o}, 22.92^{o}, 34.38^{o}, 45.84^{o}, 57.30^{o} and 90^{o} respectively. The computed results of the higher coupled modes, up to fifth mode are presented in Table 19. The results are presented in graphical form (plotted to a base of pretwist angle) in Figure 24. It should be noted that the vertical frequency scale is discontinuous and in addition that its magnitude is adjusted to a suitable value in relation to the curve being considered, this procedure being adopted for convenience of present ation.

The first coupled mode is little affected by pretwist angle. With increase in pretwist angle, a small rise in frequency is apparent which is caused by coupling between the first flap bending mode frequency and first drag bending mode frequency. The amount of coupling increases with pretwist angle. Rosard (39) quoted a definition which states "if two vibrating systems having nearly equal natural frequencies are coupled together, the resulting system has one natural frequency below the low uncoupled frequency and one natural frequency above the higher uncoupled frequency". In pretwisted blade problem the vibrating systems considered are the second mode vibration in the drag bending plane and the first mode vibration in the flap bending plane. This is well understood in Figure 24; by the increasing values of first mode frequencies with the increase of pretwist angle, decreasing values of second mode frequencies with the increase of pretwist angle, increasing values of third mode frequencies with the increase of pretwist angle, decreasing values of fourth mode frequencies with the increase of pretwist angle and increasing values of fifth mode frequencies with the increase of pretwist angle. No attempt is made to present all the mode shapes for different pretwist angles as more numbers of pretwisted blades are analysed. However, the coupled mode shapes up to five modes are presented for a case of 1 radian (57.30^{o}) pretwist angle (blade no.11) in Figures 25-27.

The first coupled mode shape is of the combination of first flap bending mode shape type and the first drag bending mode shape type; the contribution of the flap bending displacement being more than the drag bending displacement. The second coupled mode shape is also of the combination of first flap bending displacement and first drag bending displacement, but in this case, drag bending displacement being more than flap bending displacement. The third coupled mode shape has two predominantly coupled second bending type mode shapes. The fourth coupled mode shape is a combination of the third flap bending type of mode shape and second drag bending type of mode shape. The fifth coupled mode shape consists of a combination of two second bending type of mode shapes. All these five coupled mode shapes for the case of 1 radian pretwist angle are presented in Figures 25-27. It has to be remarked that all the torsional and longitudinal frequencies are in uncoupled form as would be expected.

4.2 CASES WHERE NO COMPARATIVE RESULTS ARE PRESENTED

In the previous section most of the cases analysed have exact analytical results to compare. However, as the method is developed for a more general case the following blades were also considered:

(a) Pretwisted blade with shear centre offset from c.g. with 1 radian pretwist - blade no.13.

(b) Swept back blade, the tip element being swept at 90^{o} as prescribed in blade no.14.

(c) A special case with very large second moment of area about z axis and 1 radian pretwist angle - blade no.15.

(d) As above with 90^{o} pretwist angle - blade no.16 and

(e) A zig-zag blade as in Table 5, blade no.17.

For these cases, there are no comparative results, but it can be argued that as the method has been found acceptable, the results computed for the above cases should be in the same region of accuracy level. The coupled mode frequencies of blade no.13 are presented in Table 20 and the frequencies are compared to that of blade no.1 and blade no.12. In fact, very little change is noticed in the coupled mode frequencies compared to those of blade no.12. This is expected as the blade no.13 is the same as blade no.12 with a slight shear centre offset being introduced. ($e_y = e_z = 0.1$").

The mode shapes were also similar to those of blade no.12 with negligible torsional coupling and the mode shapes are, therefore, not presented. However, the torsional and longitudinal frequencies in their uncoupled form of blades nos. 1 and 12 are compared to the corresponding frequencies in Table 21. It can be stated that there are little changes in the frequency values due to such a small offset value although there are traces of coupling in the mode shapes.

A blade kinked as in the case of blade 14, could be diagramatically represented as in figure 5e and the disturbed position for the drag bending mode could be represented as in figure 5f (exaggerated representation). For this type of blade the drag bending would have a noticiable displacement in X direction also. The flapping displacements would lead to displacements in Z direction coupled with torsional displacements. The coupled values of frequencies are presented in Table 22. These frequencies are compared with the frequencies of blade 1. This can better be appreciated by reference to the mode shapes plotted in figures 28 - 30. The first mode shape is that of a combination of flap bending mode shape and torsional mode shape. The second mode shape is a combination of drag bending mode shape and longitudinal mode shape. The third mode shape is a combination of flap bending mode shape coupled with torsional mode shape. The abrupt change of direction of the tip member causes the kinks that can be observed in the above mode shape curves.The fourth mode

shape is a combination of flap bending mode shape and torsional mode shape with the kinking effect being present. The fifth coupling mode shape is that of drag bending mode shape coupled with longitudinal mode shape with the kinking effect predominantly present.

The results computed for blades nos. 15 and 16 are presented in Table 23 and these results are compared with those of blades nos. 11 and 12. It is obvious that the second moments of area in both cases are very high and naturally the blade will become stiffer and especially with pretwist being present higher values in frequencies will result. This has been found so as shown in Table 23.

The computed results of blade no.17(zig-zag blade) is presented in Table 24.The interesting fact of this blade is that displacements occur in X,Y,Z directions in addition to torsional displacements in all modes. The coupled mode shapes are presented in Figures 31-33. All five modes are coupled flap-drag-torsional-longitudinal type.However for the sake of clarity, where the relative displacements are very small that particular mode shape is not drawn.

Another interesting factor in the blades 14 & 17 is that there is slight variation in the additional torsional mode shapes which are associated with $\emptyset$ in Section 3.4. Hitherto, this additional torsional mode shape has been constantly the same as the torsional mode shapes. But owing to the change of direction in the centroidal axis although too small to be represented on the graphs, does slightly change this additional torsional mode shape. This has been represented as 'sweep torsion' in the computer print outs. This has justified the introduction of two torsional deformation parameters Θ and $\emptyset$ in Section 3.4.

4.3 CASES WHERE RESULTS BY DIFFERENT APPROACHES ARE KNOWN

Carnegie's (6) rectangular and aerofoil cross section blades and Montoya's (30) aerofoil cross section blades have been considered in this section. The rectangular blade considered has geometrical configuration as in Table 6 and is referred to as blade no.23. The computed natural mode frequency values of flap, drag, torsional and longitudinal modes up to fifth mode are presented in Tables 35 and 36. The exact corresponding analytical solutions are also presented in the above Tables for comparison. The following percentage errors have been noticed. First modes: flap bending 0.062%, drag bending 0.062%, torsional 0.206%, longitudinal 0.206%; second modes: flap bending 1.078%, drag bending 1.078%, torsional 1.874%, longitudinal 1.874%; third mode: flap bending 3.596%, drag bending 3.596%,

torsional 5.194%, longitudinal 5.194%. The percentage errors are in the increasing trend for fourth and fifth modes as can be noticed in Tables 35 and 36.

The percentage errors were in the same order for blade no.1. Once again, this indicates that the errors increase with increasing mode number.

The effect of pretwist angle on the above blade is analysed by considering the pretwist angle in the range of 0^{o} to 86^{o}. The blades considered are blades no. 23 to 28 with variations as follows: blade no.23 - 0^{o} pretwist, blade no.24 - 0.3 radian pretwist (17.19^{o}), blade no.25 - 0.6 radian (34.38^{o}) pretwist, blade no.26 - 0.9 radian (51.57^{o}) pretwist, blade no.27 - 1.2 radian (68.75^{o}) pretwist and blade no.28 - 1.5 radian (85.94^{o}) pretwist angle. The coupled mode frequencies computed for these cases are presented in Tables 37 and 38, and also the results of uncoupled torsional and longitudinal mode frequencies up to fifth mode for the same range of pretwist angle are presented in Tables 39 and 40. Comparison of results is better made by reference to Tables 37 and 38. Agreement between the computed results and the results obtained by Carnegie's method (6) for the first coupled mode frequencies is very good. The percentage errors being 0.0617%, 0.0592%, 0.108%, 0.198%, 0.357% and 0.539% for pretwist angles of 0^{o}, 17.19^{o}, 34.38^{o}, 51.57^{o}, 68.75^{o} and 85.94^{o} respectively.

The computed results of the higher coupled modes up to fifth mode are presented in Table 38. Carnegie's (6) practical results are also shown on both Tables 37 and 38. These results are also presented in graphical form in Figures 34 to 36. It is remarked that the vertical frequency scale is discontinuous and in addition that its magnitude is adjusted to a suitable value in relation to the curve being studied.

Reasonable agreement is shown between the two theoretical frequency curves and also between the Carnegie's experimental results and the present results for the first coupled mode. Since the theoretical frequencies are greater than experimental ones, it would appear that stiffnesses of the actual blades are less than the values used in calculations. Carnegie (6) argued that inclusion of rotary inertia and shear deformation would reduce the theoretical frequencies. Examination of frequency curves for the higher coupled modes clearly shows the influence of pretwist and its associated coupling between flap and drag bending modes. Apart from a change in frequency values of certain modes, for example, the second coupled mode frequencies suffer a considerable reduction in frequency with increase in pretwist, a frequency doubling occurs in the higher modes as would be expected of a coupled system. This is noticeable in Figure 35, for the third coupled mode frequencies.

As the doubling effect increases with the increasing number of modes, not all his practical results are presented here. An attempt is also made to justify this frequency doubling effect by approximately the third and fourth coupled mode frequencies obtained by the present analysis. by plotting imaginary doubling effect.

There is coupling, although not very appreciable, between torsional and longitudinal frequencies. This can better be appreciated from the Tables 39 and 40. It can be concluded that for rectangular blades the first coupled mode frequencies show a slight increase with the increase of pretwist angle and the higher coupled mode frequencies are affected considerably by pretwist and hence coupled flap and drag bending effects. No attempt is made to present mode shape curves for the cases in blade nos. 23 to 28 as the coupling effect will be obvious and are observed to be similar to the rectangular blades nos 7-12 considered in 4.1.

The aerofoil cross section blade considered for a uniform untwisted case has got geometrical parameters as referred to in blade no.45. The frequencies computed by the present method and by simple beam theory are presented in Tables 41 and 42. The flap bending, drag bending, torsional and longitudinal mode frequencies are uncoupled in this particular case as s.c is assumed to coincide with c.g as a special case and the pretwist is absent. The following errors are observed for flap bending and drag bending mode frequencies: first modes: 0.062%, second modes: 1.078%, third modes: 3.596%, fourth modes: 7.428% and fifth modes 12.149%. The effors for torsional and longitudinal modes are as follows: first modes: 0.206%, second modes: 1.857%, third modes: 5.194%, fourth modes 10.284% and fifth modes: 17.238%. Once again, this confirms that the method is readily acceptable for lower modes and the percentage errors increase with mode numbers. To consider the offset shear centre effect in the above blade another one, blade no. 37, is considered. The results obtained by computing are compared to those of blade no.45 in Table 43. The coupling is of flapping-drag-torsional type. The amount of torsional coupling on the flapping modes is negligible where as torsional-drag bending coupling is considerable as can be referred to in Table 43.

The following three groups of aerofoil cross section blades are considered for further analysis.

(a) pretwist effects on blade no.45 in the range 0^{o} to 90^{o}.

The blade numbers are blade 45 - 0^{o} pretwist angle, blade 46 - 15^{o} pretwist angle, blade 47 - 30^{o} pretwist angle, blade 48 - 45^{o} pretwist angle, blade 49 - 1 radian pretwist angle, blade 50 - 60^{o} pretwist angle, blade 51 - 75^{o} pretwist angle and blade 52 - 90^{o} pretwist angle.

(b) pretwist effects on blade no.37 in the range 0^{o} to 90^{o}; blades nos. 37 to 44, the pretwist angles being in the same steps of (a).

(c) pretwist effects on a special case of aerofoil blade including higher moments of area and shear centre offset from c.g; blades nos 29 to 36 the pretwist angles being in the same steps of (a).

The computed coupled mode frequencies up to fifth mode for the pretwist angles in the range of 0^{o} - 90^{o} for the above three cases are presented in Tables 44 to 48. Carnegie's practical results are also indicated in the above tables. These coupled forms of frequencies are referred to in graphical form in Figures 37 to 41.

Referring to Figure 37, the first coupled mode frequencies show a slight increase in frequency with the increase in pretwist angle for the cases (a) and (b). But inclusion of higher moments of area terms (B1, B2, B3) in the calculation, has a decreasing effect with the increase in pretwist angle. However, it is observed that the frequencies of these cases are closer to practical results of Carnegie. In any case, his theoretical results are closer to the results of cases (a) and (b). In all the three cases the coupling is of flap-drag-torsional type as is expected of pretwisted aerofoil cross section blades. Between the cases (a) and (b) the changes in frequency values are negligible. This shows that offset in shear centre has little effect on the first coupled modes and the increases in frequency values are mainly caused by the coupling due to pretwist.

Referring to Figure 38, the second coupled mode frequencies show a steady decline of frequencies with the increase of pretwist angle. This is applicable to all the three cases considered and the practical results of Carnegie. All the coupled frequencies are of flap-drag-torsional coupling form.

The third coupled mode frequencies represented in Figure 39 show a steady increase in frequency values with the increase in pretwist angle, this being so for all the three cases considered and Carnegie's practical results.

One interesting factor noticed in the fourth coupled mode frequencies referred to in Figure 40 is that the original torsional mode frequency for case (a) is unaffected by

the increase in pretwist angle. This behaviour is like that of a rectangular cross section. This is because e_y and e_z are zero for these cases and torsional coupling is, therefore, absent for all cases considered under this category. However, the cases considered in (b) and (c) show appreciable form of coupling, as did the practical results of Carnegie.

Referring to fifth coupled mode frequencies referred to in Figure 41, all theoretical results show a steady decline of frequency values with the increase in pretwist angle with the exception of practical results of Carnegie. However, he indicated frequency doubling at this coupled mode.

It is considered voluminous to present all the mode shapes of the cases of pretwist angles in (a), (b), and (c). However, the following selected coupled mode shapes curves are presented for reference:

(1) Five coupled mode shapes of case (a) with a pretwist angle of 1 radian.

(2) Five coupled mode shapes of case (b) with a pretwist angle of 1 radian.

(3) Five coupled mode shapes of case (c) with a pretwist angle of 1 radian.

(4) Five coupled mode shapes of case (c) with a pretwist angle of 30°.

(5) Five coupled mode shapes of case (c) with a pretwist angle of 45° and

(6) Five coupled mode shapes of case (c) with a pretwist angle of 90°.

It is remarked that in all the above cases the longitudinal mode frequencies are independent and the couplings are flap-drag-torsional type.

The first five mode shapes presented in Figures 42 to 44 refer to aerofoil blade with 1 radian pretwist with $e_y = e_z = 0$ and also B1 = B2 = B3 = 0. Hence the coupled mode shapes are flap bending-drag bending coupled type. An independent torsional mode shape is also present. The first coupled mode shape is a combination of two first mode shape types. (Flap bending and drag bending). The second coupled mode shape consists of a second flap bending type of mode shape coupled with a second drag bending type mode shape. The third mode shape is an uncoupled torsional mode shape. The fourth coupled mode is a combination of two second mode shape types. The fifth coupled mode shape consists of a third flap bending mode shape coupled with another third drag bending mode shape.

The first five modes presented in Figures 45 to 47, refer to aerofoil blade with one radian pretwist with offset shear centre effect included but with B1 = B2 = B3 = 0. All mode shapes are coupled flap bending - drag bending - torsional modes.

However, the torsional coupling on the first coupled mode shape is negligible. Third and fourth coupled mode shapes are predominantly torsion and on the fifth coupled mode shape the torsional coupling is not appreciable.

The first five modes presented in Figures 48 to 50, refer to aerofoil blade with one radian pretwist including the effects of B1, B2, B3, e_y and e_z. These mode shapes are similar to the previous case with a main difference that torsional coupling becomes more significant in all the coupled mode shapes. This is considered to be mainly due to the introduction of higher moments of area terms B1, B2, and B3 in the calculations.

The other fifteen mode shapes (first five modes for three different cases) are presented in Figures 51 to 59. The blades in question are the same as in the previous paragraph but with pretwist angles of 30^o, 45^o and 90^o. Although the coupling and types of mode number are similar to the previous case one significant thing noticed is that flap-drag-torsional coupling is stronger at higher modes especially at the fifth coupled modes.

A blade in reference (30) is found to be of some interest as the author of that work included higher order moment terms similar to B1, B2, B3 terms used in the present work, in his analysis. However, his definition of B1, B2 and B3 is slightly different from the present work. The blade has geometrical details as in Table 8. These values are extrapolated values to suit an eight element idealisation. This is referred to as blade no. 53 and the variations considered on this blade are as per blade nos. 54 and 55. Montoya (30) has presented first seven frequencies with variations considered as in blades 53, 54 and 55. The computed results of the above cases are presented in Tables 49, 51 and 52. The agreement is very good for the blade no. 55. This is mainly because there are no coupling terms included in calculations. The percentage errors in the other two cases show no real pattern (e.g. no increase or decrease with mode number), although they are in reasonable range except in two cases where the errors are found to be 23.77% and 24.78%. It can be argued that Montoya's treatment of the problem is different and his geometrical data are not used in exact form in the present work as they were modified to suit the present analysis. However, the frequencies obtained without any coupling terms by the present method compare very well with those of Montoya (Table 51).

Significance of higher order terms.

Although the inclusion of higher order terms B1,B2,B3 are considered in the previous section in a general sense, it is considered essencial to make some detailed observations of the importance of these terms. Referring to table 44 for example, the first coupled mode frequencies show an increase with the increase of pretwist angle for the cases where no coupling terms are introduced(case A).There is a very small effect on frequencies on introducing the s.c. off-set.(case B) There is considerable reduction in frequencies with the increase of pretwist angle for the cases where higher order terms are introduced.(case C) Similar effects are observed on higher mode frequencies also.

The higher order terms B1,B2,B3 are defined in equations 46-48. In the flexibility matrix these terms are associated with coefficents C1,C2 &C3 (equations 69-95); where $C1=B1\beta'/A$, $C2=(B3-e_z B1)\beta'/I_y$ and $C3=(B2-e_y B1)\beta'/I_z$ It should be appreciated that C1 is affected by variation in pretwist only(uniform cross section assumed). On the other hand C2 could be affected by the values of e_z, I_y and the pretwist angle. Similarly C3 could be affected by the values of e_y, I_z and pretwist angle. The values of C2 and C3 are extreemly sensitive to the values of I_y and I_z as they are very small in the present case(.00671&.0001). They are also sensitive to the s.c. off-set terms as they are multiplied by values of B1. Note that the values of B1 are much higher than those of B2 and B3.

A blade with 1 radin pretwist(blade 33 code JNI4) is chosen to consider the changes in C1,C2 and C3 for the following variations. a)B1=B2=B3=0 b)B1≠0,B2=B3=0 c)B1=0,B2≠0,B3=0 d)B1=B2=0,B3≠0 and e)B1,B2,B3≠0. The different values of C1,C2 and C3 are presented in Table 57. Considerable changes in the values of C1,C2 and C3 are obvious for different cases analysed. In order to show how the values of flexibility matrix are affected, the flexibility matrices associated with the above 5 cases are computed and presented in Tables 58-62. The frequencies upto 5 modes of the above cases are also presented in Table 63.

It is however observed that inclusion of B1 only in the case of rectangular blades had considerable effect on frequencies(blade 23) for increasing pretwist angles. This is because s.c values are zero for rectangular blades and also B2=B3=0. For the present cases the off-set s.c terms are coupled with higher order terms resulting in considerable changes in the flexibility matrix. All the foregoing considerations indicate that the incusion of B1,B2,B3 and s.c off-set terms could have considerable effect on the normal mode frequencies.

4.4 ROTATION CASES

A number of rotating cases of blades were also considered. Blades nos. 18 to 22 represent different speeds of rotation of the blade in Table 3. The speeds of rotation being 3 radians/sec, 6 radians/sec, 10 radians/sec, 15 radians/sec and 20 radians/sec for the blades nos. 18, 19, 20, 21 and 22 respectively. These cases were run by the present programme and by Williams' programme. The normal mode flap bending and drag bending frequencies up to fifth mode computed by both methods are presented in Tables 25-34.

The percentage differences of the first flap bending mode frequencies for different speeds of rotation are as follows: 3 radians - 0.227%, 6 radians - 0.38%, 10 radians - 0.512%, 15 radians - 0.57%, 20 radians - 0.56%. The percentage differences of the first drag bending modes for different speeds of rotation are as follows: 3 radians - 0.18%, 6 radians 0.48%, 10 radians - 1.11%, 15 radians - 2.28% and 20 radians - 3.81%. The agreement between these two methods are remarkably good for the first mode frequencies. Similar percentage differences, for the second flap bending modes are 0.598%, 0.32%, 0.19%, 0.156% and 0.17%; and for second drag bending mode frequencies are 1.0%, 0.83%, 0.625%, 0.45%,0.33%. The agreement between the two methods on second mode frequencies are also good.

The percentage differences on the third flap bending mode frequencies are 2.91%, 2.19%, 1.82%, 1.76% and 1.76% and the differences in the cases of drag bending mode frequencies are 3.51%, 3.28%, 2.91% 2.48% and 2.20%. The agreement in these cases could be considered as reasonable. The errors on the higher mode frequencies increases with the increase of mode number as can be referred to in Tables 25 to 34.

Once again, it can be concluded that Williams' results and the present results are in good agreement for the lower mode frequencies. Williams' results are better for higher modes also mainly because his method is a 25 element idealisation and also he has used sophisticated deflection curve patterns and bending of moments. However, the present method is in close agreement with those of Williams' results especially for lower modes. As the percentage errors caused by the present method for non-rotating cases are in the same region of errors by Williams' 10 element idealisation technique, it can be argued that a 25 element idealisation of the present method would result in the same sort of accuracy of Williams' for both rotating and non-rotating cases. In fact, improvement in accuracy has been shown, by increasing the number of elements to 20. (See Section 4.1).

The frequency variations on each mode due to different speeds are better understood from Figures 60 to 64. The analysis of mode shapes of all these cases would be voluminous. However, mode shapes of the first five modes of flap bending and the first five modes of drag bending for one rotation case are presented (3 radians/sec). These are in Figures 65 to 70. On all these mode shape curves, the mode shapes obtained by Williams 25 element idealisation are also indicated. It can be seen from Figures 65 to 70 the mode shapes of all the flap bending modes and drag bending modes are in very good agreement with those of Williams.

The mode shapes obtained for torsional and longitudinal modes are also presented, up to fifth mode in Figures 71 to 73.

Another known case of rotating blade is that of Montoya's (30) which is adopted for running by the present programme. Although he did not present the calculated results, the results of his work were read off from the graph (30) and compared with the present results. The blades used for these runs are referred to as blade nos. 56 to 61. The results obtained for the first mode frequencies for different rotation speeds are presented in Table 50. The results are also presented in Figure 74. From the above figure it can be seen that the present results are closer to Montoya's practical results than his theoretical results.

Another known case where computed frequency values and mode shapes are available, is that of Wilde (48). The blade parameters used in his blade were idealised into ten elements and run on the present programme. The results obtained are encouraging. His values of first and second mode frequencies of 3.183 and 8.781 compare well with the present values of 3.236 and 8.807. The bending mode shape presented by him compares very well with the mode shape obtained by the present method which can be referred to in Figure 75.

CONCLUSIONS

A discrete element method has been developed for the solution of normal mode frequencies and their mode shapes. The method is suitable for both rotating and non rotating blades having complexities such as pretwist, off-set shear centre from centroid, variable mass per unit length and abrupt changes in the centroidal axis. Various checks have been made for different cases with known standard analytical solutions and other investigator's results where available. The results obtained indicate that the method is stable and the accuracy to be good especially for lower modes.

The accuracy of the method decreases with the increase of mode number. On the other hand the accuracy of the method increases by increasing the number of elements. This has been established by computing the results using 20 element idealisation and comparing with those of 10 element idealisation, blade geometrical properties being the same in either case.

For rectangular cross section blades, the natural frequencies and mode shapes of vibration obtained by this method gives good agreement with those obtained by Williams' metod. Similar agreement is shown with the results of Carnegie's method. The displacements in flap, drag and longitudinal and torsion are independent for a uniform rectangular blade. When a blade is positioned at equal inclination to overall X,Y,Z directions (54.7°) the following displacement patterns have been observed. The flap bending displacements have components in global X,Y,Z directions and drag bending displacements have components in global X and Y directions. The displacements in the longitudinal mode have components in global X,Y,Z directions. However torsional displacements do not form any coupling. In the above cases the values of normal mode frequencies are not changed from the values of those laid in one axis. It can be concluded that the natural frequencies are independent of the position in which the blade is laid whereas the mode shapes are dependent on the position of the blade.

For a swept back bade (as in the case of bade 14 with 90° sweep back) the flapping displacements would lead to displacements in Z direction coupled with torsional displacements. The drag bending displacements would lead to displacements in Y direction coupled with longitudinal (X) displacements. A kink is noticeable on the mode shapes of this

blade which is predominent on the higher modes.

A zig-zag blade (blade 23) causes displacements in X,Y,Z directions in addition to torsion on all modes of frequencies. The mode shapes are very copmlex compared to those of normal mode shape curves. It is concluded that abrupt changes in the centroidal axis causes changes in the frequency values compared to those of straight blades and the torsional mode shapes in particular result in complexities.

For rectangular blades with pretwist being present, the flapping and drag mode frequencies couple together to give complex modes which are best identified by the ascending order of frequencies. The inclusion of the higher order term B1 (B2=B3=0) in a pretwisted rectangular blade calculation indicated an increasing trend of first mode frequency with the increase of pretwist angle.

For blades with off-set shear centre from centroid, e.g aerofoil cross section blade, the mode of vibration is that of coupled flap-drag-torsional type and the longitudinal mode is independent. However the coupling is appreciable only in the higher modes. For pretwisted aerofoil cross section blades the coupled modes are predominantly flap-drag-torsional type. Traces of longitudinal coupling are however observed on certain modes. The complex mode shapes are better identified in the ascending order of frequency.

The introduction of higher order terms B1,B2,B3 in the pretwisted aerofoil cross section blades results in significant changes in the flexibility matrix. Considerable changes to the frequency values and their mode shapes have been observed due to the inclusion of higher order terms. For example the first normal mode frequencies, show a decreasing trend with the increase of pretwist angle. This is mainly because the higher order terms coupled with off-set shear centre co-ordinates decrease the flexibility. Torsional coupling is more significant in all the coupled mode shapes for the cases when the higher order terms B1,B2 and B3 are introduced in the calculations. It is concluded that calculation of natural frequencies and mode shapes of vibration of asymmetrical beams neglecting higher order terms or with inaccurate values of shear centre co-ordinates could result in unacceptable values. Therefore due consideration must be given in establishing the higher order terms and the s.c position, during the design stage. It is concluded that natural mode frequencies and mode shapes can be calculated using this method at design stage.

6

FUTURE WORK

To improve the accuracy of the method a more sophesticated stress and deformation pattern could be introduced. For example in calculating the blade bending moment each discrete blade length could be assumed to be deflected into a circular arc. In evaluating the displacement of the blade at the ends of the discrete elements the blade bending moment in each short blade length could be assumed to vary cubically. The number of elements could be increased to increase the accuracy of the method.

The changes in steady state geometry, some times known as centrifugal untwisting moment, could affect the normal mode frequencies and the mode shapes. There may be sizable steady state deformation of the rotating blades. This could be studied in some detail as a pre-analysis package. The shear deformation and Coriolis' forces could be included in the theory to study their effect on normal mode frequencies and mode shapes.

The importance of the inclusion of the higher order terms could be analysed further to include accurate prediction of the values of the higher order terms and the shear centre location; and their sensitiveness to other terms they are coupled with. The present method could be extended to establish the bending moment distributions.

FLEXIBILITY MATRIX

TABLE 1

	P_{x1}	P_{x2}	M_{x1}	M_{x2}	M_{y1}	M_{y2}	M_{z1}	M_{z2}
P_{x1}	$\frac{L}{3EA} + \frac{C_1^2 L}{3GJ}$	$\frac{L}{6EA} + \frac{C_1^2 L}{6GJ}$	$\frac{C_1 L}{3GJ}$	$\frac{C_1 L}{6GJ}$	$\frac{C_1 C_2 L}{3GJ} - \frac{C_1 C_2 \beta^2 L}{60GJ}$ $- C_1 C_3 \beta L / 12GJ$	$\frac{C_1 C_2 L}{6GJ} - \frac{C_1 C_2 \beta^2 L}{40GJ}$ $-C_1 C_3 \beta L / 12GJ$	$\frac{C_1 C_2 \beta L}{12GJ} + \frac{C_1 C_3 L}{3GJ}$ $-C_1 C_3 \beta^2 L / 60GJ$	$\frac{C_1 C_2 \beta L}{12GJ} + \frac{C_1 C_3 L}{6GJ}$ $-C_1 C_3 \beta^2 L / 40GJ$
P_{x2}	$\frac{L}{6EA} + \frac{C_1^2 L}{6GJ}$	$\frac{L}{3EA} + \frac{C_1^2 L}{3GJ}$	$\frac{C_1 L}{6GJ}$	$\frac{C_1 L}{3GJ}$	$\frac{C_1 C_2 L}{6GJ} - \frac{C_1 C_2 \beta^2 L}{40GJ}$ $-C_1 C_3 \beta L / 12GJ$	$\frac{C_1 C_2 L}{3GJ} - \frac{C_1 C_2 \beta^2 L}{10GJ}$ $- C_1 C_3 \beta L / 4GJ$	$\frac{C_1 C_2 \beta L}{12GJ} + \frac{C_1 C_3 L}{6GJ}$ $- C_1 C_3 \beta^2 L / 40GJ$	$\frac{C_1 C_2 \beta L}{4GJ} + \frac{C_1 C_3 L}{3GJ}$ $- C_1 C_3 \beta^2 L / 10GJ$
M_{x1}	$\frac{C_1 L}{3GJ}$	$\frac{C_1 L}{6GJ}$	$\frac{L}{3GJ}$	$\frac{L}{6GJ}$	$\frac{C_2 L}{3GJ} - \frac{C_2 \beta^2 L}{60GJ} - \frac{C_3 \beta L}{12GJ}$	$\frac{C_2 L}{6GJ} - \frac{C_2 \beta^2 L}{40GJ} - \frac{C_3 \beta L}{12GJ}$	$\frac{C_2 \beta L}{12GJ} + \frac{C_3 L}{3GJ} - \frac{C_3 \beta^2 L}{60GJ}$	$\frac{C_2 \beta L}{12GJ} + \frac{C_3 L}{6GJ} - \frac{C_3 \beta^2 L}{40GJ}$
M_{x2}	$\frac{C_1 L}{6GJ}$	$\frac{C_1 L}{3GJ}$	$\frac{L}{6GJ}$	$\frac{L}{3GJ}$	$\frac{C_2 L}{6GJ} - \frac{C_2 \beta^2 L}{40GJ} - \frac{C_3 \beta L}{12GJ}$	$\frac{C_2 L}{3GJ} - \frac{C_2 \beta^2 L}{10GJ} - \frac{C_3 \beta L}{4GJ}$	$\frac{C_2 \beta L}{12GJ} + \frac{C_3 L}{6GJ} - \frac{C_3 \beta^2 L}{40GJ}$	$\frac{C_2 \beta L}{4GJ} + \frac{C_3 L}{3GJ} - \frac{C_3 \beta^2 L}{10GJ}$
M_{y1}	$\frac{C_1 C_2 L - C_1 C_2 \beta^2 L}{3GJ} - \frac{60GJ}{C_1 C_3 L}$ $-\frac{}{12GJ}$	$\frac{C_1 C_2 L}{6GJ} - \frac{C_1 C_2 \beta^2 L}{40GJ}$ $- C_1 C_3 \beta L / 12GJ$	$\frac{C_2 L}{3GJ} - \frac{C_2 \beta^2 L}{60GJ}$ $- C_3 \beta L / 12GJ$	$\frac{C_2 L}{6GJ} - \frac{C_2 \beta^2 L}{40GJ}$ $- C_3 \beta L / 12GJ$	$\frac{LC_2^2}{3GJ} - \frac{C_2^2 \beta^2 L}{30GJ} - \frac{C_3 C_2 \beta L}{6GJ}$ $+L + \frac{C_3^2 \beta^2 L}{30GJ} +$ $(\frac{1}{I_y} - \frac{1}{I_z}) \beta^2 L / 30E$	$\frac{LC_2^2}{6GJ} - \frac{C_2^2 \beta^2 L}{20GJ} - \frac{C_2 C_3 \beta L}{6GJ}$ $+L + \frac{C_3^2 \beta^2 L}{20GJ} +$ $(\frac{1}{I_z} - \frac{1}{I_y}) \beta^2 L / 20E$	$\frac{C_2^2 \beta L}{12GJ} - \frac{C_2^2 \beta L}{12GJ} + \frac{C_2 C_3 L}{3GJ}$ $- \frac{C_2 C_3 \beta^2 L}{15GJ} +$ $(\frac{1}{I_y} - \frac{1}{I_z}) \beta L / 12E$	$\frac{C_2^2 \beta L}{12GJ} - \frac{C_2^2 \beta L}{12GJ} + \frac{C_2 C_3 L}{6GJ}$ $- \frac{C_2 C_3 \beta^2 L}{10GJ} +$ $(\frac{1}{I_y} - \frac{1}{I_z}) \beta L / 12E$
M_{y2}	$\frac{C_1 C_2 L}{6GJ} - \frac{C_1 C_2 \beta^2 L}{40GJ}$ $-\frac{C_1 C_3 \beta L}{12GJ}$	$\frac{C_1 C_2 L}{3GJ} - \frac{C_1 C_2 \beta^2 L}{10GJ}$ $- \frac{C_1 C_3 \beta L}{4GJ}$	$\frac{C_2 L}{6GJ} - \frac{C_2 \beta^2 L}{40GJ}$ $- \frac{C_3 \beta L}{12GJ}$	$\frac{C_2 L}{3GJ} - \frac{C_2 \beta^2 L}{10GJ}$ $- \frac{C_3 \beta L}{4GJ}$	$\frac{LC_2^2}{6GJ} - \frac{C_2^2 \beta^2 L}{20GJ} - \frac{C_2 C_3 \beta L}{6GJ}$ $+ L + \frac{C_3^2 \beta L}{20GJ} +$ $(1/I_z - 1/I_y) \beta^2 L / 20E$	$\frac{LC_2^2}{3GJ} - \frac{C_2^2 \beta^2 L}{5GJ} - \frac{C_2 C_3 \beta L}{2GJ}$ $+ L + \frac{C_3^2 \beta^2 L}{5GJ} +$ $(1/I_z - 1/I_y) \beta^2 L / 5E$	$\frac{C_2^2 \beta L}{12GJ} - \frac{C_2^2 \beta L}{12GJ} + \frac{C_2 C_3 L}{6GJ}$ $- \frac{C_2 C_3 \beta^2 L}{10GJ} +$ $(1/I_y - 1/I_z) \beta L / 12E$	$\frac{C_2^2 \beta L}{4GJ} - \frac{C_2^2 \beta L}{4GJ} + \frac{C_2 C_3 L}{3GJ}$ $- \frac{C_2 C_3 \beta^2 L}{2.5GJ} +$ $(1/I_y - 1/I_z) \beta L / 4E$
M_{z1}	$\frac{C_1 C_2 \beta L}{12GJ} + \frac{C_1 C_3 L}{3GJ}$ $-\frac{C_1 C_3 \beta^2 L}{60GJ}$	$\frac{C_1 C_2 \beta L}{12GJ} + \frac{C_1 C_3 L}{6GJ}$ $- \frac{C_1 C_3 \beta^2 L}{40GJ}$	$\frac{C_2 \beta L}{12GJ} + \frac{C_3 L}{3GJ}$ $- \frac{C_3 \beta^2 L}{60GJ}$	$\frac{C_2 \beta L}{12GJ} + \frac{C_3 L}{6GJ}$ $- \frac{C_3 \beta^2 L}{40GJ}$	$\frac{C_2^2 \beta L}{12GJ} - \frac{C_2^2 \beta L}{12GJ} + \frac{C_2 C_3 L}{3GJ}$ $- \frac{C_2 C_3 \beta^2 L}{15GJ} +$ $(1/I_y - 1/I_z) \beta L / 12E$	$\frac{C_2^2 \beta L}{12GJ} - \frac{C_2^2 \beta L}{12GJ} + \frac{C_2 C_3 L}{6GJ}$ $- \frac{C_2 C_3 \beta^2 L}{10GJ} +$ $(1/I_y - 1/I_z) \beta L / 12E$	$\frac{C_2 C_3 \beta L}{6GJ} + \frac{C_2^2 \beta^2 L}{30GJ} + \frac{C_3^2 L}{3GJ}$ $- \frac{C_3^2 \beta^2 L}{30GJ} + L + \frac{}{3EI_z} +$ $(1/I_y - 1/I_z) \beta^2 L / 30E$	$\frac{C_2 C_3 \beta L}{6GJ} + \frac{C_2^2 \beta^2 L}{20GJ} + \frac{C_3^2 L}{6GJ}$ $- \frac{C_3^2 \beta^2 L}{20GJ} + L + \frac{}{6EI_z} +$ $(1/I_y - 1/I_z) \beta^2 L / 20E$
M_{z2}	$\frac{C_1 C_2 \beta L}{12GJ} + \frac{C_1 C_3 L}{6GJ}$ $-\frac{C_1 C_3 \beta^2 L}{40GJ}$	$\frac{C_1 C_2 \beta L}{4GJ} + \frac{C_1 C_3 L}{3GJ}$ $- \frac{C_1 C_3 \beta^2 L}{10GJ}$	$\frac{C_2 \beta L}{12GJ} + \frac{C_3 L}{6GJ}$ $- \frac{C_3 \beta^2 L}{40GJ}$	$\frac{C_2 \beta L}{4GJ} + \frac{C_3 L}{3GJ}$ $-\frac{C_3 \beta^2 L}{10GJ}$	$\frac{C_2^2 \beta L}{12GJ} - \frac{C_2^2 \beta L}{12GJ} + \frac{C_2 C_3 L}{6GJ}$ $- \frac{C_2 C_3 \beta^2 L}{10GJ} +$ $(1/I_y - 1/I_z) \beta L / 12E$	$\frac{C_2^2 \beta L}{4GJ} - \frac{C_2^2 \beta L}{4GJ} + \frac{C_2 C_3 L}{3GJ}$ $- \frac{C_2 C_3 \beta^2 L}{2.5GJ} +$ $(1/I_y - 1/I_z) \beta L / 4E$	$\frac{C_2 C_3 \beta L}{6GJ} + \frac{C_2^2 \beta^2 L}{6GJ} + \frac{C_3^2 L}{6GJ}$ $- \frac{C_3^2 \beta^2 L}{20GJ} + L + \frac{}{6EI_z} E$ $(1/I_y - 1/I_z) \beta^2 L / 20E$	$\frac{C_2 C_3 \beta L}{2GJ} + \frac{C_2^2 \beta^2 L}{5GJ} + \frac{C_3^2 L}{3GJ}$ $- \frac{C_3 \beta^2 L}{5GJ} + L + \frac{}{3EI_z} +$ $(1/I_y - 1/I_z) \beta^2 L / 5E$

FLEXIBILITY MATRIX TABLE 1

BLADE DESCRIPTIONS TABLE 2

Blade No	Blade Code in the Data File	Description Of Blade Details
1	KUMN	As in Table 3
2	SHRT	As in Table 4
3	SUND	As in Table 3 ; with E = 10×10^6 lbf/ in^2 and ρ = 18 lbf/ in ; (To consider variation in ρ)
4	SHER	As in Table 3 with changes; J = 3 in^4 & I_p = 2 lbs.sec^2 e_y = 1 in ; To consider s.c off-set in y axis
5	CESH	As in Table 3 ; with $e_y = e_z = 0.1"$
6	SHCE	As in Table 3 ; with $e_y = e_z = 1.0"$
7	PTO2	As in Table 3 ; with Pretwist angle 0.2 radian
8	PTO4	As in Table 3 ; with Pretwist angle 0.4 radian
9	PTO6	As in Table 3 ; with Pretwist angle 0.6 radian
10	PTO8	As in Table 3 ; with Pretwist angle 0.8 radian
11	PTC2	As in Table 3 ; with Pretwist angle 1.0 radian
12	PTC1	As in Table 3 ; with Pretwist angle 1.5708(90^0) radian
13	PTCS	As in Table 3 ; with 1 radian pretwist& $e_y=e_z=0.1"$
14	KUSP	As in Table 3 ; with a sweep back of 90^0 of 1st element
15	HIIZ	As in Blade 11 with IZ=10000 (To consider the effect of large second moment of area)
16	HINZ	As in Blade 12 with IZ=10000 (To consider the effect of large second moment of area)
17	KINK	As in Table 5
18	RTO3	As in Table 3 with speed of rotation =3 radians/sec
19	RTO6	As in Table 3 with speed of rotation =6 radians/sec
20	RT10	As in Table 3 with speed of rotation =10 radians/sec
21	RT15	As in Table 3 with speed of rotation =15 radians/sec
22	RT20	As in Table 3 with speed of rotation =20 radians/sec
23	TAMO	As in Table 6
24	TAM1	AS in Table 6 with Pretwist angle 0.3 radian
25	TAM2	As in Table 6 with Pretwist angle 0.6 radian
26	TAM3	As in Table 6 with Pretwist angle 0.9 radian
27	TAM4	As in Table 6 with Pretwist angle 1.2 radians
28	TAM5	As in Table 6 with Pretwist angle 1.5 radians
29	JNIO	As in Table 7
30	JNI1	As in Table 7 with Pretwist angle of 15^0

Contd.

Table 2 Continued

Blade No	Blade Code in the Data File	Description Of Blade Details
31	JNI2	As in Table 7 with a Pretwist angle of 30°
32	JNI3	As in Table 7 with a Pretwist angle of 45°
33	JNI4	As in Table 7 with a Pretwist angle of 57.30°(1 radian)
34	JNI5	As in Table 7 with a Pretwist angle of 60°
35	JNI6	As in Table 7 with a Pretwist angle of 75°
36	JNI7	As in Table 7 with a Pretwist angle of 90°
37	JNTO	As in Table 7 with B1 =B2 =B3 =0
38	JNT1	As in Blade 37 with a Pretwist angle 15°
39	JNT2	As in Blade 37 with a Pretwist angle 30°
40	JNT3	As in Blade 37 with a Pretwist angle 45°
41	JNT4	As in Blade 37 with a Pretwist angle 57.30°(1 radian)
42	JNT5	As in Blade 37 with a Pretwist angle 60°
43	JNT6	As in Blade 37 with a Pretwist angle 75°
44	JNT7	As in Blade 37 with a Pretwist angle 90°
45	CAMO	As in Table 7 with $e_y = e_z$ = B1 = B2 = B3 = 0
46	CAM1	As in Blade 45 with a Pretwist angle 15°
47	CAM2	As in Blade 45 with a Pretwist angle 30°
48	CAM3	As in Blade 45 with a Pretwist angle 45°
49	CAM4	As in Blade 45 with a Pretwist angle 57.3°(1 radian)
50	CAM5	As in Blade 45 with a Pretwist angle 60°
51	CAM6	As in Blade 45 with a Pretwist angle 75°
52	CAM7	As in Blade 45 with a Pretwist angle 90°
53	MON5	As in Table 8
54	MON1	As in Table 8 with a pretwist angle of 1.121 radians
55	MON4	As Blade 54 with $e_y = e_z$ = B1 = B2 = B3 = 0
56	SUB1	As in Table 8; e_y=e_z=B1=B2=B3=0;Rotation 0 r.p.m
57	SUB4	As in Table 8; e_y=e_z=B1=B2=B3=0;Rotation 1000 r.p.m
58	SUB5	As in Table 8; e_y=e_z=B1=B2=B3=0;Rotation 1500 r.p.m
59	SUB6	As in Table 8; e_y=e_z=B1=B2=B3=0;Rotation 2000 r.p.m
60	SUB7	As in Table 8; e_y=e_z=B1=B2=B3=0;Rotation 2500 r.p.m
61	SUB2	As in Table 8; e_y=e_z=B1=B2=B3=0;Rotation 3000 r.p.m
62	EWDE	As in Table 9 and Speed of rotation = 20 radians/sec

BLADE DESCRIPTIONS

TABLE 2

Description of the parameter	ELEMENT NUMBERS									
	1	2	3	4	5	6	7	8	9	10
A :Area :in^2	10	10	10	10	10	10	10	10	10	10
I_y :2nd moment of area about y axis:in^4	1	1	1	1	1	1	1	1	1	1
I_z :2nd moment of area about z axis:in^4	10	10	10	10	10	10	10	10	10	10
J :Torsional stiffness :in^4	10	10	10	10	10	10	10	10	10	10
e_y :Off-set between c.s&c.g :in	0	0	0	0	0	0	0	0	0	0
e_z :Off-set between c.s&c.g :in	0	0	0	0	0	0	0	0	0	0
B1 :Higher moment 1 :in^4	0	0	0	0	0	0	0	0	0	0
B2 :Higher moment 2 :in^5	0	0	0	0	0	0	0	0	0	0
B3 :Higher moment 3 :in^5	0	0	0	0	0	0	0	0	0	0
ρ :Mass per unit length lbf/in	1	1	1	1	1	1	1	1	1	1
I_p :Pitching inertia lbs sec^2/in	10	10	10	10	10	10	10	10	10	10
X :X Co-ordinate of c.g :in	100	90	80	70	60	50	40	30	20	10
Y :Y Co-ordinate of c.g :in	0	0	0	0	0	0	0	0	0	0
Z :Z Co-ordinate of c.g :in	0	0	0	0	0	0	0	0	0	0

E :Young's Modulus 11×10^6 lbf/in^2

G :Rigidity Modulus 5×10^6 lbf/in^2

L :Length 100 in

β :Pretwist angle -tip to root 0 radian

Short title of the blade:Uniform rectangular blade laid in X axis

Blade code :KUMN

BLADE PARAMETERS OF BLADE No 1

TABLE 3

Description of the parameter	ELEMENT NUMBERS 1	2	3	4	5	6	7	8	9	10
A :Area :in^2	10	10	10	10	10	10	10	10	10	10
I_y :2nd moment of area about y axis:in^4	1	1	1	1	1	1	1	1	1	1
I_z :2nd moment of area about z axis:in^4	10	10	10	10	10	10	10	10	10	10
J :Torsional stiffness :in^4	10	10	10	10	10	10	10	10	10	10
e_y :Off-set between c.s&c.g :in	0	0	0	0	0	0	0	0	0	0
e_z :Off-set between c.s&c.g :in	0	0	0	0	0	0	0	0	0	0
B1 :Higher moment 1 :in^4	0	0	0	0	0	0	0	0	0	0
B2 :Higher moment 2 :in^5	0	0	0	0	0	0	0	0	0	0
B3 :Higher moment 3 :in^5	0	0	0	0	0	0	0	0	0	0
ρ :Mass per unit length lbf/in	1	1	1	1	1	1	1	1	1	1
I_p :Pitching inertia lbs sec^2/in	10	10	10	10	10	10	10	10	10	10
X :X CO-Ordinate of c.g :in	57.735	51.962	46.188	40.415	34.641	28.868	23.094	17.321	11.547	5.774
Y :Y Co-ordinate of c.g :in	57.735	51.962	46.188	40.415	34.641	28.868	23.094	17.321	11.547	5.774
Z :Z Co-ordinate of c.g :in	57.735	51.962	46.188	40.415	34.641	28.868	23.094	17.321	11.547	5.774

E :Young's Modulus 11×10^6 lbf/in^2

G :Rigidity Modulus 5×10^6 lbf/in^2

L :Length 100 in

β :Pretwist angle-tip to root 0 radian

Short title of the blade:Blade 1 laid in 54.7356° to all three axes, but equivalent length of each element=10"

Blade code :SHRT

BLADE PARAMETERS OF BLADE No 2

TABLE 4

Description of the parameter	ELEMENT NUMBERS									
	1	2	3	4	5	6	7	8	9	10
A :Area :in^2	10	10	10	10	10	10	10	10	10	10
I_y :2nd moment of area about y axis:in^4	1	1	1	1	1	1	1	1	1	1
I_z :2nd moment of area about z axis:in^4	10	10	10	10	10	10	10	10	10	10
J :Torsional stiffness :in^4	10	10	10	10	10	10	10	10	10	10
e_y :Off-set between c.s&c.g :in	0	0	0	0	0	0	0	0	0	0
e_z :Off-set between c.s&c.g :in	0	0	0	0	0	0	0	0	0	0
B1 :Higher moment 1 :in^4	0	0	0	0	0	0	0	0	0	0
B2 :Higher moment 2 :in^5	0	0	0	0	0	0	0	0	0	0
B3 :Higher moment 3 :in^5	0	0	0	0	0	0	0	0	0	0
ρ :Mass per unit length lbf/in	1	1	1	1	1	1	1	1	1	1
I_p :Pitching inertia lbs sec^2/in	10	10	10	10	10	10	10	10	10	10
X :X Co-ordinate of c.g :in	100	90	80	70	60	50	40	30	20	10
Y :Y Co-ordinate of c.g :in	0	10	0	10	0	10	0	10	0	10
Z :Z Co-ordinate of c.g :in	0	0	10	0	10	0	10	0	10	0

E :Young's Modulus 11×10^6 lbf/in^2

G :Rigidity Modulus 5×10^6 lbf/in^2

L :Length 166.84

β :Pretwist angle-tip to root 0 radian

Short title of the blade:Zig-zag Blade

Blade code :KINK

BLADE PARAMETERS OF BLADE No 17

TABLE 5

Description of the parameter		ELEMENT NUMBERS									
		1	2	3	4	5	6	7	8	9	10
A :Area	:in^2	0.068	0.068	0.068	0.068	0.068	0.068	0.068	0.068	0.068	0.068
I_y :2nd moment of area about y axis	:$in^4 x10^{-4}$	0.262	0.262	0.262	0.262	0.262	0.262	0.262	0.262	0.262	0.262
I_z :2nd moment of area about z axis	:$in^4 x10^{-2}$	0.5667	0.5667	0.5667	0.5667	0.5667	0.5667	0.5667	0.5667	0.5667	0.5667
J :Torsional stiffness	:$in^4 x10^{-3}$	0.1048	0.1048	0.1048	0.1048	0.1048	0.1048	0.1048	0.1048	0.1048	0.1048
e_y :Off-set between c.s&c.g	:in	0	0	0	0	0	0	0	0	0	0
e_z :Off-set between c.s&c.g	:in	0	0	0	0	0	0	0	0	0	0
B1 :Higher moment 1	:$in^4 x10^{-2}$	0.5693	0.5693	0.5693	0.5693	0.5693	0.5693	0.5693	0.5693	0.5693	0.5693
B2 :Higher moment 2	:in^5	0	0	0	0	0	0	0	0	0	0
B3 :Higher moment 3	:in^5	0	0	0	0	0	0	0	0	0	0
ρ :Mass per unit length (10^{-4})	lbf/in	0.4998	0.4998	0.4998	0.4998	0.4998	0.4998	0.4998	0.4998	0.4998	0.4998
I_p :Pitching inertia	lbs sec^2/ $in x10^{-5}$	0.4184	0.4184	0.4184	0.4184	0.4184	0.4184	0.4184	0.4184	0.4184	0.4184
X :X Co-ordinate of c.g	:in	6	5.4	4.8	4.2	3.6	3	2.4	1.8	1.2	0.6
Y :Y Co-ordinate of c.g	:in	0	0	0	0	0	0	0	0	0	0
Z :Z Co-ordinate of c.g	:in	0	0	0	0	0	0	0	0	0	0

E :Young's Modulus $30x10^6$ lbf/in^2

G :Rigidity Modulus $11.54 x10^6$ lbf/in^2

L :Length 6 in

β :Pretwist angle-tip to root 0 radian

Short title of the blade:Carnegie's rectangular Blade without pretwist

Blade code :TAMO

BLADE PARAMETERS OF BLADE No 23

TABLE 6

Description of the parameter		ELEMENT NUMBERS									
		1	2	3	4	5	6	7	8	9	10
A :Area	:in^2	0.0914	0.0914	0.0914	0.0914	0.0914	0.0914	0.0914	0.0914	0.0914	0.0914
I_y :2nd moment of area about y axis	:$in^4 x10^{-3}$	0.1	0.1	0.1	0.1	0.1	0.1	0.1	0.1	0.1	0.1
I_z :2nd moment of area about z axis	:$in^4 x10^{-2}$	0.671	0.671	0.671	0.671	0.671	0.671	0.671	0.671	0.671	0.671
J :Torsional stiffness	:$in^4 x10^{-3}$	0.2708	0.2708	0.2708	0.2708	0.2708	0.2708	0.2708	0.2708	0.2708	0.2708
e_y :Off-set between c.s&c.g	:in	0.007	0.007	0.007	0.007	0.007	0.007	0.007	0.007	0.007	0.007
e_z :Off-set between c.s&c.g	:in	0.0469	0.0469	0.0469	0.0469	0.0469	0.0469	0.0469	0.0469	0.0469	0.0469
B1 :Higher moment 1	:$in^4 x10^{-2}$	0.681	0.681	0.681	0.681	0.681	0.681	0.681	0.681	0.681	0.681
B2 :Higher moment 2	:$in^5 x10^{-4}$	0.106	0.106	0.106	0.106	0.106	0.106	0.106	0.106	0.106	0.106
B3 :Higher moment 3	:$in^5 x10^{-3}$	0.2	0.2	0.2	0.2	0.2	0.2	0.2	0.2	0.2	0.2
ρ :Mass per unit length ($x10^{-4}$)	lbf/in	0.6718	0.6718	0.6718	0.6718	0.6718	0.6718	0.6718	0.6718	0.6718	0.6718
I_p :Pitching inertia	lbs $sec^2/in x10^{-5}$	0.5005	0.5005	0.5005	0.5005	0.5005	0.5005	0.5005	0.5005	0.5005	0.5005
X :X Co-ordinate of c.g	:in	6	5.4	4.8	4.2	3.6	3.0	2.4	1.8	1.2	0.6
Y :Y Co-ordinate of c.g	:in	0	0	0	0	0	0	0	0	0	0
Z :Z Co-ordinate of c.g	:in	0	0	0	0	0	0	0	0	0	0

E :Young's Modulus 31×10^6 lbf/in^2

G :Rigidity Modulus 12×10^6 lbf/in^2

L :Length 6 in

β :Pretwist angle-tip to root 0 radian

Short title of the blade:Carnegie's aerofoil cross section blade without pretwist

Blade code :JNIO

BLADE PARAMETERS OF BLADE No 29

TABLE 7

Description of the parameter	ELEMENT NUMBERS 1	2	3	4	5	6	7	8		
A :Area :cm^2	4.64	5.451	6.451	7.854	10.26	14.16	19.24	25.19		
I_y :2nd moment of area about y axis:cm^4	0.199	0.5907	1.526	3.4	7.047	13.79	24.79	39.87		
I_z :2nd moment of area about z axis:cm^4	36.1	41.37	50.17	65.11	93.99	151.1	244.2	385.1		
J :Torsional stiffness :cm^4	0.3886	0.6511	1.02	1.694	3.263	6.573	13.04	23.98		
e_y :Off-set between c.s&c.g :cm	0.7206	0.7702	0.7447	0.6155	0.4715	0.3971	0.2382	0.0152		
e_z :off-set between c.s&c.g :cm	0.1847	0.3787	0.6449	0.8924	1.170	1.395	1.566	1.766		
B1 :Higher moment 1 :cm^4	36.2	41.96	51.7	68.5	101	164.9	268.9	424.9		
B2 :Higher moment 2 :cm^5	39.7	54.9	75.02	106.1	152.6	225.4	333.1	510.5		
B3 :Higher moment 3 :cm^5	13.7	21.9	34.4	57.6	95.1	143.2	166.3	153.1		
ρ :Mass per unit length kgf/cm $x10^{-4}$	0.37	0.43	0.51	0.62	0.81	1.1	1.5	2.0		
I_p :Pitching inertia kg sec^2/cm $x10^{-3}$	0.29	0.33	0.41	0.54	0.8	1.3	2.1	3.4		
X :X Co-ordinate of c.g :cm	71.68	62.72	53.76	44.8	35.84	26.88	17.92	8.96		
Y :Y Co-ordinate of c.g :cm	0	0	0	0	0	0	0	0		
Z :Z Co-ordinate of c.g :cm	0	0	0	0	0	0	0	0		

E :Young's Modulus 2050000 kgf/cm^2

G :Rigidity Modulus 800000 kgf/cm^2

L :Length 71.68 cm

β :Pretwist angle-tip to root 0 radian

Short title of the blade:Brown Boveri Blade

Blade code :MON5

BLADE PARAMETERS OF BLADE No 53

TABLE 8

Description of the parameter		ELEMENT NUMBERS									
		1	2	3	4	5	6	7	8	9	10
A :Area	:in^2	7.56	7.56	7.56	7.56	7.56	7.56	7.56	7.56	7.56	7.56
I_y :2nd moment of area about y axis	:in^4	1	1	1	1	1	1	1	1	1	1
I_z :2nd moment of area about z axis	:in^4	22.68	22.68	22.68	22.68	22.68	22.68	22.68	22.68	22.68	22.68
J :Torsional stiffness	:in^4	4	4	4	4	4	4	4	4	4	4
e_y :Off-set between c.s&c.g	:in	0	0	0	0	0	0	0	0	0	0
e_z :Off-set between c.s&c.g	:in	0	0	0	0	0	0	0	0	0	0
B1 :Higher moment 1	:in^4	0	0	0	0	0	0	0	0	0	0
B2 :Higher moment 2	:in^5	0	0	0	0	0	0	0	0	0	0
B3 :Higher moment 3	:in^5	0	0	0	0	0	0	0	0	0	0
ρ :Mass per unit length ($x10^{-2}$)	lbf/in	0.667	0.667	0.667	0.667	0.667	0.667	0.667	0.667	0.667	0.667
I_p :Pitching inertia	lbs sec^2/ in	0.159	0.159	0.159	0.159	0.159	0.159	0.159	0.159	0.159	0.159
X : X Co-ordinate of c.g	:in	300	270	240	210	180	150	120	90	60	30
Y :Y Co-ordinate of c.g	:in	0	0	0	0	0	0	0	0	0	0
Z :Z Co-ordinate of c.g	:in	0	0	0	0	0	0	0	0	0	0

E :Young's Modulus 10×10^6 lbf/in^2

G :Rigidity Modulus 4×10^6 lbf/in^2

L :Length 300 in

β :Pretwist angle-tip to root 0 radian

Short title of the blade: Wilde's blade laid in X axis

Blade code :EWDE

BLADE PARAMETERS OF BLADE No 62

TABLE 9

Flapping Mode Frequencies	Frequencies In Hz		% Difference
	Solution By Present Analysis	Exact Analyt- ical Solution	Compared To Present Analysis
First Mode	0.185460	0.185575	0.054
Second Mode	1.175735	1.163061	1.075
Third Mode	3.378427	3.256932	3.596
Fourth Mode	6.894546	6.382427	7.427
Fifth Mode	12.008414	10.549476	12.150

FLAPPING MODE FREQUENCIES OF UNIFORM RECTANGULAR BLADE

BLADE CODE : KUMN

TABLE 10

Drag Mode Frequencies	Frequencies In Hz		% Difference
	Solution By Present Analysis	Exact Analyt- ical Solution	Compared To Present Analysis
First Mode	0.586477	0.586839	0.075
Second Mode	3.718002	3.677922	1.079
Third Mode	10.683523	10.299324	3.596
Fourth Mode	21.802470	20.183005	7.428
Fifth Mode	37.973938	33.360371	12.149

DRAG MODE FREQUENCIES OF UNIFIRM RECTANGULAR BLADE

BLADE CODE : KUMN

TABLE 11

Torsional Mode Frequencies	Frequencies In Hz		% Difference
	Solution By Present Analysis	Exact Analytical Solution	Compared To Present Analysis
First Mode	5.601691	5.590169	0.205
Second Mode	17.087902	16.770506	1.857
Third Mode	29.482156	27.950843	5.194
Fourth Mode	43.616851	39.131180	10.284
Fifth Mode	60.790329	50.311517	17.238

TORSIONAL MODE FREQUENCIES OF UNIFORM RECTANGULAR BLADE

BLADE CODE : KUMN

TABLE 12

Longitudinal Mode Frequencies	Frequencies In Hz		% Difference
	Solution By Present Analysis	Exact Analytical Solution	Compared To Present Analysis
First Mode	26.274261	26.220214	0.206
Second Mode	80.149376	78.660643	1.857
Third Mode	138.283434	131.101072	5.194
Fourth Mode	204.580318	183.541501	10.284
Fifth Mode	285.131312	235.981930	17.237

LONGITUDINAL MODE FREQUENCIES OF UNIFORM RECTANGULAR BLADE

BLADE CODE : KUMN

TABLE 13

Frequency In Hz (KUMN)	Type Of Mode (KUMN)	Frequency In Hz (SHRT)	Type Of Displacement (SHRT)
0.185460	Flap	0.185460	X,Y,Z
0.586477	Drag	0.586477	X,Y
1.175735	Flap	1.175735	X,Y,Z
3.378427	Flap	3.378426	X,Y,Z
3.718002	Drag	3.718002	X,Y
5.601691	Torsion	5.601691	Torsion
6.894546	Flap	6.894546	X,Y,Z
10.683523	Drag	10.683523	X,Y
12.008414	Flap	12.008414	X,Y,Z
17.087902	Torsion	17.087901	Torsion
19.035802	Flap	19.035804	X,Y,Z
21.802470	Drag	21.802468	X,Y
26.274261	Longitudinal	26.274259	X,Y,Z

CHANGES IN MODE SHAPES WHEN A BLADE IS ARRANGED TO LAY IN
(a) X AXIS AND
(b) 54.736° INCLINATION IN X,Y,Z DIRECTIONS
BLADE CODES : KUMN,SHRT
NOTE : No Change in frequency values

TABLE 14

Type Of Normal Mode	Frequencies In Hz Solution by Present Analysis	Solution by Analytical Method	% Difference Compared To Present Results	Freqencies In Hz Solution by Williams Method	% Difference Compared To Present Results
I Flapping	0.041679	0.041705	0.062	0.041666	0.024
II Flapping	0.264227	0.261375	1.078	0.260712	1.328
III Flapping	0.759245	0.731941	3.596	0.728834	4.005
IV Flapping	1.549434	1.434344	7.428	1.425836	7.979
V Flapping	2.698690	2.370818	12.149	2.353009	12.917
I Drag	0.131801	0.131882	0.061		
II Drag	0.835559	0.826552	1.078		
III Drag	2.400943	2.314601	3.596	-	-
IV Drag	4.899741	4.535793	7.428		
V Drag	8.534008	7.497186	12.149		
I Torsional	5.601691	5.590169	0.206		
II Torsional	17.087902	16.770506	1.857		
III Torsional	29.482069	27.950843	5.194	-	-
IV Torsional	43.616873	39.131180	10.284		
V Torsional	60.791035	50.311517	17.239		
I Longitudinal	5.904701	5.892555	0.206		
II Longitudinal	18.012231	17.677665	1.857		
III Longitudinal	31.076932	29.462775	5.194	-	-
IV Longitudinal	45.976102	41.247885	10.284		
V Longitudinal	64.078610	53.032995	17.238		

COMPARISION OF NORMAL MODE FREQUENCIES OF A KNOWN CASE WHERE $\rho = 18$

BLADE CODE : SUND

TABLE 15

Coupled Frequencies	Solution By Present Analysis Frequencies In Hz	Solution By Williams Method Frequencies In Hz	% Difference Compared To Present Results	Solution By Carnegie's Principle Frequencies In Hz	% Difference Compared To Present Results
First Mode	0.185429	0.19	2.481	0.186313	0.485
Second Mode	1.174325	1.18	0.485	1.167690	0.562
Third Mode	3.368637	3.31	1.751	3.269814	2.933
Fourth Mode	6.766925	6.49	4.092	6.407828	5.307
Fifth Mode	6.961976	6.87	1.320	6.846532	1.658
Sixth Mode	11.913319	10.71	10.100	10.593137	11.081
Seventh Mode	18.821202	15.63	16.955	15.825130	15.919

COMARISION OF COUPLED MODE FREQUENCIES OF A BLADE WITH OFF-SET S.C IN y DIRECTION ONLY

BLADE CODE : SHER

TABLE 16

Type Of Mode Of Case (A)	Straight Blade without s.c Off-set Frequencies in Hz (A)	Blade With s.c Off-set $e_y=e_z=0.1$ Frequencies in Hz (B)	Blade With s.c Off-set $e_y=e_z=1.0$ Frequencies in Hz (C)	% Variation in Frequencies Between Blades (B) and (C)
I Flapping	0.185460	0.185460	0.185451	0.000
II Flapping	1.175735	1.175731	1.175308	0.034
III Flapping	3.378427	3.378396	3.375370	0.089
IV Flapping	6.894546	6.894462	6.886086	0.198
V Flapping	12.008414	12.008107	11.977887	0.253
I Drag	0.586477	0.586474	0.586176	0.051
II Drag	3.718002	3.717819	3.699946	0.484
III Drag	10.683523	10.682425	10.576465	1.002
IV Drag	21.802470	21.797668	21.355360	2.071
V Drag	37.973938	37.954336	36.430780	4.182
I Torsion	5.601691	5.601867	5.619026	0.305
II Torsion	17.087902	17.089012	17.195441	0.619
III Torsion	29.482156	29.487066	29.935143	1.497
IV Torsion	43.616851	43.635536	45.076699	3.197
V Torsion	60.790329	61.032468	64.992217	6.093

EFFECT OF VARIATION IN OFF-SET S.C ON FREQUENCIES

BLADE CODES : KUMN :NO OFF-SET (A)

: CESH :$e_y = e_z$=0.1 (B)

: SHCE :$e_y = e_z$=1.0 (C)

TABLE 17

Pretwist Angle In Degrees	Frequencies In Hz		% Difference Compared To Present Results
	Solution By Present Analysis	Solution By Carnegie's Method	
0.00	0.185460	0.185575	0.062
11.46	0.185542	0.185766	0.121
22.92	0.185786	0.185957	0.092
34.38	0.186192	0.186474	0.151
45.84	0.186755	0.187200	0.238
57.30	0.187473	0.188134	0.353
90.00	0.190318	0.191940	0.852

FIRST COUPLED MODE FREQUENCIES DUE TO PRETWIST:RECTANGULAR CROSS SECTION
BLADE CODES : KUMN,PTO2,PTO4,PTO6,PTO8,
PTC2,PTC1

TABLE 18

Pretwist Angle	Frequencies In Hz			
	2nd Coupled Mode	3rd Coupled Mode	4th Coupled Mode	5th Coupled Mode
0.00	0.586477	1.175735	3.378427	3.718002
11.46	0.583202	1.182368	3.309239	3.794287
22.92	0.573871	1.201685	3.177293	3.947341
34.38	0.559739	1.232172	3.036037	4.123167
45.84	0.542352	1.271866	2.897665	4.308650
57.30	0.523144	1.318771	2.765683	4.498967
90.00	0.467130	1.476792	2.433323	5.039600

II,III,IV,V COUPLED MODE FREQUENCIES DUE TO PRETWIST
RECTANGULAR CROSS SECTION BLADES
BLADE CODES : KUMN,PTO2,PTO4,PTO6,PTO8,
PTC2,PTC1

TABLE 19

Frequencies In Hz $\beta=0, e_y=e_z=0$ (A)	Frequencies In Hz $\beta=1, e_y=e_z=0$ (B)	Frequencies In Hz $\beta=1, e_y=e_z=0.1$ (C)
0.185460	0.187473	0.187473
0.586477	0.523144	0.523142
1.175735	1.318771	1.318757
3.378427	2.765683	2.765663
3.718002	4.498967	4.498706
6.894546	6.457741	6.457678
10.683523	11.226743	11.225750
12.008414	11.617026	11.616636
19.035802	18.633475	18.632824
21.802470	22.185948	22.181766

COMPARISION OF UNCOUPLED AND COUPLED FREQUENCIES

(A) STRAIGHT RECTANGULAR BLADE :UNCOUPLED : BLADE CODE : KUMN

(B) 1 RADIAN PRETWIST. NO S.C OFF-SET : BLADE CODE : PTC2

(C) 1 RADIAN PRETWIST. S.C OFF-SET INCLUDED : BLADE CODE : PTCS

NOTE : (B) AND (C) COUPLED FLAPPING AND DRAG

TABLE 20

Frequencies In Hz $\beta=0, e_y=e_z=0$ (A)	Frequencies In Hz $\beta=1, e_y=e_z=0$ (B)	Frequencies In Hz $\beta=1, e_y=e_z=0.1$ (C)	
5.601691	5.601691	5.601902	Torsional Modes
17.087902	17.087902	17.088934	
29.482156	29.482162	29.486605	
43.616851	43.616851	43.632693	
60.790329	60.790251	60.944683	
26.274261	26.274261	26.181766	Longitudinal Modes
80.149376	80.149373	80.149373	
138.283434	138.283645	138.283645	
204.580318	204.580656	204.580656	
285.131312	285.135616	285.135616	

COMPARISION OF TORSIONAL AND LONGITUDINAL FREQUENCIES

A,B,C : DETAILS AND BLADE CODES SAME AS TABLE 20

TABLE 21

Frequencies in Hz			
Uncoupled Flap & Torsion Frequencies Straight Blade	Frequencies Z – Torsion Displacements Sweep Back Blade	Uncoupled Drag &Longitudinal Frequencies Straight Blade	Frequencies Y & X Displacements Sweep Back Blade
0.185460+	0.190138	0.586477x	0.600798
1.175735+	1.255662	3.718002x	3.936380
3.378427+	3.607882	10.683523x	11.270022
5.601691*	5.192255	21.802470x	20.980338
6.894546+	7.780935	26.274261e	26.975620
12.008414+	13.117677	37.973938x	36.017098
17.087902*	15.429861	80.149376e	51.360512
29.482156*	20.477351	138.283434e	76.786847
43.616851*	24.648670	204.580318e	88.655404
60.790329*	29.473873	285.131312e	112.537234

+ Uncoupled Flapping Mode Frequencies
* Uncoupled Torsional Mode Frequencies
x Uncoupled Drag Mode Frequencies
e Uncoupled Longitudinal Mode Frequencies

FREQUENCIES OF A SWEEP BACK BLADE: 90° SWEEP BACK IN FIRST(TIP) ELEMENT

TABLE 22

Frequencies in Hz			
Blade With 1 Radian Pretwist & IZ = 10	Blade With 1 Radian Pretwist & IZ = 10000	Blade With 90° Pretwist & IZ= 10	Blade With 90° Pretwist & IZ = 10000
0.187473	0.187696	0.190318	0.190870
0.523144	0.863767	0.467130	0.670805
1.318771	2.993376	1.476792	2.642201
2.765683	4.660998	2.433323	3.989742
4.498967	6.608550	5.039600	6.247057
6.457741	11.677828	6.013479	11.158582
11.226743	18.740134	11.076876	17.234562
11.617026	23.416319	11.876742	18.408955
18.633475	28.090114	18.116685	27.511635
22.185948	39.227745	22.610499	38.606608

FREQUENCIES OF SPECIAL CASES WITH LARGE IZ (10000 in^4)
COMPARED TO PRETWISTED UNIFORM RECTANGULAR BLADE
PRETWIST ANGLES 1 RADIAN AND 90°

BLADE CODES :KUMN,HIIZ,HINZ

TABLE 23

Frequency No	Coupled Frequencies in Hz	Type of Coupling Displacement
1	0.146557	
2	0.316827	
3	0.870757	X, Y, Z &
4	1.297063	Torsion-
5	1.907401	
6	2.057154	
7	2.555002	
8	3.650142	
9	4.780083	
10	4.953222	

COUPLED FREQUENCIES OF A ZIG -ZAG BLADE

BLADE CODE : KINK

TABLE 24

Flapping Mode Frequencies	Solution By Present Analysis Frequencies In Hz	Solution By Williams Method Frequencies In Hz	% Difference Compared To Present Results
First Mode	0.540867	0.5420918	0.227
Second Mode	1.691472	1.6813609	0.598
Third Mode	3.941190	3.8262274	2.910
Fourth Mode	7.492762	6.9935720	6.660
Fifth Mode	12.626227	11.1915300	11.360

FLAPPING MODE FREQUENCIES OF ROTATING BLADE
SPEED OF ROTATION 3 RADIANS/ SEC
BLADE CODE : RT03

TABLE 25

Flapping Mode Frequencies	Solution By Present Analysis Frequencies In Hz	Solution By Williams Method Frequencies In Hz	% Difference Compared To Present Results
First Mode	0.620521	0.6216732	0.18
Second Mode	3.882899	3.8441492	1.00
Third Mode	10.865465	10.4841410	3.51
Fourth Mode	21.994675	20.3837910	7.32
Fifth Mode	38.171298	33.5900270	12.00

DRAG MODE FREQUENCIES OF ROTATING BLADE
SPEED OF ROTATION : 3 RADIANS/ SEC
BLADE CODE : RT03

TABLE 26

Flapping Mode Frequencies	Solution By Present Analysis Frequencies In Hz	Solution By Williams Method Frequencies In Hz	% Difference Compared To Present Results
First Mode	1.010385	1.0141826	0.38
Second Mode	2.688995	2.6802342	0.32
Third Mode	5.252232	5.1372534	2.19
Fourth Mode	9.026009	8.5325972	5.46
Fifth Mode	14.304657	12.8816340	9.94

FLAPPING MODE FREQUENCIES OF ROTATING BLADE
SPEED OF ROTATION 6 RADIANS/ SEC
BLADE CODE : RT06

TABLE 27

Flapping Mode Frequencies	Solution By Present Analysis Frequencies In Hz	Solution By Williams Method Frequencies In Hz	% Difference Compared To Present Results
First Mode	0.699271	0.7026457	0.48
Second Mode	4.340111	4.3039149	0.83
Third Mode	11.392082	11.0174500	3.28
Fourth Mode	22.560294	20.9611600	7.08
Fifth Mode	38.756727	34.1911800	11.78

DRAG MODE FREQUENCIES OF ROTATING BLADE
SPEED OF ROTATION : 6 RADIANS/ SEC
BLADE CODE : RT06

TABLE 28

Flapping Mode Frequencies	Solution By Present Analysis Frequencies In Hz	Solution By Williams Method Frequencies In Hz	% Difference Compared To Present Results
First Mode	1.640518	1.6489549	0.512
Second Mode	4.167953	4.1597522	0.190
Third Mode	7.425322	7.2898314	1.820
Fourth Mode	11.812890	11.2717750	4.580
Fifth Mode	17.586766	16.0967000	8.470

FLAPPING MODE FREQUENCIES OF ROTATING BLADE

SPEED OF ROTATION 10 RADIANS/ SEC

BLADE CODE : RT10

TABLE 29

Flapping Mode Frequencies	Solution By Present Analysis Frequencies In Hz	Solution By Williams Method Frequencies In Hz	% Difference Compared To Present Results
First Mode	0.818518	0.8276715	1.110
Second Mode	5.264394	5.2314195	0.625
Third Mode	12.543539	12.1780160	2.910
Fouth Mode	23.838875	22.2613210	6.170
Fifth Mode	40.119591	35.5698410	11.340

DRAG MODE FREQUENCIES OF ROTATING BLADE

SPEED OF ROTATION : 10 RADIANS/ SEC

BLADE CODE : RT10

TABLE 30

Flapping Mode Frequencies	Solution By Present Analysis Frequencies In Hz	Solution By Williams Method Frequencies In Hz	% Difference Compared To Present Results
First Mode	2.429048	2.4430511	0.570
Second Mode	6.074007	6.0645040	0.156
Third Mode	10.360628	10.1775230	1.760
Fourth Mode	15.761508	15.0976470	4.210
Fifth Mode	22.496212	20.7968340	7.550

FLAPPING MODE FREQUENCIES OF ROTATING BLADE
SPEED OF ROTATION 15 RADIANS/ SEC
BLADE CODE : RT 15

TABLE 31

Flapping Mode Frequencies	Solution By Present Analysis Frequencies In Hz	Solution By Williams Method Frequencies In Hz	% Difference Compared To Present Results
First Mode	0.952979	0.9747217	2.28
Second Mode	6.698661	6.6681297	0.45
Third Mode	14.502411	14.1419530	2.48
Fourth Mode	26.135481	24.5737660	5.97
Fifth Mode	42.617097	38.0976680	10.60

DRAG MODE FREQUENCIES OF ROTATING BLADE
SPEED OF ROTATION : 15 RADIANS/ SEC
BLADE CODE : RT 15

TABLE 32

Flapping Mode Frequencies	Solution By Present Analysis Frequencies In Hz	Solution By Williams Method Frequencies In Hz	% Difference Compared To Present Results
First Mode	3.218774	3.2369619	0.56
Second Mode	8.001711	7.9879378	0.17
Third Mode	13.375840	13.1401940	1.76
Fourth Mode	19.939240	19.0782180	4.31
Fifth Mode	27.759853	25.7852500	7.11

FLAPPING MODE FREQUENCIES OF ROTATING BLADE
SPEED OF ROTATION 20 RADIANS/ SEC
BLADE CODE : RT 20

TABLE 33

Flapping Mode Frequencies	Solution By Present Analysis Frequencies In Hz	Solution By Williams Method Frequencies In Hz	% Difference Compared To Present Results
First Mode	1.065372	1.1059061	3.81
Second Mode	8.280013	8.2519186	0.33
Third Mode	16.828773	16.4580560	2.20
Fourth Mode	29.030752	27.4352140	5.49
Fifth Mode	45.914430	41.3366700	9.97

DRAG MODE FREQUENCIES OF ROTATING BLADE
SPEED OF ROTATION : 20 RADIANS/ SEC
BLADE CODE : RT 20

TABLE 34

Natural Mode Frequency	Solution By Present Analysis Frequencies in Hz	Exact Analytical Solution Frequencies in Hz	% Difference Compared to Present Results
FLAPPING			
First Mode	61.597814	61.635824	0.062
Second Mode	390.502591	386.292993	1.078
Third Mode	1122.092863	1081.740374	3.596
Fourth Mode	2289.918324	2119.825622	7.428
Fifth Mode	3988.411393	3503.847361	12.149
DRAG			
First Mode	905.922941	906.481959	0.062
Second Mode	5743.146316	5681.235493	1.078
Third Mode	16502.689891	15909.224115	3.596
Fourth Mode	33677.922672	31176.409538	7.428
Fifth Mode	58658.117609	51531.304809	12.150

FLAPPING AND DRAG MODE FREQUENCIES OF RECTANGULAR BLADE

BLADE CODE : TAMO

TABLE 35

Natural Mode Frequency	Solution By Present Analysis Frequencies in Hz	Exact Analytical Solution Frequencies in Hz	% Difference Compared to Present Results
TORSIONAL			
First Mode	709.856590	708.396415	0.206
Second Mode	2165.410339	2125.189246	1.874
Third Mode	3736.033647	3541.982077	5.194
Fourth Mode	5527.207695	4958.774908	10.284
Fifth Mode	7703.452018	6375.567739	17.238
LONGITUDINAL			
First Mode	8435.287139	8417.935716	0.206
Second Mode	25731.765223	25253.807149	1.857
Third Mode	44395.525734	42089.678582	5.194
Fourth Mode	65680.413181	58925.550014	10.284
Fifth Mode	91540.782268	75761.421449	17.238

TORSIONAL AND LONGITUDINAL MODE FREQUENCIES OF RECTANGULAR BLADE

BLADE CODE : TAMO

TABLE 36

Pretwist Angle in Degrees	Solution By Present Analysis Frequencies in Hz	Solution By Carnegie's Method Frequencies in Hz	% Difference Compared to Present Results	Carnegie's Practical Results Read off From Graph
0.00	61.597814	61.635824	0.0617	58.0
17.19	61.665114	61.701646	0.0592	57.5
34.38	61.866115	61.932853	0.1080	58.0
51.57	62.198057	62.320538	0.1980	59.0
68.75	62.656177	62.867192	0.3370	60.0
85.94	63.233473	63.574721	0.5390	61.0

EFFECT OF PRETWIST ON FIRST COUPLED FREQUENCIES OF RECTANGULAR BLADE

BLADE CODES : TAMO,TAM1,TAM2,TAM3,TAM4,TAM5

TABLE 37

Pretwist Angle in Degrees	Frequencies in Hz			
	2nd Coupled Mode	3rd Coupled Mode	4th Coupled Mode	5th Coupled Mode
0.00	390.502591	905.922941	1122.092863	2289.918324
17.19	374.062628	915.752045	1116.198910	2280.160409
34.38	335.869198	932.905865	1101.517120	2251.714268
51.57	293.415206	935.607690	1087.639195	2206.903320
68.75	255.679055	912.633779	1084.178116	2149.140658
85.94	224.780755	870.814826	1089.054390	2080.457661
Carnegie's Practical Results Read Off from Graph: Frequencies in Hz				
0.00	370	1050	1050	1990
17.19	350	1000	1000	1970
34.38	315	950	1100	1950
51.57	290	910	1250	1970
68.75	250	900	1350	1990
85.94	210	850	1500	2000

EFFECT OF PRETWIST ANGLES ON FREQUENCIES OF RECTANGULAR BLADE

II,III,IV & V MODES COMARED TO CARNEGIE'S PRACTICAL RESULTS

BLADE CODES : TAMO,TAM1,TAM2,TAM3,TAM4,TAM5

TABLE 38

Pretwist Angle in Degrees	Frequencies in Hz		
	1st Normal Mode	2nd Normal Mode	3rd Normal Mode
0.00	709.856590	2165.410339	3736.033647
17.19	709.781778	2165.182126	3735.639861
34.38	709.557488	2164.497950	3734.459306
51.57	709.184147	2163.359057	3732.494538
68.75	708.662467	2161.767678	3729.748901
85.94	707.993441	2159.726836	3726.227714

TORSIONAL MODE FREQUENCIES OF RECTANGULAR PRETWISTED BLADES
BLADE CODES : TAMO,TAM1,TAM2,TAM3,TAM4,TAM5

TABLE 39

Pretwist Angle in Degrees	Frequencies in Hz		
	1st Normal Mode	2nd Normal Mode	3rd Normal Mode
0.00	8435.287139	25731.765223	44395.525734
17.19	8436.176286	25734.470835	44400.333503
34.38	8438.842925	25742.605569	44414.302073
51.57	8443.285346	25756.157646	44437.083841
68.75	8449.503154	25775.118101	44470.365131
85.94	8457.485766	25799.473301	44511.923877

LONGITUDINAL MODE FREQUENCIES OF RECTANGULAR PRETWISTED BLADES
BLADE CODES : TAMO,TAM1,TAM2,TAM3,TAM4,TAM5

TABLE 40

Natural Mode	Frequencies in Hz		% Difference Compared to Present Results
	Solution By Present Analysis	Solution By Analytical Method	
FLAPPING			
First	105.514707	105.579817	0.062
Second	668.916054	661.705175	1.078
Third	1922.102307	1852.980032	3.596
Fourth	3922.542821	3631.180487	7.428
Fifth	6831.996632	6001.956985	12.149
DRAG			
First	864.319392	864.852738	0.062
Second	5479.398423	5420.330787	1.078
Third	15744.821698	15178.609894	3.596
Fourth	32131.344323	29744.666042	7.428
Fifth	55964.048506	49164.784365	12.149

FREQUENCIES OF AEROFOIL CROSS SECTION BLADE

FLAPPING AND DRAG MODES : $e_y = e_z = 0$

BLADE CODE : CAMO

TABLE 41

Natural Mode	Frequencies in Hz		% Difference Compared to Present Results
	Solution By Present Analysis	Solution By Analytical Method	
TORSIONAL			
First	1063.887785	1061.699369	0.206
Second	3245.378916	3185.098107	1.857
Third	5599.328962	5308.496845	5.194
Fourth	8283.826394	7431.895583	10.284
Fifth	11545.442595	9555.294321	17.238
LONGITUDINAL			
First	8574.659001	8557.020889	0.206
Second	26156.914569	25671.062666	1.857
Third	45129.103520	42785.104443	5.194
Fourth	66765.497299	59899.146220	10.284
Fifth	93053.259686	77013.187998	17.238

FREQUENCIES OF AEROFOIL CROSS SECTION BLADE

TORSIONAL AND LONGITUDINAL MODES : $e_y = e_z = 0$

BLADE CODE : CAMO

TABLE 42

Frequencies in Hz Shear Centre Off-set Neglected	Type of Normal Mode	Frequencies in Hz Shear Centre Off-set Included	Type of Normal Mode
105.514707	I Flapping	105.514387	
668.916054	II Flapping	668.896989	
864.319392	I Drag	844.004342	Flap-Drag-Torsion Coupled
1063.887785	I Torsion	1088.077344	
1922.102307	III Flapping	1921.989672	
3245.378916	II Torsion	3184.764705	
3922.542821	IV Flapping	3922.059854	
5479.398423	II Drag	5362.977383	

COMPARISION OF FREQUENCIES OF AEROFOIL CROSS SECTION BLADE WITH AND WITHOUT SHEAR CENTRE OFF-SET EFFECT

BLADE CODES : CAMO , JNTO

TABLE 43

Pretwist Angle In Degrees	(A) Blade without Coupling Terms $e_y=e_z$=B1=B2 B=3=0 Frequencies In Hz	(B) Blade With Shear Centre Off-set But B1=B2=B3=0 Frequencies In Hz	Carnegie's Practical Results in Hz From Graph	(C) Blade With Shear Centre Off-set And B1,B2,B3 Terms Frequencies In Hz	Carnegie's Analytical Solution Frequencies In Hz
0.00	105.514707	105.514387	94.00	105.514387	105.579817
15.00	105.600806	105.600538	93.00	105.452548	105.661825
30.00	105.858192	105.857871	96.00	105.292434	105.963788
45.00	106.284094	106.283613	95.00	105.036849	106.467461
57.30	106.767944	106.767250	96.50	104.746104	107.036040
60.00	106.873786	106.873038	97.00	104.689945	107.178986
75.00	107.620405	107.619283	97.00	104.256647	108.099261
90.00	108.514748	108.513148	98.00	103.741984	109.229192

COMPARISION OF FIRST COUPLED FREQUENCIES OF PRETWISTED AEROFOIL CROSS-SECTION BLADES

BLADE CODES

(A) PRETWISTED BLADES WITHOUT COUPLING TERMS :CAMO,CAM1,CAM2,CAM3,CAM4,CAM5,CAM6,CAM7

(B) PRETWISTED BLADES WITH S.C EFFECT BUT WITHOUT B1,B2,B3 TERMS:JNTO,JNT1,JNT2,JNT3,JNT4,JNT5,JNT6,JNT7

(C) PRETWISTED BLADES WITH S.C AND B1,B2,B3 TERMS INCLUDED :JNIO,JNI1,JNI2,JNI3,JNI4,JNI5,JNI6,JNI7

TABLE 44

Pretwist Angle In Degrees	(A) Blade without Coupling Terms $e_y=e_z$=B1=B2 B=3=0 Frequencies In Hz	(B) Blade With Shear Centre Off-set But B1=B2=B3=0 Frequencies In Hz	Carnegie's Practical Results in Hz From Graph	(C) Blade With Shear Centre Off-set And B1,B2,B3 Terms Frequencies In Hz
0.00	668.916054	668.896989	590	668.896989
15.00	631.578239	630.772082	560	629.275307
30.00	564.815214	563.734887	510	559.876411
45.00	500.361764	499.450417	450	492.952567
57.30	452.891940	452.164221	400	443.330667
60.00	444.527536	443.833506	390	434.452188
75.00	397.801432	397.285847	350	384.856612
90.00	359.198469	358.815157	310	343.257821

COMPARISION OF SECOND COUPLED FREQUENCIES OF PRETWISTED AEROFOIL CROSS-SECTION BLADES

BLADE CODES

(A) PRETWISTED BLADES WITHOUT COUPLING TERMS :CAMO,CAM1,CAM2,CAM3,CAM4,CAM5,CAM6,CAM7

(B) PRETWISTED BLADES WITH S.C EFFECT BUT WITHOUT B1,B2,B3 TERMS:JNTO,JNT1,JNT2,JNT3,JNT4,JNT5,JNT6,JNT7

(C) PRETWISTED BLADES WITH S.C AND B1,B2,B3 TERMS INCLUDED :JNIO,JNI1,JNI2,JNI3,JNI4,JNI5,JNI6,JNI7

TABLE 45

Pretwist Angle In Degrees	(A) Blade without Coupling Terms $e_y=e_z=B1=B2$ $B=3=0$ Frequencies In Hz	(B) Blade With Shear Centre Off-set But B1=B2=B3=0 Frequencies In Hz	Carnegie's Practical Results in Hz From Graph	(C) Blade With Shear Centre Off-set And B1,B2,B3 Terms Frequencies In Hz
0.00	864.319392	844.004342	790	844.004342
15.00	909.817314	886.002575	820	888.339015
30.00	999.292018	959.781829	920	967.914863
45.00	1096.345034	1014.147899	1010	1033.809248
57.30	1173.104298	1034.883646	1150	1064.188554
60.00	1188.328547	1037.387801	1160	1068.591375
75.00	1266.802480	1046.357995	1190	1089.026183
90.00	1319.636922	1050.457746	1150	1106.528961

COMPARISION OF THIRD COUPLED FREQUENCIES OF PRETWISTED AEROFOIL CROSS-SECTION BLADES

BLADE CODES

(A) PRETWISTED BLADES WITHOUT COUPLING TERMS :CAMO,CAM1,CAM2,CAM3,CAM4,CAM5,CAM6,CAM7

(B) PRETWISTED BLADES WITH S.C EFFECT BUT WITHOUT B1,B2,B3 TERMS:JNTO,JNT1,JNT2,JNT3,JNT4,JNT5,JNT6,JNT7

(C) PRETWISTED BLADES WITH S.C AND B1,B2,B3 TERMS INCLUDED :JNIO,JNI1,JNI2,JNI3,JNI4,JNI5,JNI6,JNI7

TABLE 46

Pretwist Angle In Degrees	(A) Blade without Coupling Terms $e_y=e_z=B1=B2\ B=3=0$ Frequencies In Hz	(B) Blade With Shear Centre Off-set But B1=B2=B3=0 Frequencies In Hz	Carnegie's Practical Results in Hz From Graph	(C) Blade With Shear Centre Off-set And B1,B2,B3 Terms Frequencies In Hz
0.00	1063.887785	1088.077344	1100	1088.077344
15.00	1063.887785	1092.472948	1100	1091.889210
30.00	1063.887785	1108.465496	1120	1105.497414
45.00	1063.887785	1150.944806	1130	1140.424629
57.30	1063.887785	1206.707636	1140	1189.515580
60.00	1063.887785	1219.383278	1150	1200.696334
75.00	1063.887785	1288.456752	1200	1258.564200
90.00	1063.887785	1335.916533	1250	1284.047035

Note:Torsional Mode uncoupled as $e_y = e_z = 0$

COMPARISION OF FOURTH COUPLED FREQUENCIES OF PRETWISTED AEROFOIL CROSS-SECTION BLADES

BLADE CODES

(A) PRETWISTED BLADES WITHOUT COUPLING TERMS :CAMO,CAM1,CAM2,CAM3,CAM4,CAM5,CAM6,CAM7

(B) PRETWISTED BLADES WITH S.C EFFECT BUT WITHOUT B1,B2,B3 TERMS:JNTO,JNT1,JNT2,JNT3,JNT4,JNT5,JNT6,JNT7

(C) PRETWISTED BLADES WITH S.C AND B1,B2,B3 TERMS INCLUDED :JNIO,JNI1,JNI2,JNI3,JNI4,JNI5,JNI6,JNI7

TABLE 47

Pretwist Angle In Degrees	(A) Blade without Coupling Terms $e_y=e_z$=B1=B2 B=3=0 Frequencies In Hz	(B) Blade With Shear Centre Off-set But B1=B2=B3=0 Frequencies In Hz	Carnegie's Practical Results in Hz From Graph	(C) Blade With Shear Centre Off-set And B1,B2,B3 Terms Frequencies In Hz
0.00	1922.102307	1921.989672	1640	1921.989672
15.00	1906.711868	1906.537807	1630	1902.375751
30.00	1863.184189	1862.681622	1590	1847.455171
45.00	1798.546027	1797.637027	1580	1767.090047
57.30	1738.462621	1737.276862	1510	1693.325938
60.00	1722.310979	1721.087528	1510	1673.846150
75.00	1645.681223	1644.417181	1510	1582.331643
90.00	1584.499263	1584.174367	1620	1514.770320

COMPARISION OF FIFTH COUPLED FREQUENCIES OF PRETWISTED AEROFOIL CROSS-SECTION BLADES

BLADE CODES

(A) PRETWISTED BLADES WITHOUT COUPLING TERMS :CAMO,CAM1,CAM2,CAM3,CAM4,CAM5,CAM6,CAM7

(B) PRETWISTED BLADES WITH S.C EFFECT BUT WITHOUT B1,B2,B3 TERMS:JNTO,JNT1,JNT2,JNT3,JNT4,JNT5,JNT6,JNT7

(C) PRETWISTED BLADES WITH S.C AND B1,B2,B3 TERMS INCLUDED :JNIO,JNI1,JNI2,JNI3,JNI4,JNI5,JNI6,JNI7

TABLE 48

Frequency No	Solution By Present Analysis Frequencies in Hz	Solution By Montoya's Analysis Frequencies in Hz	% Difference Compared to Present Results
1	89.528641	93.45	4.38
2	267.092727	203.60	23.77
3	288.582727	299.40	3.75
4	372.601963	443.80	19.11
5	610.591330	606.10	0.74
6	663.070198	618.20	6.77
7	958.353367	883.30	7.83

FREQUENCIES OF BROWN BOVERI BLADE : SHEAR CENTRE OFF-SET EFFECT AND COUPLING TERMS INCLUDED: PRETWIST ANGLE = 0

BLADE CODE : MON5

TABLE 49

Speed in r.p.m	Frequencies in Hz		
	Solution By Present Analysis	Montoya's Solution From Graph	Montoya's Practical Results From Graph
0	89.730921	93	83
1000	91.265521	96	87
1500	93.061146	100	91
2000	95.372024	106	99
2500	98.042602	113	105
3000	97.886275	121	114

I MODE FREQUENCIES OF BROWN BOVERI BLADE : ROTATING CASES STRAIGHT BLADES WITHOUT PRETWIST AND COUPLING TERMS

BLADE CODES : SUB1,SUB4,SUB5,SUB6,SUB7,SUB2

TABLE 50

Frequency No	Frequencies in Hz		% difference Compared to Present Results	Montoya's Practical Results Frequencies In Hz
	Solution By Present Analysis	Solution By Montoya's Analysis		
1	93.142100	93.58	0.47	83.4
2	202.077973	206.90	2.39	184.80
3	307.479445*	303.50	1.29	344.30
4	435.539816	441.22	1.30	399.70
5	628.226766	621.70	1.04	500.00
6	645.269708*	626.70	2.88	655.00
7	1021.607226*	928.80	9.08	840.00

* :Torsion

FREQUENCIES OF BROWN BOVERI BLADE:PRETWISTED WITHOUT COUPLING TERMS

BLADE CODE : MON4

TABLE 51

Frequency No	Frequencies in Hz		% Difference Compared to Present Results
	Solution By Present Analysis	Solution By Montoya's Analysis	
1	89.801832	80.3	10.58
2	193.957733	185.5	4.36
3	285.548715	356.3	24.78
4	452.885400	410.3	9.40
5	572.590820	535.7	6.44
6	677.693448	724.3	6.88
7	943.446994	847.1	10.21

FREQUENCIES OF BROWN BOVERI BLADE INCLUDING COUPLING TERMS AND PRETWIST

BLADE CODE : MON1

TABLE 52

Frequencies in Hz			% Difference Compared to 10 Element Idealisation	% Difference Compared to 20 Element Idealisation
Results By 10 Element Idealisation	Results By 20 Element Idealisation	Exact Analytical Solution		
0.185460	0.185562	0.185575	0.054	0.00701
1.175735	1.166312	1.163061	1.075	0.27900
3.378427	3.287718	3.256932	3.596	0.93600
6.894546	6.512889	6.382427	7.427	2.00300
12.008414	10.926156	10.549476	12.150	3.44700

COMPARISION OF FREQUENCIES AND ERRORS
10 ELEMENT AND 20 ELEMENT IDEALISATIONS
FLAPPING MODE FREQUENCIES; BLADE CODE : KUMN

TABLE 53

Frequencies in Hz			% Difference Compared to 10 Element Idealisation	% Difference Compared to 10 Element Idealisation
Results By 10 Element Idealisation	Results By 20 Element Idealisation	Exact Analytical Solution		
0.586477	0.586799	0.586839	0.075	0.00682
3.718002	3.688202	3.677922	1.079	0.27800
10.683523	10.396676	10.299324	3.596	0.93600
21.802470	20.595566	20.183005	7.428	2.00300
37.973938	34.551537	33.360371	12.149	3.44700

COMPARISION OF FREQUENCIES AND ERRORS
10 ELEMENT AND 20 ELEMENT IDEALISATIONS
DRAG MODE FREQUENCIES : BLADE CODE : KUMN

TABLE 54

Frequencies in Hz			% Difference Compared to 10 Element Idealisation	% Difference Compared to 20 Element Idealisation
Results By 10 Element Idealisation	Results By 20 Element Idealisation	Exact Analytical Solution		
5.601691	5.593044	5.590169	0.205	0.0514
17.087902	16.848525	16.770506	1.857	0.4630
29.482156	28.315663	27.950843	5.194	1.2880
43.616851	40.147544	39.131180	10.284	2.5310
60.790329	52.516641	50.311517	17.238	4.1990

COMPARISION OF FREQUENCIES AND ERRORS
10 ELEMENT AND 20 ELEMENT IDEALISATIONS
TORSIONAL MODE FREQUENCIES ; BLADE CODE : KUMN

TABLE 55

Frequencies in Hz			% Difference Compared to 10 Element Idealisation	% Difference Compared to 20 Element Idealisation
Results By 10 Element Idealisation	Results By 20 Element Idealisation	Exact Analytical Solution		
26.274261	26.233701	26.220214	0.206	0.0514
80.149376	79.026704	78.660643	1.857	0.4630
138.283434	132.811269	131.101072	5.194	1.2880
204.580318	188.307614	183.541501	10.284	2.5310
285.131312	246.331155	235.981930	17.237	4.2010

COMPARISION OF FREQUENCIES AND ERRORS
10 ELEMENT AND 20 ELEMENT IDEALISATION
LONGITUDINAL MODE FREQUENCIES ; BLADE CODE : KUMN

TABLE 56

Cases	C1	C2	C3	Details of variations
Case a	0	0	0	B1 = B2 = B3 = 0
Case b	-0.0124	0.5322	0.0019	B1 ≠ 0, B2 = B3 = 0
Case c	0	0	-0.0003	B1 = 0, B2 ≠ 0, B3 = 0
Case d	0	-0.3333	0	B1 = B2 = 0, B3 ≠ 0
Case e	-0.0124	0.1988	0.0009	B1,B2,B3 ≠ 0

Blade Code JNI4

VARIATIONS IN C1,C2 AND C3 FOR DIFFERENT CASES

TABLE 57

10^{-6}

0.0706	0.0353	0	0	0	0	0	0
0.0353	0.0706	0	0	0	0	0	0
0	0	61.5460	30.7730	0	0	0	0
0	0	30.7730	61.5460	0	0	0	0
0	0	0	0	64.5161	32.2581	0	0
0	0	0	0	32.2581	64.5161	0	0
0	0	0	0	0	0	0.9615	0.4807
0	0	0	0	0	0	0.4807	0.9615

FLEXIBILITY MATRIX FOR CASE (a) IN TABLE 57

TABLE 58

10^{-6}

0.0795	0.0397	-0.7153	-0.3577	-0.3806	-0.1901	0.0087	0.0091
0.0397	0.0795	-0.3577	-0.7153	-0.1901	-0.3797	0.0091	0.0277
-0.7153	-0.3577	57.6049	28.8024	30.6503	15.3107	-0.6784	-0.7325
-0.3577	-0.7153	28.8024	57.6049	15.3107	30.5771	-0.7325	-2.2318
-0.3807	-0.1901	30.6503	15.3107	80.7607	40.3015	-2.0333	-1.9989
-0.1901	-0.3797	15.3017	30.5771	40.3015	80.3652	-1.9989	-5.9549
0.0087	0.0091	-0.6984	-0.7325	-2.0333	-1.9989	1.0396	0.5988
0.0091	0.0277	-0.7325	2.2318	-1.9989	-5.9549	0.5988	1.4354

FLEXIBILITY MATRIX FOR CASE (b) IN TABLE 57

TABLE 59

10^{-6}

0.0706	0.0353	0	0	0	0	0	0
0.0353	0.0706	0	0	0	0	0	0
0	0	57.6049	28.8024	-0.0004	-0.0004	-0.0152	-0.0076
0	0	28.8024	57.6049	-0.0004	-0.0011	-0.0076	-0.0151
0	0	-0.0004	-0.0004	64.4526	32.1627	-1.5889	-1.5889
0	0	-0.0004	-0.0011	32.1627	64.1348	-1.5887	-4.7666
0	0	-0.0152	-0.0076	-1.5889	-1.5889	1.0251	0.5761
0	0	-0.0076	-0.0151	-1.5889	-4.7666	0.5761	1.3428

FLEXIBILITY MATRIX FOR CASE (c) IN TABLE 57

TABLE 60

$$10^{-6}\begin{bmatrix}
0.0706 & 0.0353 & 0 & 0 & 0 & 0 & 0 & 0 \\
0.0353 & 0.0706 & 0 & 0 & 0 & 0 & 0 & 0 \\
0 & 0 & 57.6049 & 28.8024 & -19.1920 & -9.5864 & 0.4800 & 0.4800 \\
0 & 0 & 28.8024 & 57.6049 & -9.5864 & -19.1440 & 0.4800 & 1.4401 \\
0 & 0 & -19.1920 & -9.5864 & 70.8467 & 35.3534 & -1.7489 & -1.7489 \\
0 & 0 & -9.5864 & -19.1440 & 35.3534 & 70.4969 & -1.7489 & -5.2467 \\
0 & 0 & 0.4800 & 0.4800 & -1.7489 & -1.7489 & 1.0315 & 0.5857 \\
0 & 0 & 0.4800 & 1.4401 & -1.7489 & -5.2466 & 0.5857 & 1.3812
\end{bmatrix}$$

FLEXIBILITY MATRIX FOR CASE (d) IN TABLE 57

TABLE 61

$$10^{-6}\begin{bmatrix}
0.0745 & 0.0397 & -0.7153 & -0.3577 & -0.1423 & -0.0711 & 0.0029 & 0.0032 \\
0.0397 & 0.0795 & -0.3577 & -0.7153 & -0.0711 & -0.1420 & 0.0032 & 0.0100 \\
-0.7153 & -0.3577 & 57.6049 & 28.8024 & 11.4579 & 5.7239 & -0.2335 & -0.2601 \\
-0.3577 & -0.7153 & 28.8024 & 57.6049 & 5.7239 & 11.4319 & -0.2601 & -0.8068 \\
-0.1423 & -0.0711 & 11.4579 & 5.7239 & 66.7316 & 33.3002 & -1.6565 & -1.6464 \\
-0.0711 & -0.1420 & 5.7239 & 11.4319 & 33.3002 & 66.4035 & -1.6464 & -4.9272 \\
0.0029 & 0.0032 & -0.2335 & -0.2601 & -1.6565 & -1.6464 & 1.0269 & 0.5790 \\
0.0032 & 0.0100 & -0.2601 & -0.8068 & -1.6464 & -4.9272 & 0.5790 & 1.3550
\end{bmatrix}$$

FLEXIBILITY MATRIX FOR CASE (e) IN TABLE 57

TABLE 62

	Frequencies in Hz				
Mode No	Case a B1=B2=B3=0	Case b B1≠0, B2=B3=0	Case c B1=0, B2≠0, B3=0	Case d B1=B2=0, B3≠0	Case e B1, B2, B3≠0
1	106.767944	95.233870	106.767239	101.546098	104.746104
2	452.891940	407.099304	452.141697	436.047833	443.330667
3	1173.104298	1124.406143	1034.323398	1042.509220	1064.188554
4	1063.887785	1236.740521	1207.427629	1229.820965	1189.515580
5	1738.462621	1532.540186	1737.270241	1662.759445	1693.325938

FREQUENCIES UPTO FIFTH MODE OF CASES (a) TO (e) IN TABLE 57

TABLE 63

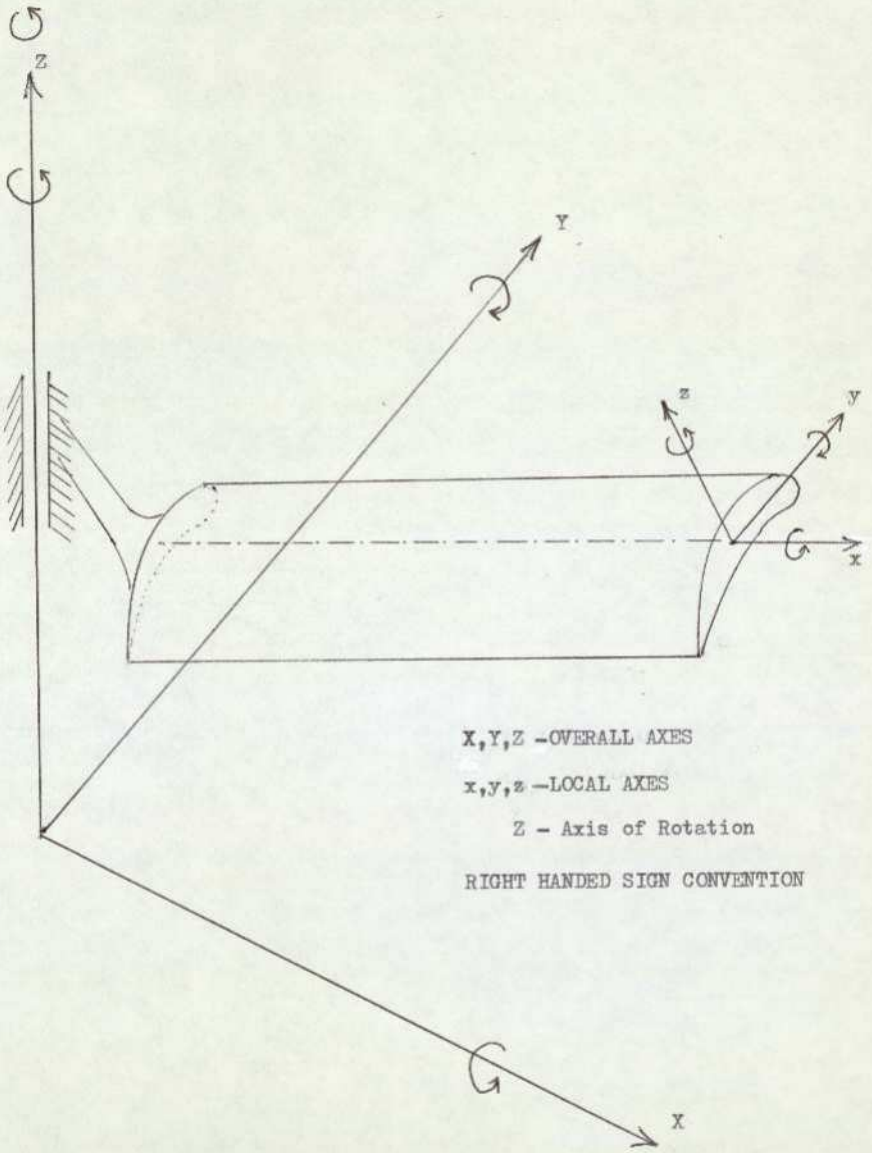

REPRESENTATION OF OVERALL AND LOCAL AXES SYSTEMS

FIGURE 1

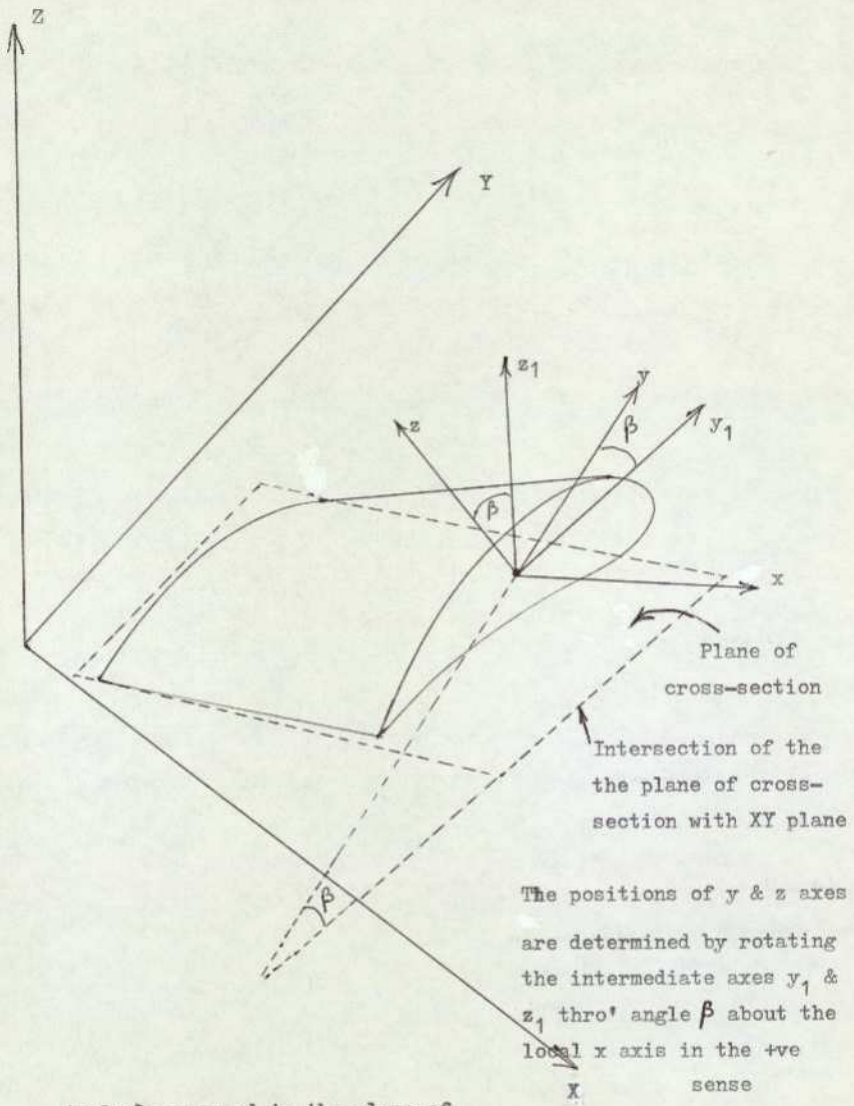

Angle β measured in the plane of cross-section

REPRESENTATION OF A PRE-TWISTED BLADE

FIGURE 2

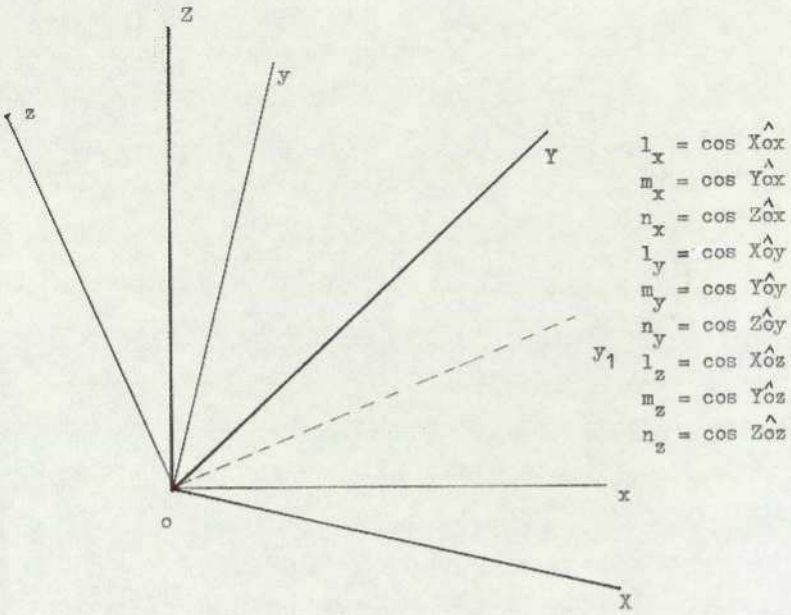

$l_x = \cos X\hat{o}x$
$m_x = \cos Y\hat{o}x$
$n_x = \cos Z\hat{o}x$
$l_y = \cos X\hat{o}y$
$m_y = \cos Y\hat{o}y$
$n_y = \cos Z\hat{o}y$
$l_z = \cos X\hat{o}z$
$m_z = \cos Y\hat{o}z$
$n_z = \cos Z\hat{o}z$

DIRECTION COSINES BETWEEN TWO SYSTEMS OF REFERENCE AXES

X,Y,Z – Overall axes directions x,y,z – Local axes directions

oy_1 – Intermediate axis

FIGURE 2a

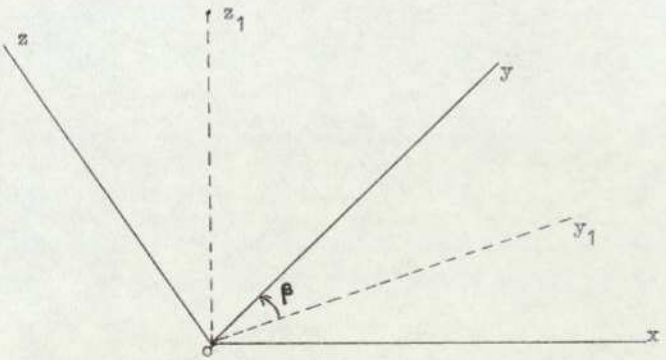

POSITION OF THE INTERMEDIATE AXES oy_1 & oz_1

The positions of oy and oz are established by rotating the intermediate axes oy_1 and oz_1 thro' angle β about the local x axis in the positive sense

$y = y_1\cos\beta + z_1\sin\beta$; $z = -y_1\sin\beta + z_1\cos\beta$

FIGURE 2b

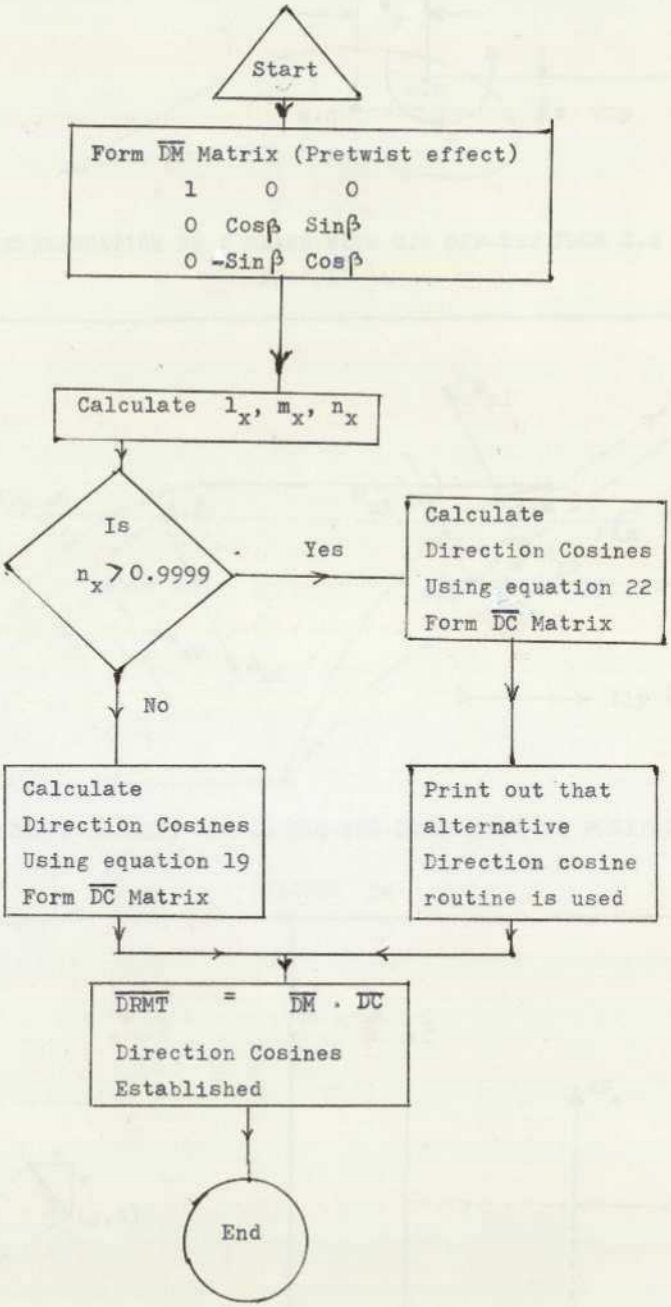

DIRECTION COSINES SUBROUTINE COSN(I) LOGIC

FIGURE 3

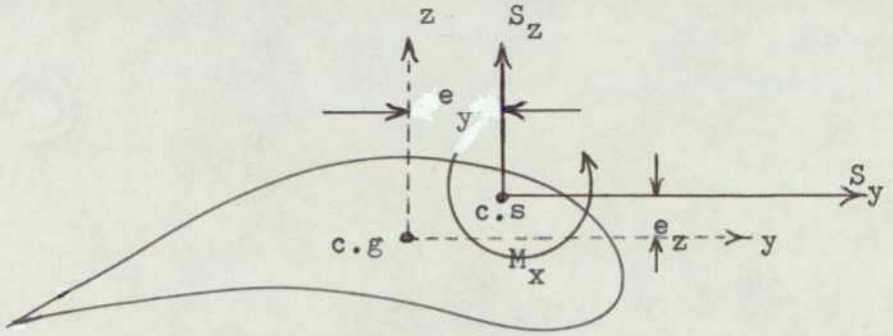

REPRESENATION OF A BLADE WITH C.S OFF-SET FROM C.G

FIGURE 4

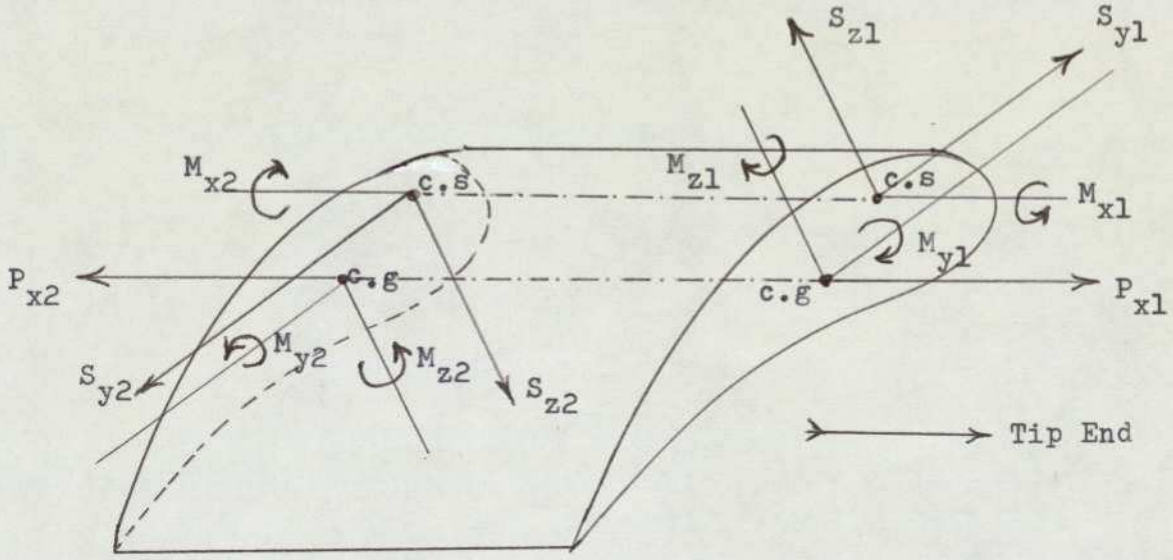

A DISCRETE ELEMENT INDICATING THE DIRECTIONS OF POSITIVE LOADS

FIGURE 5a

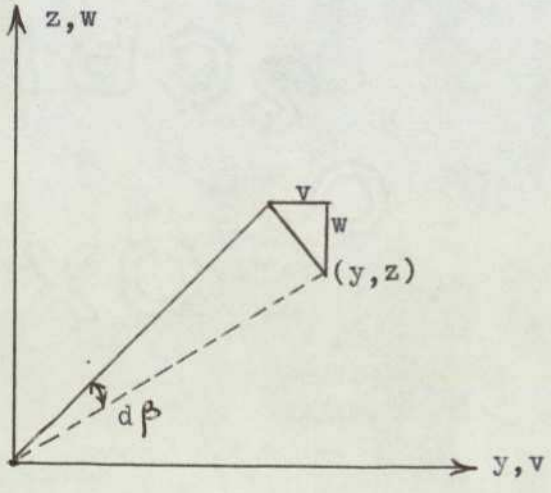

$v = -z\, d\beta$

$w = y\, d\beta$

END LOAD FIBRES:EFFECT DUE TO PRETWIST

FIGURE 5b

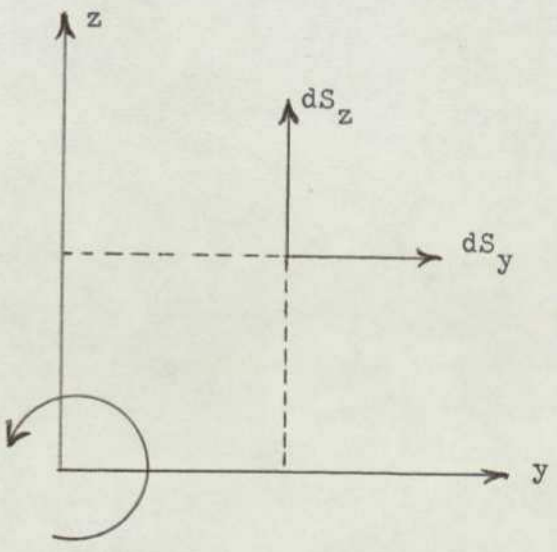

SIGN CONVENTION FOR POSITIVE MOMENTS

FIGURE 5c

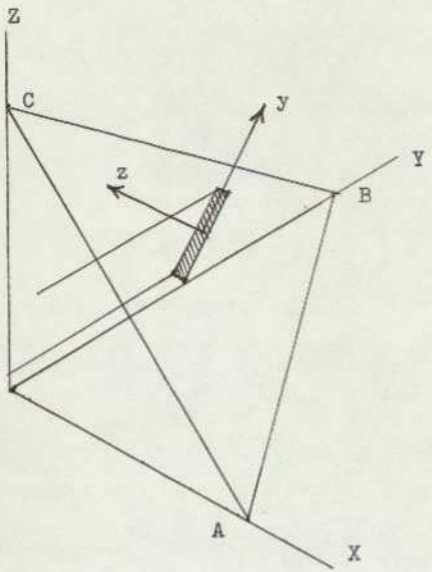

ABC is the plane of cross section
Directions of local axes corresponding to $\beta = 0$ of a blade positioned at equal inclination to X,Y,Z axes

REPRESENTATION OF BLADE 2

FIGURE 5d

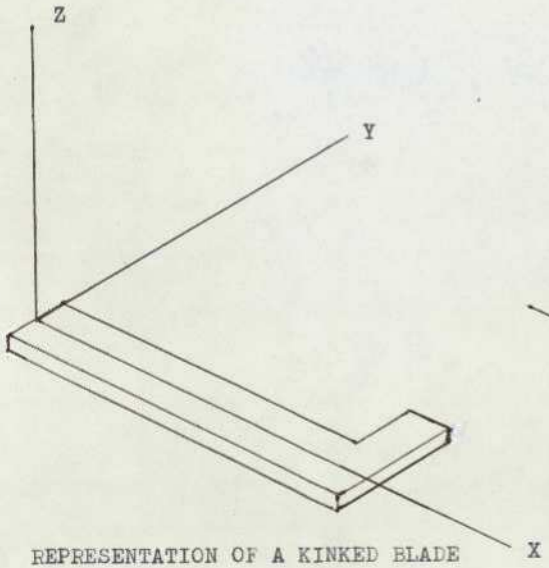

REPRESENTATION OF A KINKED BLADE

FIGURE 5e

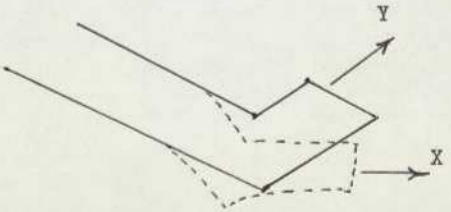

Drag bending distorsion of a kinked blade

FIGURE 5f

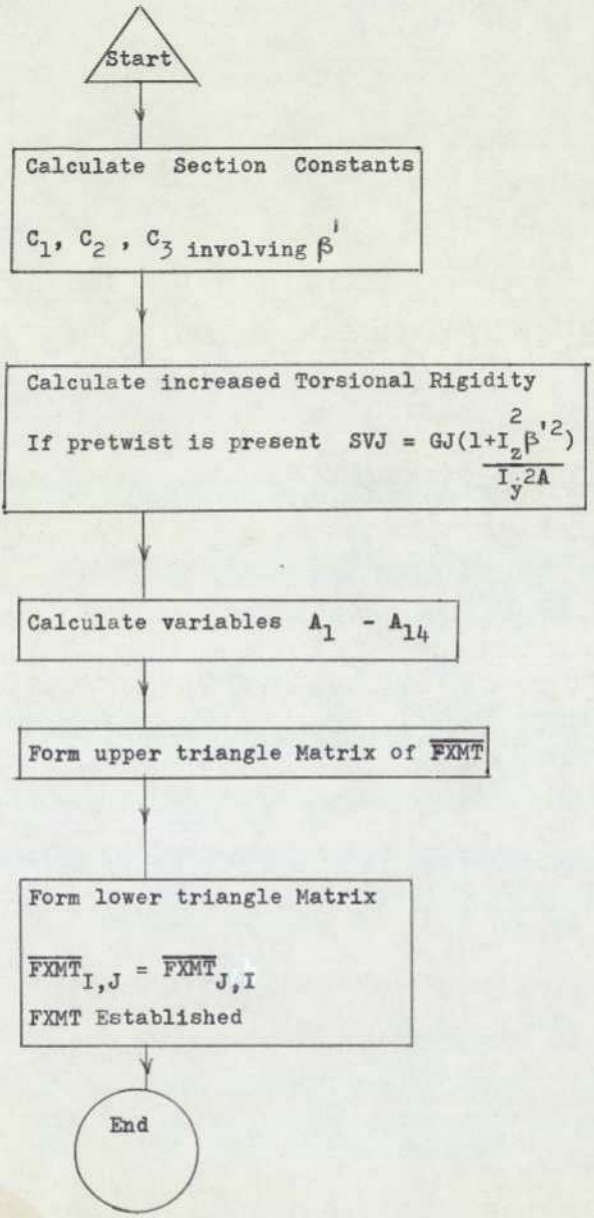

FLEXIBILITY MATRIX SUBROUTINE FLEX(I) LOGIC

FIGURE 6

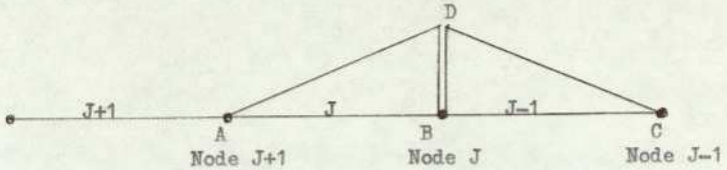

ASSUMED SHAPE OF ELEMENTS J AND J-1 DUE TO FORCES CAUSED BY DISPLACEMENT AT J

BD - Assumed displacement at node J

AD - Assumed shape of element AB(element J)

CD - Assumed shape of element BC(element J-1)

FIGURE 7

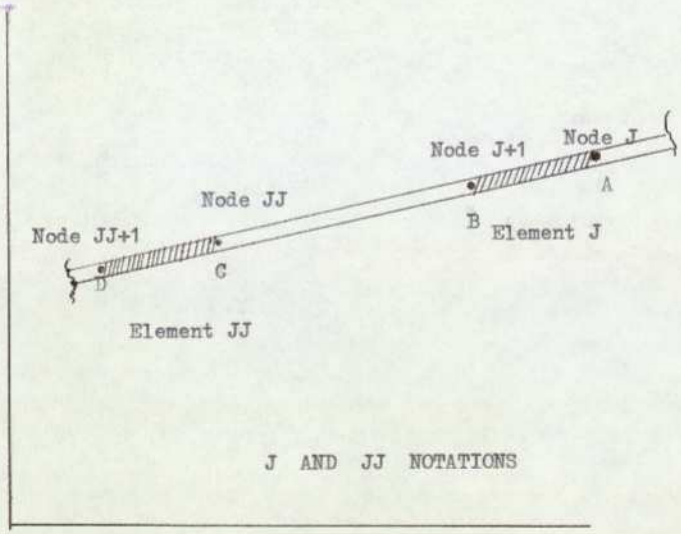

J AND JJ NOTATIONS

AB - Element J

A - Node J

B - Node J+1

CD - Element JJ

C - Node JJ

D - Node JJ+1

FIGURE 8

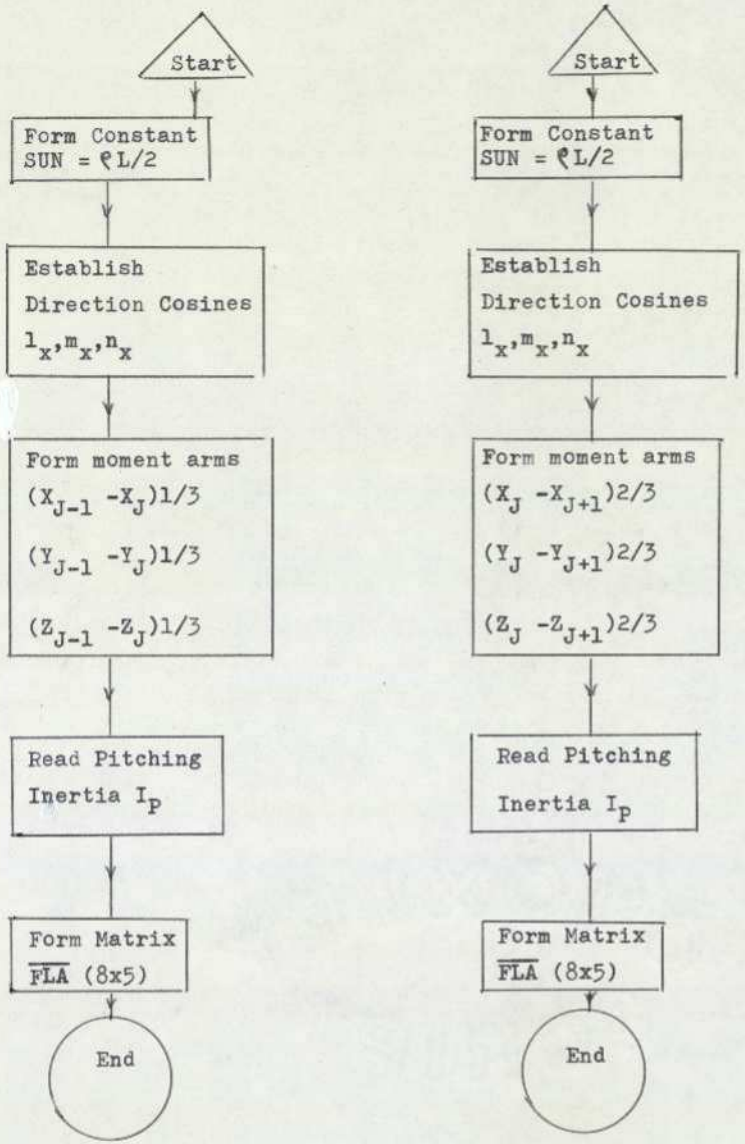

LOGIC OF SUBROUTINES FLAP AND FLAB

FIGURE 9

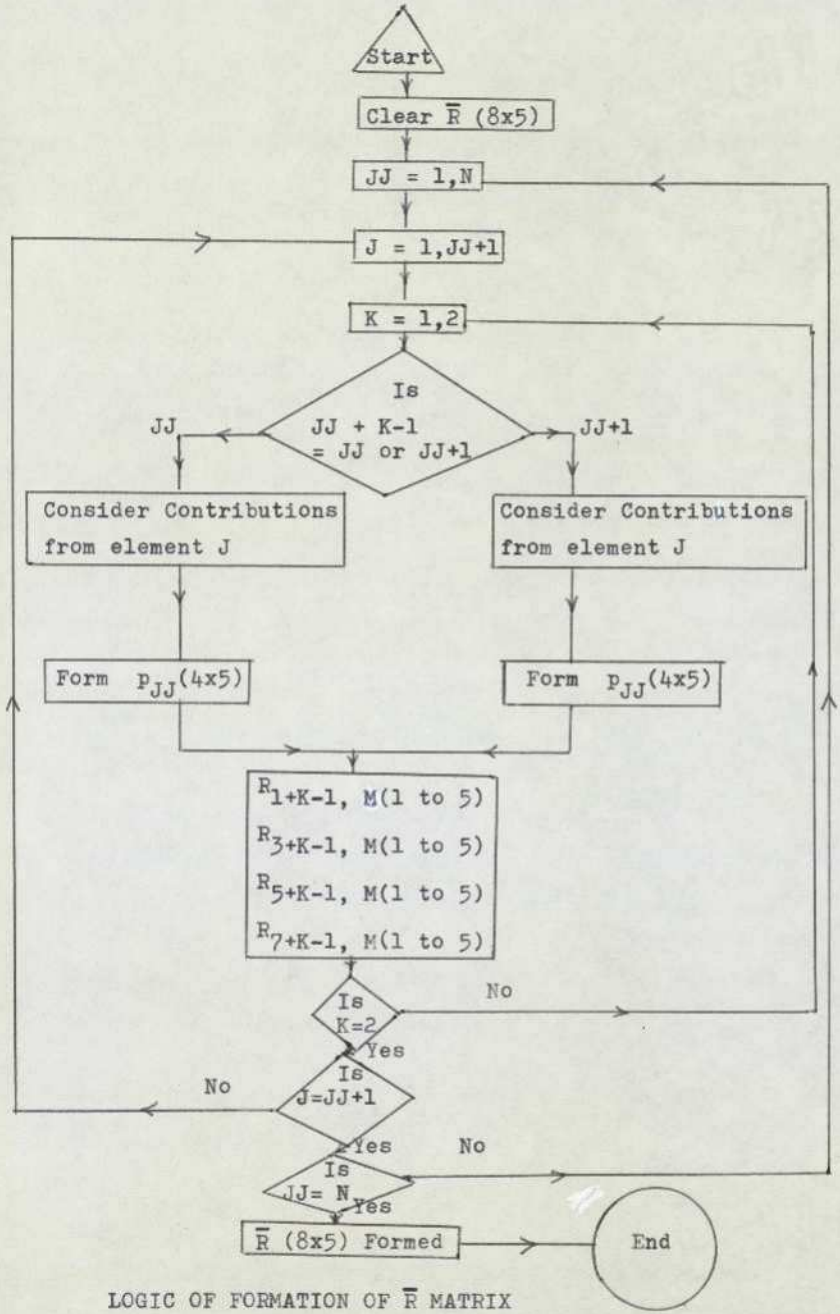

LOGIC OF FORMATION OF $\bar{R}$ MATRIX

FIGURE 10

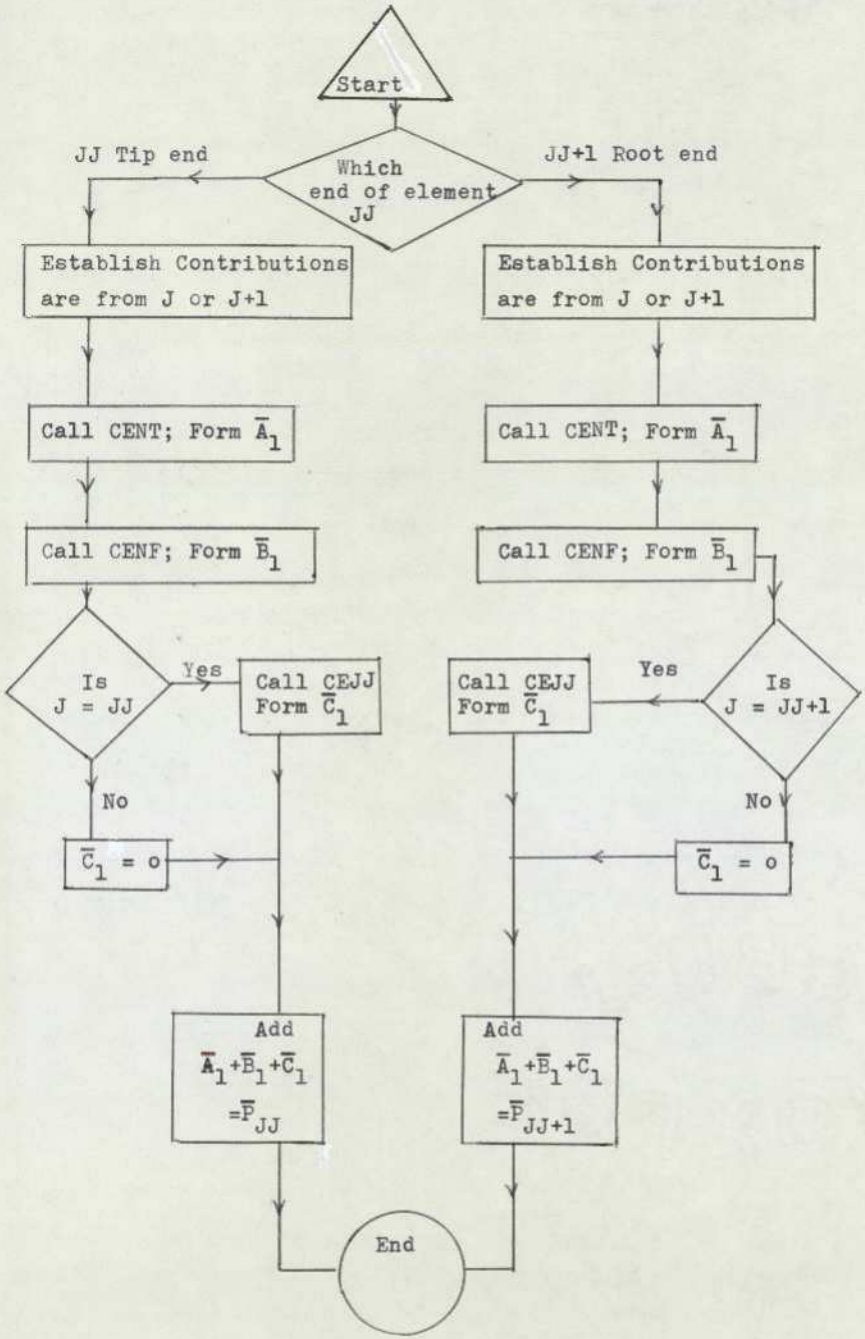

LOGIC OF ESTABLISHING LOADS ON ELEMENT JJ

FIGURE 11

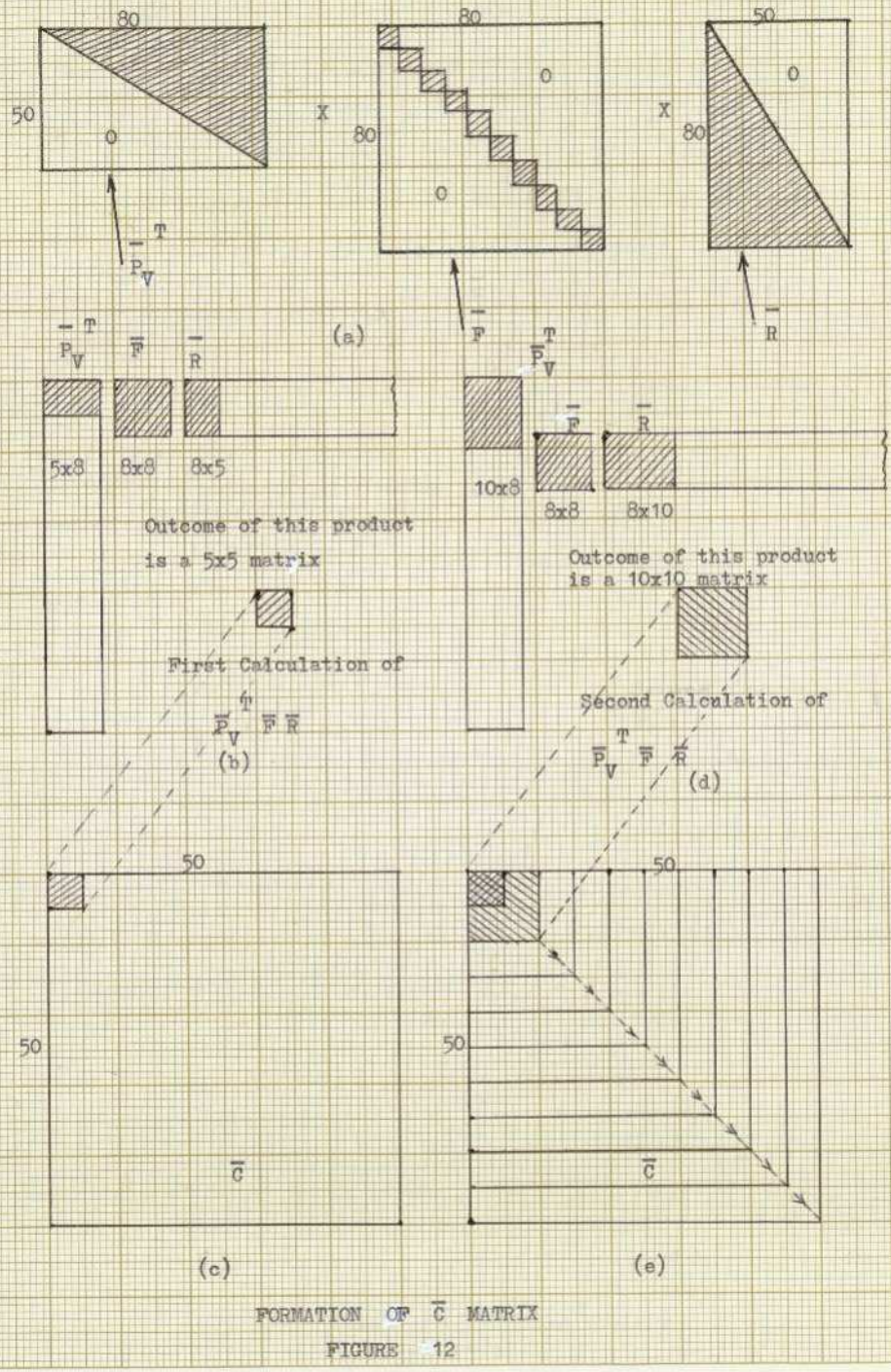

FORMATION OF $\overline{C}$ MATRIX

FIGURE 12

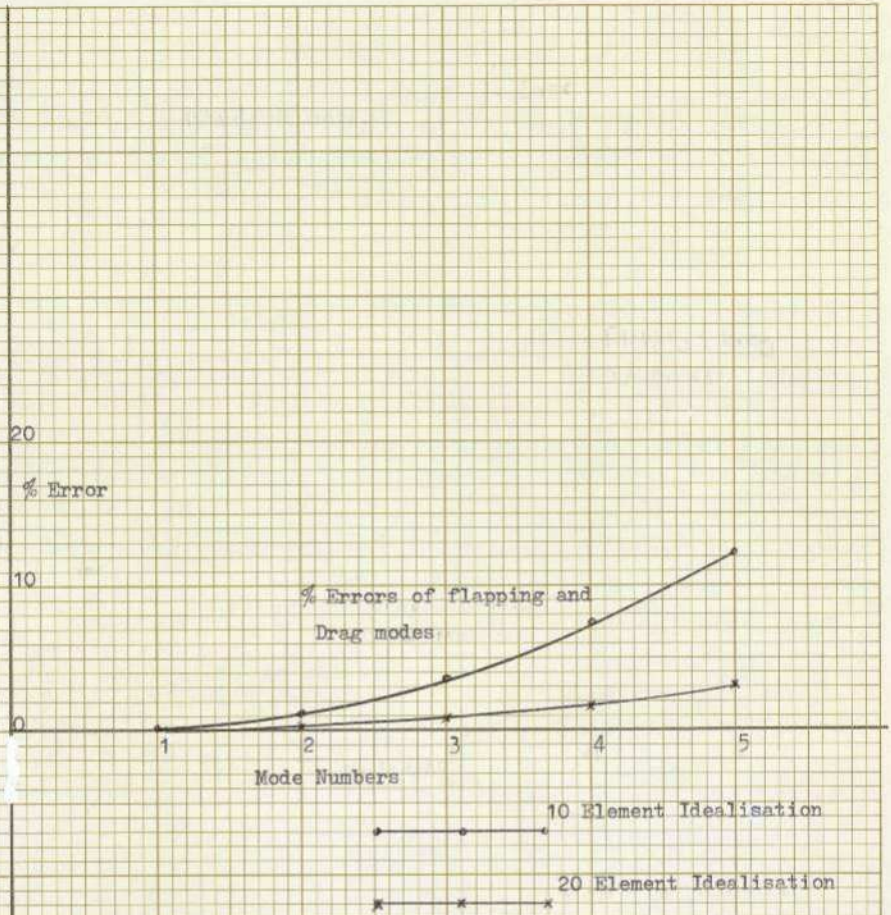

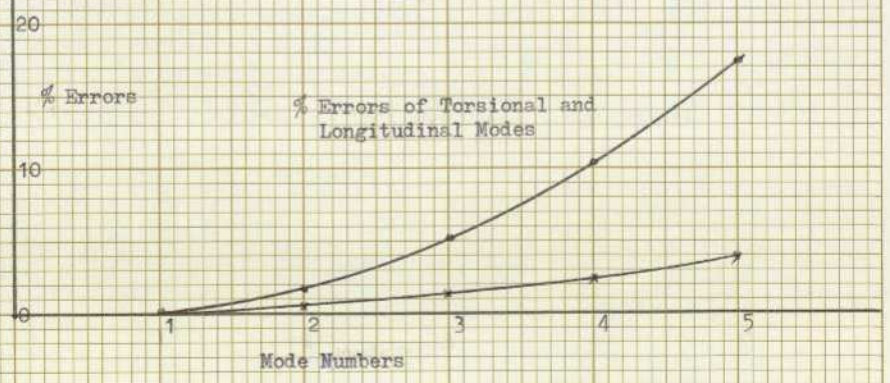

ERROR ANALYSIS OF A SIMPLE BLADE : BLADE CODE KUMN

FIGURE 13

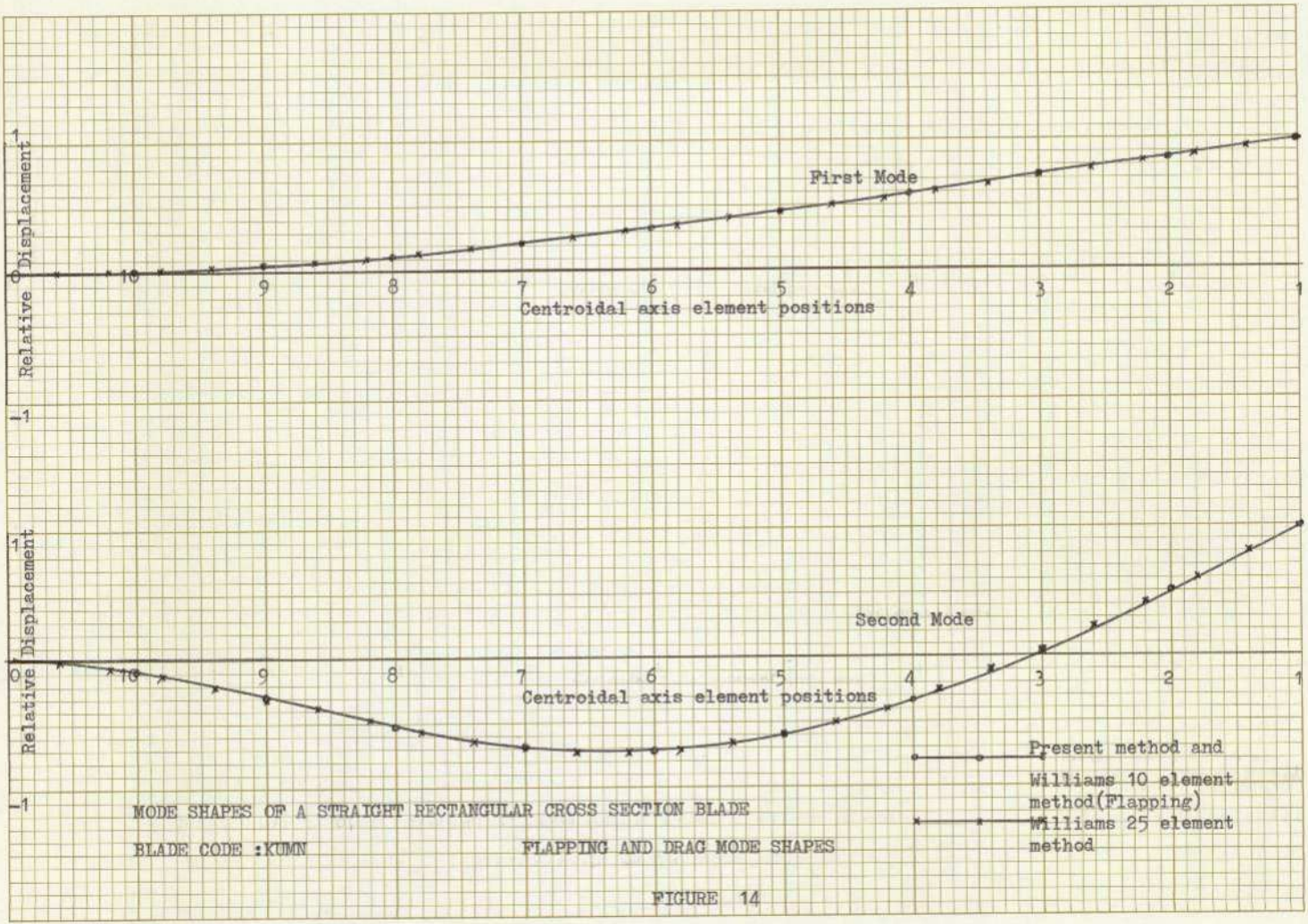

MODE SHAPES OF A STRAIGHT RECTANGULAR CROSS SECTION BLADE

BLADE CODE :KUMN

FLAPPING AND DRAG MODE SHAPES

FIGURE 14

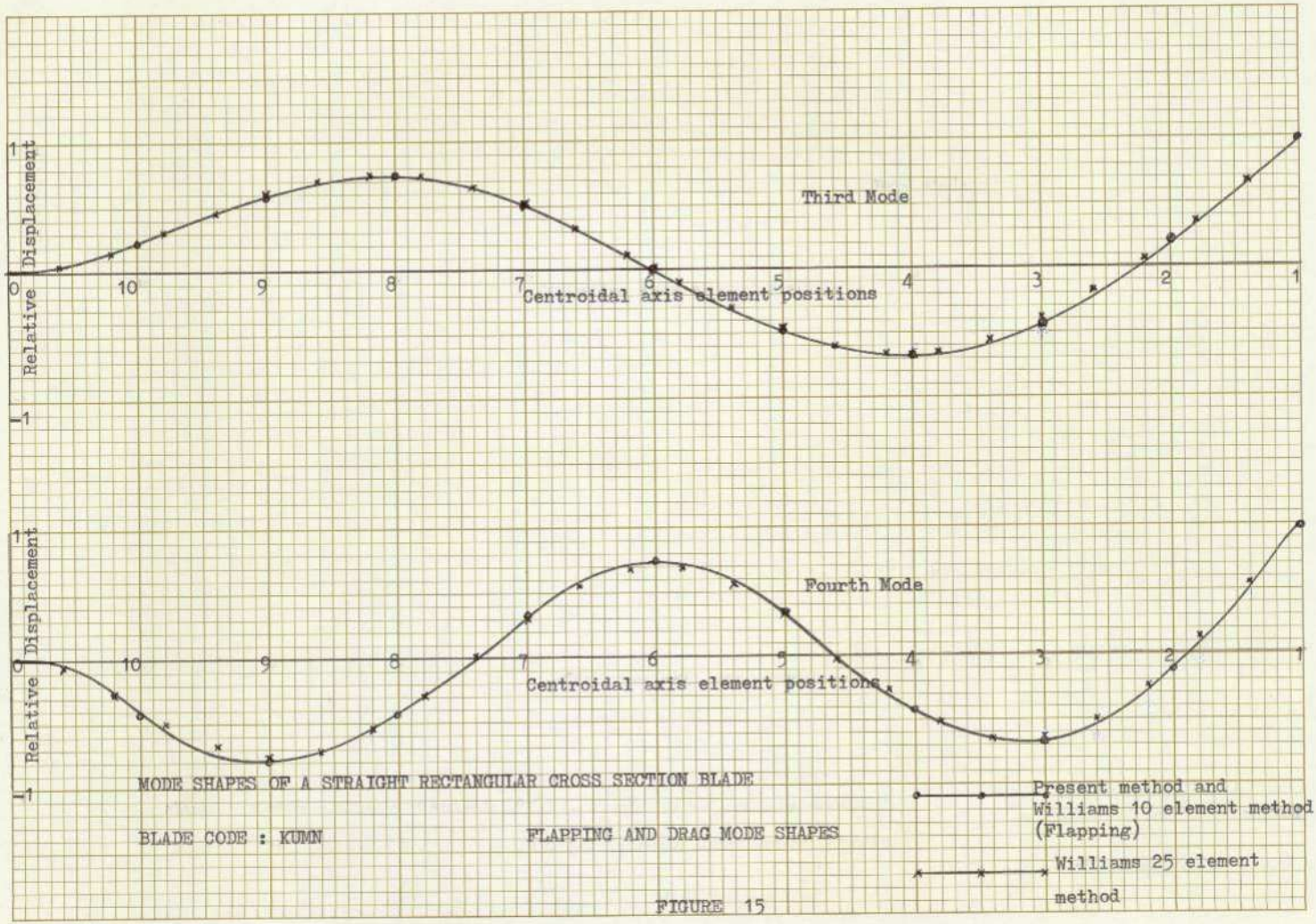

MODE SHAPES OF A STRAIGHT RECTANGULAR CROSS SECTION BLADE

BLADE CODE : KUMN

FLAPPING AND DRAG MODE SHAPES

FIGURE 15

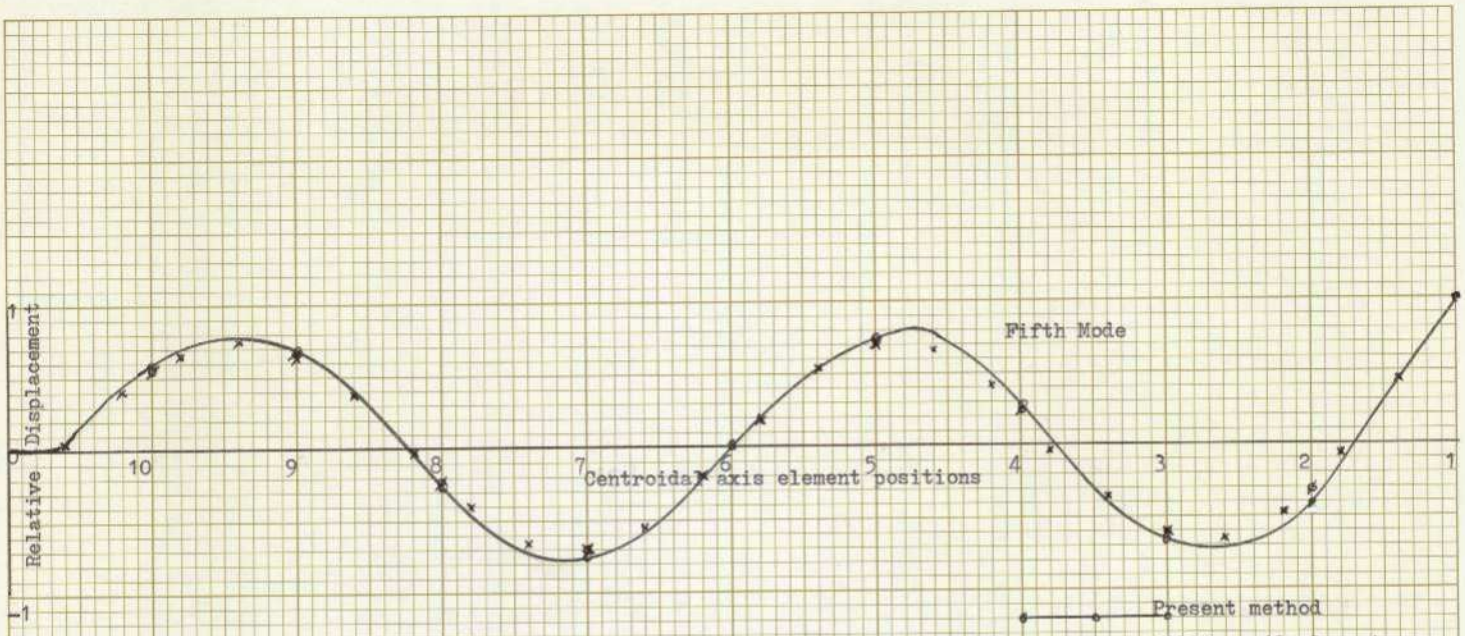

MODE SHAPES OF A STRAIGHT RECTANGULAR CROSS SECTION BLADE

BLADE CODE : KUMN

FLAPPING AND DRAG MODE SHAPES

FIGURE 16

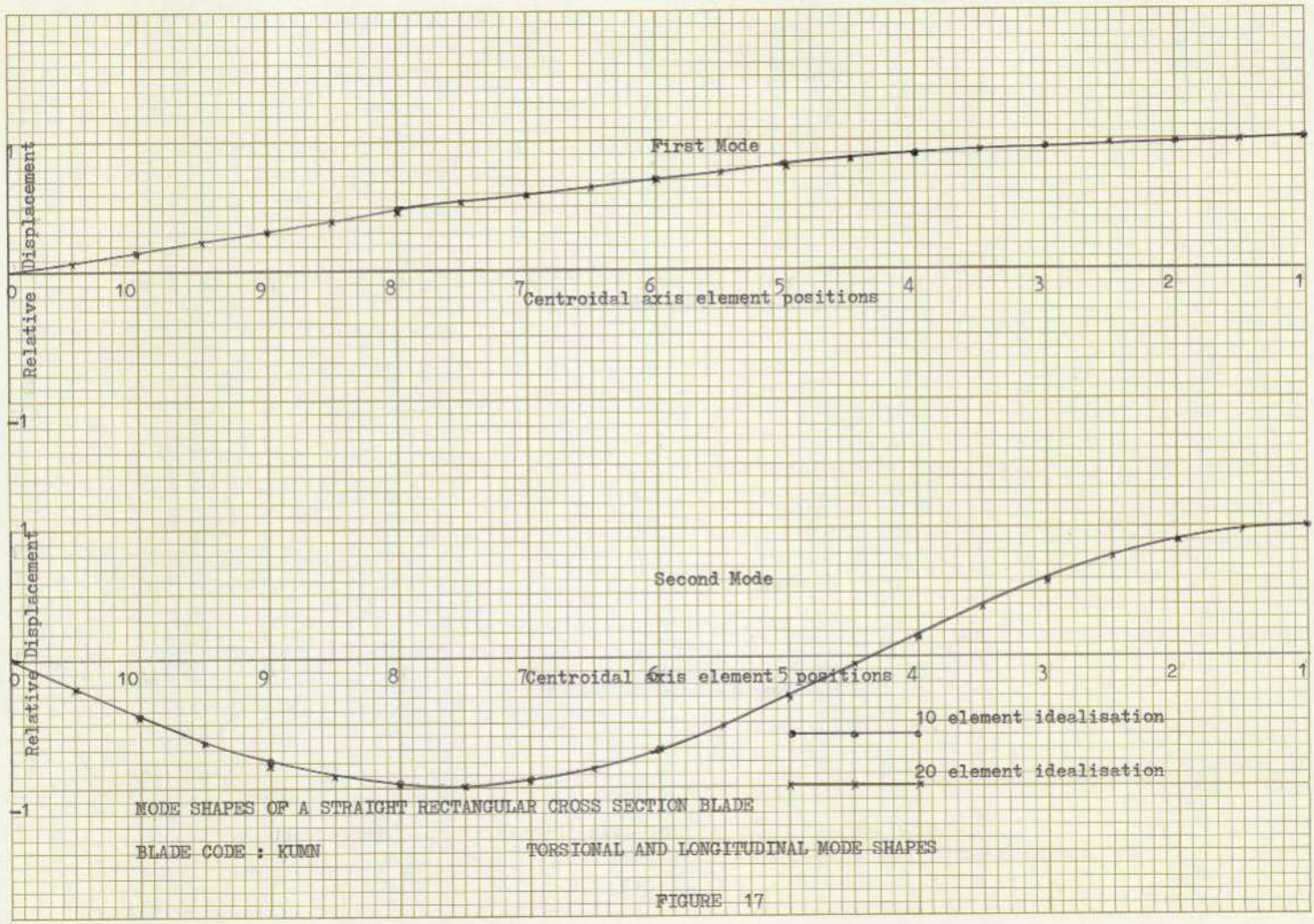

MODE SHAPES OF A STRAIGHT RECTANGULAR CROSS SECTION BLADE

BLADE CODE : KUMN

TORSIONAL AND LONGITUDINAL MODE SHAPES

FIGURE 17

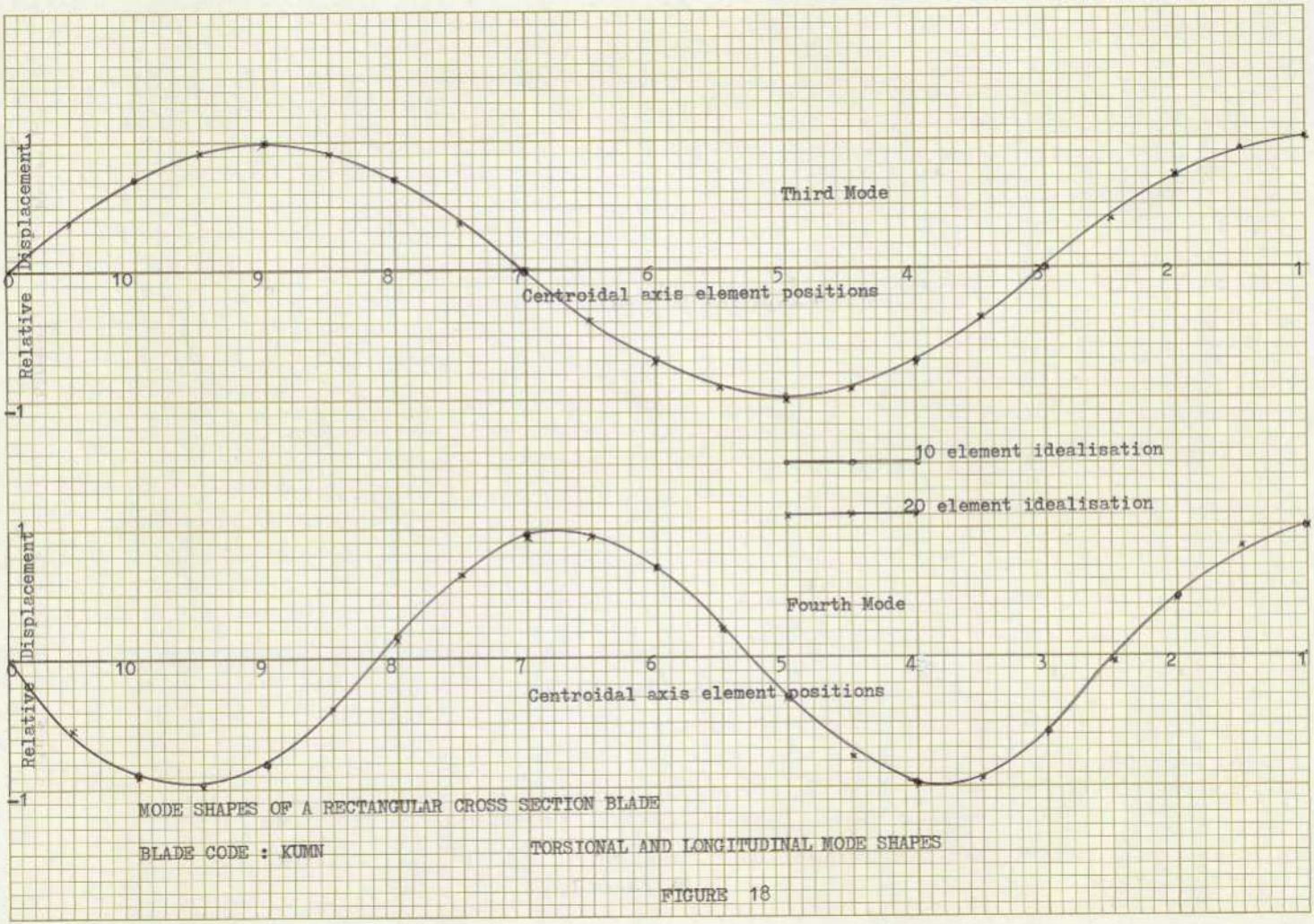

MODE SHAPES OF A RECTANGULAR CROSS SECTION BLADE

BLADE CODE : KUMN

TORSIONAL AND LONGITUDINAL MODE SHAPES

FIGURE 18

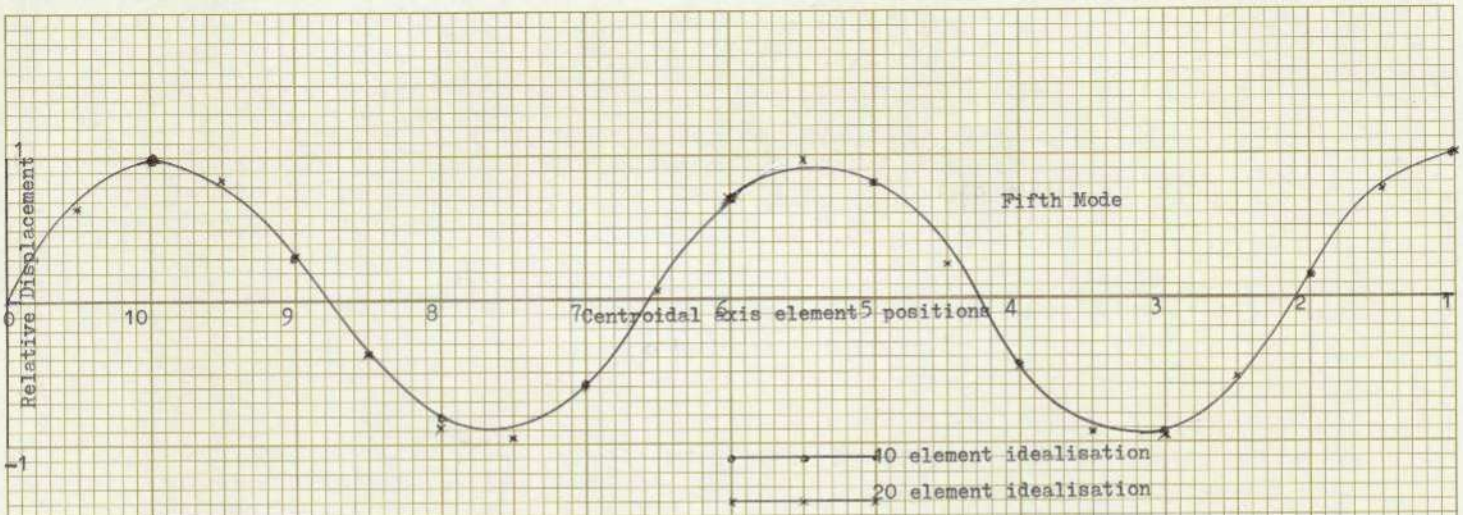

MODE SHAPES OF A RECTANGULAR CROSS SECTION BLADE

BLADE CODE : KUMN

TORSIONAL AND LONGITUDINAL MODE SHAPES

FIGURE 19

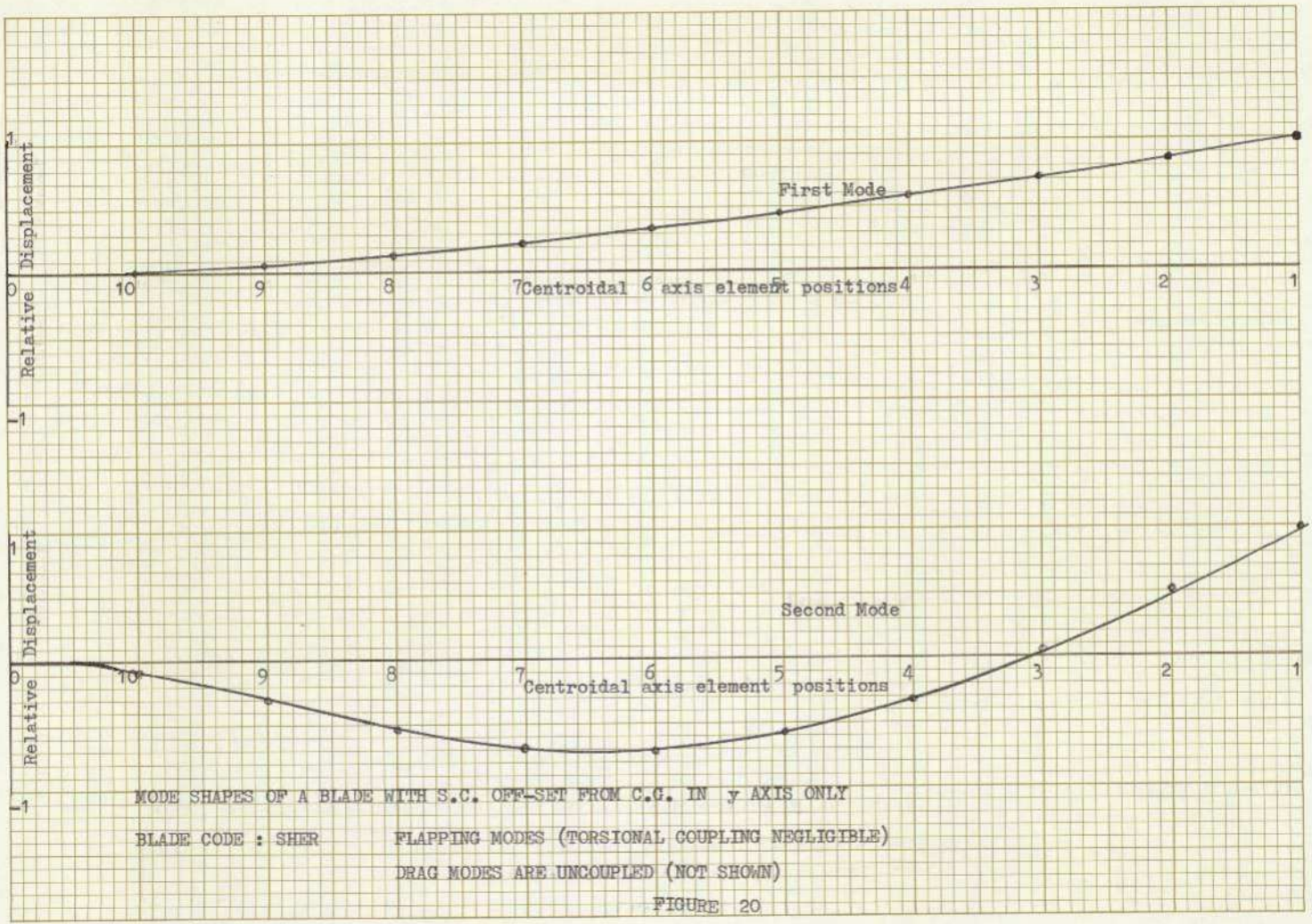

MODE SHAPES OF A BLADE WITH S.C. OFF-SET FROM C.G. IN y AXIS ONLY

BLADE CODE : SHER FLAPPING MODES (TORSIONAL COUPLING NEGLIGIBLE)

DRAG MODES ARE UNCOUPLED (NOT SHOWN)

FIGURE 20

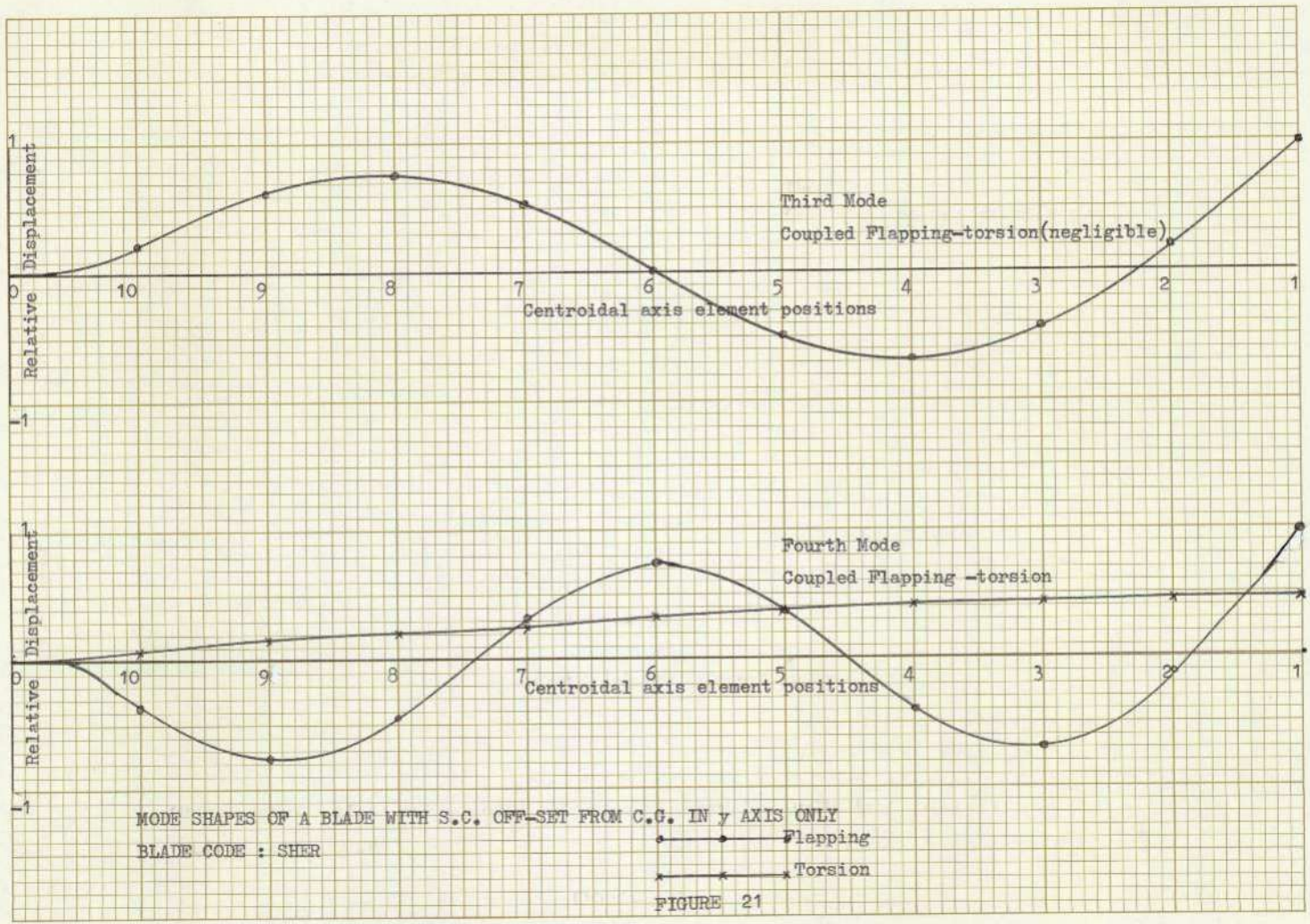

MODE SHAPES OF A BLADE WITH S.C. OFF-SET FROM C.G. IN y AXIS ONLY

BLADE CODE : SHER

FIGURE 21

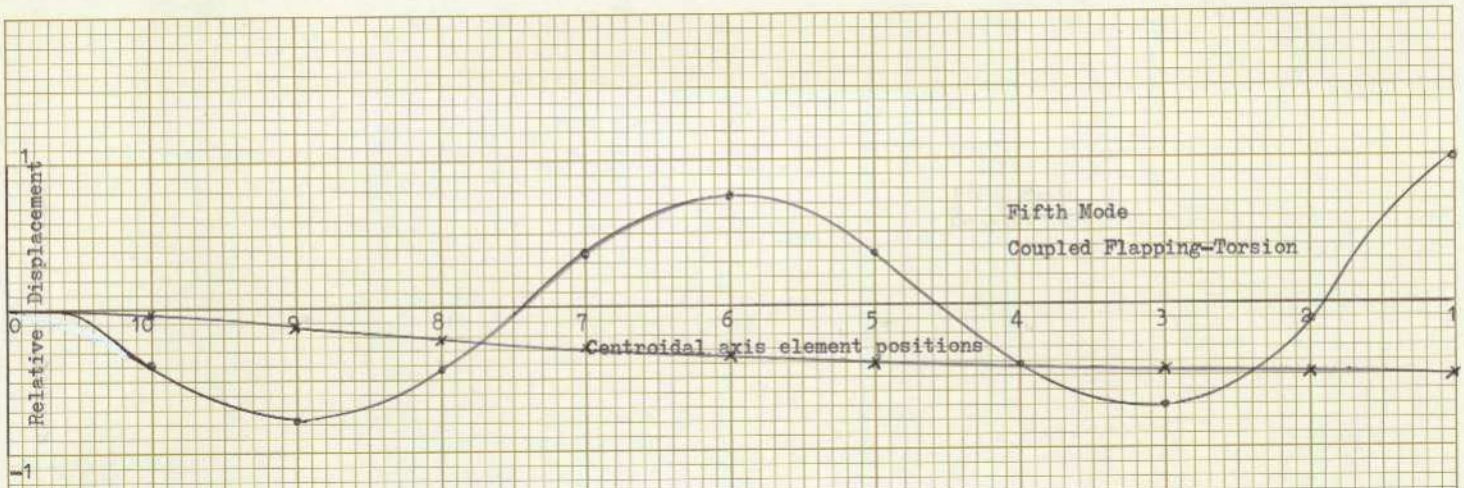

MODE SHAPES OF A BLADE WITH OFF-SET S.C. FROM C.G. IN y axis only

Flapping

Torsional

FIGURE 22

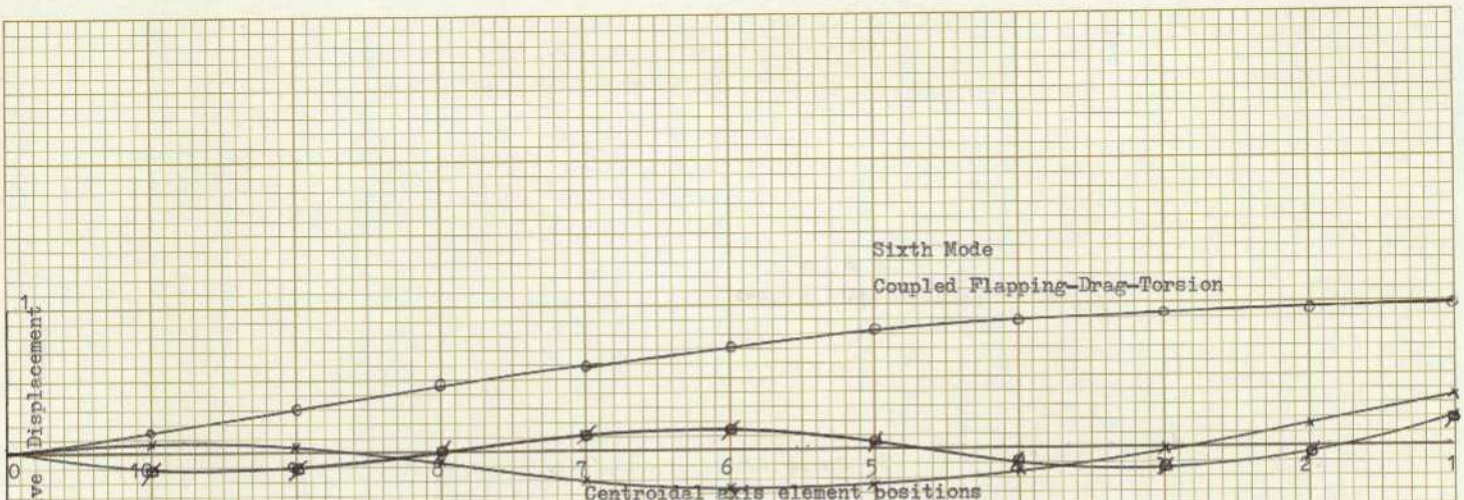

MODE SHAPES OF A BLADE WITH S.C. OFF-SET FROM C.G

FIGURE 23

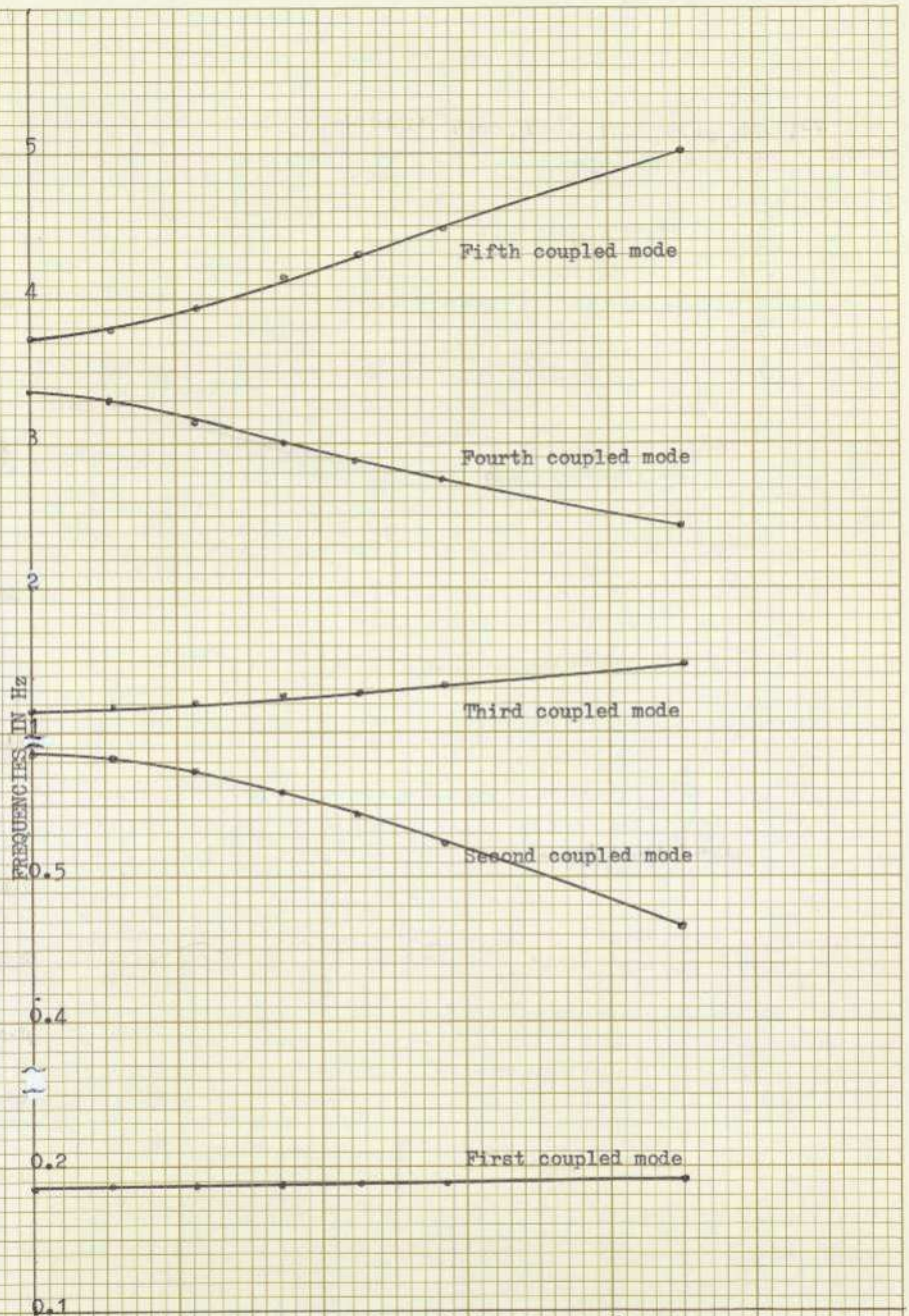

BLADE CODES :KUMN,PTO2,PTO4,PTO6,PTO8,PTC2,PTC1

FREQUENCIES OF PRETWISTED RECTANGULAR BLADES

FIGURE 24

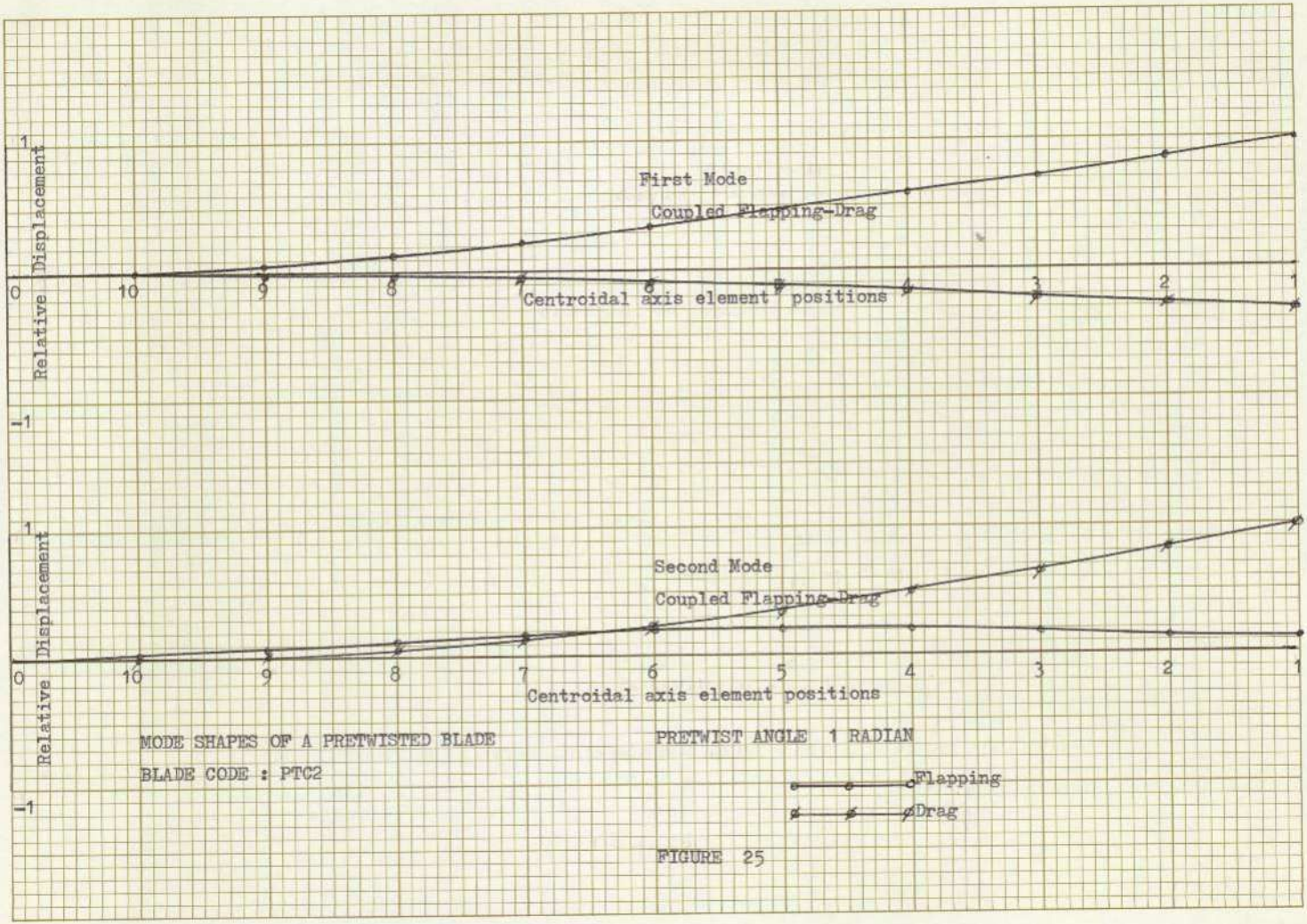
First Mode
Coupled Flapping-Drag
Relative Displacement
1
0
-1
10
9
8
7
6
5
4
3
2
1
Centroidal axis element positions
Second Mode
Coupled Flapping-Drag
Relative Displacement
1
0
-1
10
9
8
7
6
5
4
3
2
1
Centroidal axis element positions
MODE SHAPES OF A PRETWISTED BLADE
BLADE CODE : PTC2
PRETWIST ANGLE 1 RADIAN
Flapping
Drag

FIGURE 25

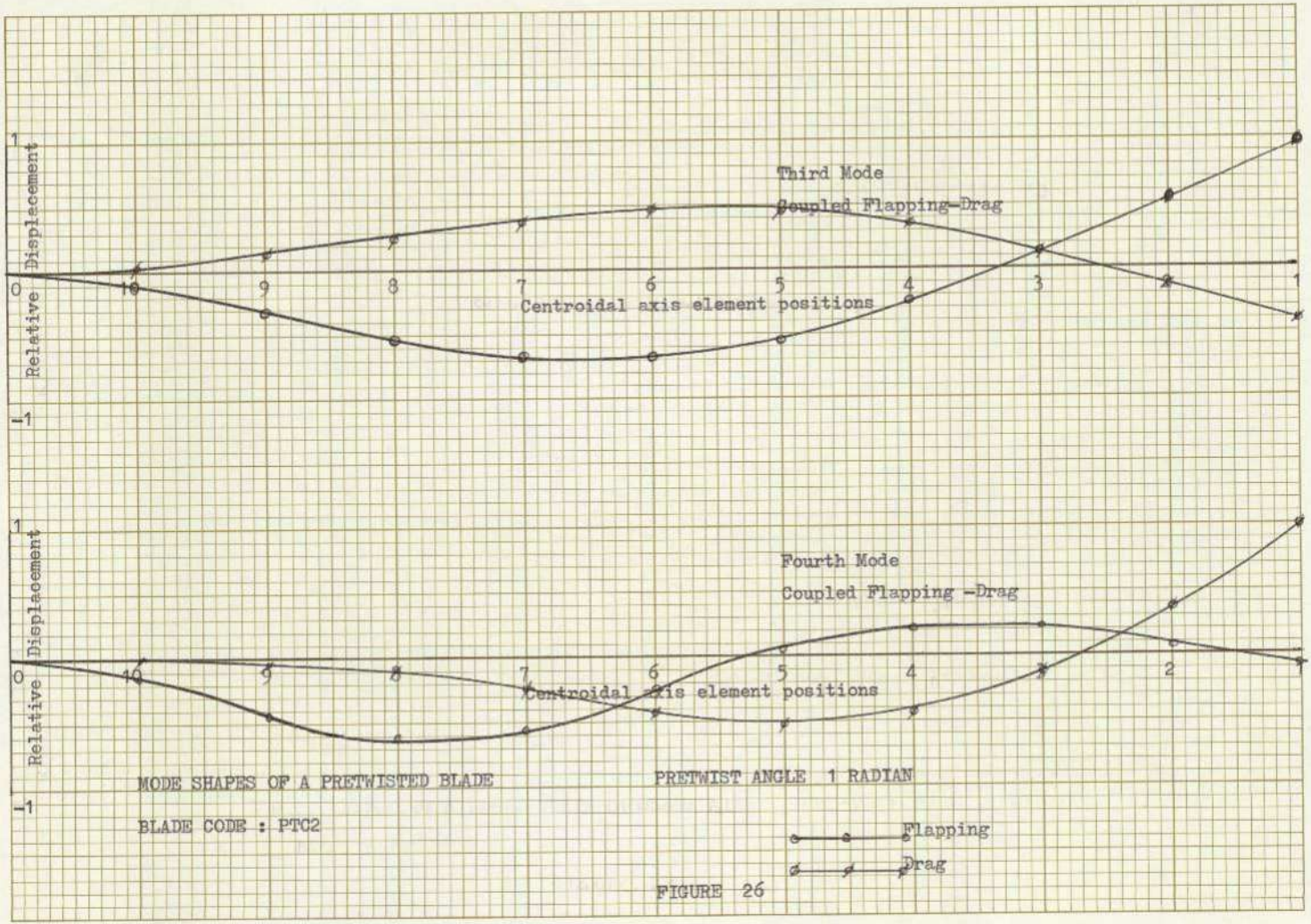
Third Mode
Coupled Flapping-Drag
Relative Displacement
1
0
-1
10
9
8
7
6
5
4
3
2
1
Centroidal axis element positions
Fourth Mode
Coupled Flapping -Drag
Relative Displacement
1
0
-1
10
9
8
7
6
5
4
2
1
Centroidal axis element positions
MODE SHAPES OF A PRETWISTED BLADE
BLADE CODE : PTC2
PRETWIST ANGLE 1 RADIAN
Flapping
Drag

FIGURE 26

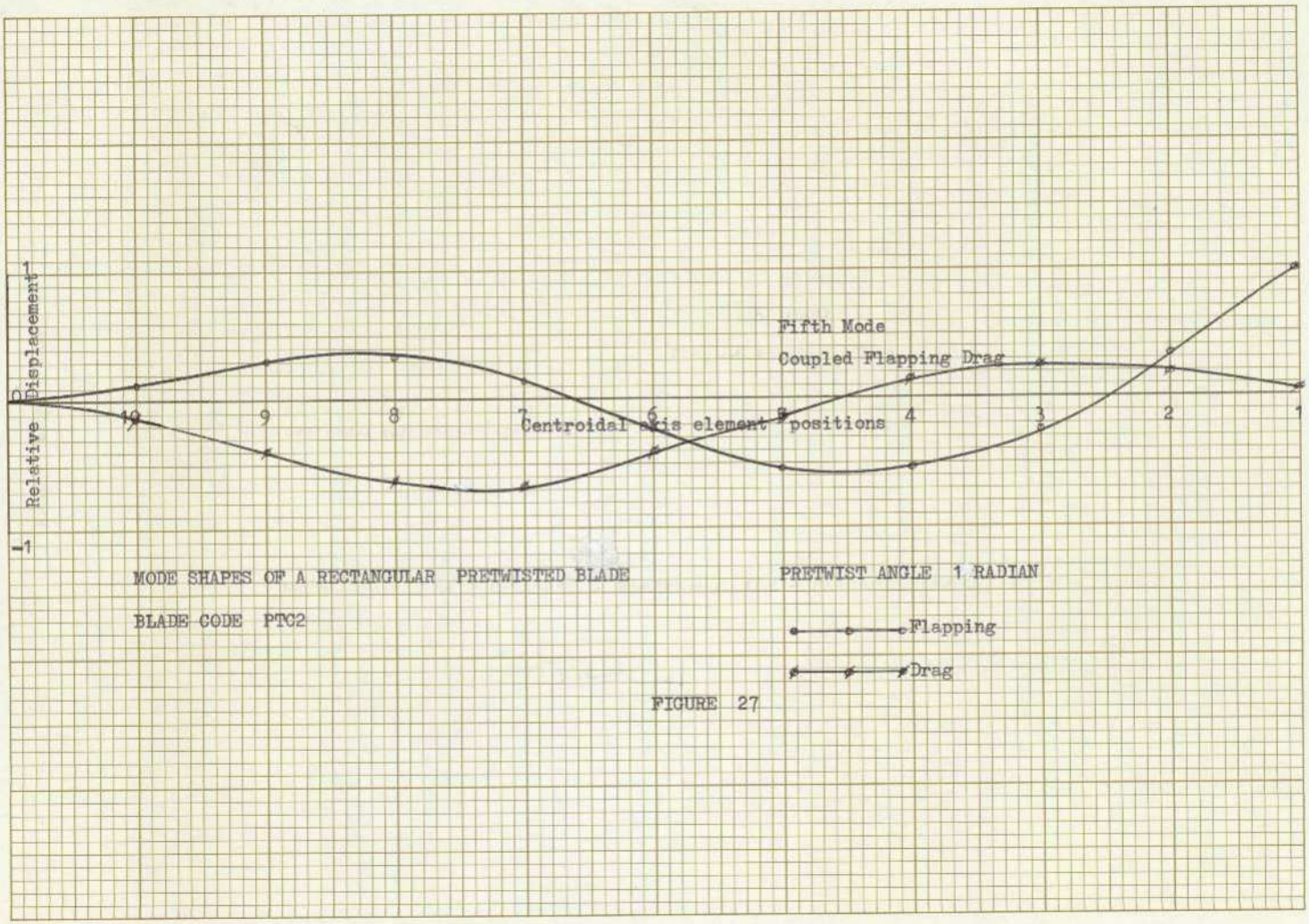
Relative Displacement
1
0
-1
10
9
8
7
6
5
4
3
2
1
Centroidal axis element positions
Fifth Mode
Coupled Flapping Drag
MODE SHAPES OF A RECTANGULAR PRETWISTED BLADE
BLADE CODE PTC2
PRETWIST ANGLE 1 RADIAN
Flapping
Drag

FIGURE 27

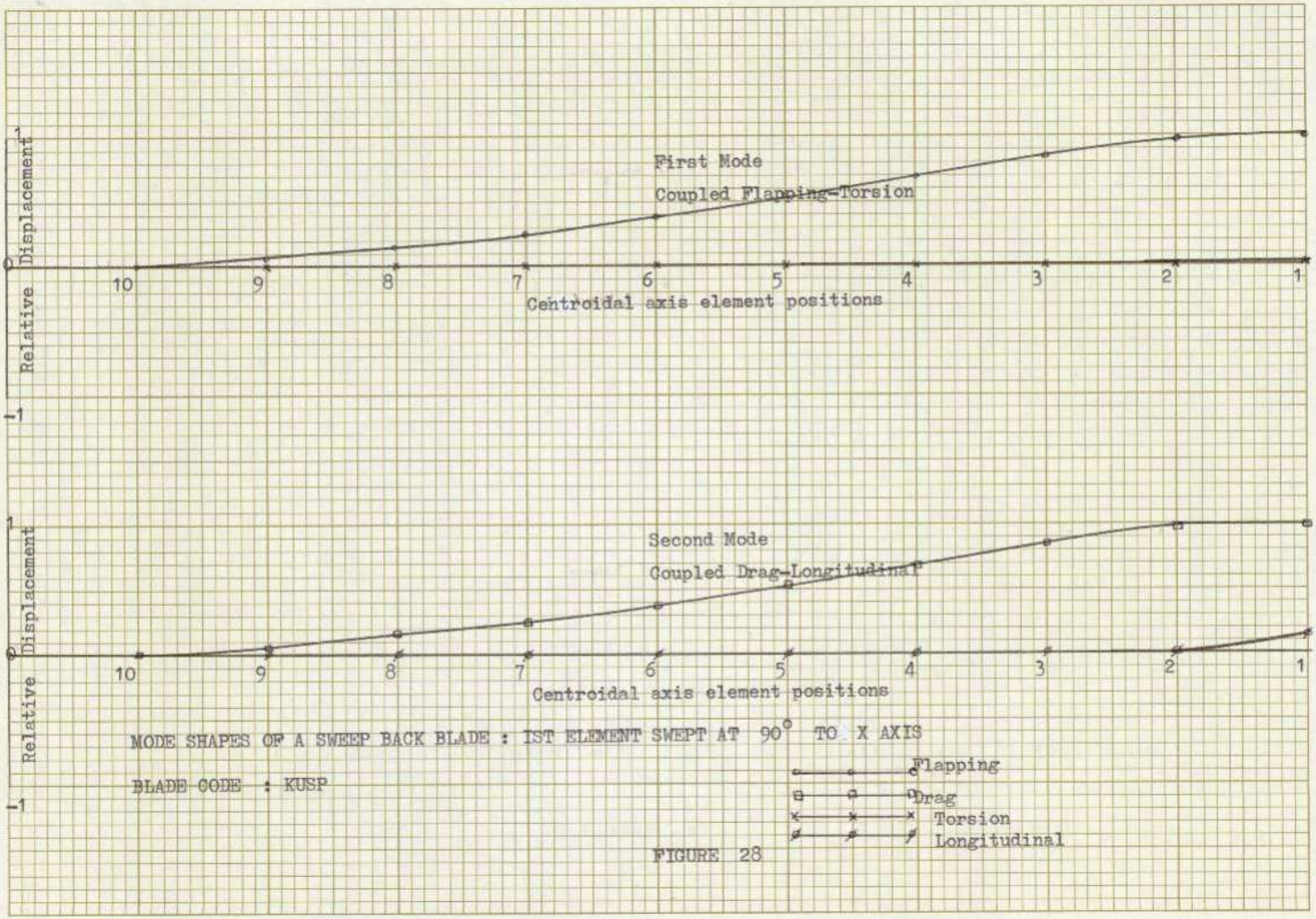
First Mode
Coupled Flapping-Torsion
Relative Displacement
1
0
1
10
9
8
7
6
5
4
3
2
1
Centroidal axis element positions
Second Mode
Coupled Drag-Longitudinal
Relative Displacement
1
0
1
10
9
8
7
6
5
4
3
2
1
Centroidal axis element positions
MODE SHAPES OF A SWEEP BACK BLADE : IST ELEMENT SWEPT AT 90° TO X AXIS
BLADE CODE : KUSP
Flapping
Drag
Torsion
Longitudinal

FIGURE 28

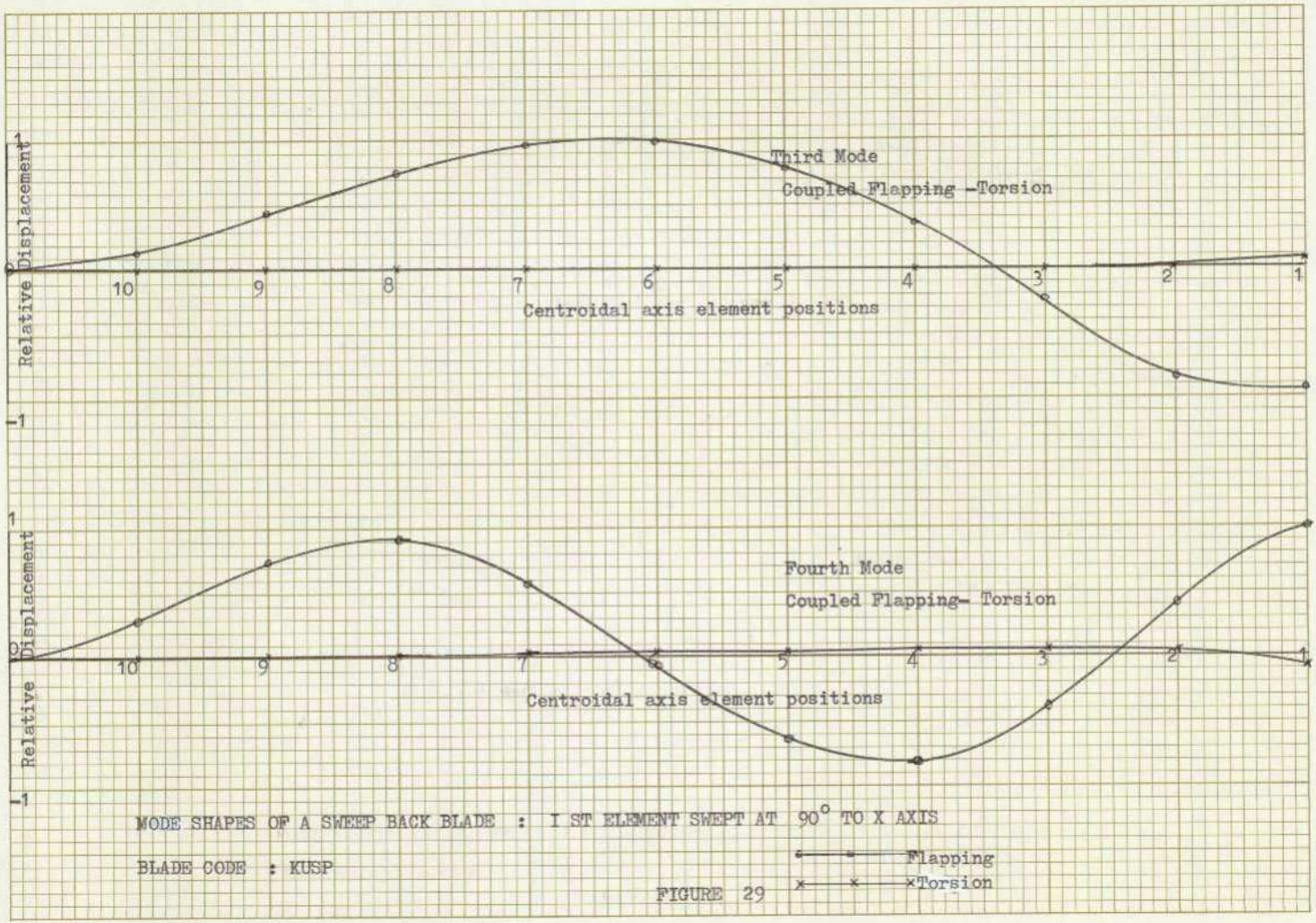
Third Mode
Coupled Flapping -Torsion
Relative Displacement
10
9
8
7
6
5
4
3
2
1
Centroidal axis element positions
Fourth Mode
Coupled Flapping- Torsion
Relative Displacement
Centroidal axis element positions
MODE SHAPES OF A SWEEP BACK BLADE : I ST ELEMENT SWEPT AT 90° TO X AXIS
BLADE CODE : KUSP
Flapping
Torsion

FIGURE 29

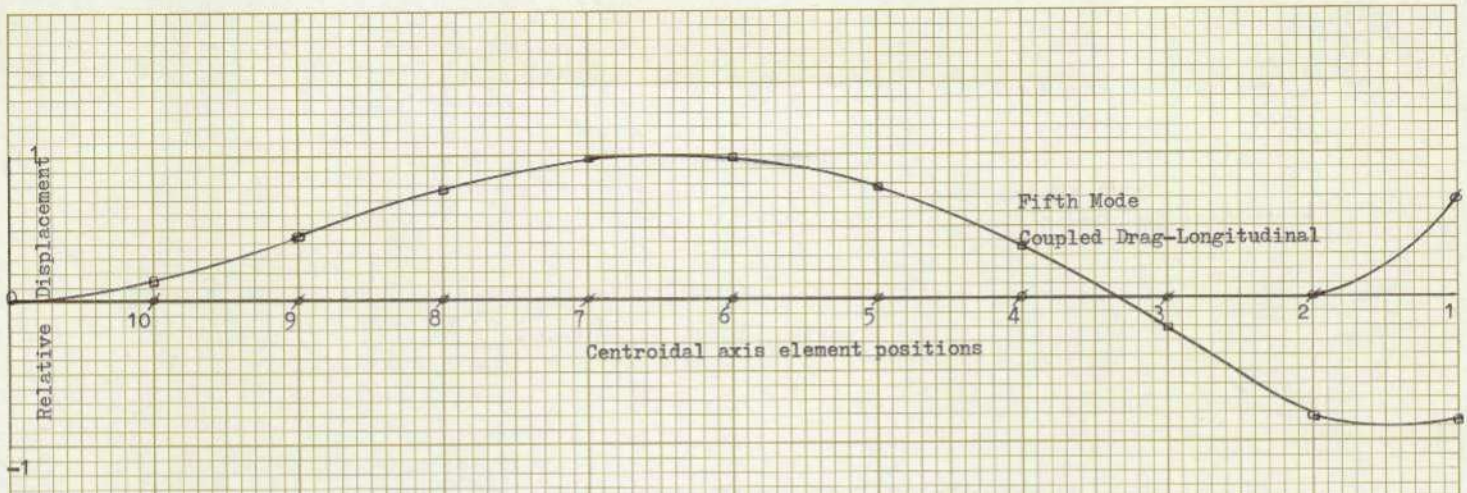

MODE SHAPES OF A SWEEP BACK BLADE : I ST ELEMENT SWEPT AT 90° TO X AXIS

Drag

Longitudinal

BLADE CODE : KUSP

FIGURE 30

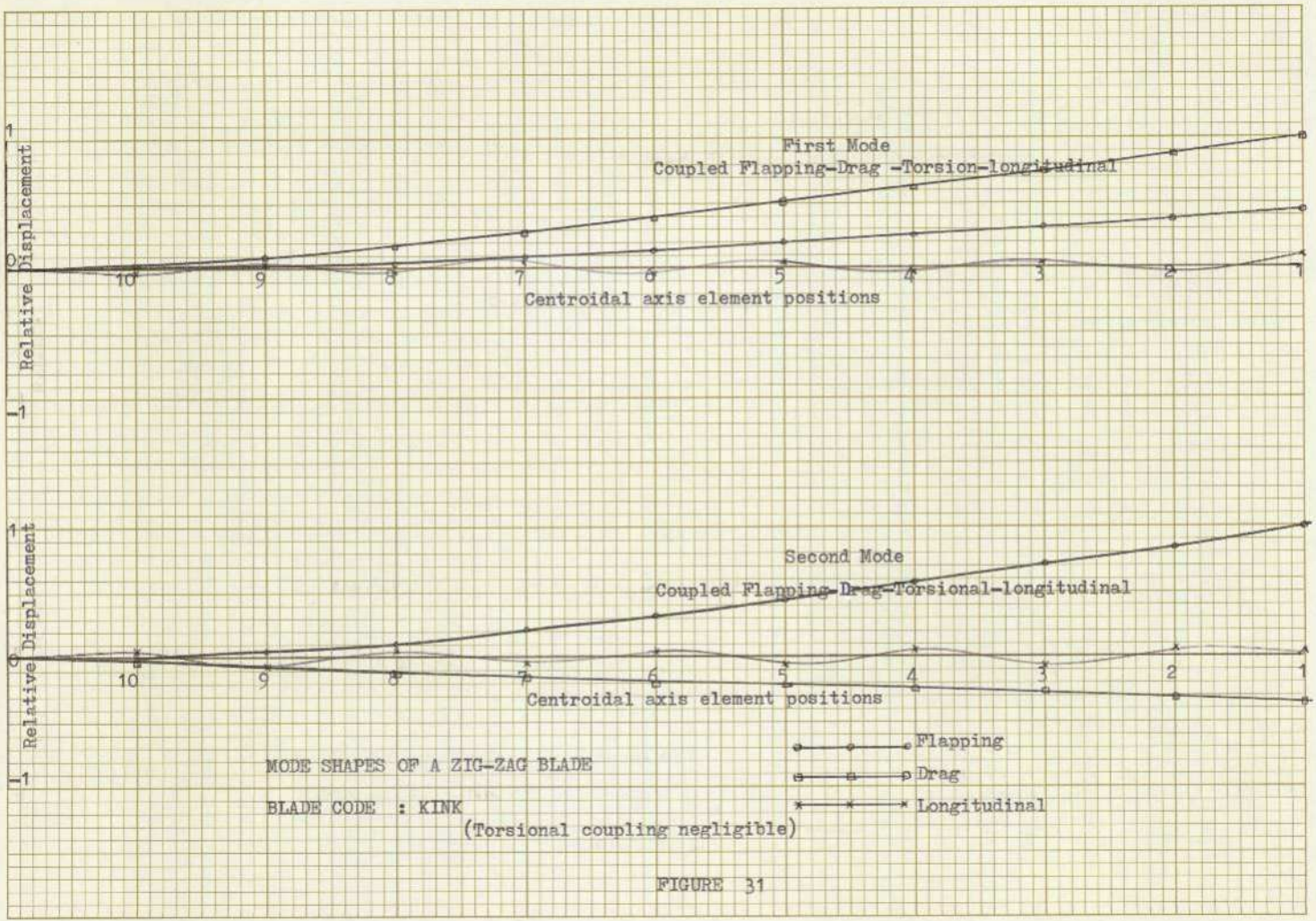

MODE SHAPES OF A ZIG-ZAG BLADE

BLADE CODE : KINK

(Torsional coupling negligible)

FIGURE 31

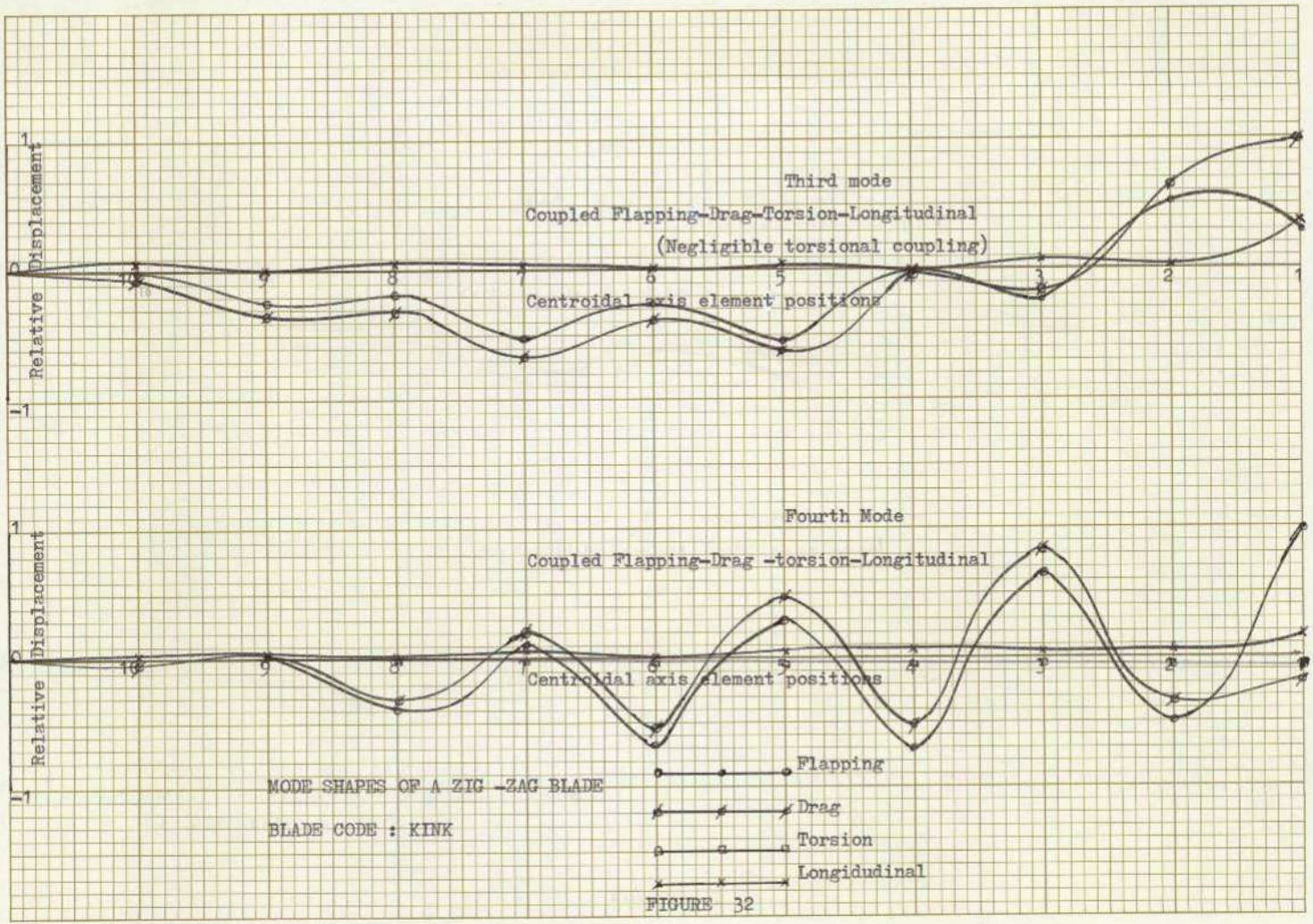
Third mode
Coupled Flapping-Drag-Torsion-Longitudinal
(Negligible torsional coupling)
Centroidal axis element positions
Relative Displacement
1
0
-1
Fourth Mode
Coupled Flapping-Drag -torsion-Longitudinal
Centroidal axis element positions
Relative Displacement
1
0
-1
MODE SHAPES OF A ZIG -ZAG BLADE
BLADE CODE : KINK
Flapping
Drag
Torsion
Longidudinal

FIGURE 32

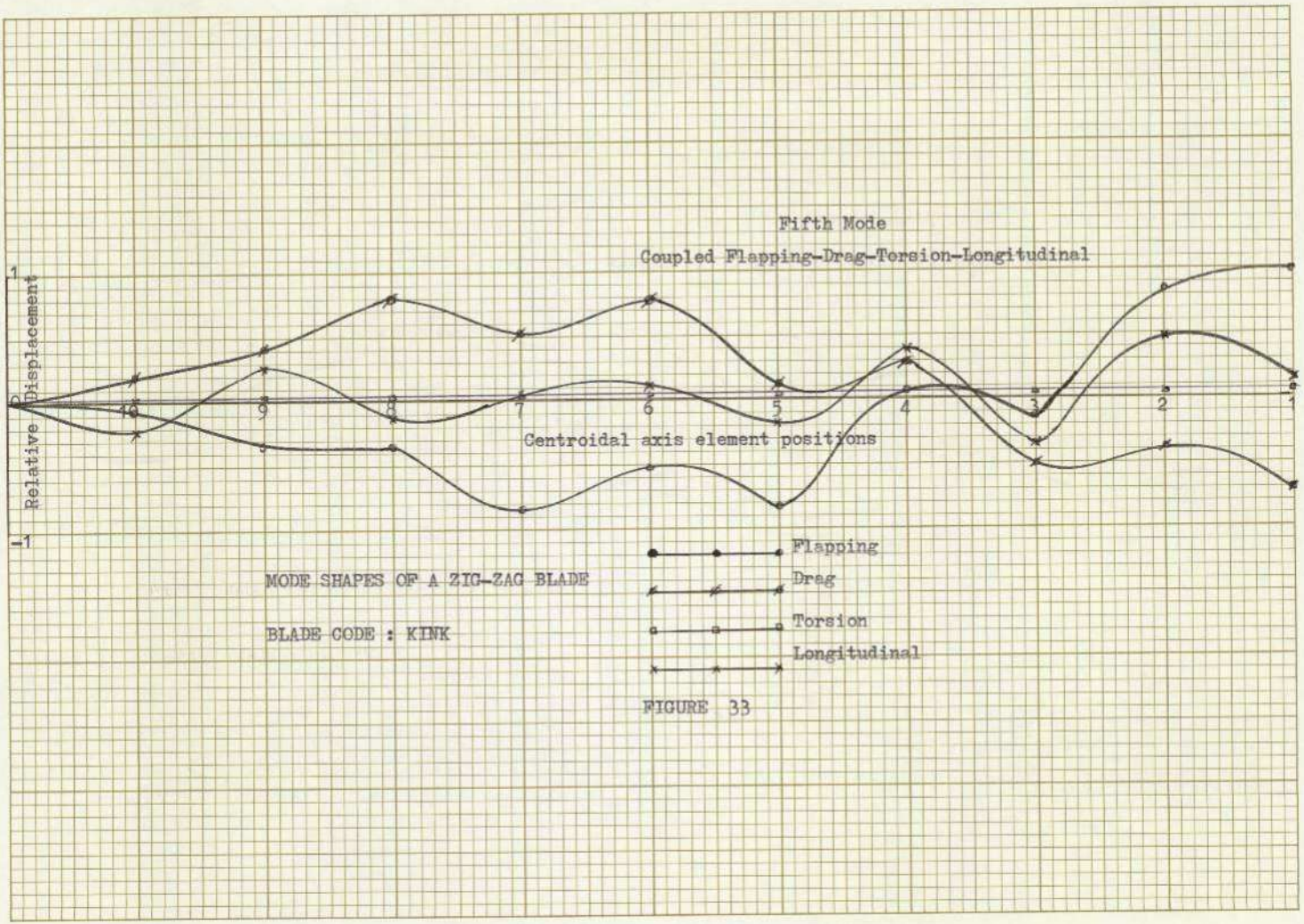

MODE SHAPES OF A ZIG-ZAG BLADE

BLADE CODE : KINK

FIGURE 33

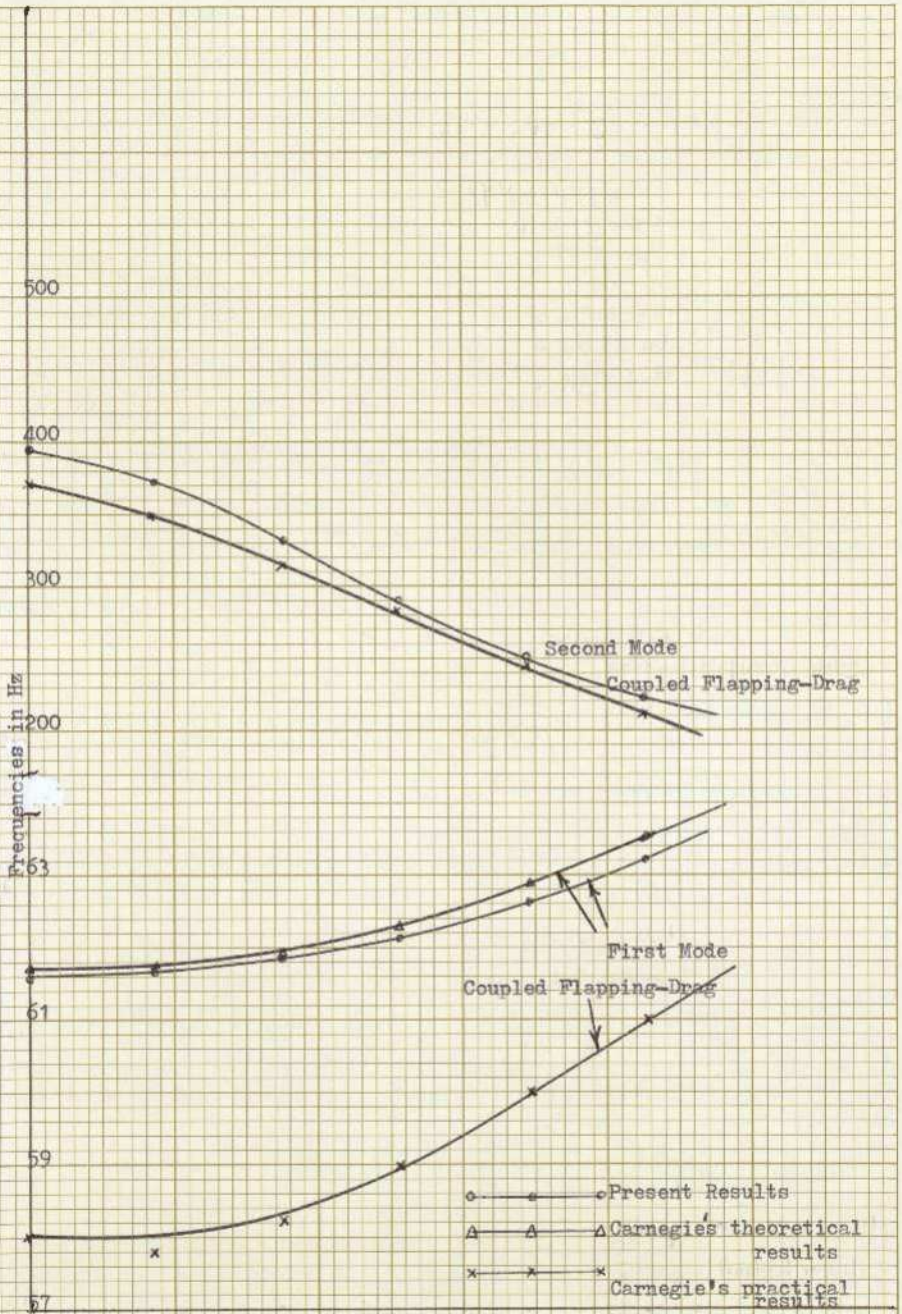

FREQUENCIES OF PRETWISTED RECTANGULAR BLADES

BLADE CODES :TAM0, TAM1, TAM2, TAM3, TAM4, TAM5

FIGURE 34

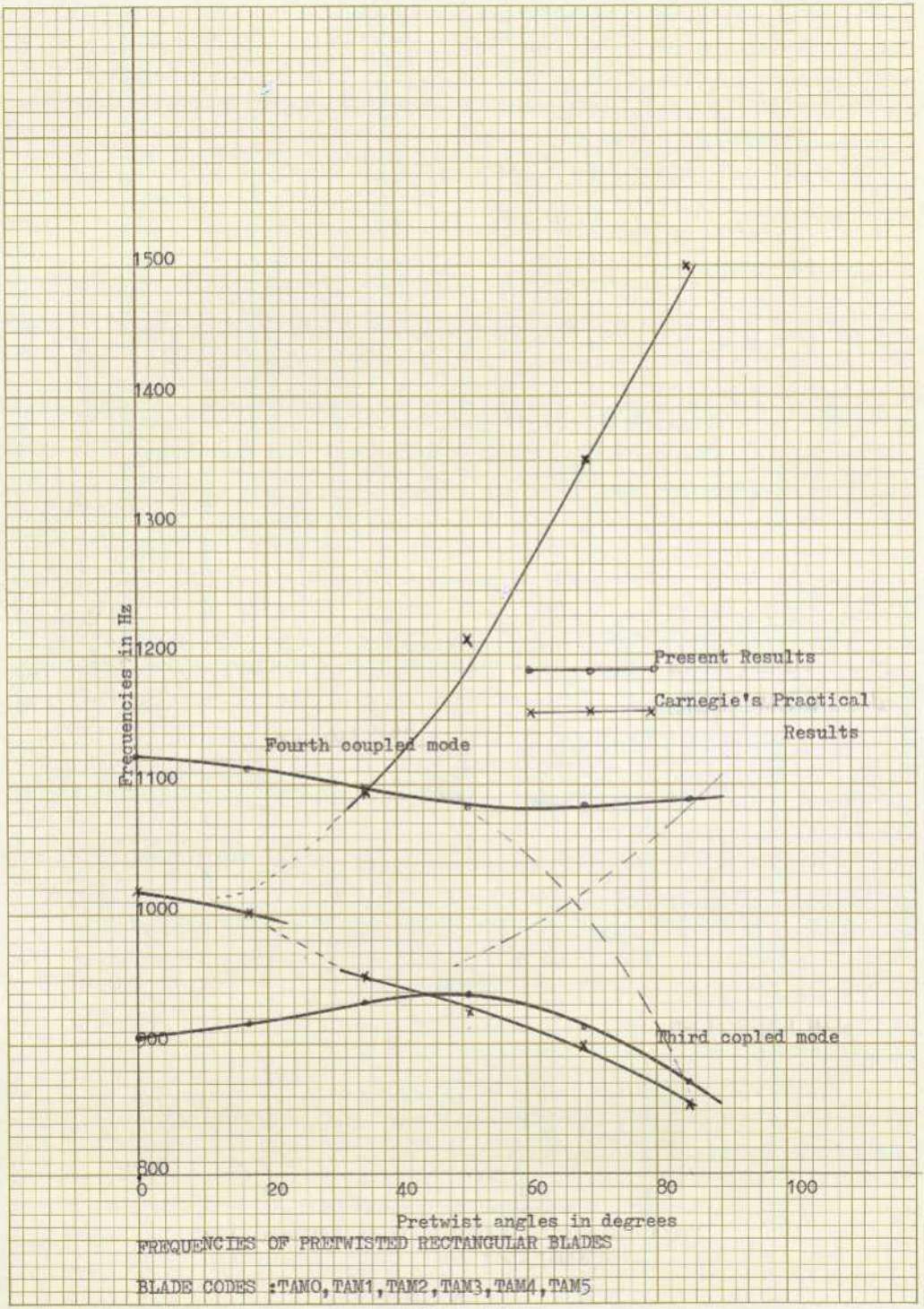

FREQUENCIES OF PRETWISTED RECTANGULAR BLADES

BLADE CODES :TAM0, TAM1, TAM2, TAM3, TAM4, TAM5

FIGURE 35

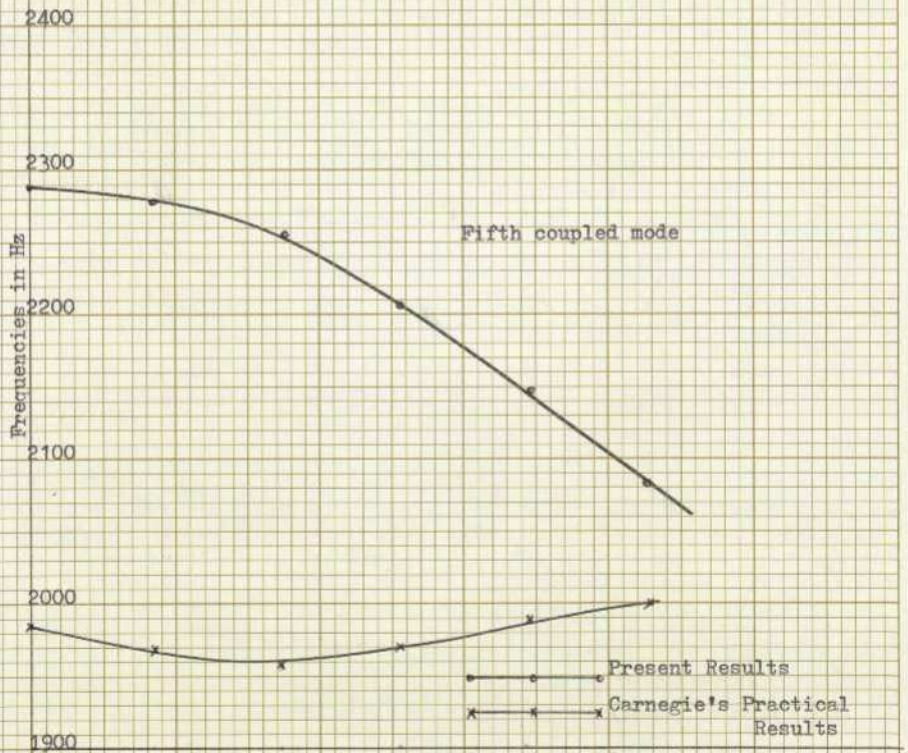

FREQUENCIES OF PRETWISTED RECTANGULAR BLADE

BLADE CODES: TAM0, TAM1, TAM2, TAM3, TAM4, TAM5

FIGURE 36

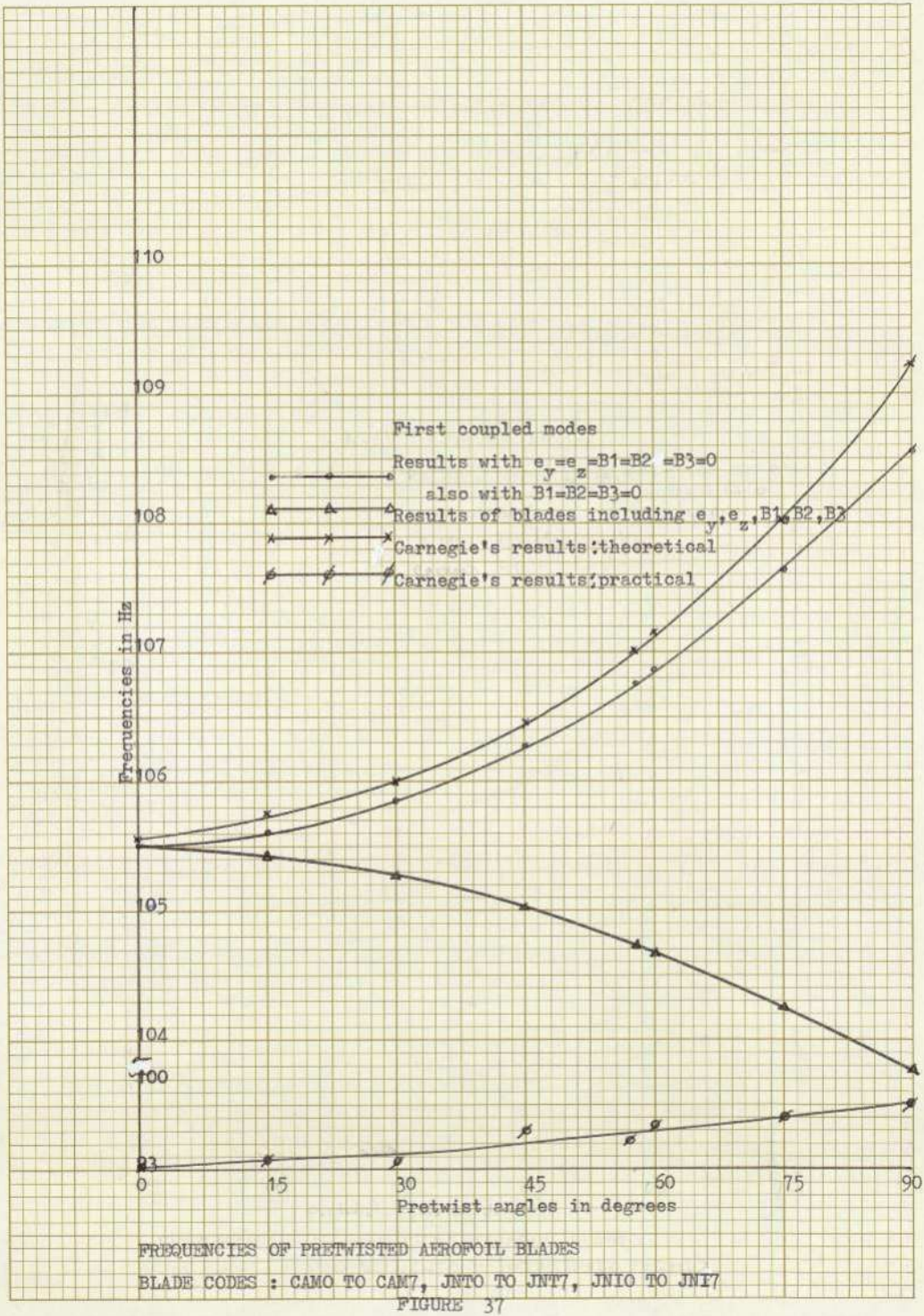

FREQUENCIES OF PRETWISTED AEROFOIL BLADES

BLADE CODES : CAM0 TO CAM7, JNT0 TO JNT7, JNI0 TO JNI7

FIGURE 37

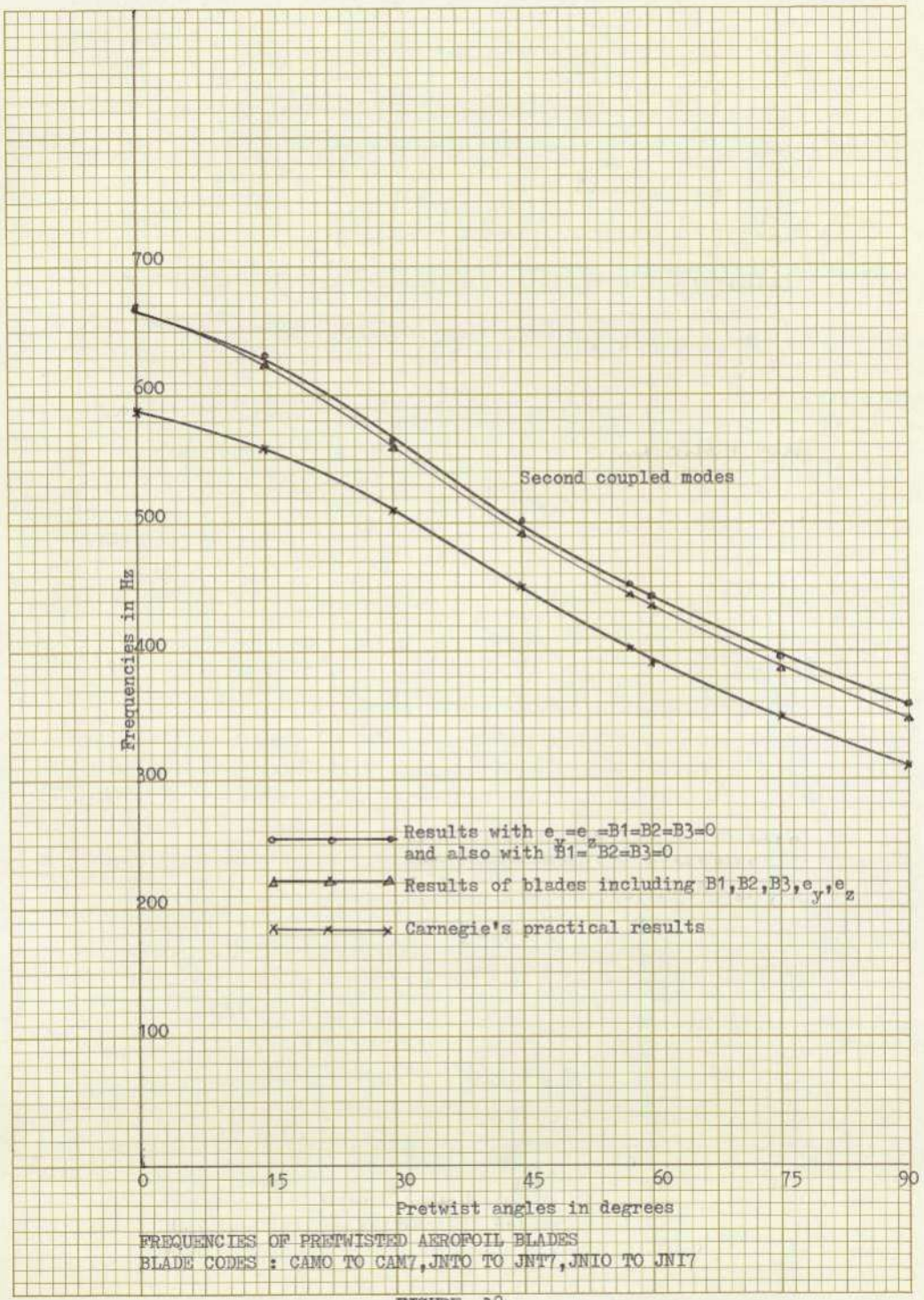

FREQUENCIES OF PRETWISTED AEROFOIL BLADES
BLADE CODES : CAM0 TO CAM7, JNT0 TO JNT7, JNI0 TO JNI7

FIGURE 38

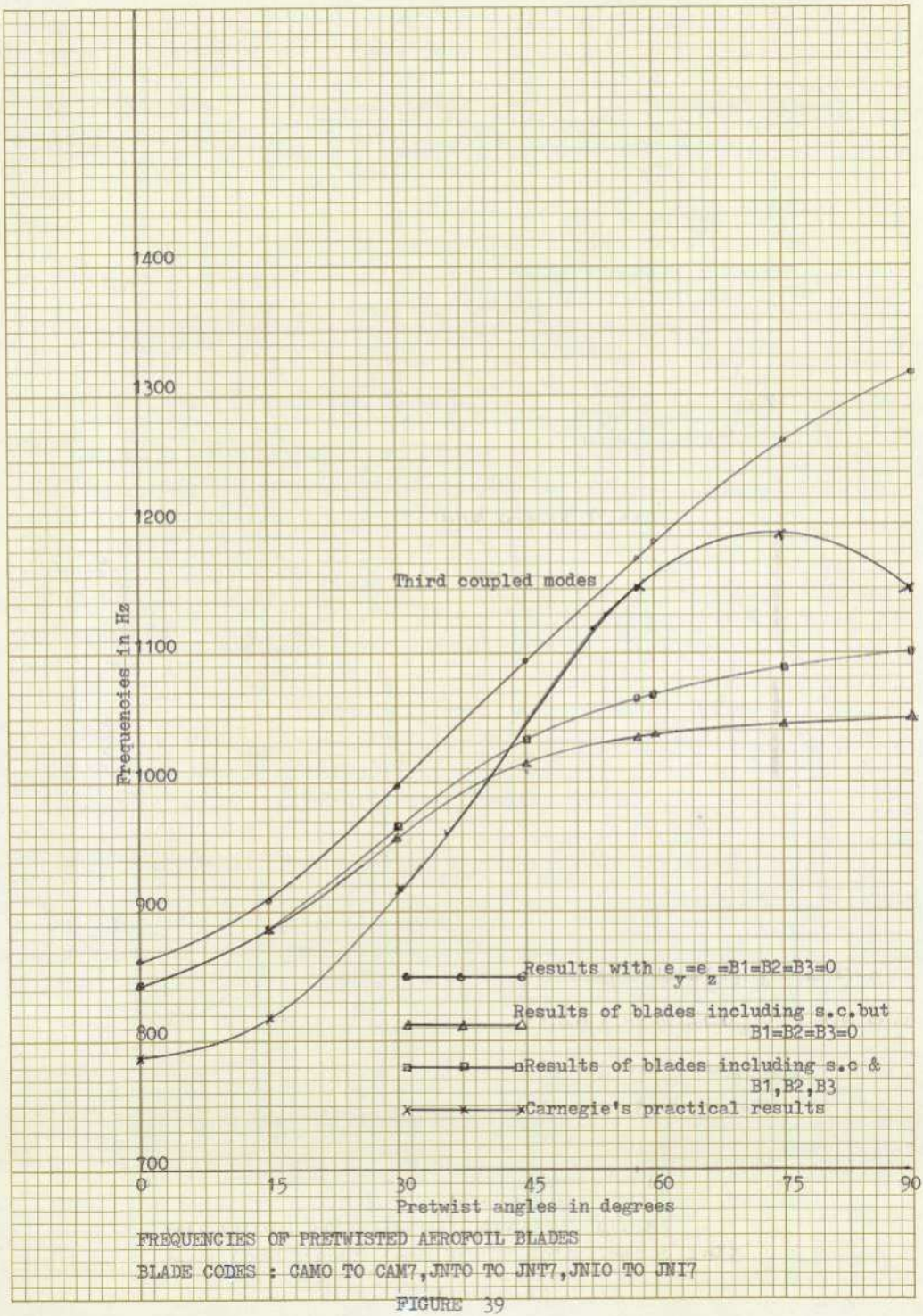

FREQUENCIES OF PRETWISTED AEROFOIL BLADES

BLADE CODES : CAM0 TO CAM7, JNT0 TO JNT7, JNI0 TO JNI7

FIGURE 39

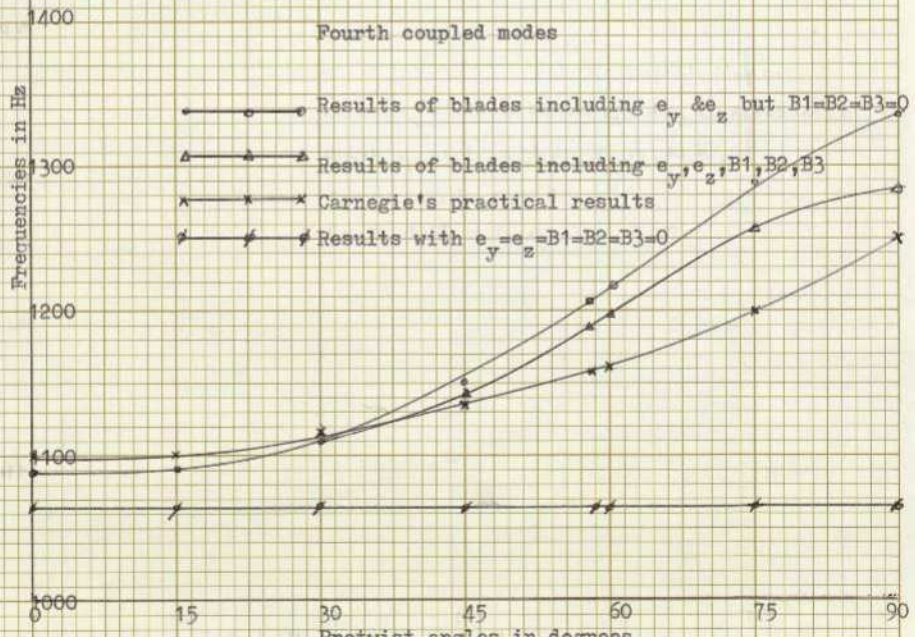

FREQUENCIES OF PRETWISTED AEROFOIL BLADES

BLADE CODES : CAMO TO CAM7, JNTO TO JNT7, JNIO TO JNI7

FIGURE 40

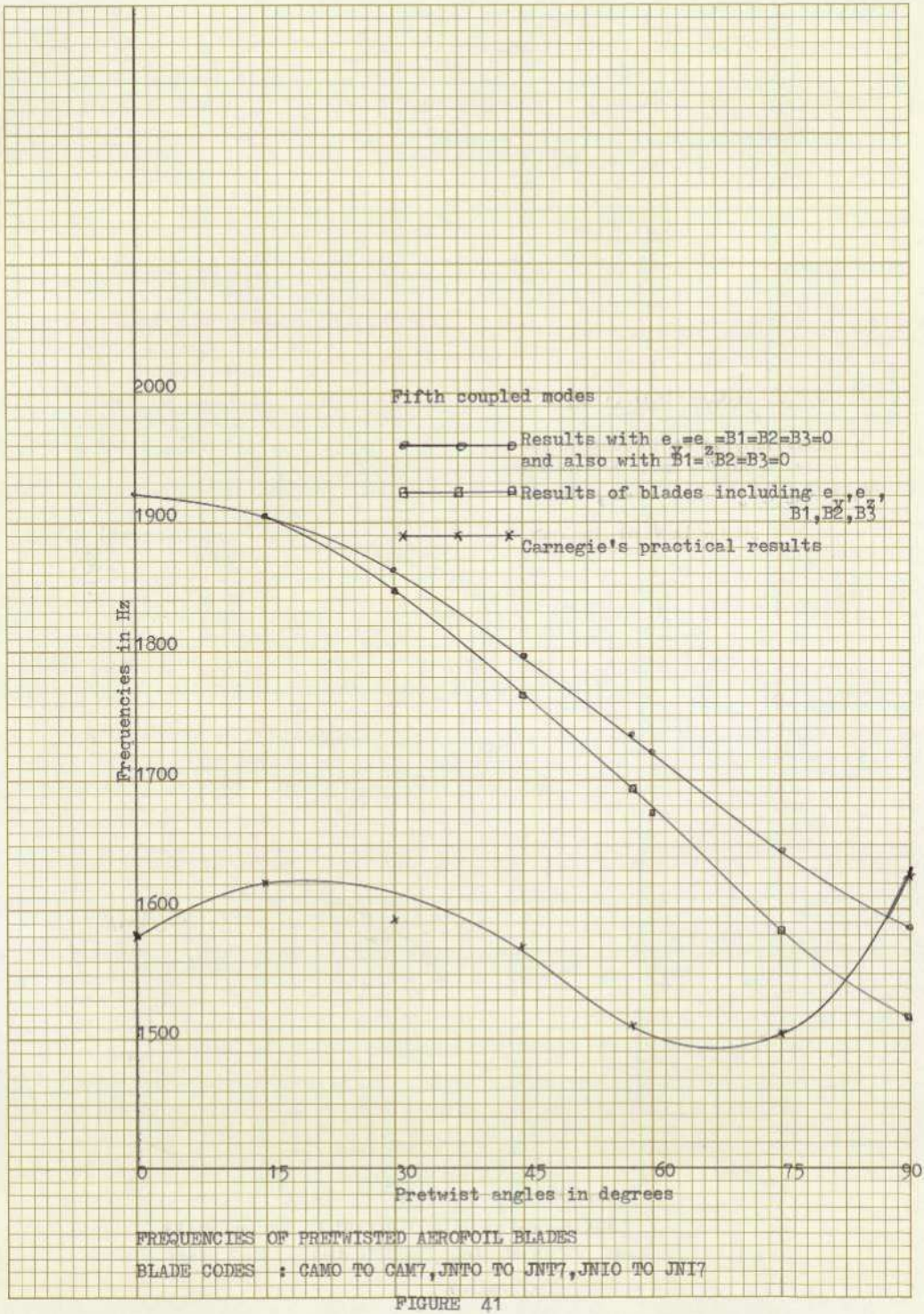

FREQUENCIES OF PRETWISTED AEROFOIL BLADES

BLADE CODES : CAM0 TO CAM7, JNT0 TO JNT7, JNI0 TO JNI7

FIGURE 41

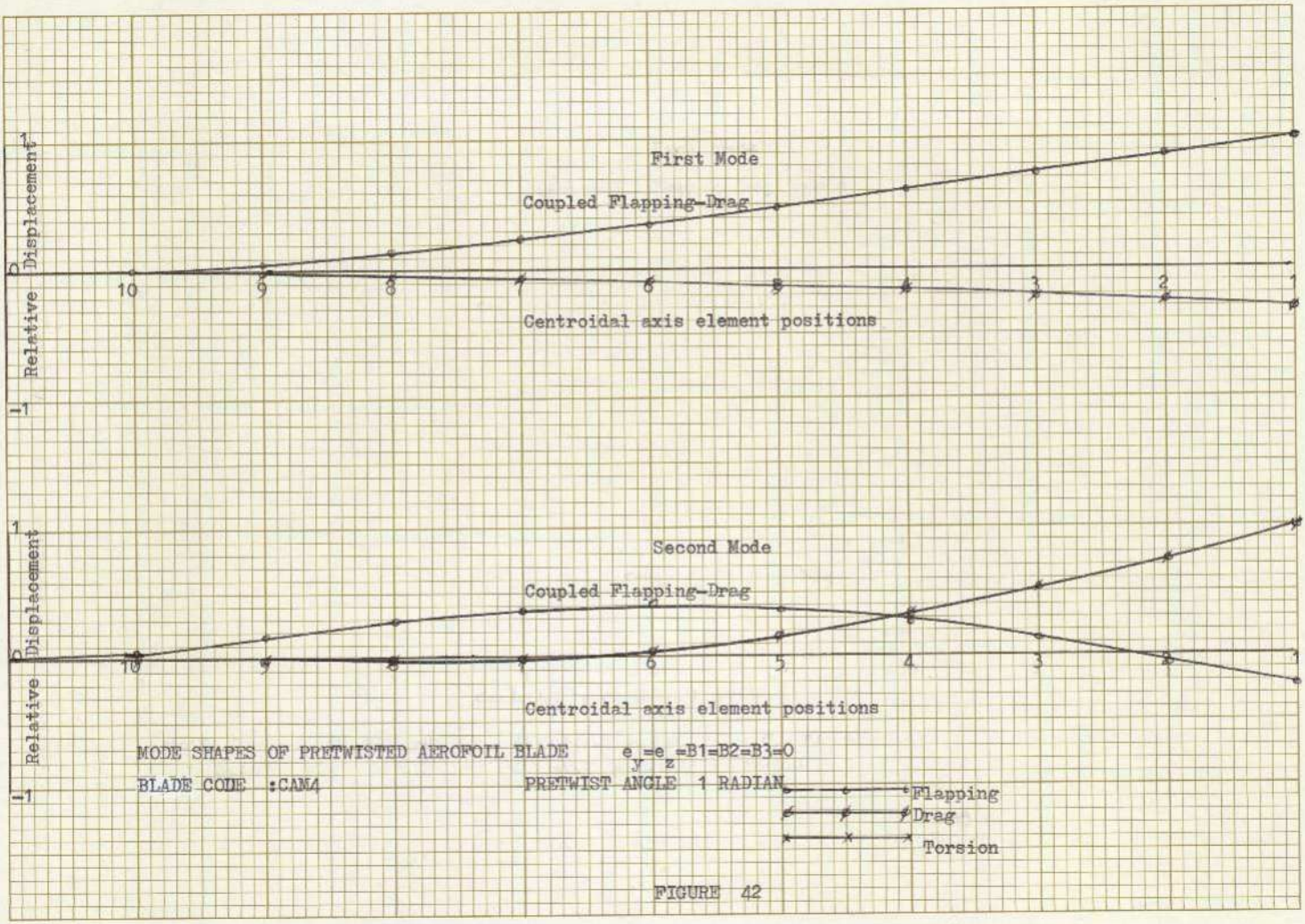
First Mode
Coupled Flapping-Drag
Relative Displacement
Centroidal axis element positions
Second Mode
Coupled Flapping-Drag
Relative Displacement
Centroidal axis element positions
MODE SHAPES OF PRETWISTED AEROFOIL BLADE e_y=e_z=B1=B2=B3=0
BLADE CODE :CAM4
PRETWIST ANGLE 1 RADIAN
Flapping
Drag
Torsion

FIGURE 42

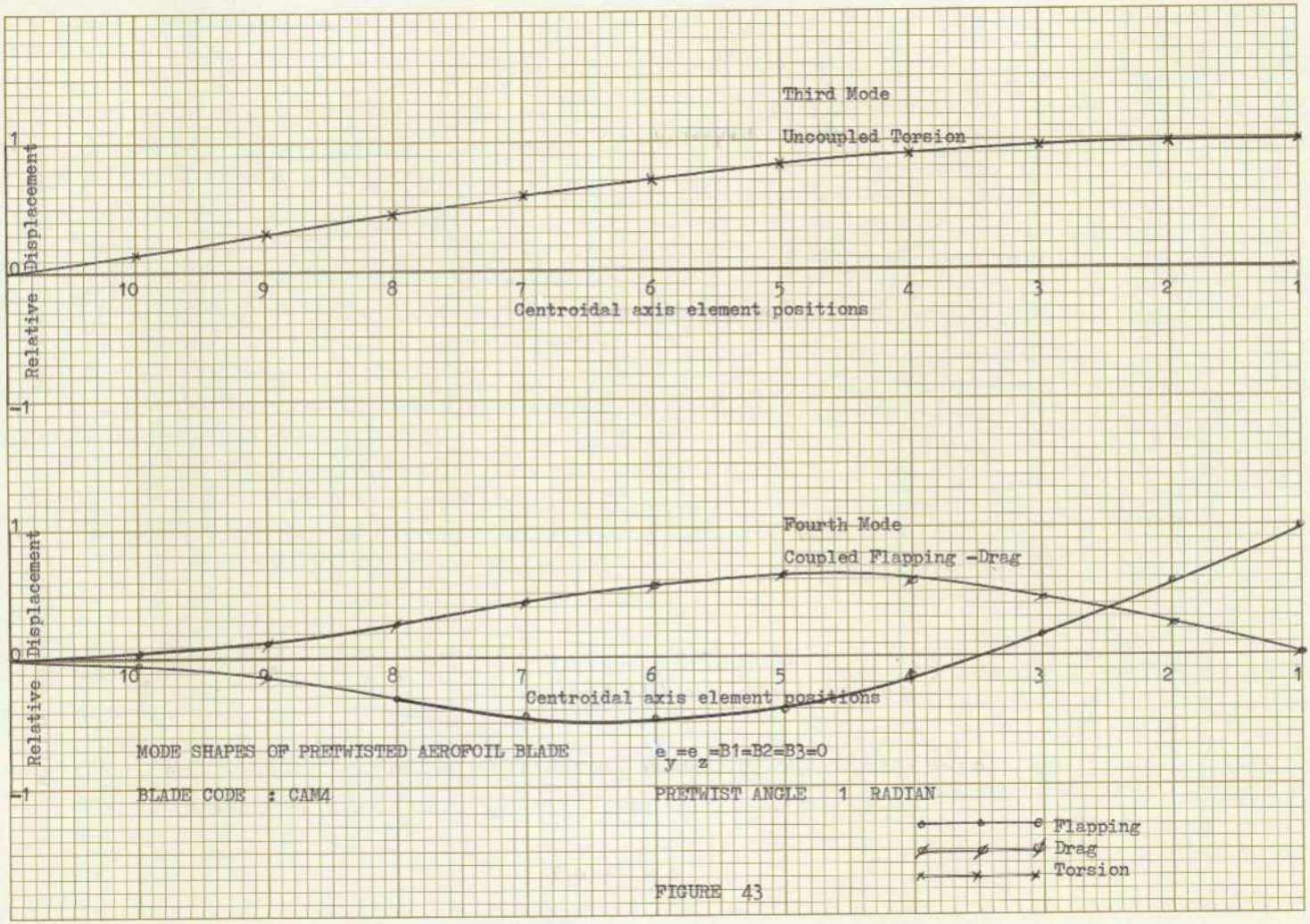
Third Mode
Uncoupled Torsion
Relative Displacement
1
0
10
9
8
7
6
5
4
3
2
1
Centroidal axis element positions
Fourth Mode
Coupled Flapping -Drag
Relative Displacement
1
0
10
9
8
7
6
5
4
3
2
1
Centroidal axis element positions
MODE SHAPES OF PRETWISTED AEROFOIL BLADE
$e_y = e_z = B1 = B2 = B3 = 0$
BLADE CODE : CAM4
PRETWIST ANGLE 1 RADIAN
Flapping
Drag
Torsion

FIGURE 43

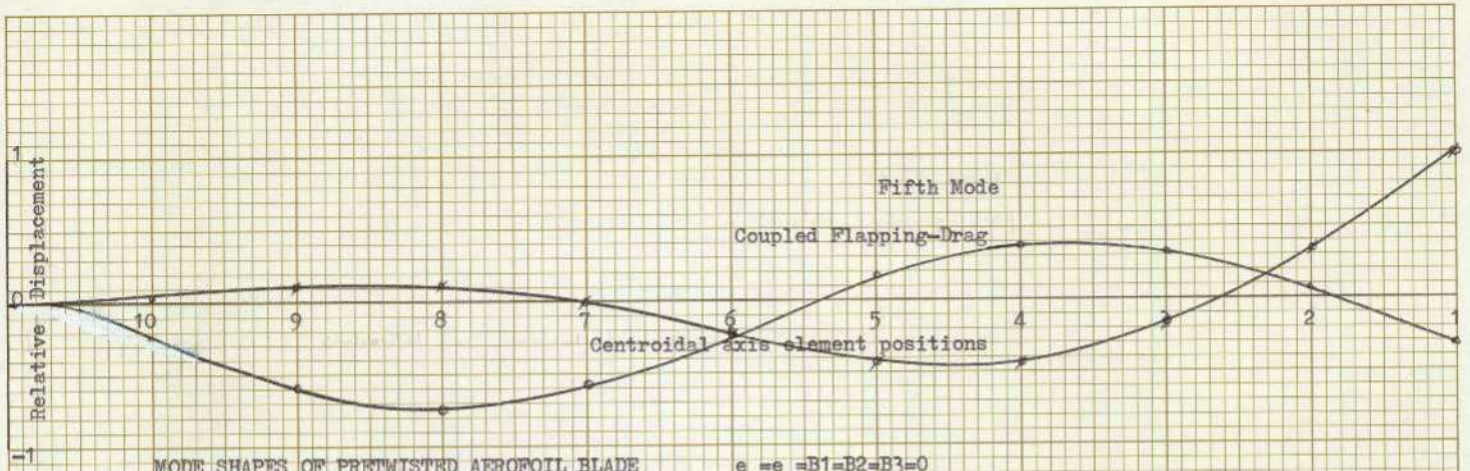

MODE SHAPES OF PRETWISTED AEROFOIL BLADE

BLADE CODE : CAM4

$e_y = e_z = B1 = B2 = B3 = 0$

PRETWIST ANGLE 1 RADIAN

Flapping

Drag

FIGURE 44

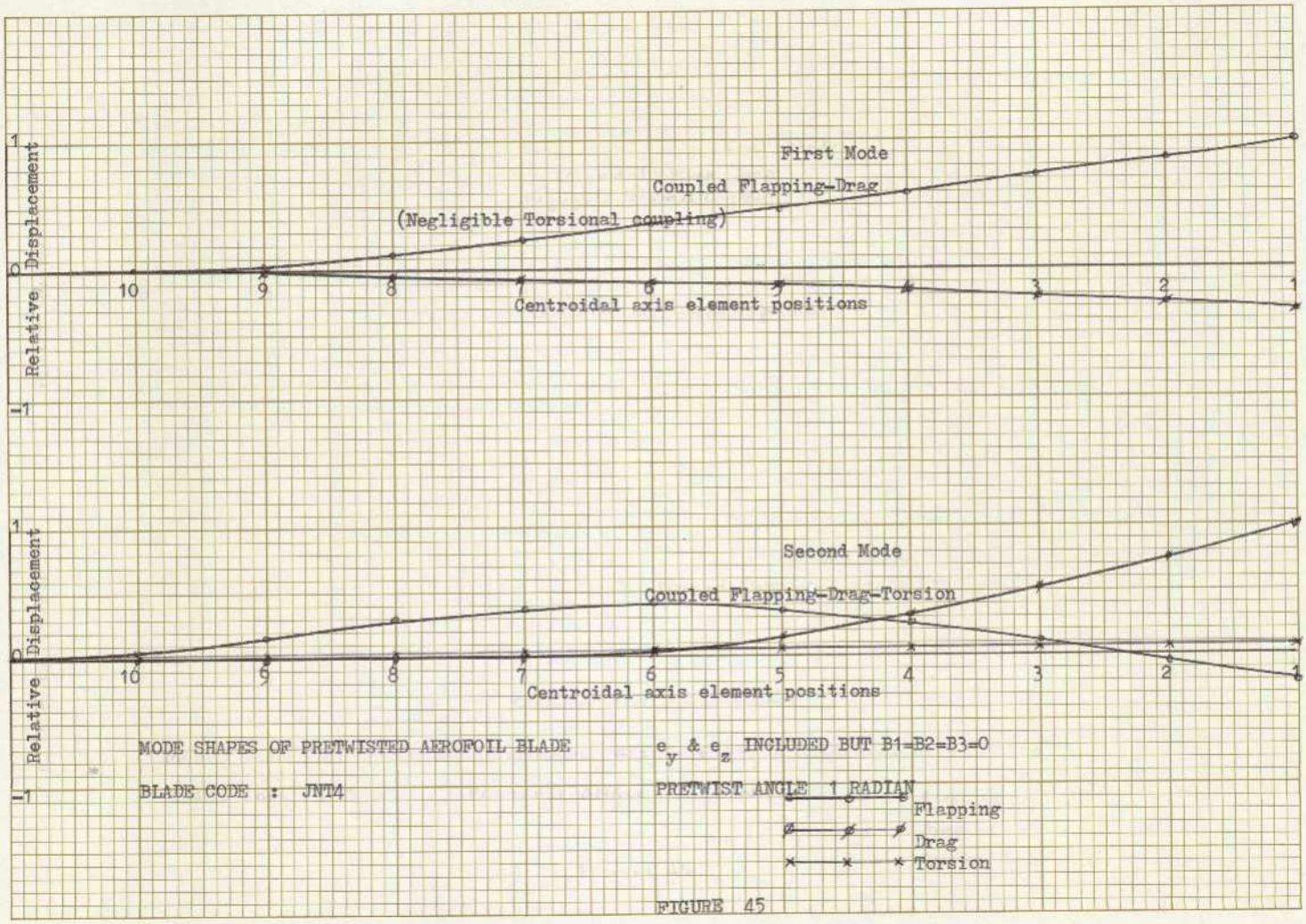
First Mode
Coupled Flapping-Drag
(Negligible Torsional coupling)
Relative Displacement
10
9
8
7
6
5
4
3
2
1
Centroidal axis element positions
Second Mode
Coupled Flapping-Drag-Torsion
Relative Displacement
10
9
8
7
6
5
4
3
2
1
Centroidal axis element positions
MODE SHAPES OF PRETWISTED AEROFOIL BLADE
e_y & e_z INCLUDED BUT B1=B2=B3=0
BLADE CODE : JNT4
PRETWIST ANGLE 1 RADIAN
Flapping
Drag
Torsion

FIGURE 45

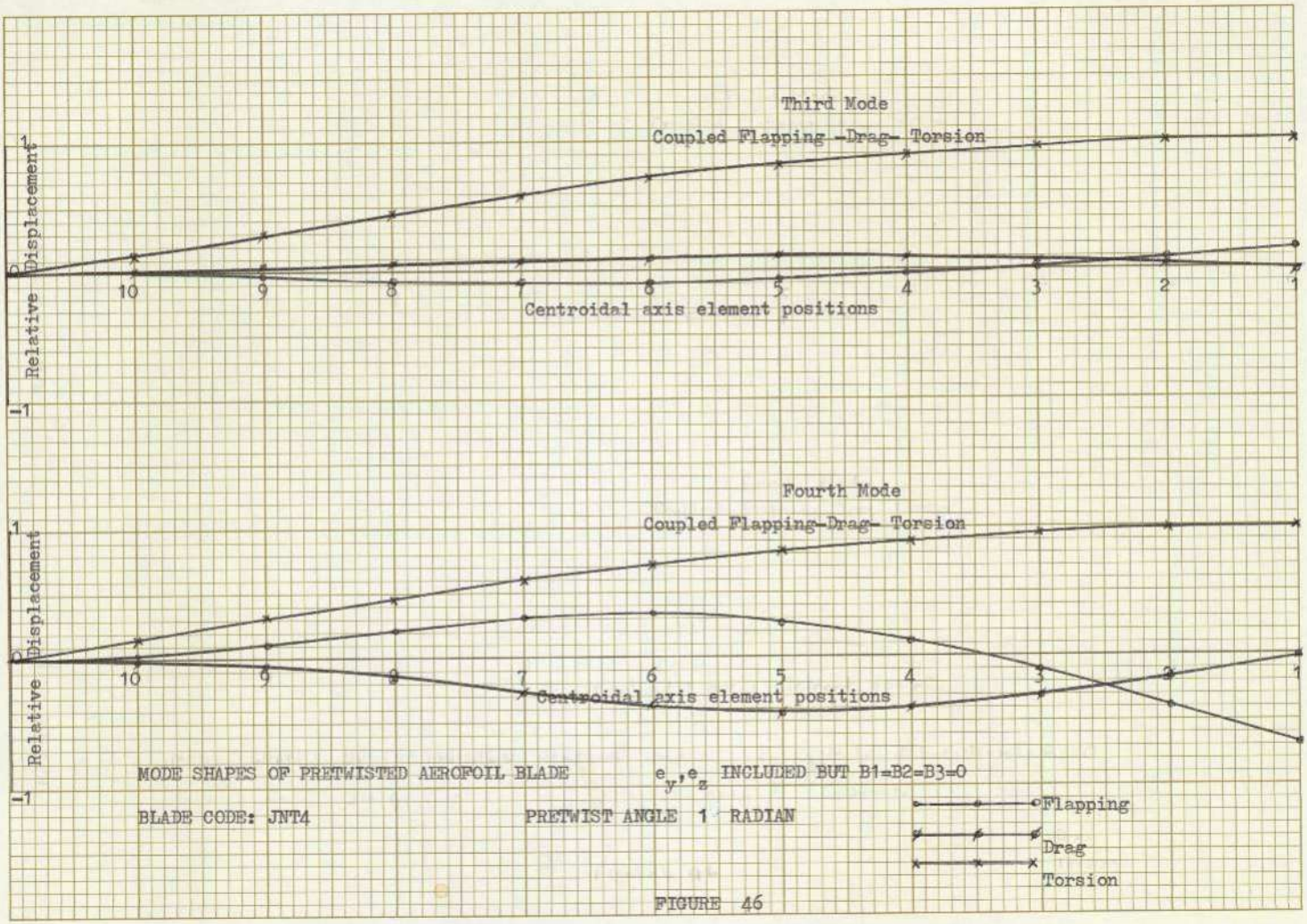
Third Mode
Coupled Flapping -Drag- Torsion
Relative Displacement
1
0
-1
10
9
8
7
6
5
4
3
2
1
Centroidal axis element positions
Fourth Mode
Coupled Flapping-Drag- Torsion
Relative Displacement
1
0
-1
10
9
8
7
6
5
4
3
2
1
Centroidal axis element positions
MODE SHAPES OF PRETWISTED AEROFOIL BLADE e_y, e_z INCLUDED BUT B1=B2=B3=0
BLADE CODE: JNT4
PRETWIST ANGLE 1 RADIAN
Flapping
Drag
Torsion

FIGURE 46

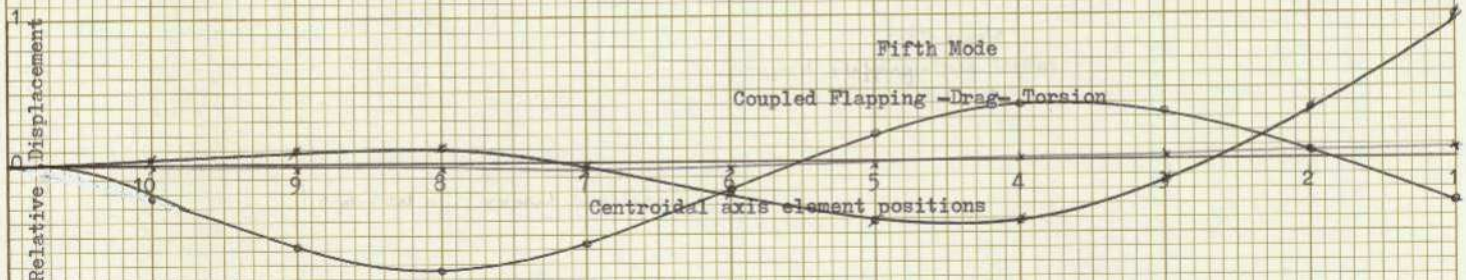

MODE SHAPES OF PRETWISTED AEROFOIL BLADE

BLADE CODE : JNT4

e_y, e_z INCLUDED BUT B1=B2=B3=0

PRETWIST ANGLE 1 RADIAN

Flapping

Drag

Torsion

FIGURE 47

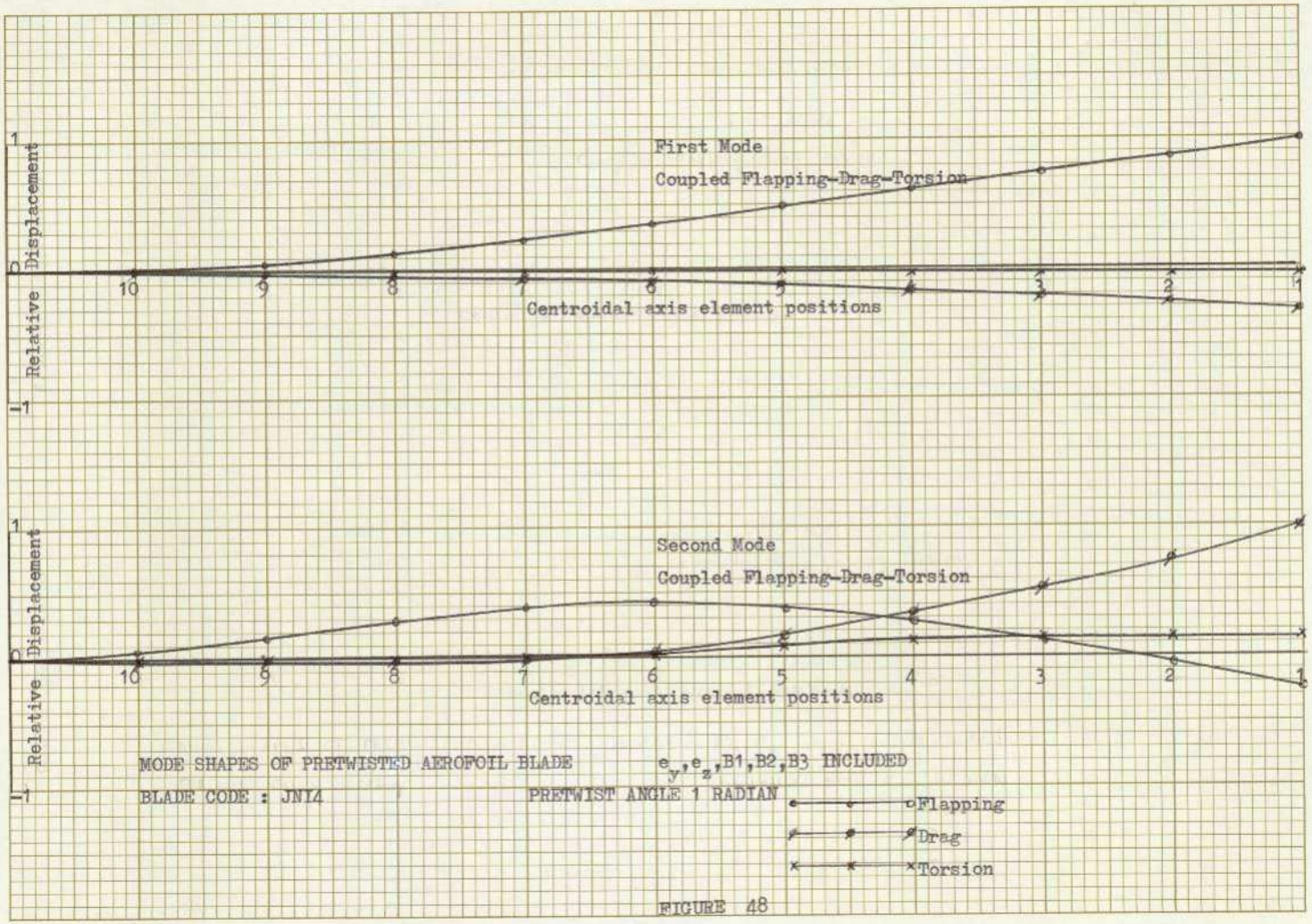
First Mode
Coupled Flapping-Drag-Torsion
Relative Displacement
1
0
-1
10
9
8
7
6
5
4
3
2
1
Centroidal axis element positions
Second Mode
Coupled Flapping-Drag-Torsion
Relative Displacement
1
0
-1
10
9
8
7
6
5
4
3
2
1
Centroidal axis element positions
MODE SHAPES OF PRETWISTED AEROFOIL BLADE e_y, e_z, B1, B2, B3 INCLUDED
BLADE CODE : JN14
PRETWIST ANGLE 1 RADIAN
Flapping
Drag
Torsion

FIGURE 48

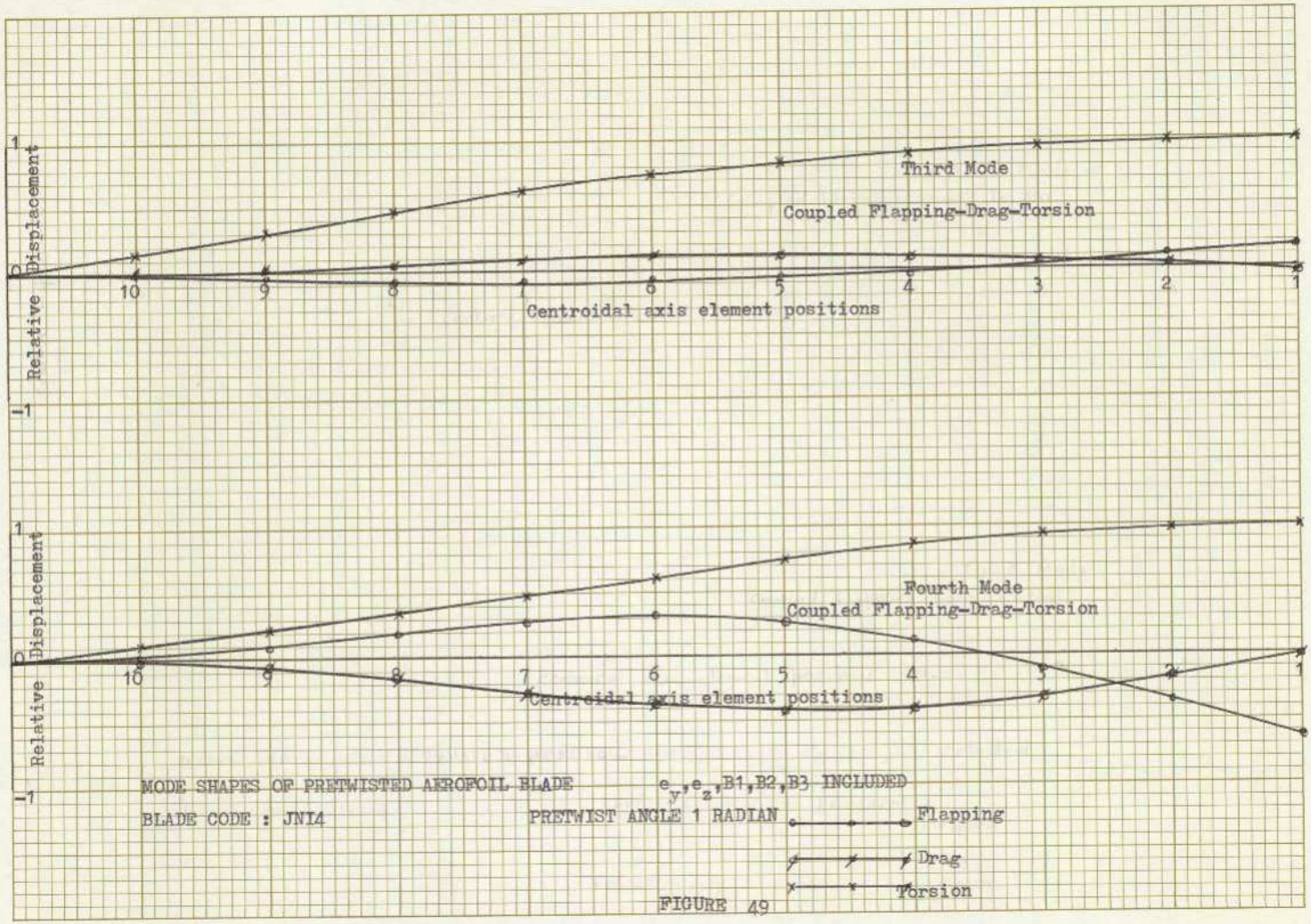
Third Mode
Coupled Flapping-Drag-Torsion
Relative Displacement
1
-1
10
9
8
7
6
5
4
3
2
1
Centroidal axis element positions
Fourth Mode
Coupled Flapping-Drag-Torsion
Relative Displacement
1
-1
10
9
8
7
6
5
4
3
2
1
Centroidal axis element positions
MODE SHAPES OF PRETWISTED AEROFOIL BLADE e_y, e_z, B1, B2, B3 INCLUDED
BLADE CODE : JNI4
PRETWIST ANGLE 1 RADIAN
Flapping
Drag
Torsion

FIGURE 49

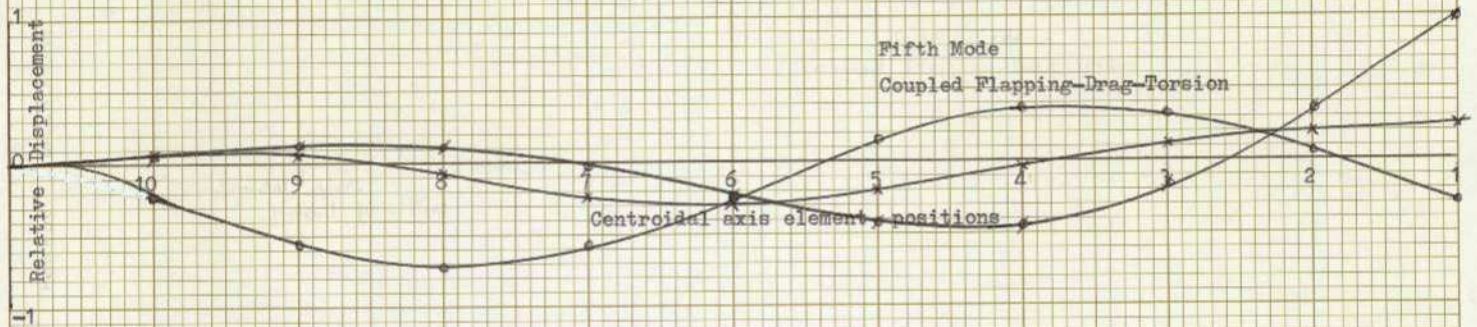

MODE SHAPES OF PRETWISTED AEROFOIL BLADE e_y, e_z, B1, B2, B3 INCLUDED

BLADE CODE : JNI4 PRETWIST ANGLE 1 RADIAN

Flapping

Drag

Torsion

FIGURE 50

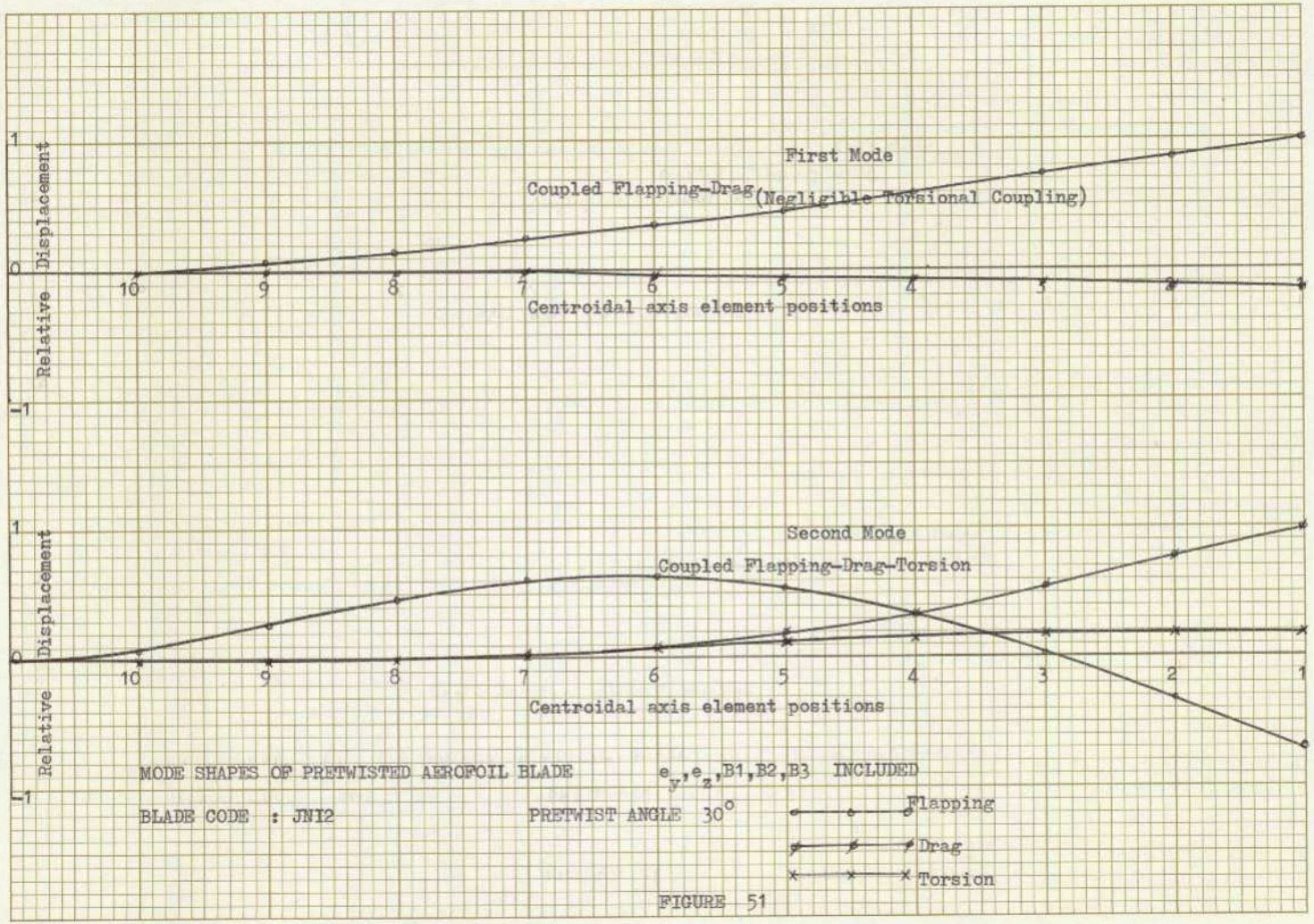
First Mode
Coupled Flapping-Drag (Negligible Torsional Coupling)
Relative Displacement
1
0
-1
10
9
8
7
6
5
4
3
2
Centroidal axis element positions
Second Mode
Coupled Flapping-Drag-Torsion
Relative Displacement
1
0
-1
10
9
8
7
6
5
4
3
2
1
Centroidal axis element positions
MODE SHAPES OF PRETWISTED AEROFOIL BLADE e_y, e_z, B1, B2, B3 INCLUDED
BLADE CODE : JNI2
PRETWIST ANGLE 30°
Flapping
Drag
Torsion

FIGURE 51

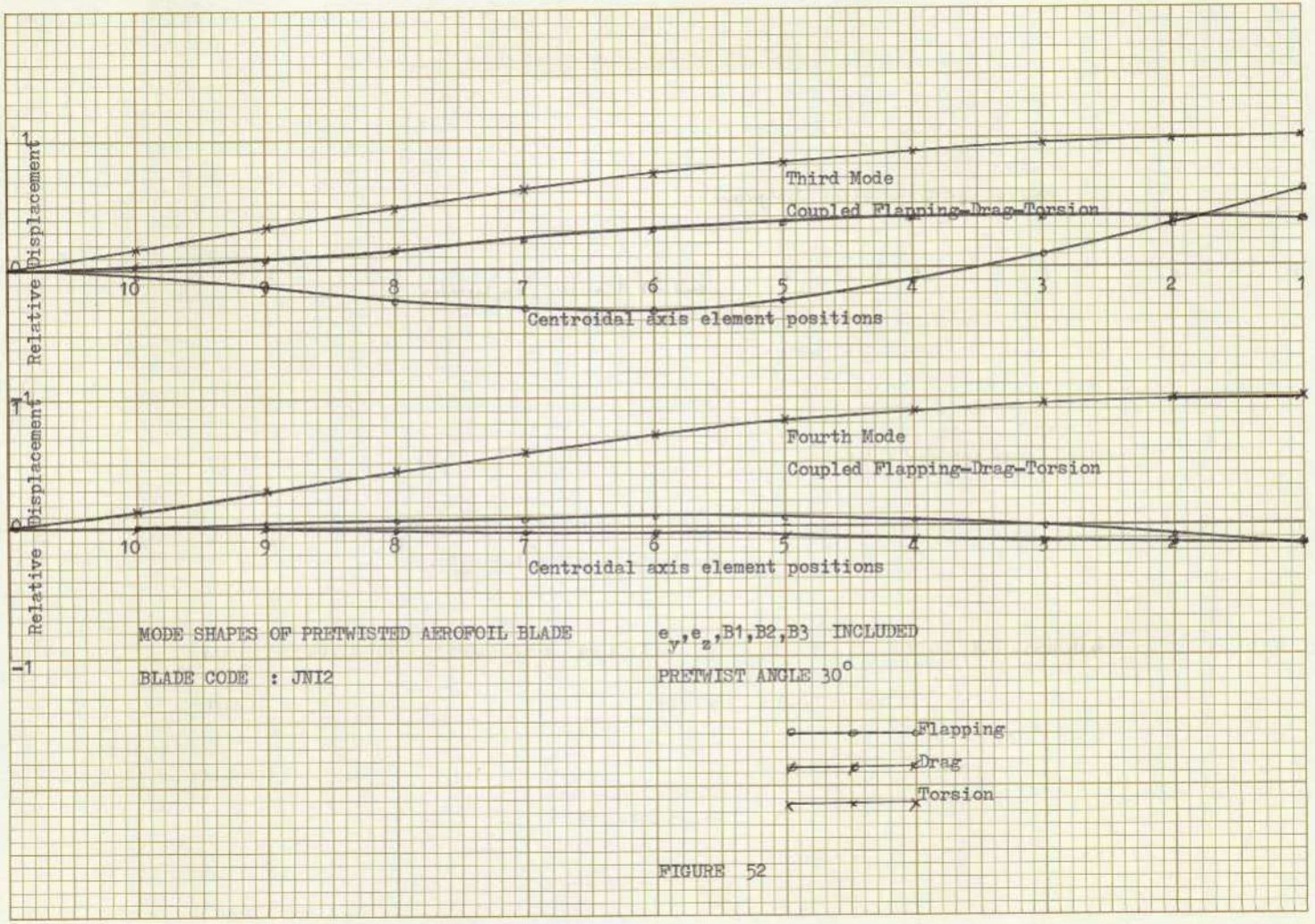
Relative Displacement
Third Mode
Coupled Flapping-Drag-Torsion
10
9
8
7
6
5
4
3
2
1
Centroidal axis element positions
Relative Displacement
Fourth Mode
Coupled Flapping-Drag-Torsion
10
9
8
7
6
5
4
3
2
1
Centroidal axis element positions
Relative Displacement
MODE SHAPES OF PRETWISTED AEROFOIL BLADE
e_y, e_z, B1, B2, B3 INCLUDED
BLADE CODE : JNI2
PRETWIST ANGLE 30°
Flapping
Drag
Torsion

FIGURE 52

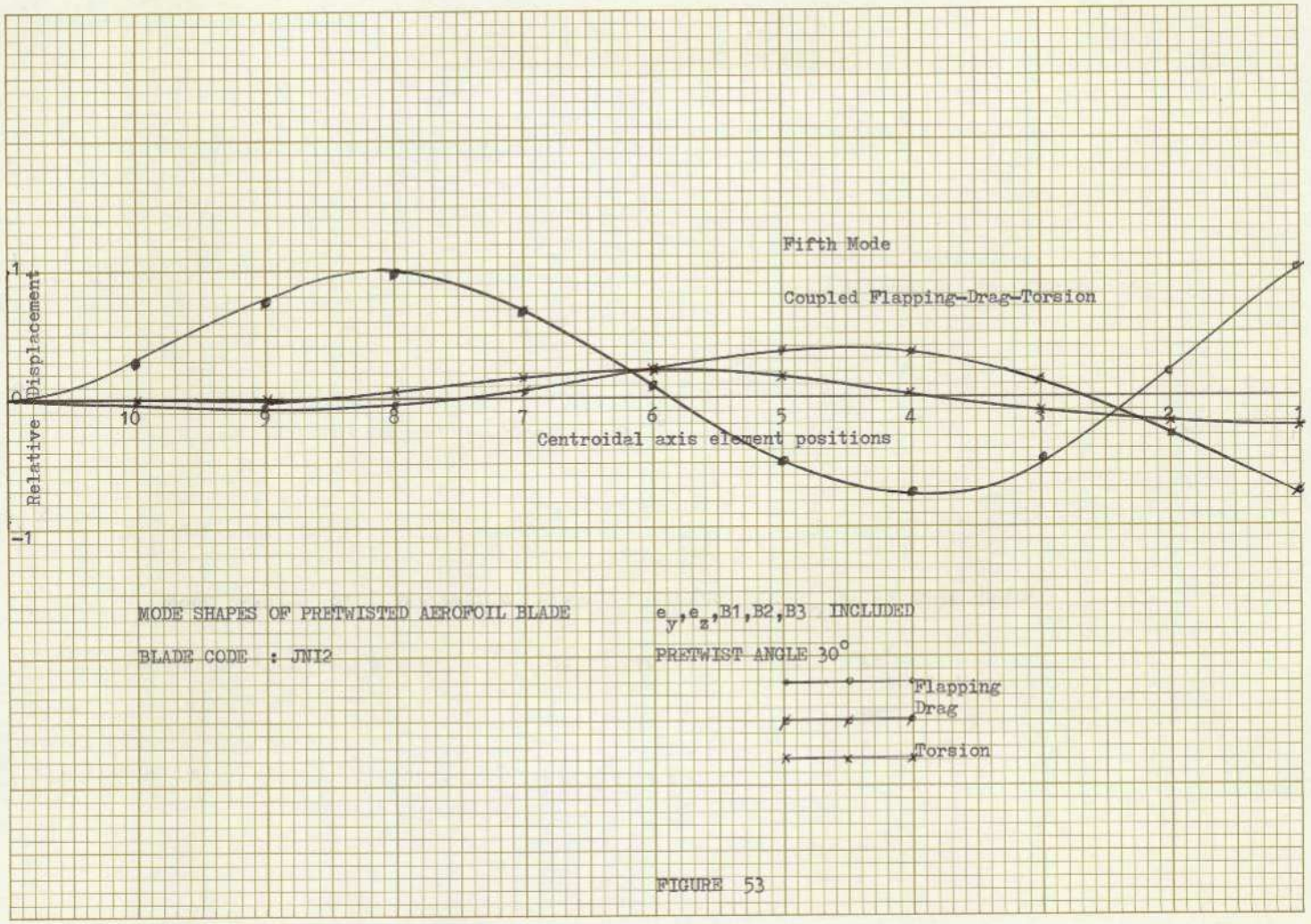
Fifth Mode
Coupled Flapping-Drag-Torsion
1
0
-1
Relative Displacement
10
9
8
7
6
5
4
3
2
1
Centroidal axis element positions
MODE SHAPES OF PRETWISTED AEROFOIL BLADE
BLADE CODE : JNI2
e_y, e_z, B1, B2, B3 INCLUDED
PRETWIST ANGLE 30°
Flapping
Drag
Torsion

FIGURE 53

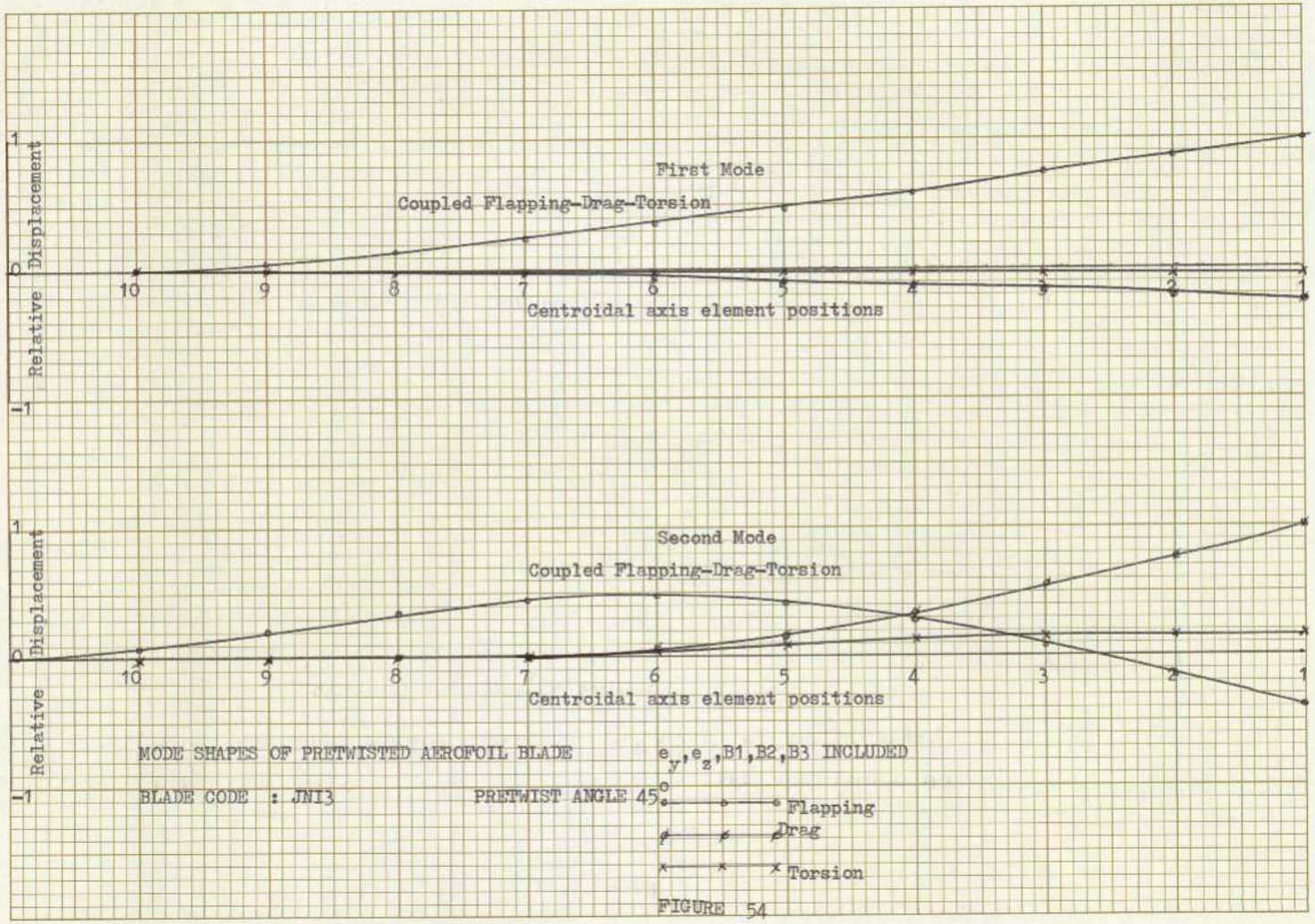
First Mode
Coupled Flapping-Drag-Torsion
Relative Displacement
10
9
8
7
6
5
4
3
2
1
Centroidal axis element positions
Second Mode
Coupled Flapping-Drag-Torsion
Relative Displacement
10
9
8
7
6
5
4
3
2
1
Centroidal axis element positions
MODE SHAPES OF PRETWISTED AEROFOIL BLADE
e_y, e_z, B1, B2, B3 INCLUDED
BLADE CODE : JNI3
PRETWIST ANGLE 45°
Flapping
Drag
Torsion

FIGURE 54

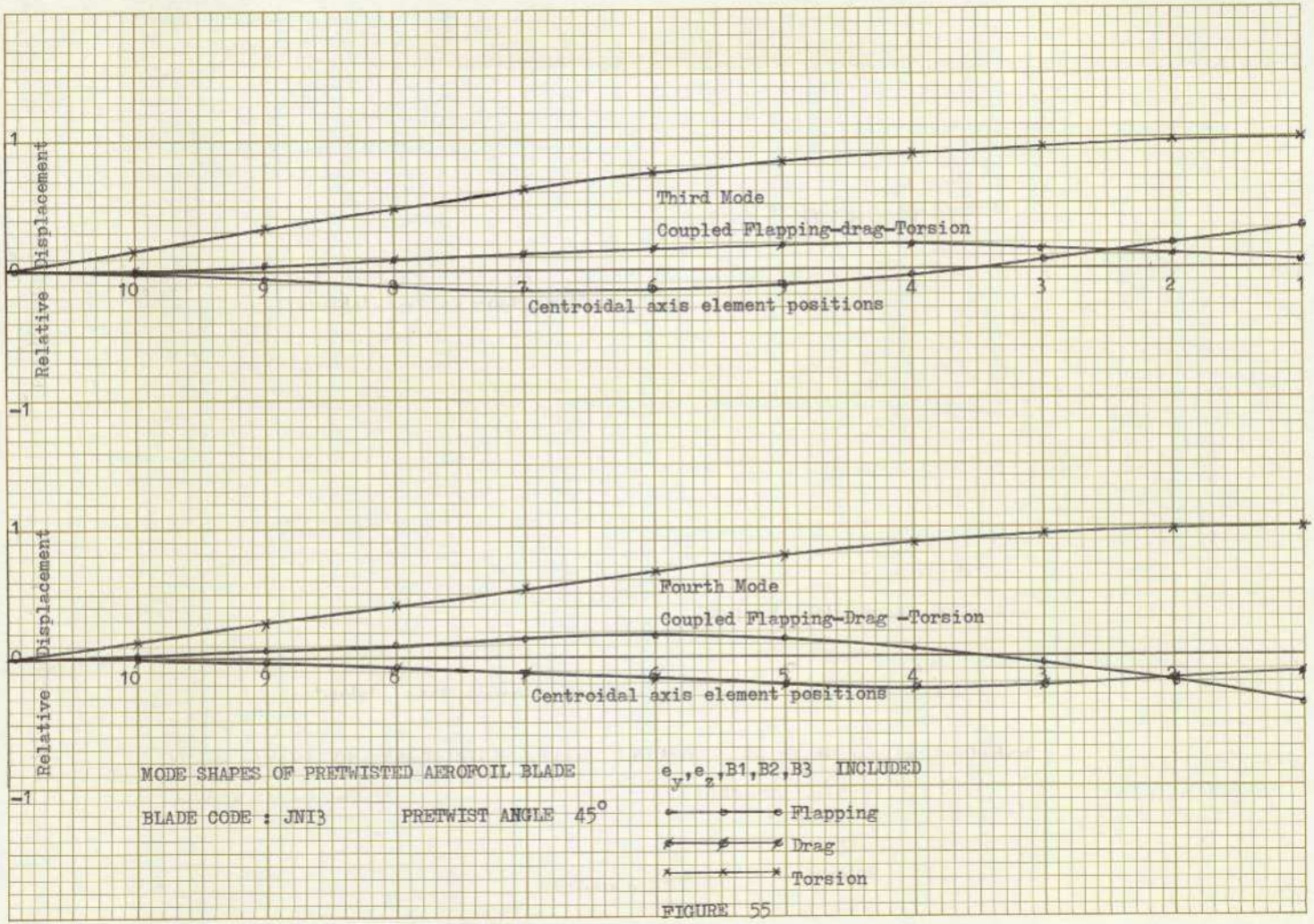
Third Mode
Coupled Flapping-drag-Torsion
Relative Displacement
Centroidal axis element positions
10
9
8
7
6
5
4
3
2
1
Fourth Mode
Coupled Flapping-Drag -Torsion
Relative Displacement
Centroidal axis element positions
MODE SHAPES OF PRETWISTED AEROFOIL BLADE
BLADE CODE : JNI3
PRETWIST ANGLE 45°
e_y, e_z, B1, B2, B3 INCLUDED
Flapping
Drag
Torsion

FIGURE 55

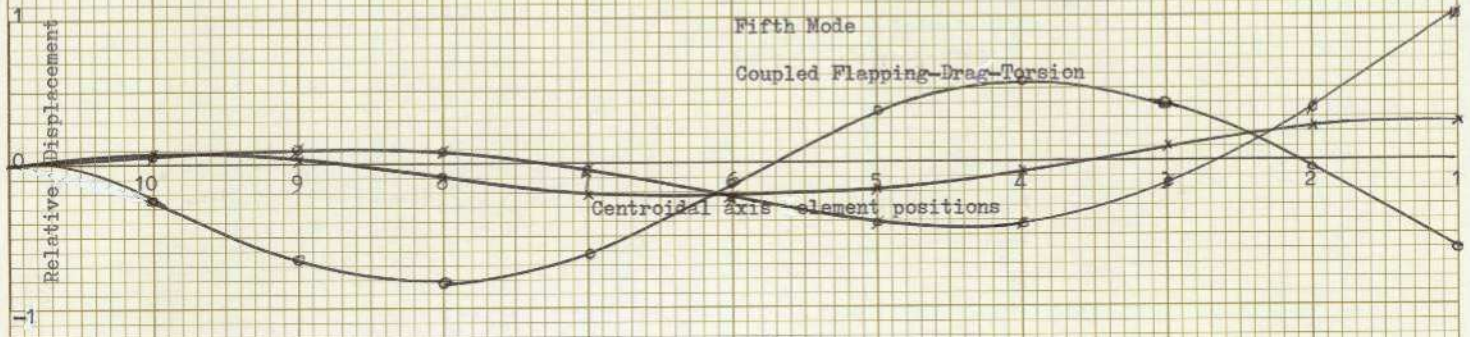

MODE SHAPES OF PRETWISTED AEROFOIL BLADE e_y, e_z, B1, B2, B3 INCLUDED

BLADE CODE : JNI3 PRETWIST ANGLE 45°

Flapping
Drag
Torsion

FIGURE 56

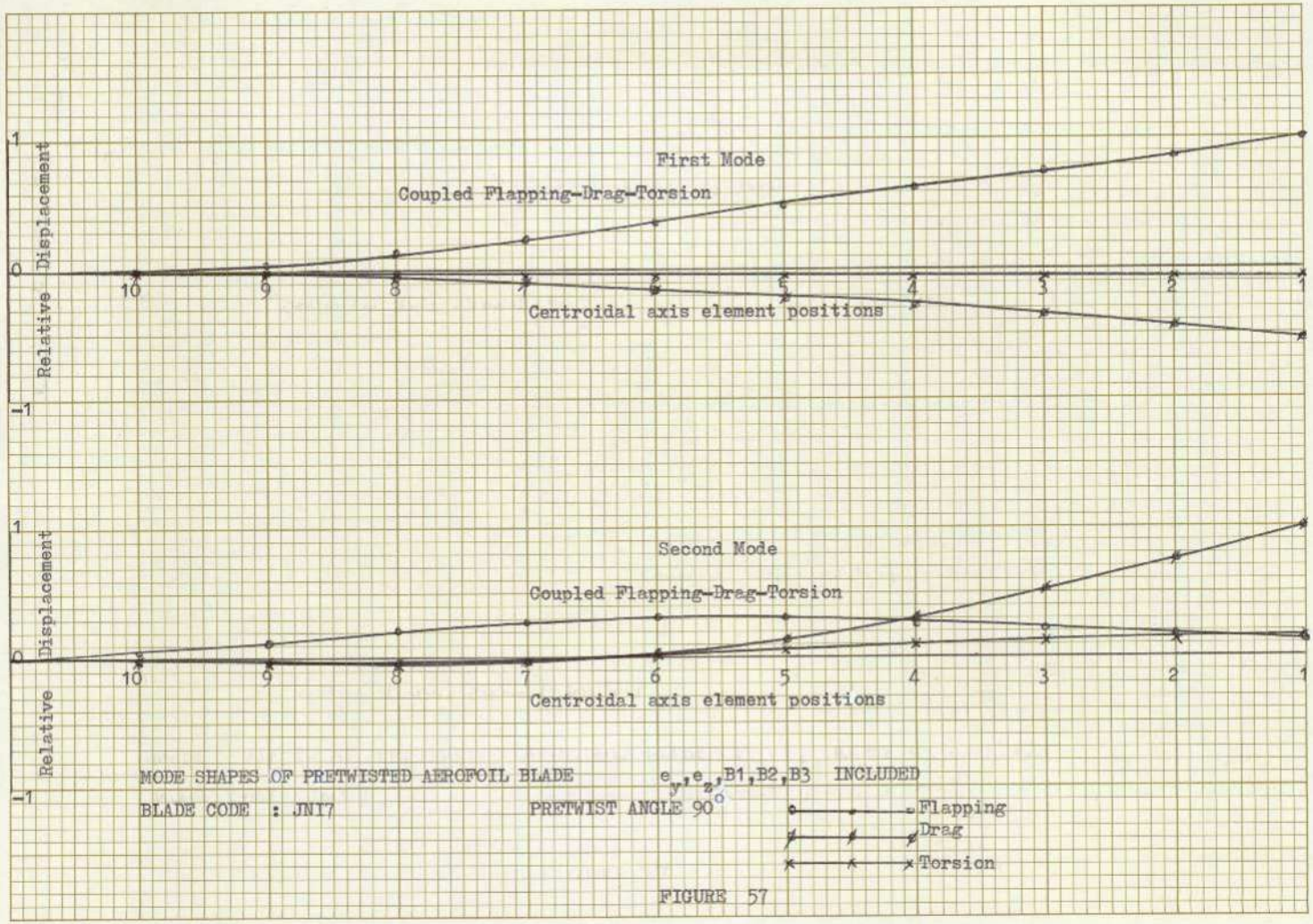
First Mode
Coupled Flapping-Drag-Torsion
Relative Displacement
1
0
-1
10
9
8
7
6
5
4
3
2
1
Centroidal axis element positions
Second Mode
Coupled Flapping-Drag-Torsion
Relative Displacement
1
0
-1
10
9
8
7
6
5
4
3
2
1
Centroidal axis element positions
MODE SHAPES OF PRETWISTED AEROFOIL BLADE $e_y, e_z, B1, B2, B3$ INCLUDED
BLADE CODE : JNI7
PRETWIST ANGLE 90°
Flapping
Drag
Torsion

FIGURE 57

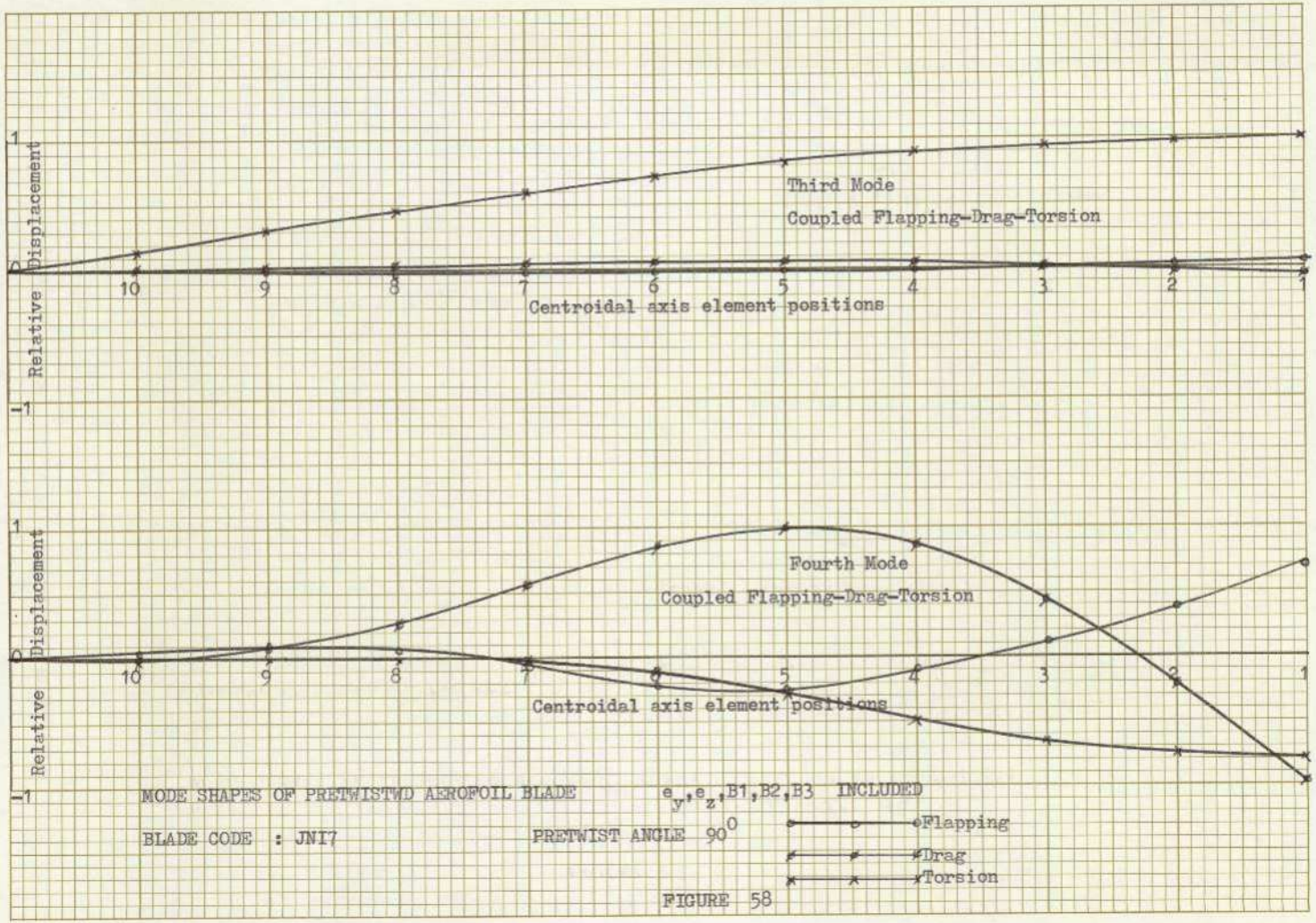
Relative Displacement
1
0
-1
Third Mode
Coupled Flapping-Drag-Torsion
10
9
8
7
6
5
4
3
2
1
Centroidal axis element positions
Relative Displacement
1
0
-1
Fourth Mode
Coupled Flapping-Drag-Torsion
10
9
8
7
6
5
4
3
2
1
Centroidal axis element positions
MODE SHAPES OF PRETWISTWD AEROFOIL BLADE
e_y, e_z, B1, B2, B3 INCLUDED
BLADE CODE : JNI7
PRETWIST ANGLE 90^0
Flapping
Drag
Torsion

FIGURE 58

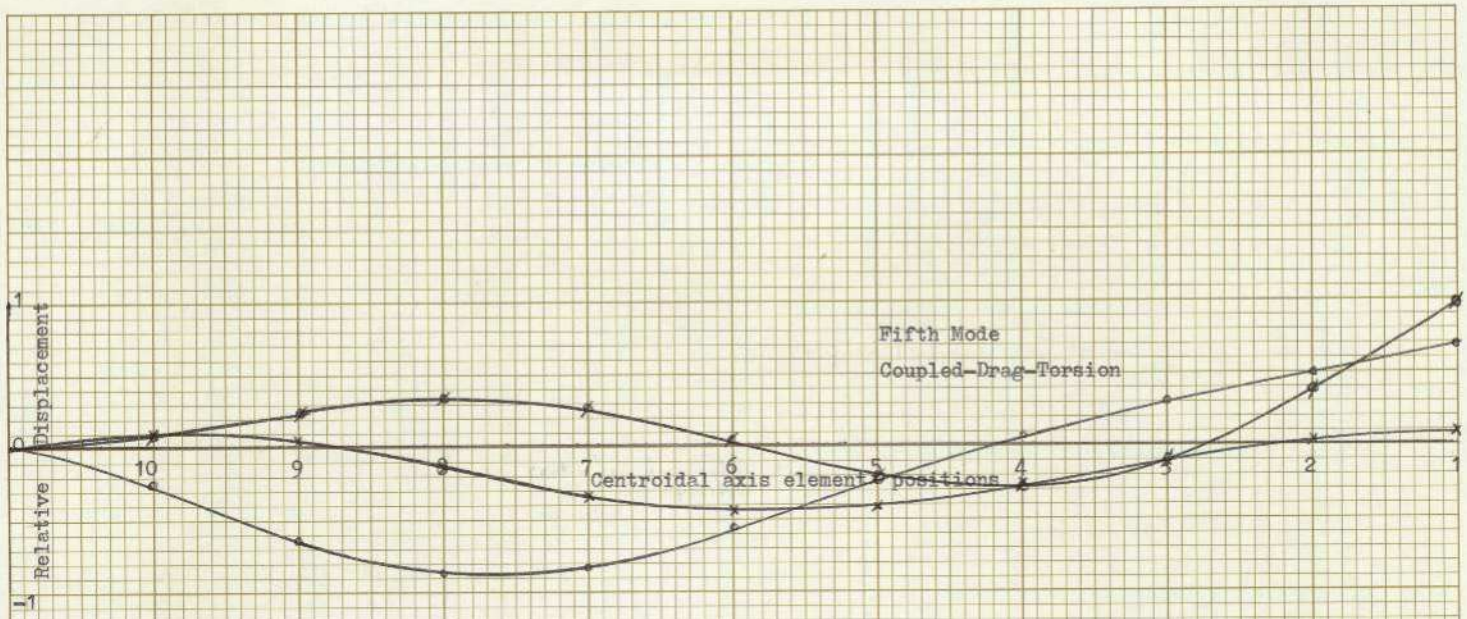

MODE SHAPES OF PRETWISTED AEROFOIL BLADE e_y, e_z, B1, B2, B3 INCLUDED

BLADE CODE : JN17 PRETWIST ANGLE 90°

Flapping

Drag

Torsion

FIGURE 59

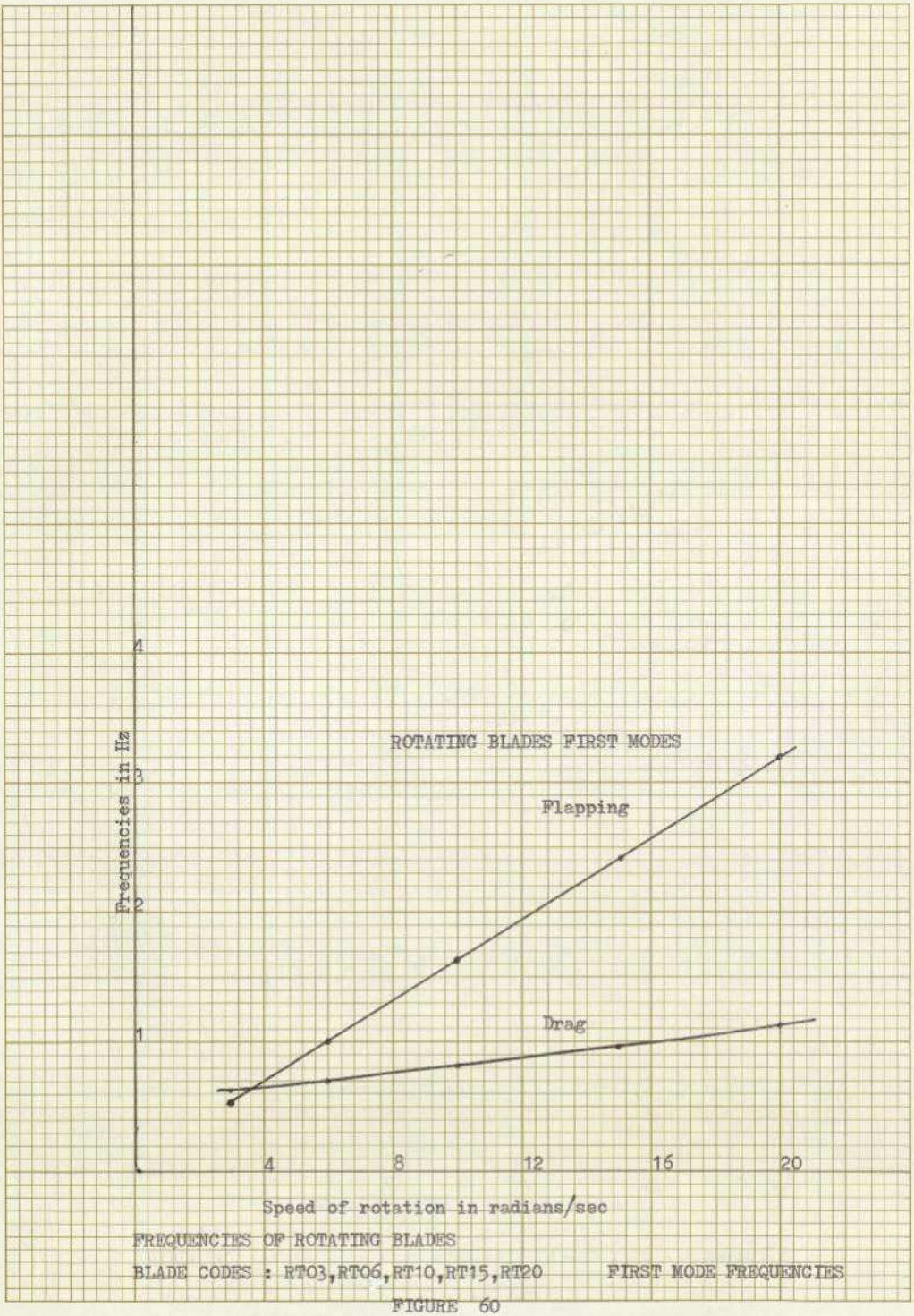

FREQUENCIES OF ROTATING BLADES

BLADE CODES : RT03,RT06,RT10,RT15,RT20 FIRST MODE FREQUENCIES

FIGURE 60

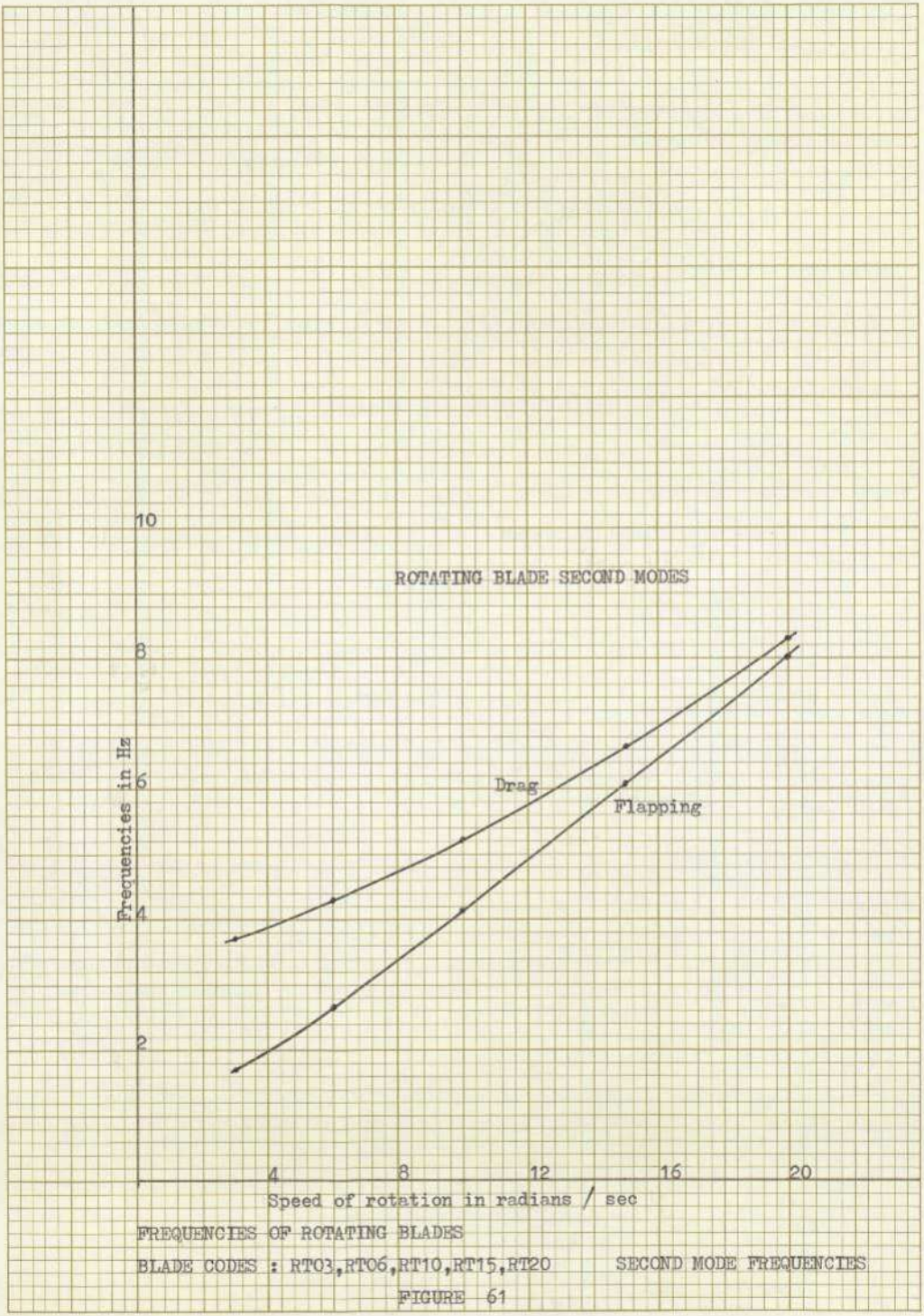

FREQUENCIES OF ROTATING BLADES

BLADE CODES : RT03,RT06,RT10,RT15,RT20 SECOND MODE FREQUENCIES

FIGURE 61

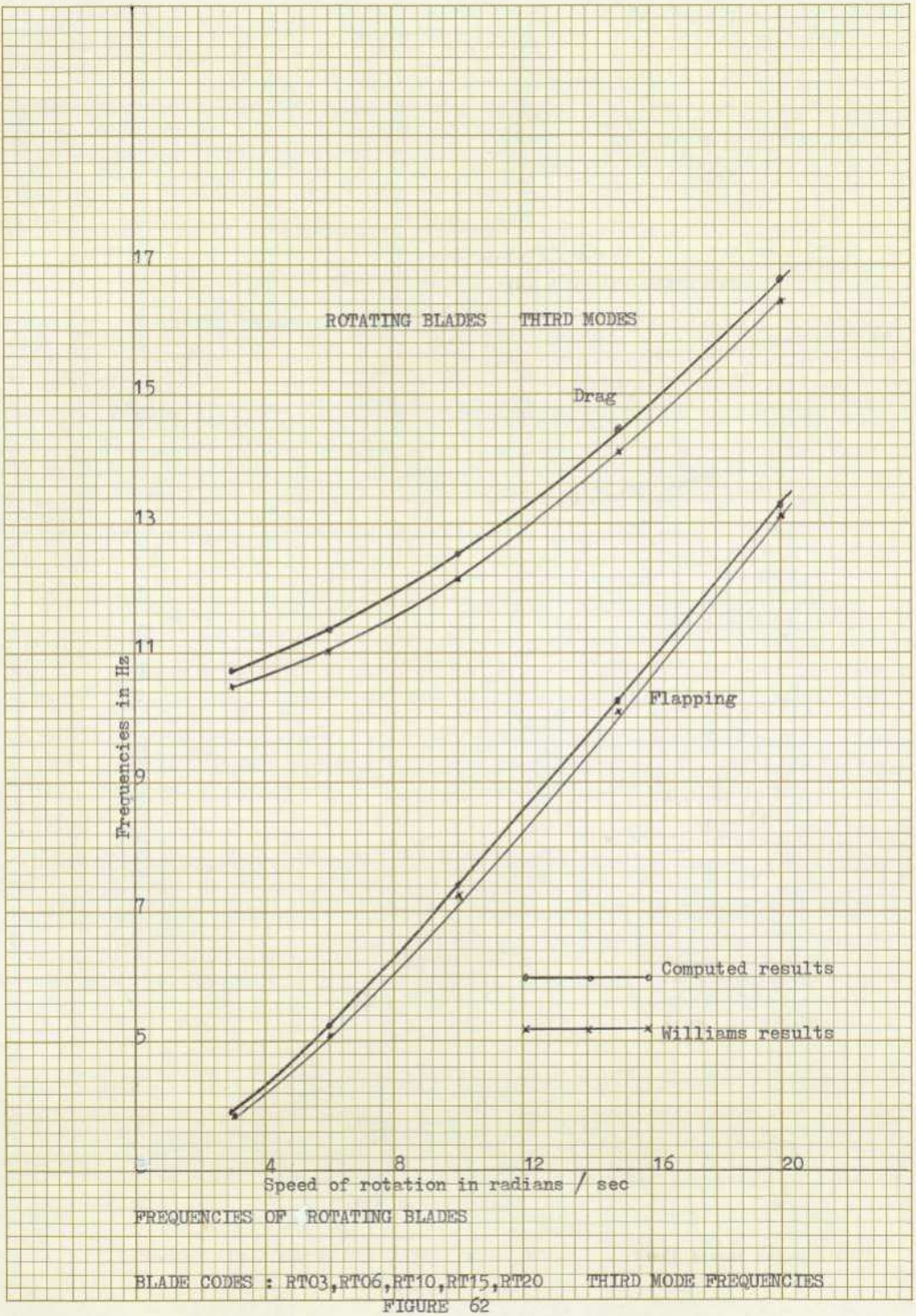

FREQUENCIES OF ROTATING BLADES

BLADE CODES : RT03,RT06,RT10,RT15,RT20 THIRD MODE FREQUENCIES

FIGURE 62

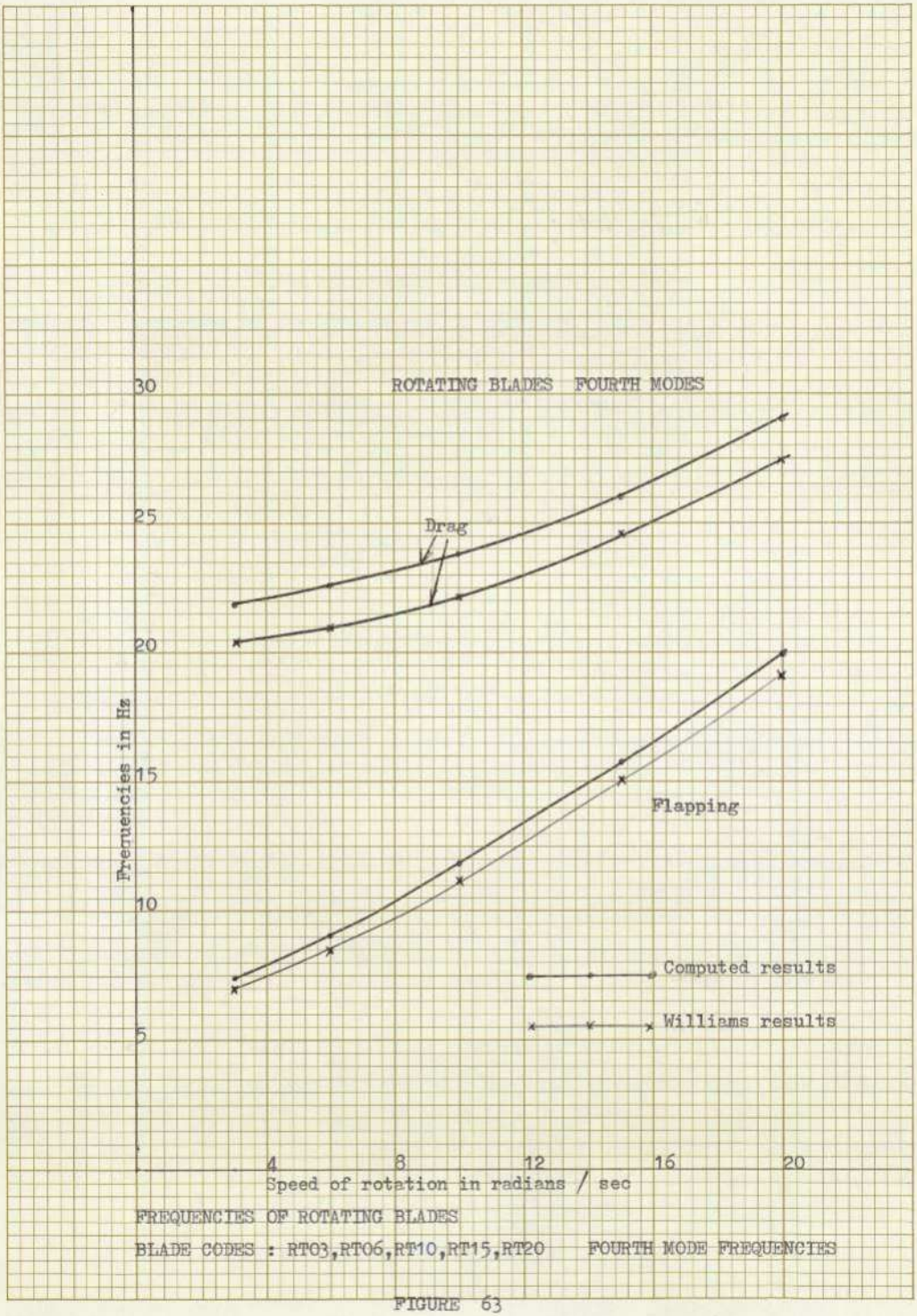

FREQUENCIES OF ROTATING BLADES

BLADE CODES : RT03,RT06,RT10,RT15,RT20 FOURTH MODE FREQUENCIES

FIGURE 63

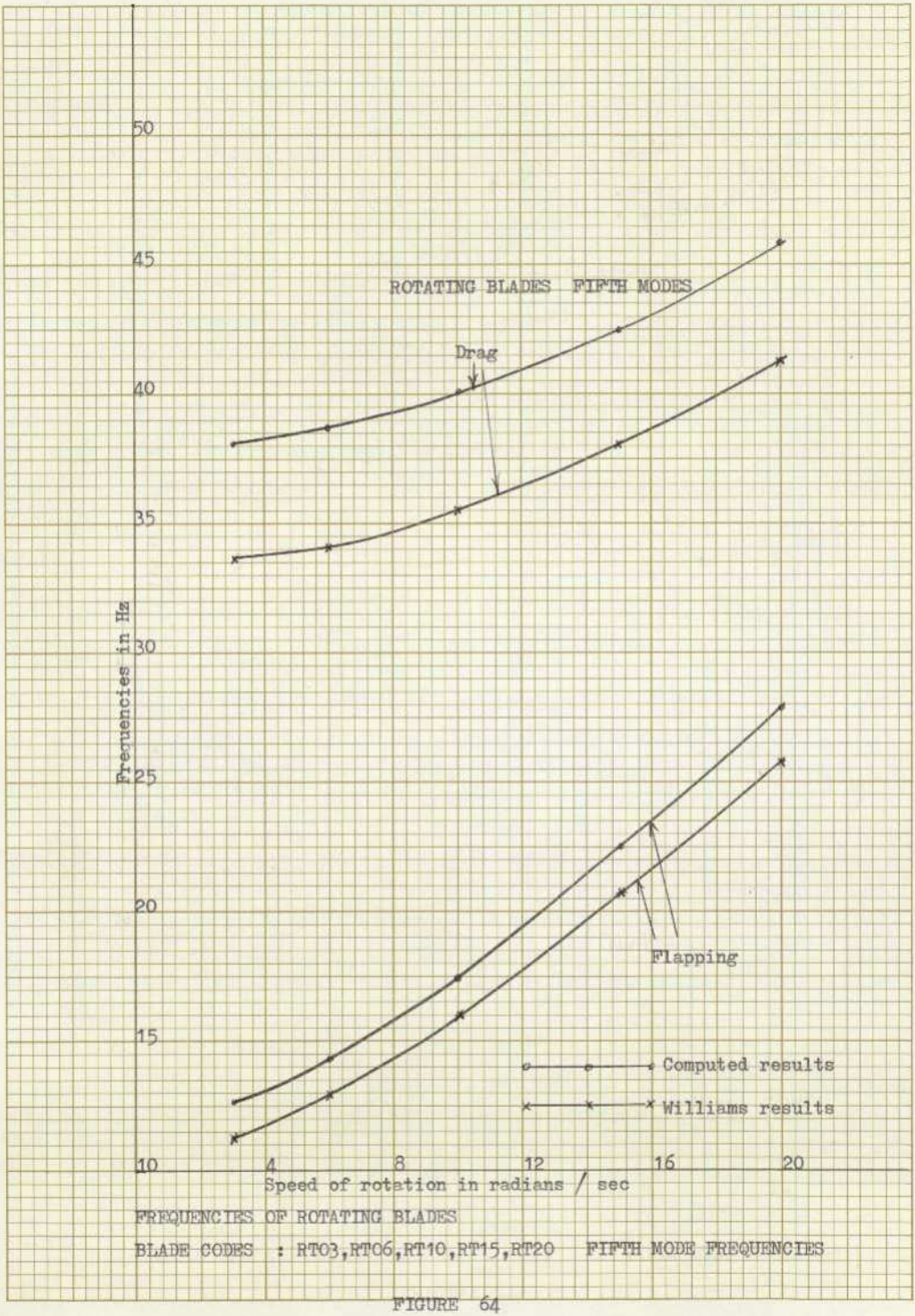

FREQUENCIES OF ROTATING BLADES

BLADE CODES : RT03,RT06,RT10,RT15,RT20 FIFTH MODE FREQUENCIES

FIGURE 64

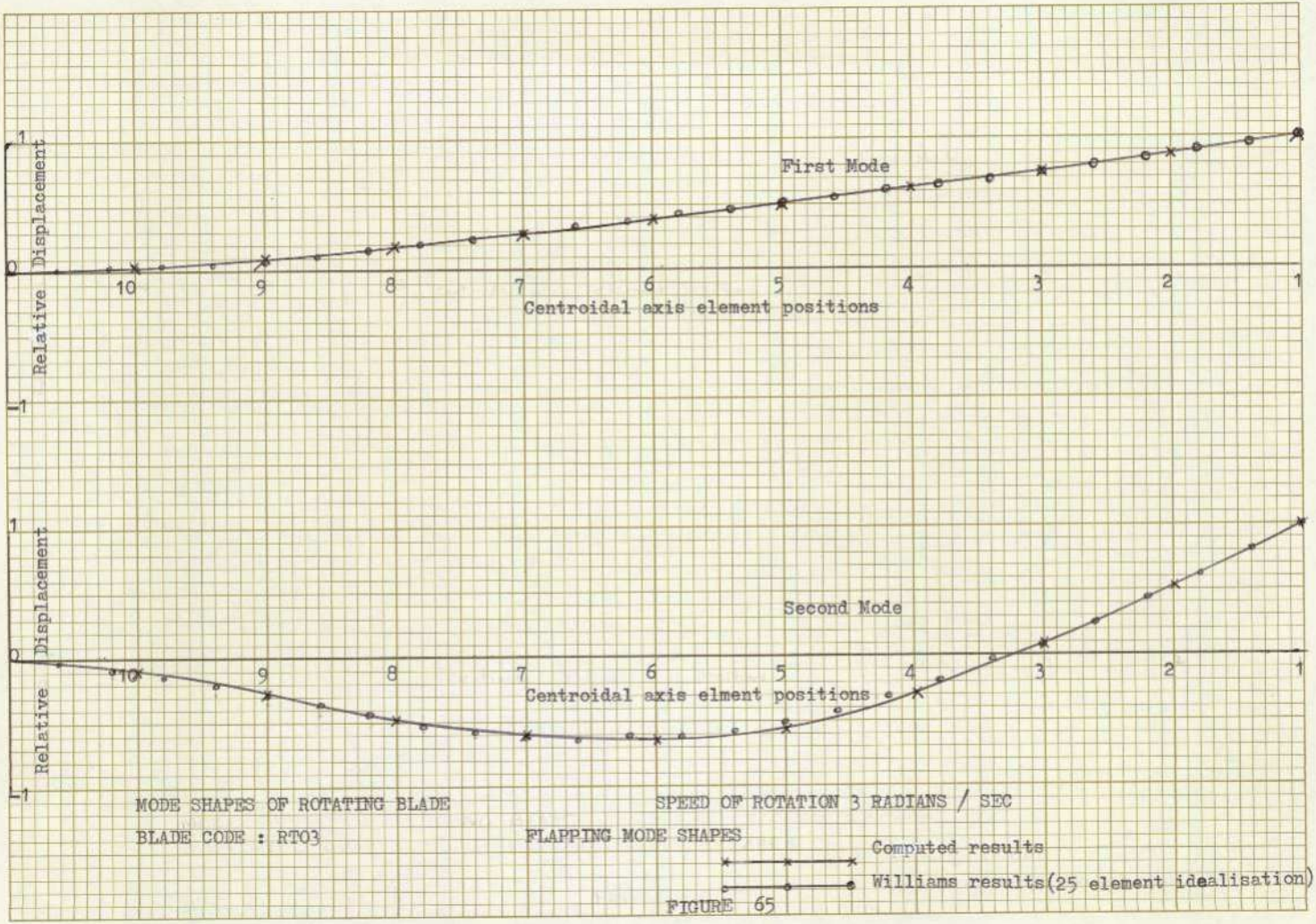

MODE SHAPES OF ROTATING BLADE

BLADE CODE : RTO3

SPEED OF ROTATION 3 RADIANS / SEC

FLAPPING MODE SHAPES

Computed results

Williams results (25 element idealisation)

FIGURE 65

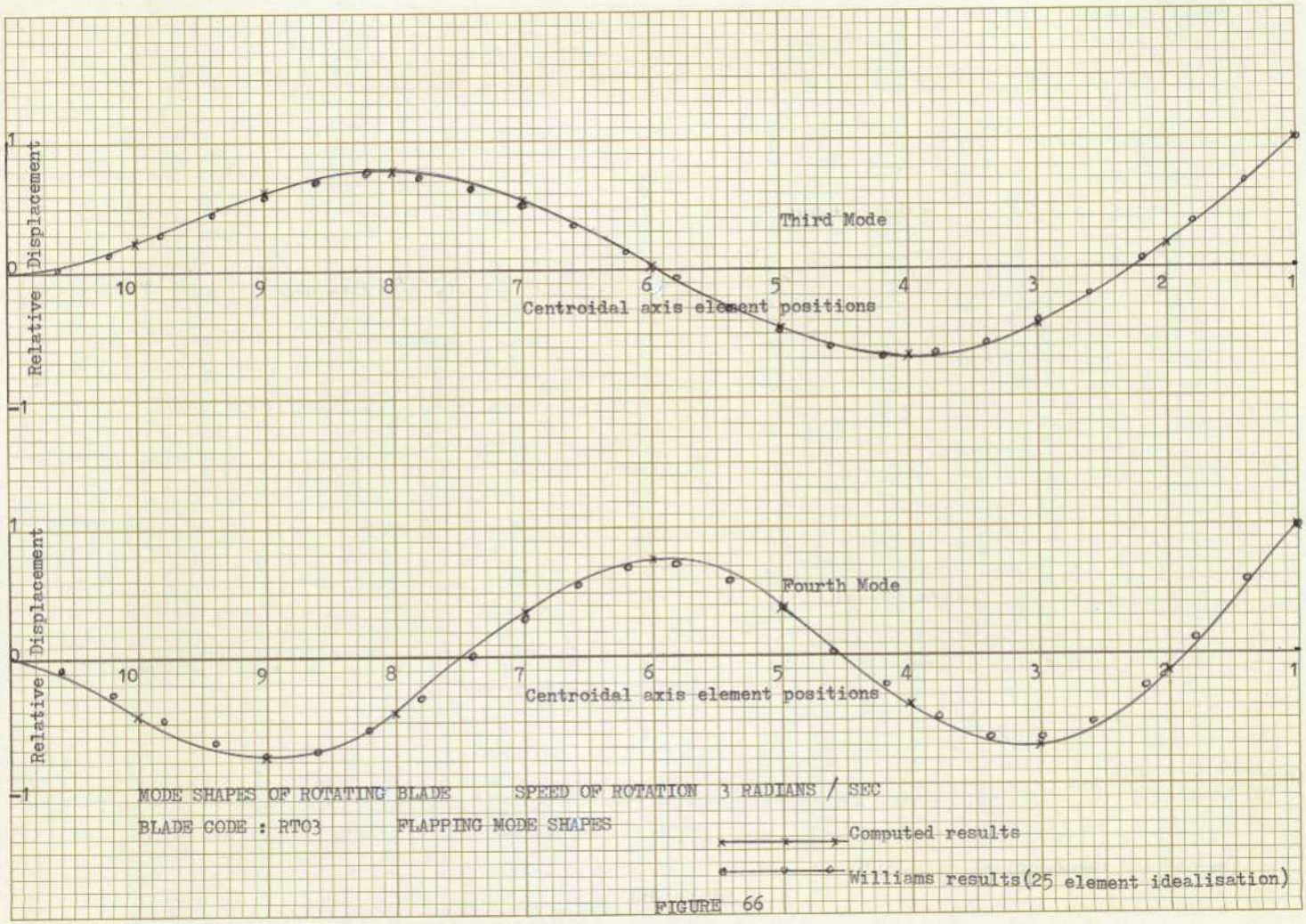
Relative Displacement
1
0
-1
10
9
8
7
6
5
4
3
2
1
Third Mode
Centroidal axis element positions
Relative Displacement
1
0
-1
10
9
8
7
6
5
4
3
2
1
Fourth Mode
Centroidal axis element positions
MODE SHAPES OF ROTATING BLADE
SPEED OF ROTATION 3 RADIANS / SEC
BLADE CODE : RT03
FLAPPING MODE SHAPES
Computed results
Williams results (25 element idealisation)

FIGURE 66

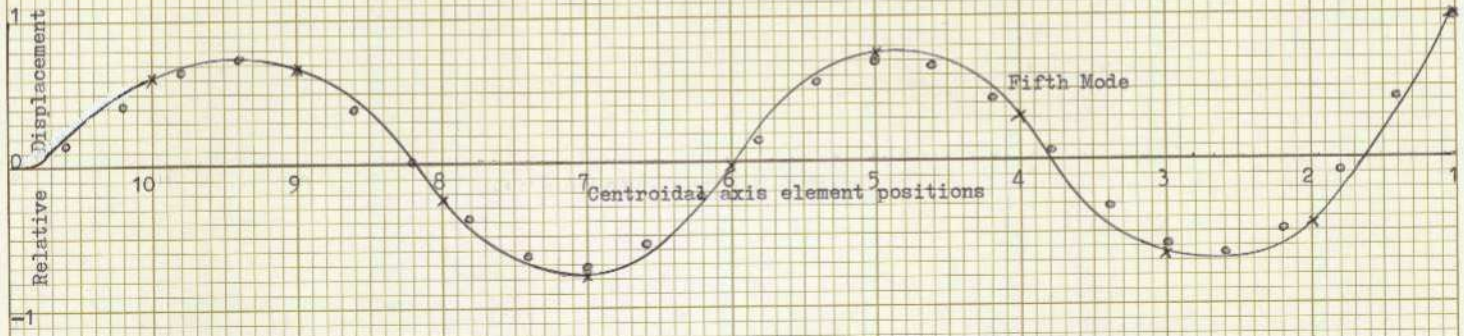

MODE SHAPES OF ROTATING BLADE

SPEED OF ROTATION 3 RADIANS / SEC

BLADE CODES : RTO3

FLAPPING MODE SHAPES

×——×——× Computed results

•——•——• Williams results(25 element idealisation)

FIGURE 67

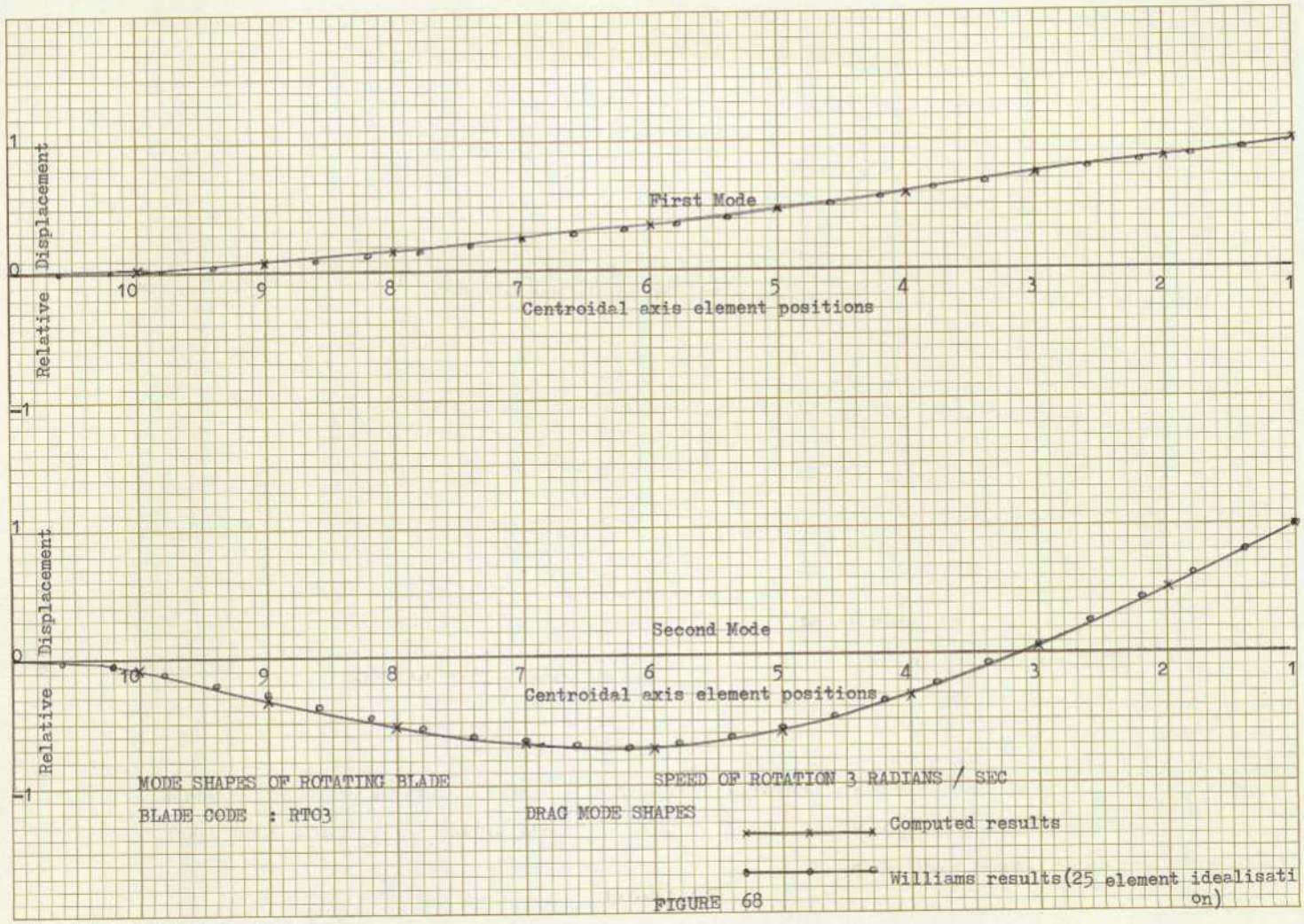
First Mode
Relative Displacement
1
0
-1
10
9
8
7
6
5
4
3
2
1
Centroidal axis element positions
Second Mode
Relative Displacement
1
0
-1
10
9
8
7
6
5
4
3
2
1
Centroidal axis element positions
MODE SHAPES OF ROTATING BLADE
BLADE CODE : RTO3
DRAG MODE SHAPES
SPEED OF ROTATION 3 RADIANS / SEC
Computed results
Williams results(25 element idealisation)

FIGURE 68

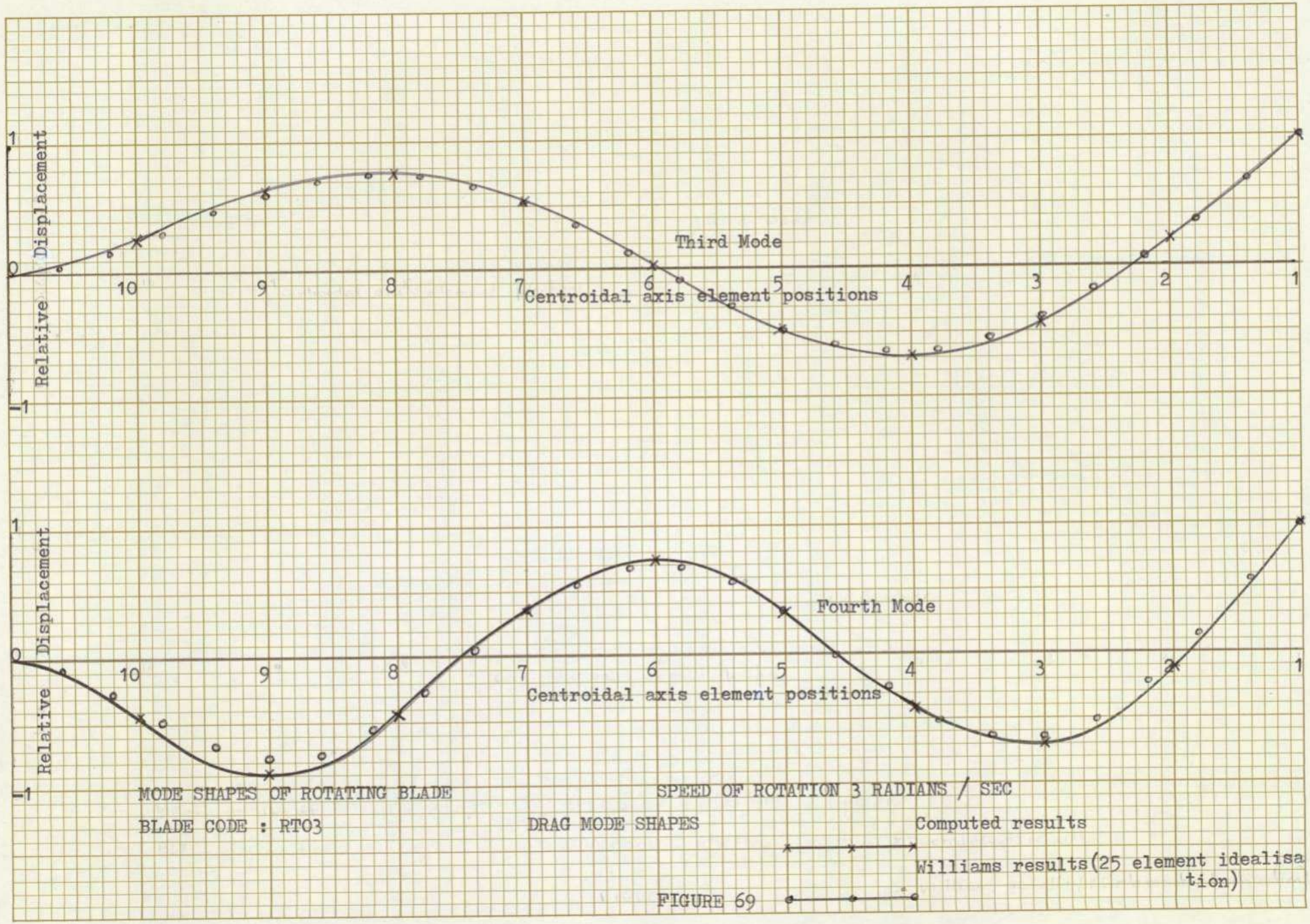
Third Mode
Relative Displacement
1
0
-1
10
9
8
7
6
5
4
3
2
1
Centroidal axis element positions
Fourth Mode
Relative Displacement
1
0
-1
10
9
8
7
6
5
4
3
2
1
Centroidal axis element positions
MODE SHAPES OF ROTATING BLADE
BLADE CODE : RT03
SPEED OF ROTATION 3 RADIANS / SEC
DRAG MODE SHAPES
Computed results
Williams results(25 element idealisation)

FIGURE 69

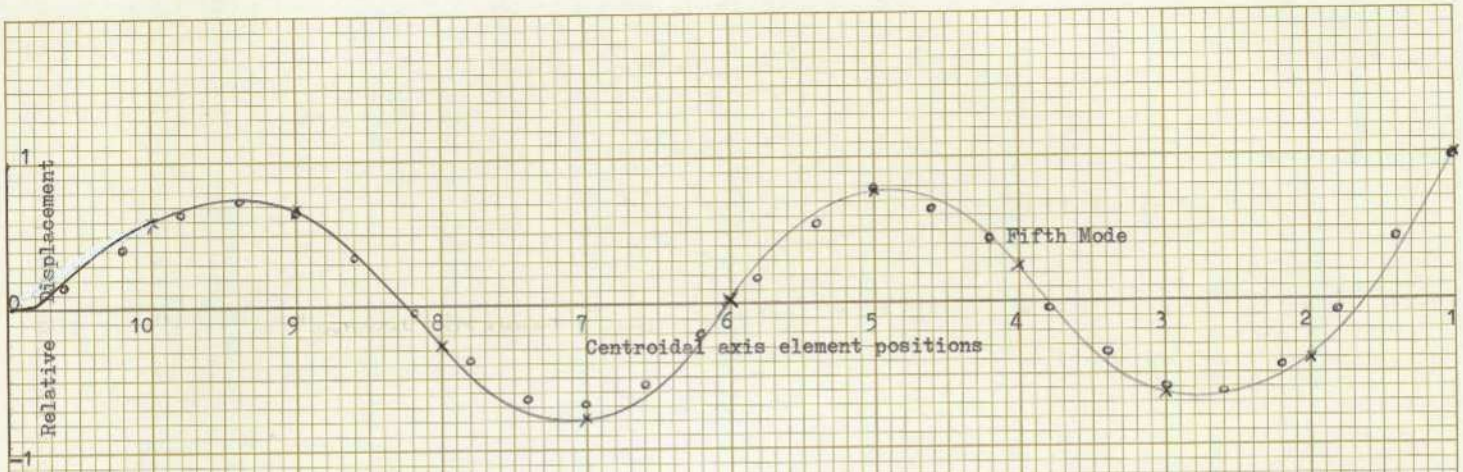

MODE SHAPES OF ROTATING BLADE

SPEED OF ROTATION 3 RADIANS / SEC

BLADE CODE : RTO3

DRAG MODE SHAPES

Computed results

Williams results(25 element idealisation)

FIGURE 70

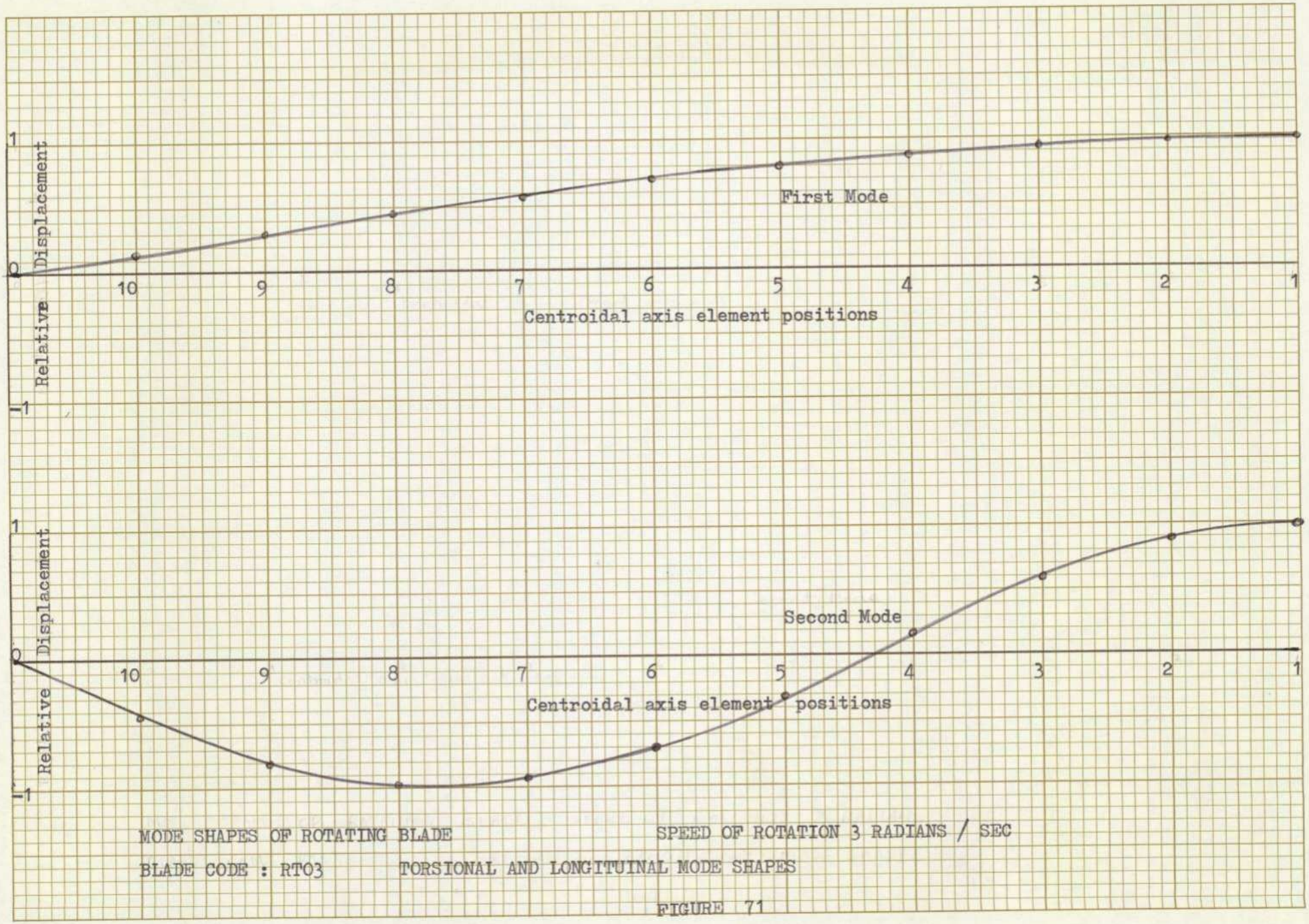

MODE SHAPES OF ROTATING BLADE SPEED OF ROTATION 3 RADIANS / SEC

BLADE CODE : RTO3 TORSIONAL AND LONGITUINAL MODE SHAPES

FIGURE 71

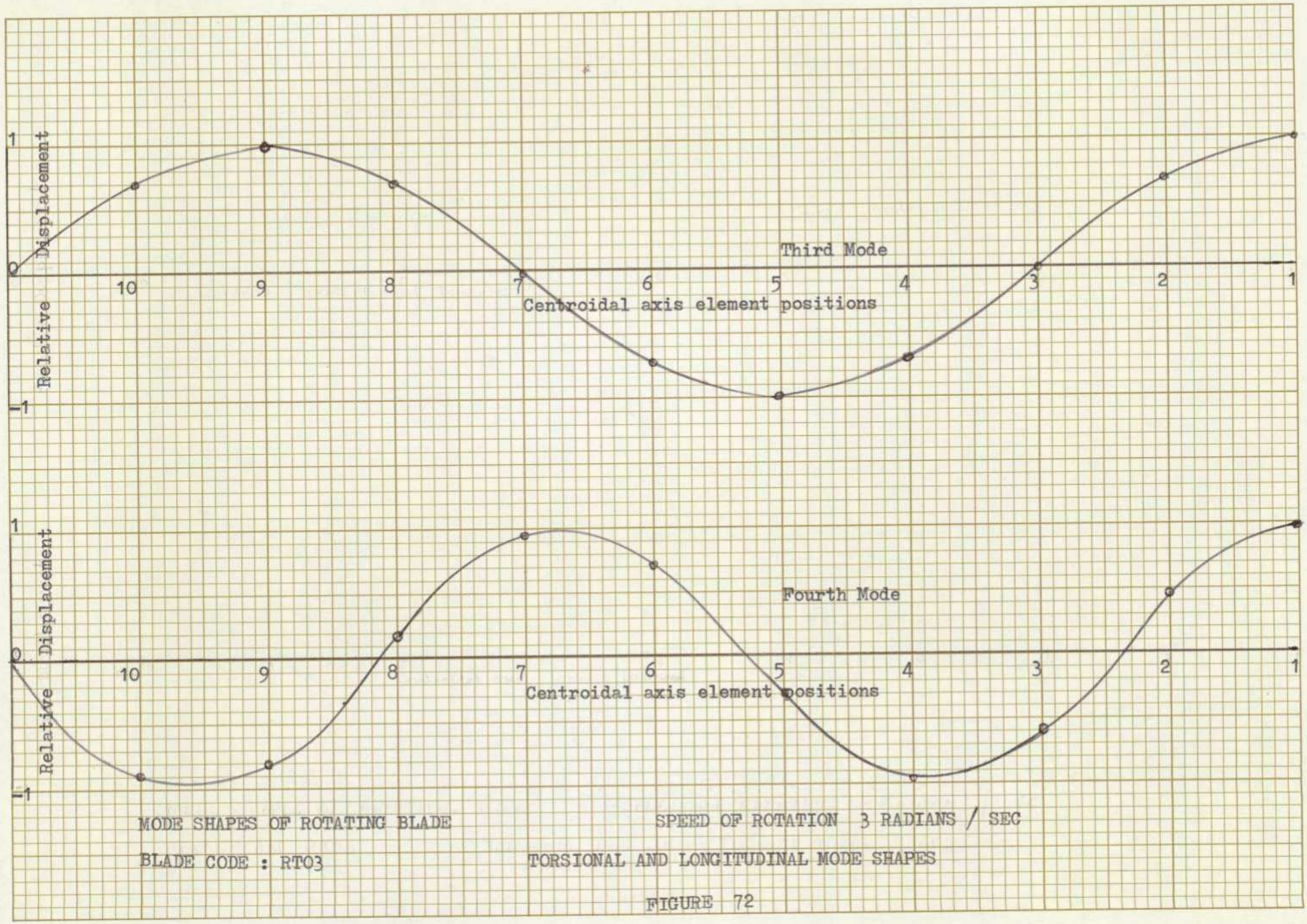

MODE SHAPES OF ROTATING BLADE

BLADE CODE : RT03

SPEED OF ROTATION 3 RADIANS / SEC

TORSIONAL AND LONGITUDINAL MODE SHAPES

FIGURE 72

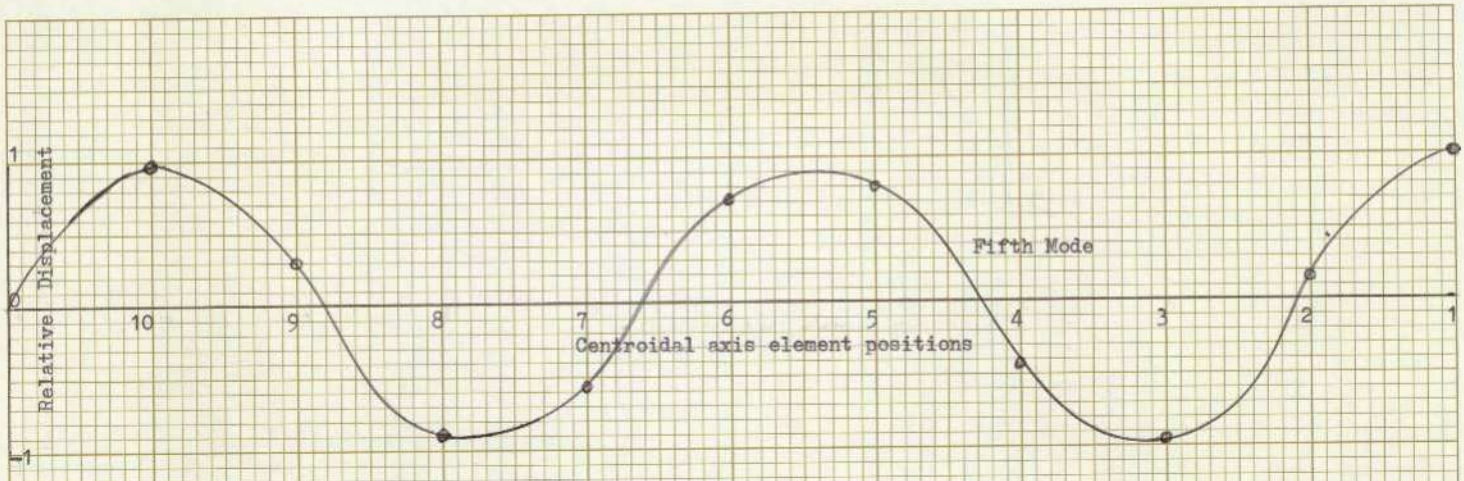

MODE SHAPES OF ROTATING BLADE

SPEED OF ROTATION 3 RADIANS / SEC

BLADE CODE :RT03

TORSIONAL AND LONGITUDINAL MODE SHAPES

FIGURE 73

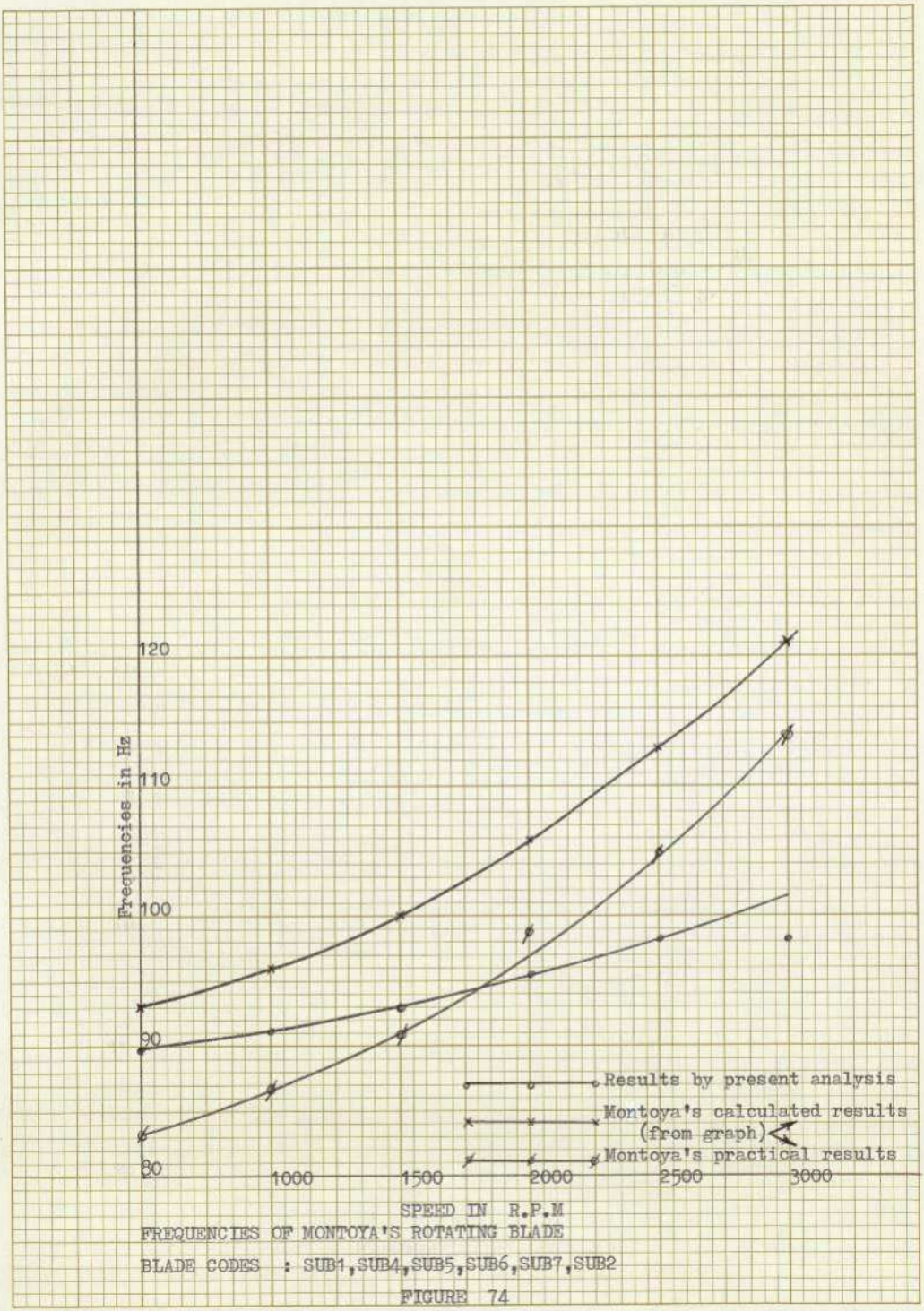

FREQUENCIES OF MONTOYA'S ROTATING BLADE

BLADE CODES : SUB1, SUB4, SUB5, SUB6, SUB7, SUB2

FIGURE 74

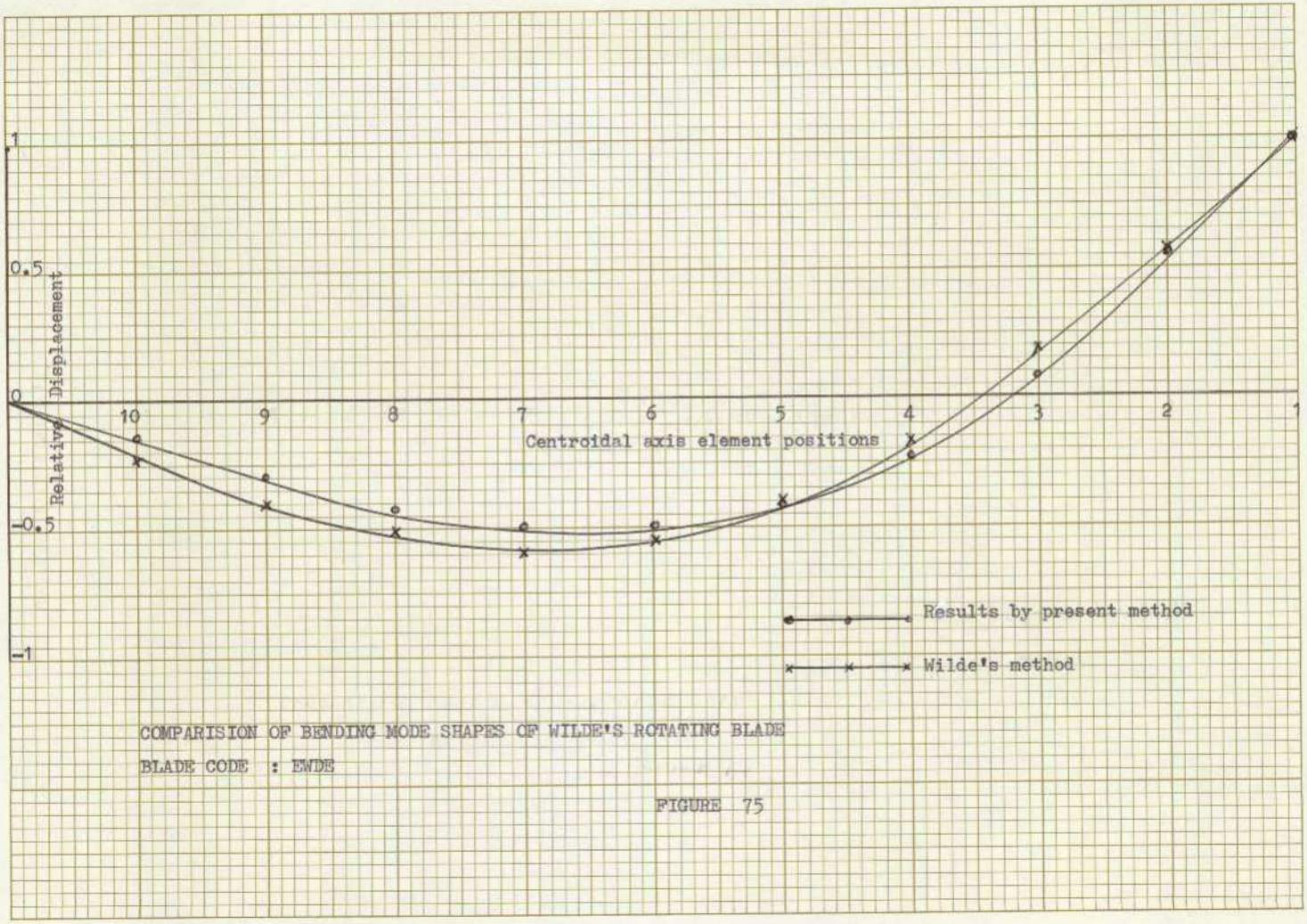

COMPARISION OF BENDING MODE SHAPES OF WILDE'S ROTATING BLADE

BLADE CODE : EWDE

FIGURE 75

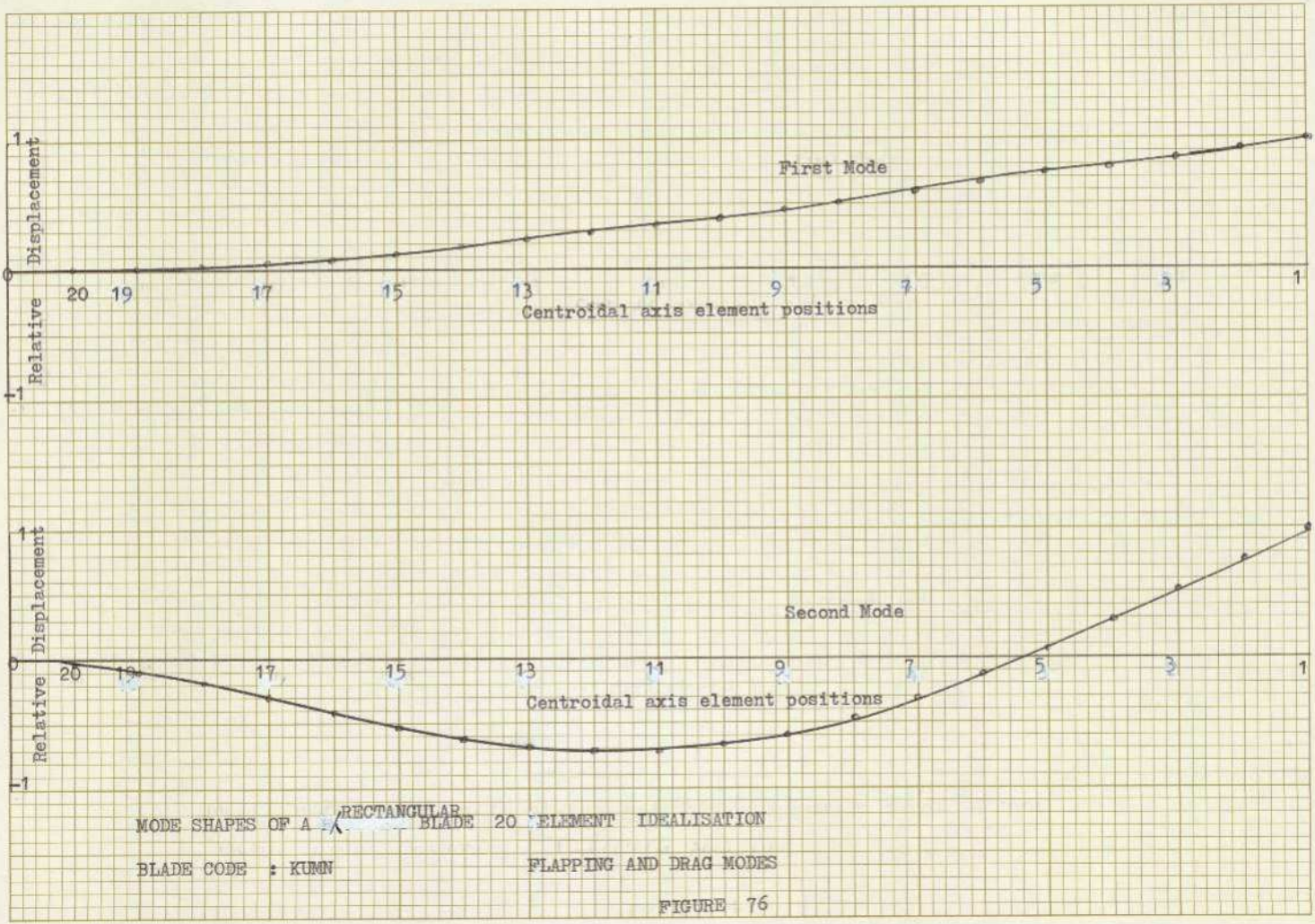

MODE SHAPES OF A RECTANGULAR BLADE 20 ELEMENT IDEALISATION

BLADE CODE : KUMN

FLAPPING AND DRAG MODES

FIGURE 76

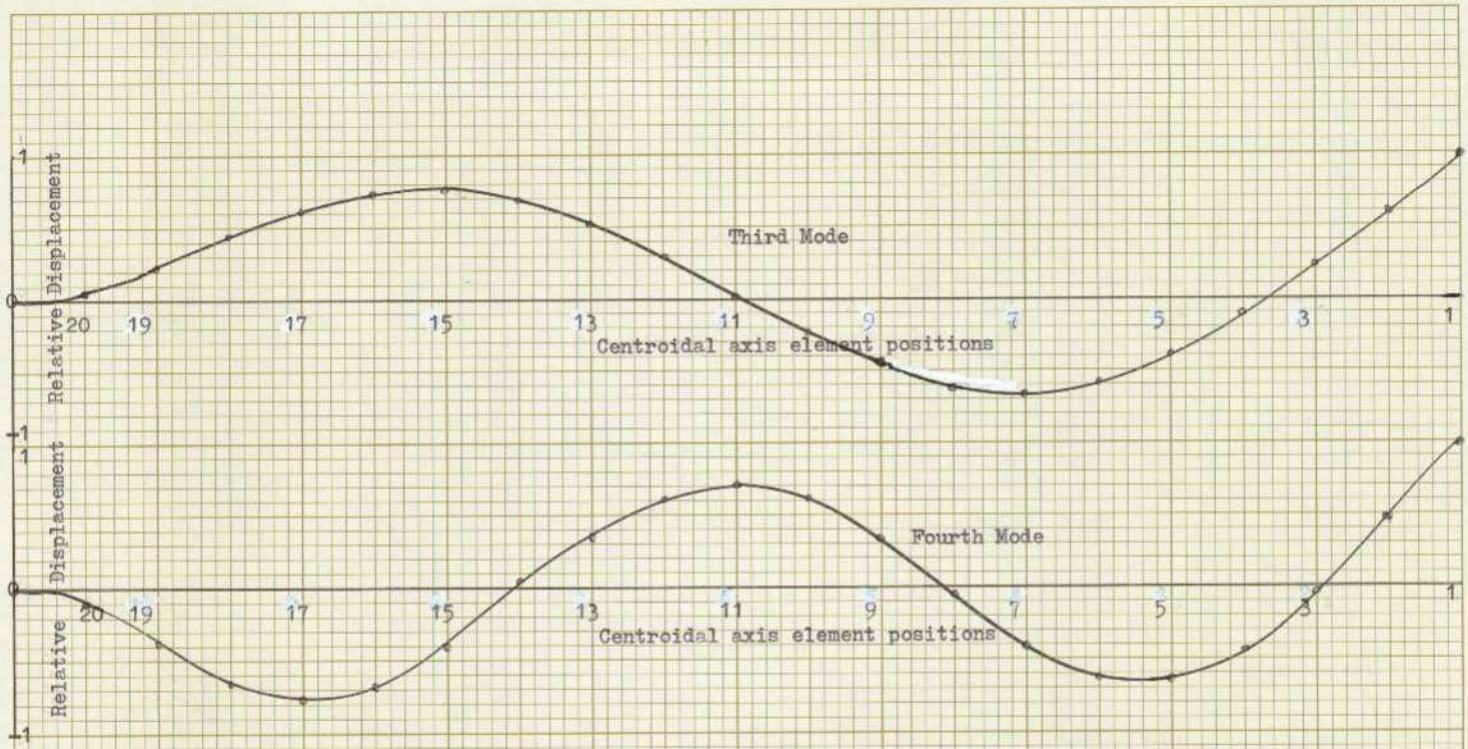

MODE SHAPES OF A RECTANGULAR BLADE 20 ELEMENT IDEALISATION

BLADE CODE : KUMN FLAPPING AND DRAG MODES

FIGURE 77

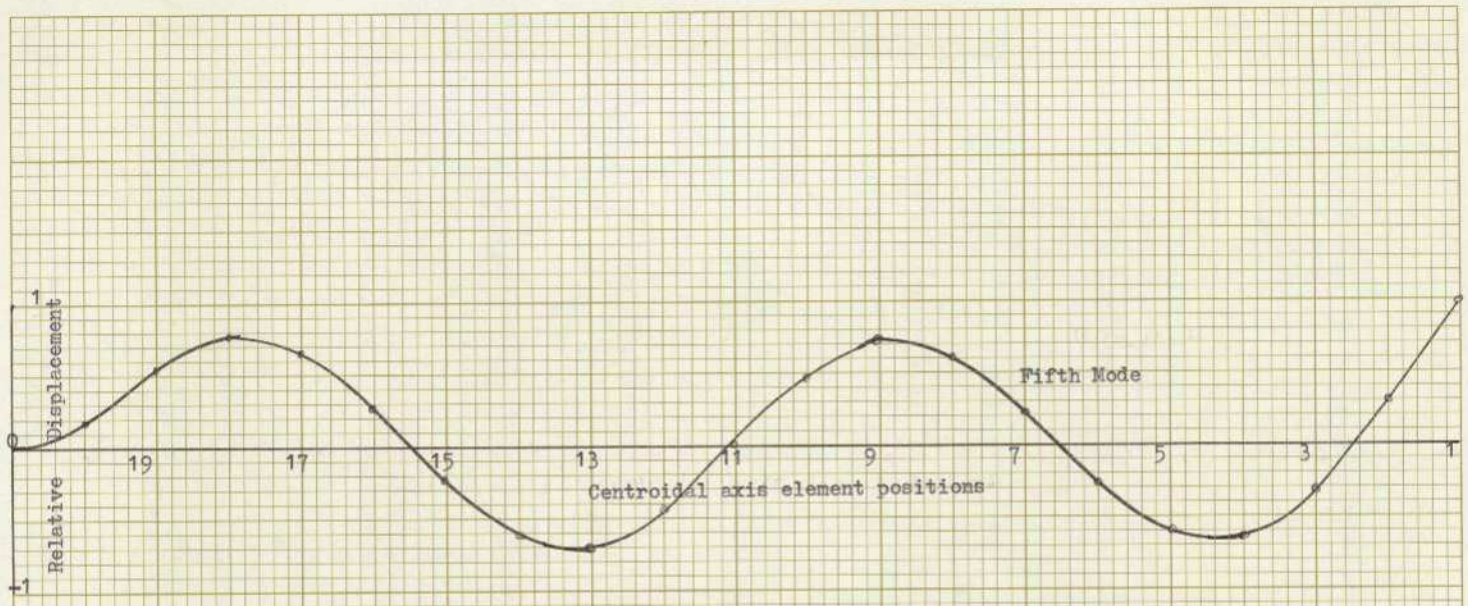

MODE SHAPES OF A RECTANGULAR BLADE 20 ELEMENT IDEALISATION

BLADE CODE : KUMN FLAPPING AND DRAG MODES

FIGURE 78

PROPERTIES OF DIRECTION COSINES BETWEEN ORTHOGONAL SETS OF AXES

The two reference axes are referred as Global or Overall axes and Local member axes which are represented in Figure A1.

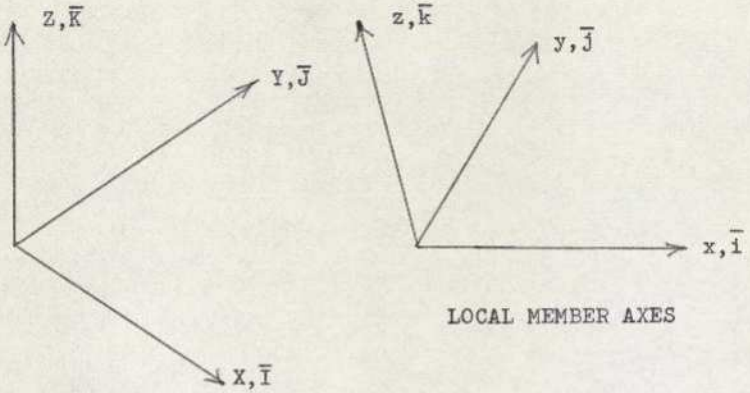

FIGURE A1

Unit vectors in the direction of the local axes x, y, z are denoted by $\bar{i}$, $\bar{j}$, $\bar{k}$ whilst unit vectors in the overall axes directions X, Y, Z are denoted by $\bar{I}$, $\bar{J}$, $\bar{K}$. The direction cosines between the positive axes directions are given by

		Overall axes X	Y	Z
local axes	x	l_x	m_x	n_x
	y	l_y	m_y	n_y
	z	l_z	m_z	n_z

The rows of the table represent the projection of unit vectors in the local axes directions on to the overall axes.

Thus
$$\bar{i} = l_x\bar{I} + m_x\bar{J} + n_x\bar{K} \quad \text{..... A1}$$
$$\bar{j} = l_y\bar{I} + m_y\bar{J} + n_y\bar{K} \quad \text{..... A2}$$
$$\bar{k} = l_z\bar{I} + m_z\bar{J} + n_z\bar{K} \quad \text{..... A3}$$

The columns of the table give the projection of unit vectors in the overall axes directions onto the local axes.

Thus
$$\bar{I} = {}^{l}x\bar{i} + {}^{l}y\bar{j} + {}^{l}z\bar{k} \quad \ldots\ldots\ldots\ldots\ldots \text{A4}$$
$$\bar{J} = {}^{m}x\bar{i} + {}^{m}y\bar{j} + {}^{m}z\bar{k} \quad \ldots\ldots\ldots\ldots\ldots \text{A5}$$
$$\bar{K} = {}^{n}x\bar{i} + {}^{n}y\bar{j} + {}^{n}z\bar{k} \quad \ldots\ldots\ldots\ldots\ldots \text{A6}$$

Relationships between the direction cosines can be derived by using the properties of the scalar and vector products.

Scalar Products

$$\bar{i}.\bar{i} = {}^{l2}x + {}^{m2}x + {}^{n2}x = 1 \quad \ldots\ldots\ldots\ldots\ldots \text{A7}$$
$$\bar{j}.\bar{j} = {}^{l2}y + {}^{m2}y + {}^{n2}y = 1 \quad \ldots\ldots\ldots\ldots\ldots \text{A8}$$
$$\bar{k}.\bar{k} = {}^{l2}z + {}^{m2}z + {}^{n2}z = 1 \quad \ldots\ldots\ldots\ldots\ldots \text{A9}$$
$$\bar{I}.\bar{I} = {}^{l2}x + {}^{l2}y + {}^{l2}z = 1 \quad \ldots\ldots\ldots\ldots\ldots \text{A10}$$
$$\bar{J}.\bar{J} = {}^{m2}x + {}^{m2}y + {}^{m2}z = 1 \quad \ldots\ldots\ldots\ldots\ldots \text{A11}$$
$$\bar{K}.\bar{K} = {}^{n2}x + {}^{n2}y + {}^{n2}z = 1 \quad \ldots\ldots\ldots\ldots\ldots \text{A12}$$
$$\bar{i}.\bar{j} = l_x l_y + m_x m_y + n_x n_y = 0 \quad \ldots\ldots\ldots\ldots\ldots \text{A13}$$
$$\bar{j}.\bar{k} = l_y l_z + m_y m_z + n_y n_z = 0 \quad \ldots\ldots\ldots\ldots\ldots \text{A14}$$
$$\bar{k}.\bar{i} = l_z l_x + m_z m_x + n_z n_x = 0 \quad \ldots\ldots\ldots\ldots\ldots \text{A15}$$
$$\bar{I}.\bar{J} = l_x m_x + l_y m_y + l_z m_z = 0 \quad \ldots\ldots\ldots\ldots\ldots \text{A16}$$
$$\bar{J}.\bar{K} = m_x n_x + m_y n_y + m_z n_z = 0 \quad \ldots\ldots\ldots\ldots\ldots \text{A17}$$
$$\bar{K}.\bar{I} = n_x l_x + n_y l_y + n_z l_z = 0 \quad \ldots\ldots\ldots\ldots\ldots \text{A18}$$

Vector Products

$$\bar{I} \wedge \bar{J} = \bar{k}, \qquad \bar{J} \wedge \bar{k} = \bar{I}, \qquad \bar{k} \wedge \bar{I} = \bar{J}$$

From the above vectorial product relationships considering $\bar{I} \wedge \bar{J} = \bar{k}$

$$\begin{vmatrix} \bar{I} & \bar{J} & \bar{K} \\ l_x & m_x & n_x \\ l_y & m_y & n_y \end{vmatrix} = l_z\bar{I} + m_z\bar{J} + n_z\bar{K} \quad \ldots \text{A19}$$

Expanding equation A19

$$(m_x n_y - m_y n_x)\bar{I} + (n_x l_y - l_x n_y)\bar{J} + (l_x m_y - l_y m_x)\bar{K} = l_z\bar{I} + m_z\bar{J} + n_z\bar{K}$$

Hence

$$m_x n_y - m_y n_x = l_z \quad \text{A20}$$
$$n_x l_y - l_x n_y = m_z \quad \text{A21}$$
$$l_x m_y - l_y m_x = n_z \quad \text{A22}$$

Similarly expanding the vector products $\bar{j} \wedge \bar{k} = \bar{i}$ and $\bar{k} \wedge \bar{i} = \bar{j}$ the following relationships are obtained.

$$m_z n_x - m_x n_z = l_y \quad \text{A23}$$
$$n_z l_x - l_z n_x = m_y \quad \text{A24}$$
$$l_z m_x - m_z l_x = n_y \quad \text{A25}$$
$$m_y n_z - n_y m_z = l_x \quad \text{A26}$$
$$n_y l_z - l_y n_z = m_x \quad \text{A27}$$
$$l_y m_z - l_z m_y = n_x \quad \text{A28}$$

The vector products $\bar{I} \wedge \bar{J} = \bar{K}$, $\bar{J} \wedge \bar{K} = \bar{I}$ and $\bar{K} \wedge \bar{I} = \bar{J}$ will yield the same relationships as that of equations A20–A28.

MATRIX EXPRESSIONS AND OPERATIONS

The different types of matrices which would occur in structural analysis are described in addition to the fundamental matrix operations comprising addition, subtraction, transposition, multiplication and inversion. A matrix is defined as a rectangular array of symbols arranged in rows and columns. If there are m rows and n columns the matrix can be represented by

$$\bar{A} = \begin{bmatrix} a_{11} & a_{12} & a_{13} & \cdots\cdots\cdots & a_{1n} \\ a_{21} & a_{22} & a_{23} & \cdots\cdots\cdots & a_{2n} \\ a_{31} & a_{32} & a_{33} & \cdots\cdots\cdots & a_{3n} \\ & & & & \\ a_{m1} & a_{m2} & a_{m3} & \cdots\cdots\cdots & a_{mn} \end{bmatrix} \quad \cdots\cdots\cdots (A29)$$

A typical element $a_{i,\,j}$ has two subscripts, of which the first denotes the ith row and the second one denotes the jth column. A matrix with m rows and n columns is defined as a mxn matrix.

Row and Column Matrices:

If m = 1 the matrix in (A29) reduces to a single row.

$\bar{A} = (a_{11}\ a_{12}\ a_{13} \cdots\cdots\cdots a_{1n})$ ..... (A30) which is called a row matrix. Similarly if n = 1 the matrix $\bar{A}$ reduces to a single column,

$$\bar{A} = \begin{bmatrix} a_{11} \\ a_{21} \\ a_{31} \\ \vdots \\ a_{m1} \end{bmatrix} \quad \cdots\cdots\cdots\cdots (A31)$$

which is called a column matrix.

Null Matrix:

When all the elements of a matrix are equal to zero, the matrix is called null matrix and is indicated by $\bar{0}$.

Square Matrix:

If m = n, the matrix $\bar{A}$ in (A29) reduces to a square array

$$\bar{A} = \begin{bmatrix} a_{11} & a_{12} & a_{13} & \cdots\cdots & a_{1n} \\ a_{21} & a_{22} & a_{23} & \cdots\cdots & a_{2n} \\ a_{31} & a_{32} & a_{33} & \cdots\cdots & a_{3n} \\ \cdot & \cdot & \cdot & & \\ \cdot & \cdot & \cdot & & \\ \cdot & \cdot & \cdot & & \\ a_{n1} & a_{n2} & a_{n3} & \cdots\cdots & a_{nn} \end{bmatrix} \quad \cdots\cdots\cdots \text{(A32)}$$

which is called a square matrix.

Diagonal Matrix:

A diagonal matrix is one which has zero elements everywhere outside the principal diagonal. It follows therefore that for a diagonal matrix $a_{ij} = 0$ when $i \neq j$ and not all a_{ii} are zero. A typical diagonal matrix may be given by:

$$\bar{A} = \begin{bmatrix} a_{11} & 0 & 0 & \cdots\cdots & 0 \\ 0 & a_{22} & 0 & \cdots\cdots & 0 \\ 0 & 0 & a_{33} & \cdots\cdots & 0 \\ \cdot & \cdot & \cdot & & \\ \cdot & \cdot & \cdot & & \\ \cdot & \cdot & \cdot & & \\ 0 & 0 & 0 & & a_{nn} \end{bmatrix} \quad \cdots\cdots\cdots \text{(A33)}$$

Identity Matrix:

An identity matrix is one which has unit elements on the principal diagonal and zero elsewhere It is usually denoted by symbol $\bar{I}$. A unit matrix of order 4 x 4 can be written as

$$\bar{I} = \begin{bmatrix} 1 & 0 & 0 & 0 \\ 0 & 1 & 0 & 0 \\ 0 & 0 & 1 & 0 \\ 0 & 0 & 0 & 1 \end{bmatrix} \quad \cdots\cdots\cdots \text{(A34)}$$

Triangular Matrix:

If all the elements on one side of the principal diagonal of a square matrix are zero, the matrix is called a triangular matrix. There are two types of triangular matrices: an upper triangle matrix whose elements below the principal diagonal are zero and a lower triangle matrix whose elements above diagonal are zero. A typical upper and lower triangle matrices can be written as follows:

Upper Triangle Matrix

$$\begin{bmatrix} a_{11} & a_{12} & a_{13} & \cdots & a_{1n} \\ 0 & a_{22} & a_{23} & \cdots & a_{2n} \\ 0 & 0 & a_{33} & \cdots & a_{3n} \\ 0 & 0 & 0 & \cdots & a_{4n} \\ 0 & 0 & 0 & 0 & a_{nn} \end{bmatrix}$$

Lower Triangle Matrix

$$\begin{bmatrix} a_{11} & 0 & 0 & 0 & 0 & 0 & 0 \\ a_{21} & a_{22} & 0 & 0 & 0 & 0 & 0 \\ a_{31} & a_{32} & a_{33} & 0 & 0 & 0 & 0 \\ & & & & 0 & 0 & 0 \\ a_{n1} & a_{n2} & a_{n3} & & & & a_{nn} \end{bmatrix}$$

Addition and Subtraction of Matrices

If the corresponding elements in matrices $\bar{A}$ and $\bar{B}$, of the same order, are added algebraically, the resulting elements form a third matrix, which is the sum of the first two, that is

$$\bar{A} + \bar{B} = \bar{C} \text{ where } C_{ij} = a_{ij} + b_{ij}$$

Similarly if the elements in matrices $\bar{A}$ and $\bar{B}$ are algebraically subtracted, the resulting elements form a third matrix which is the difference of the first two, that is

$$\bar{A} - \bar{B} = \bar{C} \text{ where } C_{ij} = a_{ij} - b_{ij}$$

Matrix Transposition

The transposed matrix is formed from the matrix $\bar{A}$ by interchanging all rows for the corresponding columns. The transposition of a matrix will be denoted by the superscript T. Thus $\bar{A}^T$ represents the transpose of $\bar{A}$. For example if

$$\bar{A} = \begin{bmatrix} a_{11} & a_{12} & a_{13} \\ a_{21} & a_{22} & a_{23} \end{bmatrix} \quad \text{then } \bar{A}^T = \begin{bmatrix} a_{11} & a_{21} \\ a_{12} & a_{22} \\ a_{13} & a_{23} \end{bmatrix}$$

Matrix Multiplication

Two matrices $\bar{A}$ and $\bar{B}$ can be multiplied together in order $\bar{A}\bar{B}$ only when the number of columns in $\bar{A}$ is equal to the number of rows in $\bar{B}$. When this condition is satisfied, the $\bar{A}$ and $\bar{B}$ are said to be confirmable for multiplication. The product of two conformable matrices $\bar{A}$ and $\bar{B}$ of order mxp and pxn, respectively, is defined as matrix $\bar{C}$ of order mxn whose elements are calculated from

$$C_{ij} = \sum_{r=1}^{p} a_{ir} b_{rj} \quad i = 1, 2 \ldots\ldots m \quad j = 1, 2 \ldots\ldots n \quad \ldots\ldots (A35)$$

where a_{ir} and b_{rj} are the elements of $\bar{A}$ and $\bar{B}$ respectively.

Matrix Inversion

The inverse of a square matrix $\bar{A}$ is written as $\bar{A}^{-1}$ and is defined as the matrix when multiplied by the original matrix $\bar{A}$ results in the identity matrix. The inverse is always a square matrix of the same order as the original matrix itself and only a square matrix has an inverse. The relationship between a matrix and its inverse is given by

$$\bar{A}\,\bar{A}^{-1} = \bar{A}^{-1}\,\bar{A} = \bar{I} \quad \ldots\ldots\ldots\ldots\ldots (A36)$$

Matrix Partitioning; Submatrices

The array of the elements in a matrix may be divided into smaller arrays by horizontal and vertical lines. Such a matrrix is refered to as a paritioned matrix and the smaller arrays are called submatrices. For example a square matrix of order 3 may be partitioned into four submatrices as follows:

$$\bar{A} = \left[\begin{array}{cc|c} a_{11} & a_{12} & a_{13} \\ a_{21} & a_{22} & a_{23} \\ \hline a_{31} & a_{32} & a_{33} \end{array}\right] = \begin{bmatrix} \bar{A}_{11} & \bar{A}_{12} \\ \bar{A}_{21} & \bar{A}_{22} \end{bmatrix} \quad \ldots\ldots\ldots A36'$$

Where $\bar{A}_{11} = \begin{bmatrix} a_{11} & a_{12} \\ a_{21} & a_{22} \end{bmatrix}$, $\bar{A}_{12} = \begin{bmatrix} a_{13} \\ a_{23} \end{bmatrix}$, $\bar{A}_{21} = \begin{bmatrix} a_{31} & a_{32} \end{bmatrix}$

and $\bar{A}_{22} = \begin{bmatrix} a_{33} \end{bmatrix}$

Provided the general rules for matrix operation (addition, subtraction etc) are observed, the submatrices can be treated as if they were ordinary matrix elements.

UNIT-LOAD METHOD

The unit-load method can be used not only for simple structures like beams and trusses, but also for very complicated structures having many members. Furthermore, the unit load method is suitable for finding all types of displacements, including the deflection of a point in the structure, the rotation of the axis of the member and the relative displacement between two points. This method is also known as the method of virtual work, the dummy-load method and the Maxwell-Mohr method. Two systems of loading that act upon the structure must be considered when using the unit load method

a) The first system consists of the structure subjected to the actual loads; and

b) The second system consists of a unit load acting alone on the structure.

The unit load is a fictitious or dummy load that is introduced solely for the purpose of calculating a displacement, say Δ, of the structure due to the actual loads. The term "displacement" is used here in a generalised sense; thus the displacement Δ may be a translation, a rotation or a relative displacement. The unit load acting on the structure, produces reactions at the support and stress resultants within the members. These stress resultants are designated by symbols P_v, M_v, V_v and T_v (axial stress, moments, shear stress, and Torsion). These quantities, in combination with the unit load and the reactions, constitute a force system which is in equilibrium.

According to the principle of virtual work, if the structure is given a small virtual deformation then the virtual work of the external forces is equal to the virtual work of the internal forces.

$$W_{ext} = W_{int} \quad \ldots\ldots\ldots\ldots\ldots\ldots \quad (A37)$$

During the virtual deformation the only external virtual work is by the unit load. This virtual work is the product of the unit load and the displacement Δ through which it moves; thus

$$W_{ext} = 1 \cdot \Delta \quad \ldots\ldots\ldots\ldots\ldots\ldots \quad (A38)$$

where Δ represents the desired displacement of the structure due to actual loads.

The internal virtual work is the work performed by the stress resultants P_v, M_v, V_v and T_v when the elements of the structure are deformed virtually. However, the virtual deformations are chosen to be the same as actual deformations that occur in the structure supporting the real loads. Denoting these deformations by $d\delta$, $d\theta$, $d\lambda$ and $d\phi$ the equation for internal work can be written

$$W_{int} = \int P_v d\delta + \int M_v d\theta + \int V_v d\lambda + \int T_v d\phi \quad \ldots\ldots \text{(A39)}$$

By equating external and internal work (Equations A38 and A39) the fundamental equation of the unit load method is obtained

$$\Delta = \int P_v d\delta + \int M_v d\theta + \int V_v d\lambda + \int T_v d\phi \quad \ldots\ldots \text{(A40)}$$

In the above equation Δ represents the displacement to be calculated, (translation, rotation or a relative displacement); the stress resultants P_v, M_v, V_v and T_v represent the axial force, bending moment, shear force and twisting couple caused by the unit load; and $d\delta$, $d\theta$, $d\lambda$ and $d\phi$ represent deformations caused by the actual loads. The fundamental equation of the unit load method (A40) is quite general and is not subjected to any restrictions concerning linear behaviour of the material or the structure. However, when the material of the structure follows Hook's law and the structure behaves linearly, the expressions for the deformations $d\delta$, $d\theta$, $d\lambda$ and $d\phi$ can be readily obtained. If the stress resultants in the structure due to real loads are denoted as P_A, M_A, V_A and T_A then the deformations are given by

$$d\delta = \frac{P_A dx}{EA} \quad \ldots\ldots \text{(A41)}$$

$$d\theta = \frac{M_A dx}{EI} \quad \ldots\ldots \text{(A42)}$$

$$d\lambda = \frac{V_A dx}{GA} \quad \ldots\ldots \text{(A43)}$$

$$d\phi = \frac{T_A dx}{GJ} \quad \ldots\ldots \text{(A44)}$$

Substituting these four expressions into equation A40 gives the equation of the unit load method in the following form

$$\Delta = \int \frac{P_v P_A dx}{EA} + \int \frac{M_v M_A dx}{EI} + \int \frac{\alpha_s V_v V_A dx}{GA} + \int \frac{T_v T_A dx}{GJ} \quad \ldots\ldots \text{(A45)}$$

Each integral in the above equation represents the contribution of one type of deformation to the total displacement. The procedure for calculating a displacement by means of the unit load method using equation (A45) may be summarised as follows:

a) determine the stress resultants P_A, M_A, V_A and T_A in the structure caused by the actual loads.

b) place a unit load on the structure corresponding to the displacement Δ that is to be found.

c) determine the stress resultants P_V, M_V, V_V and T_V caused by the unit load.

d) form the terms shown in A45 and integrate each term for the entire structure; and

e) sum the results to obtain the displacement Δ.

Depending upon the type of structure, it can be anticipated that some of the terms in equation (A45) will not be needed. For example, if a truss with pinned joints has loads acting only at the joints, then there will be no flexural, shearing or torsional deformations and only first term in equation (A45) is required. Similarly only flexural deformations are apt to be important in the case of a beam. Individual unit load equations depending on the load conditions can be given as follows:

For deformation due to axial loads only

$$\Delta = \int \frac{P_A P_V dx}{EA} \quad \ldots\ldots\ldots\ldots\ldots\ldots \quad (A46)$$

For flexural deformation, only due to bending

$$\Delta = \int \frac{M_A M_V dx}{EI} \quad \ldots\ldots\ldots\ldots\ldots\ldots \quad (A47)$$

For shear deformations due to shear loads only

$$\Delta = \int \frac{\alpha_s V_A V_V dx}{GA} \quad \ldots\ldots\ldots\ldots\ldots\ldots \quad (A48)$$

and twisting deformation, only due to twisting couples

$$\Delta = \int \frac{T_A T_V dx}{GJ} \quad \ldots\ldots\ldots\ldots\ldots\ldots\ldots\ldots \text{(A49)}$$

In general, it is possible to calculate displacements of structures by using any combination of equations (A46 - A49), depending upon the type of structure.

APPENDIX 4

FLEXIBILITY MATRIX - EVALUATION OF INTEGRALS.
from section 3.3

$$My' = My_1 + (My_2 - My_1)\frac{Xr}{Lr} \quad \text{.....A50}$$

$$Mz' = Mz_1 + (Mz_2 - Mz_1)\frac{Xr}{Lr} \quad \text{.....A51}$$

$$Mx = Mx_1 + (Mx_2 - Mx_1)\frac{Xr}{Lr} \quad \text{.....A52}$$

$$Px = Px_1 + (Px_2 - Px_1)\frac{Xr}{Lr} \quad \text{.....A53}$$

$$My = My' + \beta \frac{Xr}{Lr} Mz' - \frac{\beta^2 Xr^2}{2Lr^2} My' \quad \text{.....A54}$$

$$Mz = Mz' - \beta \frac{Xr}{Lr} My' - \frac{\beta^2 Xr^2}{2Lr} Mz' \quad \text{.....A55}$$

Note: $\beta = \beta_2 - \beta_1$

Substituting the values of My' and Mz' from A50 and A51

$$My = My_1 + (My_2 - My_1)\frac{Xr}{Lr} + \beta \frac{Xr}{Lr}\left\{Mz_1 + (Mz_2 - Mz_1)\frac{Xr}{Lr}\right\}$$

$$-\frac{\beta^2 Xr^2}{2Lr^2}\left\{My_1 + (My_2 - My_1)\frac{Xr}{Lr}\right\} \quad \text{.....A56}$$

$$Mz = Mz_1 + (Mz_2 - Mz_1)\frac{Xr}{Lr} - \beta \frac{Xr}{Lr}\left\{My_1 + (My_2 - My_1)\frac{Xr}{Lr}\right\}$$

$$-\frac{\beta^2 Xr^2}{2Lr^2}\left\{Mz_1 + (Mz_2 - Mz_1)\frac{Xr}{Lr}\right\} \quad \text{.....A57}$$

$$Msv = Mx_1 + (Mx_2 - Mx_1)\frac{Xr}{Lr} + C_1\left\{Px_1 + (Px_2 - Px_1)\frac{Xr}{Lr}\right\}$$

$$+C_2\left[My_1 + (My_2 - My_1)\frac{Xr}{Lr} + \left\{\frac{\beta Xr}{Lr}\left(Mz_1 + (Mz_2 - Mz_1)\frac{Xr}{Lr}\right)\right.\right.$$

$$- \frac{\beta \, Xr^2}{2Lr^2} \left\{ My_1 + (My_2 - My_1) \frac{Xr}{Lr} \right\} \Bigg]$$

$$+ C_3 \left[Mz_1 + (Mz_2 - Mz_1) \frac{Xr}{Lr} - \frac{\beta \, Xr^2}{2Lr} \left\{ My_1 + (My_2 - My_1) \frac{Xr}{Lr} \right\} \right.$$

$$\left. - \frac{\beta \, Xr^2}{2Lr} \left\{ Mz_1 + (Mz_2 - Mz_1) \frac{Xr}{Lr} \right\} \right] \quad \ldots\ldots A58$$

I II

$$P_V^T \Delta_A = \int_0^L \frac{Px_V \, Px_A}{EA} \, dx + \int_0^L \frac{My_V \, My_A}{E I_y} \, dx$$

$$+ \int_0^L \frac{Mz_V \, Mz_A}{E I_z} \, dx + \int_0^L \frac{Ms_{VV} \, Ms_{VA}}{GJ} \, dx \quad \ldots\ldots A59$$

III IV

Considering the integral I.
Substituting values of Px_V and PxA from A53.

$$\int_0^L \frac{Px_V \, Px_A}{EA} \, dx = \frac{1}{EA} \int_0^L \left\{ Px_{V_1} + (Px_{V_2} - Px_{V_1}) \frac{X}{L} \right\} \left\{ Px_1 + (Px_2 - Px_1) \frac{X}{L} \right\} dx$$

$$= \frac{1}{EA} \int_0^L \left(Px_{V_1} \left\{ Px_1 + (Px_2 - Px_1) \frac{X}{L} \right\} dx + \right.$$

$$\left. \frac{1}{EA} \int_0^L (Px_{V_2} - Px_{V_1}) \frac{X}{L} \left\{ Px_1 + (Px_2 - Px_1) \frac{X}{L} \right\} dx. \right.$$

$$= \frac{1}{EA} P_{xv_1} \left[P_{x_1} x + (P_{x_2} - P_{x_1}) \frac{X^2}{2L} \right]_0^L + \frac{1}{EA} (P_{xv_2} - P_{x_{v1}})$$

$$\left[P_{x1} \frac{x^2}{2L} (P_{x_2} - P_{x_1}) \frac{x_2^3}{3L} \right]_0^L$$

$$= \frac{1}{EA} P_{xv_1} \left(P_{x_1} L + (P_{x_2} - P_{x_1}) \frac{L}{2} \right) + \frac{1}{EA} (P_{xv_2} - P_{xv_1}) \left[\left\{ P_{x_1} L/2 + (P_{x_2} - P_{x_1}) \right\} \frac{L}{3} \right]$$

$$= \frac{L}{EA} P_{xv1} \left[\frac{P_{x1}}{2} + \frac{P_{x2}}{2}\right] + \frac{L}{EA} (P_{xv2} - P_{xv1}) \left[\frac{1}{6} P_{x1} + \frac{1}{3} P_{x2}\right]$$

$$= P_{xv1} \frac{L}{EA} \left[\frac{1}{3} P_{x1} + \frac{1}{6} P_{x2}\right] + P_{xv2} \frac{L}{EA} \left[\frac{1}{6} P_{x1} + \frac{1}{3} P_{x2}\right] \quad \ldots A60$$

Considering the integral II.
Substituting values of M_{yv} and M_{yA} from A56.

$$\int_0^L \frac{M_{yv} M_{yA}\, dx}{EI_y} = \frac{1}{EI_y} \int_0^L \left[M_{yv1} + (M_{yv2} - M_{yv1}) \frac{X}{L} + \frac{\beta X}{L} \left\{M_{zv1} + (M_{zv2} - M_{zv1}) \frac{X}{L}\right\} - \frac{\beta^2 x^2}{2L} \left\{M_{yy1} + (M_{yv2} - M_{yv1}) \frac{X}{L}\right\}\right] \left[M_{y1} + (M_{y2} - M_{y1}) \frac{X}{L} + \frac{\beta X}{L} \left\{M_{z1} + (M_{z2} - M_{z1}) \frac{X}{L}\right\} - \frac{\beta^2 x^2}{2L} \left\{M_{y1} + (M_{y2} - M_{y1}) \frac{X}{L}\right\}\right]$$

$$= \frac{1}{EI_y} \int_0^L \left\{M_{yv1} + (M_{yv2} - M_{yv1}) \frac{X}{L}\right\} \left\{M_{y1} + (M_{y2} - M_{y1}) \frac{X}{L}\right\} dx$$

$$+ \frac{\beta}{EI_y L} \int_0^L \left\{M_{yv1} + (M_{yv2} - M_{yv1}) \frac{X}{L}\right\} X \left\{M_{z1} + (M_{z2} - M_{z1}) \frac{X}{L}\right\} dx$$

$$- \frac{\beta^2}{2EI_y L^2} \int_0^L \left\{M_{yv1} + (M_{yv2} - M_{yv1}) \frac{X}{L}\right\} \left\{X^2 \left[M_{y1} + (M_{y2} - M_{y1}) \frac{X}{L}\right]\right\} dx$$

$$+ \frac{\beta}{EI_y L} \int_0^L X \left\{M_{zv1} + (M_{zv2} - M_{zv1}) \frac{X}{L}\right\} \left\{M_{y1} + (M_{y2} - M_{y1}) \frac{X}{L}\right\} dx$$

$$+ \frac{\beta^2}{EI_y L^2} \int_0^L X^2 \left\{M_{zv1} + (M_{zv2} - M_{zv1}) \frac{X}{L}\right\} \left\{M_{z1} + (M_{z2} - M_{z1}) \frac{X}{L}\right\} dx.$$

$$- \frac{\beta^3}{2EI_y L^3} \int_0^L X^3 \left\{M_{zv1} + (M_{zv2} - M_{zv1}) \frac{X}{L}\right\} \left\{M_{y1} + (M_{y2} - M_{y1}) \frac{X}{L}\right\} dx$$

$$- \frac{\beta^2}{2L^2 EI_y} \int_0^L X^2 \left\{M_{yv1} + (M_{yv2} - M_{yv1}) \frac{X}{L}\right\} \left\{M_{y1} + (M_{y2} - M_{y1}) \frac{X}{L}\right\} dx$$

$$- \frac{\beta^3}{2L^3 EI_y} \int_0^L X^3 \left\{M_{yv1} + (M_{yv2} - M_{yv1}) \frac{X}{L}\right\} \left\{M_{z1} + (M_{z2} - M_{z1}) \frac{X}{L}\right\} dx$$

$$+ \frac{\beta^4}{4L^4 EI_y} \int_0^L X^4 \left\{M_{yv1} + (M_{yv2} - M_{yv1}) \frac{X}{L}\right\} \left\{M_{y1} + (M_{y2} - M_{y1}) \frac{X}{L}\right\} dx$$

Ignoring terms containing β^3 and β^4 and integrating.

$$= \frac{M_{yv1}\,\beta L}{EI_y}\left[\frac{1}{12}M_{z1} + \frac{1}{12}M_{z2}\right] + \frac{M_{yv2}\,\beta L}{EI_y}\left[\frac{1}{12}M_{z1} + \frac{1}{4}M_{z2}\right]$$

$$+ \frac{M_{yv1}L}{EI_y}\left[\frac{M_{y1}}{3} + \frac{M_{y2}}{6}\right] + \frac{M_{yv2}L}{EI_y}\left[\frac{M_{y1}}{6} + \frac{M_{y2}}{3}\right]$$

$$+ \frac{M_{zv1}\,\beta^2 L}{EI_y}\left[\frac{M_{z1}}{30} + \frac{M_{z2}}{20}\right] + \frac{M_{zv2}\,\beta^2 L}{EI_y}\left[\frac{M_{z1}}{20} + \frac{M_{z2}}{5}\right]$$

$$- \frac{M_{yv1}\,L\beta^2}{2EI_y}\left[\frac{M_{y1}}{30} + \frac{M_{y2}}{20}\right] - \frac{M_{yv2}\,\beta^2 L}{2EI_y}\left[\frac{M_{y1}}{20} + \frac{M_{y2}}{5}\right]$$

$$- \frac{M_{yv1}\,\beta^2 L}{2EI_y}\left[\frac{M_{y1}}{30} + \frac{M_{y2}}{20}\right] - \frac{M_{yv2}\,\beta^2 L}{2EI_y}\left[\frac{M_{y1}}{20} + \frac{M_{y2}}{5}\right]$$

$$+ \frac{M_{zv1}\,\beta L}{EI_y}\left[\frac{M_{y1}}{12} + \frac{M_{y2}}{12}\right] + \frac{M_{zv2}\,\beta L}{EI_y}\left[\frac{M_{y1}}{12} + \frac{M_{y2}}{4}\right]$$

Adding appropriate terms :

$$= M_{yv1}\left[\frac{M_{y1}L}{3EI_y} + \frac{M_{y2}L}{6EI_y} + \frac{\beta LM_{z1}}{12EI_y} + \frac{\beta LM_{z2}}{12EI_y} - \frac{\beta^2 LM_{y1}}{30EI_y} - \frac{\beta^2 LM_{y2}}{20EI_y}\right]$$

$$+ M_{yv2}\left[\frac{M_{y1}L}{6EI_y} + \frac{M_{y2}L}{3EI_y} + \frac{\beta LM_{z1}}{12EI_y} + \frac{\beta LM_{z2}}{4EI_y} - \frac{\beta^2 LM_{y1}}{20EI_y} - \frac{\beta^2 LM_{y2}}{5EI_y}\right]$$

$$+ M_{zv1}\left[\frac{\beta LM_{y1}}{12EI_y} + \frac{\beta LM_{y2}}{12EI_y} + \frac{\beta^2 LM_{z1}}{30EI_y} + \frac{\beta^2 LM_{z2}}{20EI_y}\right]$$

$$+ M_{zv2}\left[\frac{\beta LM_{y1}}{12EI_y} + \frac{\beta LM_{y2}}{4EI_y} + \frac{\beta^2 LM_{z1}}{20EI_y} + \frac{\beta^2 LM_{z2}}{5EI_y}\right] \quad \ldots\ldots A61$$

Consider ing the integral III.

$$\int_0^L \frac{M_{zv}\,M_{zA}\,dx}{EI_z} = \frac{1}{EI_z}\int_0^L \left[M_{zv1} + (M_{zv2} - M_{zv1})\frac{X}{L} - \beta\frac{X}{L}\left(M_{yv1} + (M_{yv2} - M_{yv1})\frac{X}{L}\right)\right.$$

$$- \frac{\beta^2 x^2}{2L^2} \left(M_{zvi} + (M_{zv2} - M_{zvi})\frac{X}{L} \right) \left[M_{zi} + (M_{z2} - M_{zi})\frac{X}{L} \right.$$

$$\left. - \beta\frac{X}{L} \left(M_{yi} + (M_{y2} - M_{yi})\frac{X}{L} \right) - \frac{\beta^2 x^2}{2L^2} \left(M_{zi} + (M_{z2} - M_{zi})\frac{X}{L} \right) \right] dx$$

$$= \frac{1}{EI_z} \int_0^L \left(M_{zvi} + (M_{zv2} - M_{zvi})\frac{X}{L} \right) \left(M_{zi} + (M_{z2} - M_{zi})\frac{X}{L} \right) dx$$

$$- \frac{\beta}{LEI_z} \int_0^L \left(M_{zvi} + (M_{zv2} - M_{zvi})\frac{X}{L} \right) \left(M_{yi} + (M_{y2} - M_{yi})\frac{X}{L} \right) xdx$$

$$- \frac{\beta^2}{2L^2 EI_z} \int_0^L \left(M_{zvi} + (M_{zv2} - M_{zvi})\frac{X}{L} \right) \left(M_{zi} + (M_{z2} - M_{zi})\frac{X}{L} \right) x^2 dx$$

$$- \frac{\beta}{LEI_z} \int_0^L \left(M_{yvi} + (M_{yv2} - M_{yvi})\frac{X}{L} \right) \left(M_{zi} + (M_{z2} - M_{zi})\frac{X}{L} \right) xdx$$

$$+ \frac{\beta^2}{L^2 EI_z} \int_0^L \left(M_{yvi} + (M_{yv2} - M_{yvi})\frac{X}{L} \right) \left(M_{yi} + (M_{y2} - M_{yi})\frac{X}{L} \right) x^2 dx$$

$$+ \frac{\beta^3}{2L^3 EI_z} \int_0^L \left(M_{yvi} + (M_{yv2} - M_{yvi})\frac{X}{L} \right) \left(M_{zi} + (M_{z2} - M_{zi})\frac{X}{L} \right) x^3 dx$$

$$- \frac{\beta^2}{2L^2 EI_z} \int_0^L \left(M_{zvi} + (M_{zv2} - M_{zvi})\frac{X}{L} \right) \left(M_{zi} + (M_{z2} - M_{zi})\frac{X}{L} \right) x^2 dx$$

$$+ \frac{\beta^3}{2L^3 EI_z} \int_0^L \left(M_{zvi} + (M_{zv2} - M_{zvi})\frac{X}{L} \right) \left(M_{yi} + (M_{y2} - M_{yi})\frac{X}{L} \right) x^3 dx$$

$$+ \frac{\beta^4}{4L^4 EI_z} \int_0^L \left(M_{zvi} + (M_{zv2} - M_{zvi})\frac{X}{L} \right) \left(M_{zi} + (M_{z2} - M_{zi})\frac{X}{L} \right) x^4 dx$$

Ignoring terms containing β^3 and β^4 and integrating.

$$= \frac{M_{zvi}}{EI_z} \left[\frac{LM_{zi}}{3} + \frac{LM_{z2}}{6} \right] + \frac{M_{zv2}}{EI_z} \left[\frac{LM_{zi}}{6} + \frac{LM_{z2}}{3} \right]$$

$$- \frac{M_{zvi}\beta L}{EI_z} \left[\frac{M_{yi}}{12} + \frac{M_{y2}}{12} \right] - \frac{M_{zv2}\beta L}{EI_z} \left[\frac{M_{yi}}{12} + \frac{M_{y2}}{4} \right]$$

$$- \frac{M_{yv1}\,\beta L}{EI_z}\left[\frac{M_{z1}}{12} + \frac{M_{z2}}{12}\right] - \frac{M_{yv2}\,\beta L}{EI_z}\left[\frac{M_{z1}}{12} + \frac{M_{z2}}{4}\right]$$

$$+ \frac{M_{yv1}\,\beta^2 L}{EI_z}\left[\frac{M_{y1}}{30} + \frac{M_{y2}}{20}\right] + \frac{M_{yv2}\,\beta^2 L}{EI_z}\left[\frac{M_{y1}}{20} + \frac{M_{y2}}{5}\right]$$

$$- \frac{M_{zv1}\,\beta^2 L}{2EI_z}\left[\frac{M_{z1}}{30} + \frac{M_{z2}}{20}\right] - \frac{M_{zv2}\,\beta^2 L}{2EI_z}\left[\frac{M_{z1}}{20} + \frac{M_{z2}}{5}\right]$$

$$- \frac{M_{zv1}\,\beta^2 L}{2EI_z}\left[\frac{M_{z1}}{30} + \frac{M_{z2}}{20}\right] - \frac{M_{zv2}\,\beta^2 L}{2EI_z}\left[\frac{M_{z1}}{20} + \frac{M_{z2}}{5}\right]$$

Adding appropriate terms:-

$$= \frac{M_{zv1}}{EI_z}\left[\frac{LM_{z1}}{3} + \frac{LM_{z2}}{6} - \frac{\beta LM_{y1}}{12} - \frac{\beta LM_{y2}}{12} - \frac{\beta^2 LM_{z1}}{30} - \frac{\beta^2 LM_{z2}}{20}\right]$$

$$+ \frac{M_{zv2}}{EI_z}\left[\frac{LM_{z1}}{6} + \frac{LM_{z2}}{3} - \frac{\beta LM_{y1}}{12} - \frac{BLM_{y2}}{4} - \frac{\beta^2 LM_{z1}}{20} - \frac{\beta^2 LM_{z2}}{5}\right]$$

$$+ \frac{M_{yv1}}{EI_z}\left[\frac{\beta^2 LM_{y1}}{30} + \frac{\beta^2 LM_{y2}}{20} - \frac{\beta LM_{z1}}{12} - \frac{\beta LM_{z2}}{12}\right]$$

$$+ \frac{M_{yv2}}{EI_z}\left[\frac{\beta^2 LM_{y1}}{20} + \frac{\beta^2 LM_{y2}}{5} - \frac{\beta LM_{z1}}{12} - \frac{M_{z1}\beta L}{4}\right] \ldots\ldots\ldots A62$$

Considering the integral IV.

$$\int_0^L \frac{M_{svv}\, M_{svA}}{GJ}\, dx$$

$$\frac{e_1}{GJ}\int\left[M_{xv1} + (M_{xv2} - M_{xv1})\frac{X}{L} + C_1\left\{P_{xv1} + (P_{xv2} - P_{xv1})\frac{X}{L}\right\}\right.$$

$$+ C_2\left\{M_{yv1} + (M_{yv2} - M_{yv1})\frac{X}{L} + \beta\frac{X}{L}\left(M_{zv1} + (M_{zv2} - M_{zv1})\frac{X}{L}\right)\right.$$

$$\left.\left. - \frac{\beta^2 X^2}{2L^2}\left(M_{yv1} + (M_{yv2} - M_{yv1})\frac{X}{L}\right)\right\}\right.$$

$$+ C_3\left\{M_{zv1} + (M_{zv2} - M_{zv1})\frac{X}{L} - \beta\frac{X}{L}\left(M_{yv1} + (M_{yv2} - M_{yv1})\frac{X}{L}\right)\right.$$

$$\left.\left. - \frac{B^2 X^2}{2L^2}\left(M_{zv1} + (M_{zv2} - M_{zv1})\frac{X}{L}\right)\right\}\right]\left[M_{x1} + (M_{x2} - M_{x1})\frac{X}{L}\right.$$

$$+ C_1 \left(P_{x1} + (P_{x2} - P_{x1})\frac{X}{L}\right) + C_2 \left\{ M_{y1} + (M_{y2} - M_{y1})\frac{X}{L} + \beta\frac{X}{L}\left(M_{z1} + (M_{z2} - M_{z1})\frac{X}{L}\right) - \frac{\beta^2 X^2}{2L^2}\left(M_{y1} + (M_{y2} - M_{y1})\frac{X}{L}\right)\right\} + C_3 \left\{ M_{z1} + (M_{z2} - M_{z1})\frac{X}{L} - \beta\frac{X}{L}\left(M_{y1} + (M_{y2} - M_{y1})\frac{X}{L}\right) - \frac{\beta^2 X^2}{2L^2}\left(M_{z1} + (M_{z2} - M_{z1})\frac{X}{L}\right)\right\} \Bigg] dx$$

$$= \frac{1}{GJ}\int_0^L \left(M_{xv1} + (M_{xv2} - M_{xv1})\frac{X}{L}\right)\left(M_{x1} + (M_{x2} - M_{x1})\frac{X}{L}\right) dx$$

$$+ \frac{C_1}{GJ}\int_0^L \left(M_{xv1} + (M_{xv2} - M_{xv1})\frac{X}{L}\right)\left(P_{x1} + (P_{x2} - P_{x1})\frac{X}{L}\right) dx$$

$$+ \frac{C_2}{GJ}\int_0^L \left(M_{xv1} + (M_{xv2} - M_{xv1})\frac{X}{L}\right)\left(M_{y1} - (M_{y2} - M_{y1})\frac{X}{L}\right) dx$$

$$+ \frac{C_2\beta}{LGJ}\int_0^L \left(M_{xv1} + (M_{xv2} - M_{xv1})\frac{X}{L}\right)\left(M_{z1} + (M_{z2} - M_{z1})\frac{X}{L}\right) dx$$

$$- \frac{C_2\beta^2}{2L^2GJ}\int_0^L \left(M_{xv1} + (M_{xv2} - M_{xv1})\frac{X}{L}\right)\left(M_{y1} + (M_{y2} - M_{y1})\frac{X}{L}\right) x^2 dx$$

$$+ \frac{C_3}{GJ}\int_0^L \left(M_{xv1} + (M_{xv2} - M_{xv1})\frac{X}{L}\right)\left(M_{z1} + (M_{z2} - M_{z1})\frac{X}{L}\right) dx$$

$$- \frac{C_3\beta}{LGJ}\int_0^L \left(M_{xv1} + (M_{xv2} - M_{xv1})\frac{X}{L}\right)\left(M_{y1} + (M_{y2} - M_{y1})\frac{X}{L}\right) x\,dx$$

$$- \frac{C_3\beta^2}{2L^2GJ}\int_0^L \left(M_{xv1} + (M_{xv2} - M_{xv1})\frac{X}{L}\right)\left(M_{z1} + (M_{z2} - M_{z1})\frac{X}{L}\right) x^2 dx$$

$$+ \frac{C_1}{GJ}\int_0^L \left(P_{xv1} + (P_{xv2} - P_{xv1})\frac{X}{L}\right)\left(M_{x1} + (M_{x2} - M_{x1})\frac{X}{L}\right) dx$$

$$+ \frac{C_1^2}{GJ}\int_0^L \left(P_{xv1} + (P_{xv2} - P_{xv1})\frac{X}{L}\right)\left(P_{x1} + (P_{x2} - P_{x1})\frac{X}{L}\right) dx$$

$$+ \frac{C_1C_2}{GJ}\int_0^L \left(P_{xv1} + (P_{xv2} - P_{xv1})\frac{X}{L}\right)\left(M_{y1} + (M_{y2} - M_{y1})\frac{X}{L}\right) dx$$

$$+ \frac{C_1C_2\beta}{LGJ}\int_0^L \left(P_{xv1} + (P_{xv2} - P_{xv1})\frac{X}{L}\right)\left(M_{z1} + (M_{z2} - M_{z1})\frac{X}{L}\right) x\,dx$$

$$- \frac{C_1C_2\beta^2}{2L^2GJ}\int_0^L \left(P_{xv1} + (P_{xv2} - P_{xv1})\frac{X}{L}\right)\left(M_{y1} + (M_{y2} - M_{y1})\frac{X}{L}\right) x^2 dx$$

$$+ \frac{C_1C_3}{GJ}\int_0^L \left(P_{xv1} + (P_{xv2} - P_{xv1})\frac{X}{L}\right)\left(M_{z1} + (M_{z2} - M_{z1})\frac{X}{L}\right) dx$$

$$- \frac{C_1C_3\beta}{LGJ}\int_0^L \left(P_{xv1} + (P_{xv2} - P_{xv1})\frac{X}{L}\right)\left(M_{y1} + (M_{y2} - M_{y1})\frac{X}{L}\right) x\,dx$$

$$- \frac{C_1C_3\beta^2}{2L^2GJ} \int_0^L \left\{P_{xv1} + (P_{xv2} - P_{xv1})\frac{X}{L}\right\} \left\{M_{z1} + (M_{z2} - M_{z1})\frac{X}{L}\right\} x^2 dx$$

$$+ \frac{C_2}{GJ} \int_0^L \left\{M_{yv1} + (M_{yv2} - M_{yv1})\frac{X}{L}\right\} \left\{M_{x1} + (M_{x2} - M_{x1})\frac{X}{L}\right\} dx$$

$$+ \frac{C_2C_1}{GJ} \int_0^L \left\{M_{yv1} + (M_{yv2} - M_{yv1})\frac{X}{L}\right\} \left\{P_{x1} + (P_{x2} - P_{x1})\frac{X}{L}\right\} dx$$

$$+ \frac{C_2^2}{GJ} \int_0^L \left\{M_{yv1} + (M_{yv2} - M_{yv1})\frac{X}{L}\right\} \left\{M_{y1} + (M_{y2} - M_{y1})\frac{X}{L}\right\} dx$$

$$+ \frac{C_2^2\beta}{LGJ} \int_0^L \left\{M_{yv1} + (M_{yv2} - M_{yv1})\frac{X}{L}\right\} \left\{M_{z1} + (M_{z2} - M_{z1})\frac{X}{L}\right\} xdx$$

$$- \frac{C_2^2\beta^2}{2L^2GJ} \int_0^L \left\{M_{yv1} + (M_{yv2} - M_{yv1})\frac{X}{L}\right\} \left\{M_{y1} + (M_{y2} - M_{y1})\frac{X}{L}\right\} x^2 dx$$

$$+ \frac{C_2C_3}{GJ} \int_0^L \left\{M_{yv1} + (M_{yv2} - M_{yv1})\frac{X}{L}\right\} \left\{M_{z1} + (M_{z2} - M_{z1})\frac{X}{L}\right\} dx$$

$$- \frac{C_2C_3\beta}{LGJ} \int_0^L \left\{M_{yv1} + (M_{yv2} - M_{yv1})\frac{X}{L}\right\} \left\{M_{y1} - (M_{y2} - M_{y1})\frac{X}{L}\right\} xdx$$

$$- \frac{C_2C_3\beta^2}{2L^2GJ} \int_0^L \left\{M_{yv1} + (M_{yv2} - M_{yv1})\frac{X}{L}\right\} \left\{M_{z1} + (M_{z2} - M_{z1})\frac{X}{L}\right\} x^2 dx$$

$$+ \frac{C_2\beta}{LGJ} \int_0^L \left\{M_{zv1} + (M_{zv2} - M_{zv1})\frac{X}{L}\right\} \left\{M_{x1} + (M_{x2} - M_{x1})\frac{X}{L}\right\} xdx$$

$$+ \frac{C_1C_2\beta}{LGJ} \int_0^L \left\{M_{zv1} + (M_{zv2} - M_{zv1})\frac{X}{L}\right\} \left\{P_{x1} + (P_{x2} - P_{x1})\frac{X}{L}\right\} xdx$$

$$+ \frac{C_2^2\beta}{LGJ} \int_0^L \left\{M_{zv1} + (M_{zv2} - M_{zv1})\frac{X}{L}\right\} \left\{M_{y1} + (M_{y2} - M_{y1})\frac{X}{L}\right\} xdx$$

$$+ \frac{C_2^2\beta^2}{L^2GJ} \int_0^L \left\{M_{zv1} + (M_{zv2} - M_{zv1})\frac{X}{L}\right\} \left\{M_{z1} + (M_{z2} - M_{z1})\frac{X}{L}\right\} x^2 dx$$

$$- \frac{C^2{}_2\beta^3}{2L^3GJ} \int_0^L \left\{M_{zv1} + (M_{zx2} - M_{zv1})\frac{X}{L}\right\} \left\{M_{y1} + (M_{y2} - M_{y1})\frac{X}{L}\right\} x^3 dx$$

$$+ \frac{C_3C_2\beta}{LGJ} \int_0^L \left\{M_{zv1} + (M_{zv2} - M_{zv1})\frac{X}{L}\right\} \left\{M_{z1} + (M_{z2} - M_{z1})\frac{X}{L}\right\} xdx$$

$$- \frac{C_3C_2\beta^2}{L^2GJ} \int_0^L \left\{M_{zv1} + (M_{zv2} - M_{zv1})\frac{X}{L}\right\} \left\{M_{y1} + (M_{y2} - M_{y1})\frac{X}{L}\right\} x^2 dx$$

$$- \frac{C_2C_2\beta^3}{2L^3GJ} \int_0^L \left\{M_{zv1}+(M_{zv2}-M_{zv1})\frac{x}{L}\right\} \left\{M_{z1}+(M_{z2}-M_{z1})\frac{x}{L}\right\} x^3dx$$

$$- \frac{C_2\beta^2}{2L^2GJ} \int_0^L \left\{M_{yv1}+(M_{yv2}-M_{yv1})\frac{x}{L}\right\} \left\{M_{x1}+(M_{x2}-M_{x1})\frac{x}{L}\right\} x^2dx$$

$$- \frac{C_1C_2\beta^2}{2L^2GJ} \int_0^L \left\{M_{yv1}+(M_{yv2}-M_{yv1})\frac{x}{L}\right\} \left\{P_{x1}+(P_{x2}-P_{x1})\frac{x}{L}\right\} x^2dx$$

$$- \frac{C^2{}_2\beta^2}{2L^2GJ} \int_0^L \left\{M_{yv1}+(M_{yv2}-M_{yv1})\frac{x}{L}\right\} \left\{M_{y1}+(M_{y2}-M_{y1})\frac{x}{L}\right\} x^2dx$$

$$- \frac{C^2{}_2\beta^3}{2L^3GJ} \int_0^L \left\{M_{yv1}+(M_{yv2}-M_{yv1})\frac{x}{L}\right\} \left\{M_{z1}+(M_{z2}-M_{z1})\frac{x}{L}\right\} x^3dx$$

$$+ \frac{C^2{}_2\beta^4}{2L^4GJ} \int_0^L \left\{M_{yv1}+(M_{yv2}-M_{yv1})\frac{x}{L}\right\} \left\{M_{y1}+(M_{y2}-M_{y1})\frac{x}{L}\right\} x^4dx$$

$$- \frac{C_3C_2\beta^2}{2L^2GJ} \int_0^L \left\{M_{yv1}+(M_{yv2}-M_{yv1})\frac{x}{L}\right\} \left\{M_{z1}+(M_{z2}-M_{z1})\frac{x}{L}\right\} x^2dx$$

$$+ \frac{C_3C_2\beta^3}{2L^3GJ} \int_0^L \left\{M_{yv1}+(M_{yv2}-M_{yv1})\frac{x}{L}\right\} \left\{M_{y1}+(M_{y2}-M_{y1})\frac{x}{L}\right\} x^3dx$$

$$+ \frac{C_3C_2\beta^4}{4L^4GJ} \int_0^L \left\{M_{yv1}+(M_{yv2}-M_{yv1})\frac{x}{L}\right\} \left\{M_{z1}+(M_{z2}-M_{z1})\frac{x}{L}\right\} x^4dx$$

$$+ \frac{C_3}{GJ} \int_0^L \left\{M_{zv1}+(M_{zv2}-M_{zv1})\frac{x}{L}\right\} \left\{M_{x1}+(M_{x2}-M_{x1})\frac{x}{L}\right\} dx$$

$$+ \frac{C_3C_1}{GJ} \int_0^L \left\{M_{zv1}+(M_{zv2}-M_{zv1})\frac{x}{L}\right\} \left\{P_{x1}+(P_{x2}-P_{x1})\frac{x}{L}\right\} dx$$

$$+ \frac{C_3C_2}{GJ} \int_0^L \left\{M_{zv1}+(M_{zv2}-M_{zv1})\frac{x}{L}\right\} \left\{M_{y1}+(M_{y2}-M_{y1})\frac{x}{L}\right\} dx$$

$$+ \frac{C_3C_2\beta}{GJL} \int_0^L \left\{M_{zv1}+(M_{zv2}-M_{zv1})\frac{x}{L}\right\} \left\{M_{z1}+(M_{z2}-M_{z1})\frac{x}{L}\right\} xdx$$

$$- \frac{\beta^2C_3C_2}{2GJL^2} \int_0^L \left\{M_{zv1}+(M_{zv2}-M_{zv1})\frac{x}{L}\right\} \left\{M_{y1}+(M_{y2}-M_{y1})\frac{x}{L}\right\} x^2dx$$

$$+ \frac{C^2{}_3}{GJ} \int_0^L \left\{M_{zv1}+(M_{zv2}-M_{zv1})\frac{x}{L}\right\} \left\{M_{z1}+(M_{z2}-M_{z1})\frac{x}{L}\right\} dx$$

$$- \frac{C^2{}_3\beta}{GJL} \int_0^L \left\{M_{zv1}+(M_{zv2}-M_{zv1})\frac{x}{L}\right\} \left\{M_{y1}+(M_{y2}-M_{y1})\frac{x}{L}\right\} xdx$$

$$- \frac{C_3^2 \beta^2}{2GJL^2} \int_0^L \left(M_{zv1} + (M_{zv2} - M_{zv1})\frac{X}{L}\right) \left(M_{z1} + (M_{z2} - M_{z1})\frac{X}{L}\right) x^2 dx$$

$$- \frac{C_3 \beta}{LGJ} \int_0^L \left(M_{yv1} + (M_{yv2} - M_{yv1})\frac{X}{L}\right) \left(M_{x1} + (M_{x2} - M_{x1})\frac{X}{L}\right) x dx$$

$$- \frac{C_1 C_3 \beta}{LGJ} \int_0^L \left(M_{yv1} + (M_{yv2} - M_{yv1})\frac{X}{L}\right) \left(P_{x1} + (P_{x2} - P_{x1})\frac{X}{L}\right) x dx$$

$$- \frac{C_2 C_3 \beta}{LGJ} \int_0^L \left(M_{yv1} + (M_{yv2} - M_{yv1})\frac{X}{L}\right) \left(M_{y1} + (M_{y2} - M_{y1})\frac{X}{L}\right) x dx$$

$$- \frac{C_2 C_3 \beta^2}{L^2 GJ} \int_0^L \left(M_{yv1} + (M_{yv2} - M_{yv1})\frac{X}{L}\right) \left(M_{z1} + (M_{z2} - M_{z1})\frac{X}{L}\right) x^2 dx$$

$$+ \frac{C_2 C_3 \beta^3}{2L^3 GJ} \int_0^L \left(M_{yv1} + (M_{yv2} - M_{yv1})\frac{X}{L}\right) \left(M_{y1} + (M_{y2} - M_{y1})\frac{X}{L}\right) x^3 dx$$

$$- \frac{C_3^2 \beta}{LGJ} \int_0^L \left(M_{yv1} + (M_{yv2} - M_{yv1})\frac{X}{L}\right) \left(M_{z1} + (M_{z2} - M_{z1})\frac{X}{L}\right) x dx$$

$$+ \frac{C_3^2 \beta^2}{L^2 GJ} \int_0^L \left(M_{yv1} + (M_{yv2} - M_{yv1})\frac{X}{L}\right) \left(M_{y1} + (M_{y2} - M_{y1})\frac{X}{L}\right) x^2 dx$$

$$+ \frac{C_3^2 \beta^3}{2L^3 GJ} \int_0^L \left(M_{yv1} + (M_{yv2} - M_{yv1})\frac{X}{L}\right) \left(M_{z1} + (M_{z2} - M_{z1})\frac{X}{L}\right) x^3 dx$$

$$- \frac{C_3 \beta^2}{2L^2 GJ} \int_0^L \left(M_{zv1} + (M_{zv2} - M_{zv1})\frac{X}{L}\right) \left(M_{x1} + (M_{x2} - M_{x1})\frac{X}{L}\right) x^2 dx$$

$$- \frac{C_1 C_3 \beta^2}{2L^2 GJ} \int_0^L \left(M_{zv1} + (M_{zv2} - M_{zv1})\frac{X}{L}\right) \left(P_{x1} + (P_{x2} - P_{x1})\frac{X}{L}\right) x^2 dx$$

$$- \frac{C_2 C_3 \beta^2}{2L^2 GJ} \int_0^L \left(M_{zv1} + (M_{zv2} - M_{zv1})\frac{X}{L}\right) \left(M_{y1} + (M_{y2} - M_{y1})\frac{X}{L}\right) x^2 dx$$

$$- \frac{C_2 C_3 \beta^3}{2L^3 GJ} \int_0^L \left(M_{zv1} + (M_{zv2} - M_{zv1})\frac{X}{L}\right) \left(M_{z1} + (M_{z2} - M_{z1})\frac{X}{L}\right) x^3 dx$$

$$+ \frac{C_2 C_3 \beta^4}{4L^4 GJ} \int_0^L \left(M_{zv1} + (M_{zv2} - M_{zv1})\frac{X}{L}\right)\left(M_{y1} + (M_{y2} - M_{y1})\frac{X}{L}\right) x^4 dx$$

$$- \frac{C_3^2 \beta^2}{2L^2 GJ} \int_0^L \left(M_{zv1} + (M_{zv2} - M_{zv1})\frac{X}{L}\right)\left(M_{z1} + (M_{z2} - M_{z1})\frac{X}{L}\right) x^2 dx$$

$$+ \frac{C_3^2 \beta^3}{2L^3 GJ} \int_0^L \left(M_{zv1} + (M_{zv2} - M_{zv1})\frac{X}{L}\right)\left(M_{y1} + (M_{y2} - M_{y1})\frac{X}{L}\right) x^3 dx$$

$$+ \frac{C_3^2 \beta^4}{4L^4 GJ} \int_0^L \left\{M_{zv1} + (M_{zv2} - M_{zv1})\frac{X}{L}\right\}\left\{M_{z1} + (M_{z2} - M_{z1})\frac{X}{L}\right\} x^4 dx$$

Ignoring terms containing β^3 and β^4 and integrating :

$$\frac{L}{GJ} \quad M_{xv1}\left[\frac{1}{3}M_{x1} + \frac{1}{6}M_{x2}\right] + \frac{L}{GJ} M_{xv2}\left[\frac{1}{6}M_{x1} + \frac{1}{3}M_{x2}\right]$$

$$+ \frac{C_1 L}{GJ} \quad M_{xv1}\left[\frac{1}{3}P_{x1} + \frac{1}{6}P_{x2}\right] + \frac{C_1 L}{GJ} M_{xv2}\left[\frac{1}{6}P_{x1} + \frac{1}{3}P_{x2}\right]$$

$$+ \frac{C_2 L}{GJ} \quad M_{xv1}\left[\frac{1}{3}M_{y1} + \frac{1}{6}M_{y2}\right] + \frac{C_2 L}{GJ} M_{xv2}\left[\frac{1}{6}M_{y1} + \frac{1}{3}M_{y2}\right]$$

$$+ \frac{C_2 \beta L}{GJ} \quad M_{xv1}\left[\frac{1}{12}M_{z1} + \frac{1}{12}M_{z2}\right] + \frac{C_2 \beta L M_{xv2}}{GJ}\left[\frac{1}{12}M_{z1} + \frac{1}{4}M_{z2}\right]$$

$$- \frac{C_2 \beta^2 L}{2GJ} \quad M_{xv1}\left[\frac{1}{30}M_{y1} + \frac{1}{20}M_{y2}\right] - \frac{C_2 \beta^2 L}{2GJ}\left[M_{xv2}\frac{1}{20}M_{y1} + \frac{1}{5}M_{y2}\right]$$

$$+ \frac{LC_3}{GJ} \quad M_{xv1}\left[\frac{M_{z1}}{3} \quad \frac{M_{z2}}{6}\right] + \frac{LC_3 M_{xv2}}{GJ}\left[\frac{M_{z1}}{6} + \frac{M_{z2}}{3}\right]$$

$$- \frac{C_3 \beta L}{GJ} \quad M_{xv1}\left[\frac{M_{y1}}{12} + \frac{M_{y2}}{12}\right] - \frac{C_3 \beta L M_{xv2}}{GJ}\left[\frac{M_{y1}}{12} + \frac{M_{y2}}{4}\right]$$

$$- \frac{C_3 \beta^2 L M_{xv1}}{2GJ}\left[\frac{M_{z1}}{30} + \frac{M_{z2}}{20}\right] - \frac{C_3 \beta^2 L M_{xv2}}{2GJ}\left[\frac{M_{z1}}{20} + \frac{M_{z2}}{5}\right]$$

$$+ \frac{C_1 P_{xv1} L}{GJ}\left[\frac{M_{x1}}{3} + \frac{M_{x2}}{6}\right] - \frac{C_1 P_{xv2} L}{GJ}\left[\frac{M_{x1}}{6} + \frac{M_{x2}}{3}\right]$$

$$+\frac{C_1^2 P_{xv1} L}{GJ}\left[\frac{P_{x1}}{3}+\frac{P_{x2}}{6}\right]+\frac{C_1^2 P_{xv2} L}{GJ}\left[\frac{P_{x1}}{6}+\frac{P_{x2}}{3}\right]$$

$$+\frac{C_1 C_2 P_{xv1} L}{GJ}\left[\frac{M_{y1}}{3}+\frac{M_{y2}}{6}\right]+\frac{L C_1 C_2 P_{xv2}}{GJ}\left[\frac{M_{y1}}{6}+\frac{M_{y2}}{3}\right]$$

$$+\frac{C_1 C_2 \beta L P_{xv1}}{GJ}\left[\frac{M_{z1}}{12}+\frac{M_{z2}}{12}\right]+\frac{C_1 C_2 \beta L P_{xv2}}{GJ}\left[\frac{M_{z1}}{12}+\frac{M_{z2}}{4}\right]$$

$$-\frac{C_1 C_2 \beta^2 L P_{xv1}}{2GJ}\left[\frac{M_{y1}}{30}+\frac{M_{y2}}{20}\right]-\frac{C_1 C_2 \beta^2 L P_{xv2}}{2GJ}\left[\frac{M_{y1}}{20}+\frac{M_{y2}}{5}\right]$$

$$+\frac{C_1 C_3 P_{xv1}}{GJ}\left[\frac{M_{z1}}{3}+\frac{M_{z2}}{6}\right]+\frac{C_1 C_3 P_{xv2}}{GJ}\left[\frac{M_{z1}}{6}+\frac{M_{z2}}{3}\right]$$

$$-\frac{C_1 C_3 \beta L P_{xv1}}{GJ}\left[\frac{M_{y1}}{12}+\frac{M_{y2}}{12}\right]-\frac{C_1 C_3 L P_{xv2}}{GJ}\left[\frac{M_{y1}}{12}+\frac{M_{y2}}{4}\right]$$

$$-\frac{C_1 C_3 \beta^2 L P_{xv1}}{2GJ}\left[\frac{M_{z1}}{30}+\frac{M_{z2}}{20}\right]-\frac{C_1 C_3 \beta^2 L P_{xv2}}{GJ}\left[\frac{M_{z1}}{20}+\frac{M_{z2}}{5}\right]$$

$$+\frac{C_2 M_{yv1} L}{GJ}\left[\frac{M_{x1}}{3}+\frac{M_{x2}}{6}\right]+\frac{L C_2 M_{yv2}}{GJ}\left[\frac{M_{x1}}{6}+\frac{M_{x2}}{3}\right]$$

$$+\frac{L C_2 C_1 M_{yv1}}{GJ}\left[\frac{P_{x1}}{3}+\frac{P_{x2}}{6}\right]+\frac{L C_2 C_1 M_{yv2}}{GJ}\left[\frac{P_{x1}}{6}+\frac{P_{x2}}{3}\right]$$

$$+\frac{L C_2^2 M_{yv1}}{GJ}\left[\frac{M_{y1}}{3}+\frac{M_{y2}}{6}\right]+\frac{L C_2^2 M_{yv2}}{GJ}\left[\frac{M_{y1}}{6}+\frac{M_{y2}}{3}\right]$$

$$+\frac{C_2^2 \beta L M_{yv1}}{GJ}\left[\frac{M_{z1}}{12}+\frac{M_{z2}}{12}\right]+\frac{C_2^2 \beta L M_{yv2}}{GJ}\left[\frac{M_{z1}}{12}+\frac{M_{z2}}{4}\right]$$

$$-\frac{C_2^2 \beta^2 L M_{yv1}}{2GJ}\left[\frac{M_{y1}}{30}+\frac{M_{y2}}{20}\right]+\frac{C_2^2 \beta^2 L M_{yv2}}{2GJ}\left[\frac{M_{y1}}{6}+\frac{M_{y2}}{3}\right]$$

$$+\frac{L C_2 C_3 M_{yv1}}{GJ}\left[\frac{M_{z1}}{3}+\frac{M_{z2}}{6}\right]+\frac{L C_2 C_3 M_{yv2}}{GJ}\left[\frac{M_{z1}}{6}+\frac{M_{z2}}{3}\right]$$

$$- \frac{C_2C_3\beta L\, M_{yvi}}{GJ}\left[\frac{M_{yi}}{12} + \frac{M_{y2}}{12}\right] - \frac{C_2C_3\beta L\, M_{yv2}}{GJ}\left[\frac{M_{yi}}{12} + \frac{M_{y2}}{4}\right]$$

$$- \frac{C_2C_3\beta^2 L\, M_{yvi}}{2GJ}\left[\frac{M_{zi}}{30} + \frac{M_{z2}}{20}\right] - \frac{C_2C_3\beta^2 L\, M_{yv2}}{2GJ}\left[\frac{M_{zi}}{20} + \frac{M_{z2}}{5}\right]$$

$$+ \frac{C_2\beta L\, M_{zvi}}{GJ}\left[\frac{M_{xi}}{12} + \frac{M_{x2}}{12}\right] + \frac{C_2\beta L\, M_{zv2}}{GJ}\left[\frac{M_{xi}}{12} + \frac{M_{x2}}{4}\right]$$

$$+ \frac{C_1C_2\beta L\, M_{zvi}}{GJ}\left[\frac{P_{xi}}{12} + \frac{P_{x2}}{12}\right] + \frac{C_1C_2\beta L\, M_{zv2}}{GJ}\left[\frac{P_{xi}}{12} + \frac{P_{x2}}{4}\right]$$

$$+ \frac{C_2^2\beta L\, M_{zvi}}{GJ}\left[\frac{M_{yi}}{12} + \frac{M_{y2}}{12}\right] + \frac{C_2^2\beta L\, M_{zv2}}{GJ}\left[\frac{M_{yi}}{12} + \frac{M_{y2}}{4}\right]$$

$$+ \frac{C_2^2\beta^2 L\, M_{zvi}}{GJ}\left[\frac{M_{zi}}{30} + \frac{M_{z2}}{20}\right] + \frac{C_2^2\beta^2 L\, M_{zv2}}{GJ}\left[\frac{M_{zi}}{20} + \frac{M_{z2}}{5}\right]$$

$$+ \frac{C_3C_2\beta L\, M_{zvi}}{GJ}\left[\frac{M_{zi}}{12} + \frac{M_{z2}}{12}\right] + \frac{C_3C_2\beta L\, M_{zv2}}{GJ}\left[\frac{M_{zi}}{12} + \frac{M_{z2}}{4}\right]$$

$$- \frac{C_3C_2\beta^2 L\, M_{zvi}}{GJ}\left[\frac{M_{yi}}{30} + \frac{M_{y2}}{20}\right] - \frac{C_3C_2\beta^2 L\, M_{zv2}}{GJ}\left[\frac{M_{yi}}{20} + \frac{M_{y2}}{5}\right]$$

$$- \frac{C_2\beta^2 L\, M_{yvi}}{2GJ}\left[\frac{M_{xi}}{30} + \frac{M_{x2}}{20}\right] - \frac{C_2\beta^2 L\, M_{yv2}}{2GJ}\left[\frac{M_{xi}}{20} + \frac{M_{x2}}{5}\right]$$

$$- \frac{C_1C_2\beta^2 L\, M_{yvi}}{2GJ}\left[\frac{P_{xi}}{30} + \frac{P_{x2}}{20}\right] - \frac{C_1C_2\beta^2 L\, M_{yv2}}{2GJ}\left[\frac{P_{xi}}{20} + \frac{P_{x2}}{5}\right]$$

$$- \frac{C_2^2\beta^2 L\, M_{yvi}}{2GJ}\left[\frac{M_{yi}}{30} + \frac{M_{y2}}{20}\right] - \frac{C_2^2\beta^2 L\, M_{yv2}}{2GJ}\left[\frac{M_{yi}}{20} + \frac{M_{y2}}{5}\right]$$

$$- \frac{C_3C_2L\beta^2\, M_{yvi}}{2GJ}\left[\frac{M_{zi}}{30} + \frac{M_{z2}}{20}\right] - \frac{C_3C_2\beta^2 L\, M_{yv2}}{2GJ}\left[\frac{M_{zi}}{20} + \frac{M_{z2}}{5}\right]$$

$$+ \frac{LC_3\, M_{zvi}}{GJ}\left[\frac{M_{xi}}{3} + \frac{M_{x2}}{6}\right] + \frac{LC_3\, M_{zv2}}{GJ}\left[\frac{M_{xi}}{6} + \frac{M_{x2}}{3}\right]$$

$$+\frac{LC_3C_1\,M_{zv1}}{GJ}\left[\frac{P_{x1}}{3}+\frac{P_{x2}}{6}\right]+\frac{LC_3C_1\,M_{zv2}}{GJ}\left[\frac{P_{x1}}{6}+\frac{P_{x2}}{3}\right]$$

$$+\frac{LC_3C_2\,M_{zv1}}{GJ}\left[\frac{M_{y1}}{3}+\frac{M_{y2}}{6}\right]+\frac{LC_3C_2\,M_{zv2}}{GJ}\left[\frac{M_{y1}}{6}+\frac{M_{y2}}{3}\right]$$

$$+\frac{C_3C_2\,L\,M_{zv1}}{GJ}\left[\frac{M_{z1}}{12}+\frac{M_{z2}}{12}\right]+\frac{C_3C_2\,L\,M_{zv2}}{GJ}\left[\frac{M_{z1}}{12}+\frac{M_{z2}}{4}\right]$$

$$-\frac{C_3C_2\beta^2L\,M_{zv1}}{2GJ}\left[\frac{M_{y1}}{30}+\frac{M_{y2}}{20}\right]-\frac{C_3C_2\beta^2L\,M_{zv2}}{2GJ}\left[\frac{M_{y1}}{20}+\frac{M_{y2}}{5}\right]$$

$$+\frac{LC_3^2\,M_{zv1}}{GJ}\left[\frac{M_{z1}}{3}+\frac{M_{z2}}{6}\right]+\frac{LC_3^2\,M_{zv2}}{GJ}\left[\frac{M_{z1}}{6}+\frac{M_{z2}}{3}\right]$$

$$-\frac{C_3^2\beta L\,M_{zv1}}{GJ}\left[\frac{M_{y1}}{12}+\frac{M_{y2}}{12}\right]-\frac{C_3^2\beta L\,M_{zv2}}{GJ}\left[\frac{M_{y1}}{12}+\frac{M_{y2}}{4}\right]$$

$$-\frac{C_3^2\beta^2L\,M_{zv1}}{2GJ}\left[\frac{M_{z1}}{30}+\frac{M_{z2}}{20}\right]-\frac{C_3^2\beta^2L\,M_{zv2}}{2GJ}\left[\frac{M_{z1}}{20}+\frac{M_{z2}}{5}\right]$$

$$-\frac{C_3\beta L\,M_{yv1}}{GJ}\left[\frac{M_{x1}}{12}+\frac{M_{x2}}{12}\right]-\frac{C_3\beta L\,M_{yv2}}{GJ}\left[\frac{M_{x1}}{12}+\frac{M_{x2}}{4}\right]$$

$$-\frac{C_3C_1\beta L\,M_{yv1}}{GJ}\left[\frac{P_{x1}}{12}+\frac{P_{x2}}{12}\right]-\frac{C_3C_1\beta L\,M_{yv2}}{GJ}\left[\frac{P_{x1}}{12}+\frac{P_{x2}}{4}\right]$$

$$-\frac{C_2C_3\beta L\,M_{yv1}}{GJ}\left[\frac{M_{y1}}{12}+\frac{M_{y2}}{12}\right]-\frac{C_2C_3\beta L\,M_{yv2}}{GJ}\left[\frac{M_{y1}}{12}+\frac{M_{y2}}{4}\right]$$

$$-\frac{C_2C_3\beta^2L\,M_{yv1}}{GJ}\left[\frac{M_{z1}}{30}+\frac{M_{z2}}{20}\right]-\frac{C_2C_3\beta^2L\,M_{yv2}}{GJ}\left[\frac{M_{z1}}{20}+\frac{M_{z2}}{5}\right]$$

$$-\frac{C_3^2\beta L\,M_{yv1}}{GJ}\left[\frac{M_{z1}}{12}+\frac{M_{z2}}{12}\right]-\frac{C_3^2\beta L\,M_{yv2}}{GJ}\left[\frac{M_{z1}}{12}+\frac{M_{z2}}{4}\right]$$

$$+\frac{C_3^2\beta^2\,L\,M_{yv1}}{GJ}\left[\frac{M_{y1}}{30}+\frac{M_{y2}}{20}\right]+\frac{C_3^2\beta^2L\,M_{yv2}}{GJ}\left[\frac{M_{y1}}{20}+\frac{M_{y2}}{5}\right]$$

$$-\frac{C_3\beta^2L\,M_{zv1}}{2GJ}\left[\frac{M_{x1}}{30}+\frac{M_{x2}}{20}\right]-\frac{C_3\beta^2L\,M_{zv2}}{2GJ}\left[\frac{M_{x1}}{20}+\frac{M_{x2}}{5}\right]$$

$$- \frac{C_1 C_3 \beta^2 L M_{zv1}}{2GJ} \left[\frac{P_{x1}}{30} + \frac{P_{x2}}{20} \right] - \frac{C_1 C_3 \beta^2 L M_{zv2}}{2GJ} \left[\frac{P_{x1}}{20} + \frac{P_{x2}}{5} \right]$$

$$- \frac{C_2 C_3 \beta^2 L M_{zv1}}{2GJ} \left[\frac{M_{y1}}{30} + \frac{M_{y2}}{20} \right] - \frac{C_2 C_3 \beta^2 L M_{zv2}}{2GJ} \left[\frac{M_{y1}}{20} + \frac{M_{y2}}{5} \right]$$

$$- \frac{C_3^2 \beta^2 L M_{zv1}}{2GJ} \left[\frac{M_{z1}}{30} + \frac{M_{z2}}{20} \right] - \frac{C_3^2 \beta^2 L M_{zv2}}{2GJ} \left[\frac{M_{z1}}{20} + \frac{M_{z2}}{5} \right]$$

.....A63

Elements of flexibility matrix are thus formed. Equations A60, A61, A62 and A63 are rearranged and tabulated as shown in Table 1.

ESTABLISHING FLAPPING LOADS DUE TO DISPLACEMENTS AT A NODE J

Displacements: The general conventions including idealisation are explained in 3.1. The following additional definitions apply. (See figure A2). An element J is identified by its nodes namely J and J + 1, J being at the tip end and J + 1 being at the root end. Similarly an element J-1 is identified by its nodes J-1 and J; and an element J+1 is identified by its nodes J+1 and J+2. A node J is defined by its coordinates X_J, Y_J, Z_J; whereas its displacements are defined by ΔX_J, ΔY_J, ΔZ_J. A node J-1 is defined by its coordinates X_{J-1}, Y_{J-1}, Z_{J-1} and the corresponding displacement is defined by ΔX_{J-1}, ΔY_{J-1}, ΔZ_{J-1}. The same argument follows for other nodes. The twisting deformation θ_J is described with reference to local axes. However when a blade has sweep back, the twisting deformation at node J is described by two twisting deformations ϕ_{J-1} and θ_J (Figure A3). When the sweep back is absent the two twisting deformations are one and the same.

Loads: Due to the displacements at node J (ΔX_J, ΔY_J, ΔZ_J, θx_J) there are two sets of global axes forces. They are

1) Forces at J causing inertia forces on element J-1.

2) Forces $\overset{\text{at}}{\wedge}$ J+1 causing inertia forces on element J.

and the moments calculated at any node will be moments applied to the inboard section by inertia forces on the element. The moments will be about global axes. The forces due to the displacements at node J are depicted in Figure A4. These are (assuming a simple harmonic vibration with frequency ω)

a) $$P_{X_J} = \frac{\rho_{J-1}}{2}\omega^2 L_{J-1} \Delta X_J \quad \text{..... A64}$$

$$P_{Y_J} = \frac{\rho_{J-1}}{2}\omega^2 L_{J-1} \Delta Y_J \quad \text{..... A65}$$

$$P_{Z_J} = \frac{\rho_{J-1}}{2}\omega^2 L_{J-1} \Delta Z_J \quad \text{..... A66}$$

and b)

$$P_{X_{J+1}} = \rho_J \omega^2 L_J \Delta X_J \Big/ 2 \qquad \text{.....A67}$$

$$P_{Y_{J+1}} = \rho_J \omega^2 L_J \Delta Y_J \Big/ 2 \qquad \text{.....A68}$$

$$P_{Z_{J+1}} = \rho_J \omega^2 L_J \Delta Z_J \Big/ 2 \qquad \text{.....A69}$$

Moments :

Similar to the load considerations two sets of moments are applicable. They are (See figure A5) :

a) Moments about X,Y,Z axes due to displacements at J causing inertia forces on element J-1 and

b) Moments about X,Y,Z axes due to displacements at J causing inertia forces on element J

The following moments are applicable on element J-1

Taking moments about X axis

$$M_{X_J} = -\frac{\rho_{J-1}\omega^2 L_{J-1}(Z_{J-1}-Z_J)}{2}\frac{\Delta Y_J}{3} + \frac{\rho_{J-1}\omega^2 L_{J-1}(Y_{J-1}-Y_J)}{2}\frac{\Delta Z_J}{3} + \frac{\omega^2 I_P L_{J-1}}{2} l_{x(J-1)} \phi_{J-1} \qquad \text{.....A70}$$

where $\frac{\rho_{J-1}\omega^2 L_{J-1}\Delta Y_J}{2}$ and $\frac{\rho_{J-1}\omega^2 L_{J-1}\Delta Z_J}{2}$ represent the forces in Y and Z directions respectively and $1/3\,(Z_{J-1}-Z_J)$ and $1/3\,(Y_{J-1}-Y_J)$ represent the moment arms. $\frac{\omega^2 I_P L_{J-1}}{2}\phi_{J-1}$ represents the torsional moment about the local x axis. Please note that this moment is resolved into overall axes directions by applying direction cosines. Accordingly the moment component from this to the overall X axis direction is $\frac{l_x \omega^2 I_P L_{J-1}}{2}\phi_{J-1}$. Hence the total bending moment about X axis is

$$M_{X_J} = -\frac{\rho_{J-1}\omega^2 L_{J-1}(Z_{J-1}-Z_J)}{6}\Delta Y_J + \frac{\rho_{J-1}\omega^2 L_{J-1}(Y_{J-1}-Y_J)}{6}\Delta Z_J + \frac{\omega^2 I_P L_{J-1}}{2} l_{x(J-1)} \phi_{J-1} \qquad \text{.....A71}$$

Similarly taking moments about Y and Z directions

$$M_{Y_J} = +\rho_{J-1}\frac{\omega^2 L_{J-1}}{6}(Z_{J-1}-Z_J)\Delta X_J - \rho_{J-1}\frac{\omega^2 L_{J-1}}{6}(X_{J-1}-X_J)\Delta Z_J$$

$$+\frac{\omega^2 I_P L_{J-1} m_x(J-1)}{2}\phi_{J-1} \qquad \text{.....A72}$$

$$M_{Z_J} = -\rho_{J-1}\frac{\omega^2 L_{J-1}}{6}(Z_{J-1}-Z_J)\Delta X_J + \rho_{J-1}\frac{\omega^2 L_{J-1}}{6}(X_{J-1}-X_J)\Delta Y_J$$

$$+\frac{\omega^2 I_P L_{J-1} n_x(J-1)}{2}\phi_{J-1} \qquad \text{.....A73}$$

Similar arguements hold for the moments on element J and these are given by: (Please see figure 7 also for Δ distribution diagram)

$$M_{X_{J+1}} = -\rho_J\frac{\omega^2 L_J}{3}(Z_J-Z_{J+1})\Delta Y_J + \rho_J\frac{\omega^2 L_J}{3}(Y_J-Y_{J+1})\Delta Z_J$$

$$+\frac{\omega^2 I_P L_J l_{xJ}\phi_J}{2} \qquad \text{.....A74}$$

$$M_{Y_{J+1}} = +\rho_J\frac{\omega^2 L_J}{3}(Z_J-Z_{J+1})\Delta X_J - \rho_J\frac{\omega^2 L_J}{3}(X_J-X_{J+1})\Delta Z_J$$

$$+\frac{\omega^2 I_P L_J m_{xJ}\phi_J}{2} \qquad \text{.....A75}$$

$$M_{Z_{J+1}} = -\rho_J\frac{\omega^2 L_J}{3}(Y_J-Y_{J+1})\Delta X_J + \rho_J\frac{\omega^2 L_J}{3}(X_J-X_{J+1})\Delta Y_J$$

$$+\frac{\omega^2 I_P L_J n_{xJ}\phi_J}{2} \qquad \text{.....A76}$$

Thus the loads and moments due to displacements at a node J causing inrtia forces on element J-1 and element J are established.

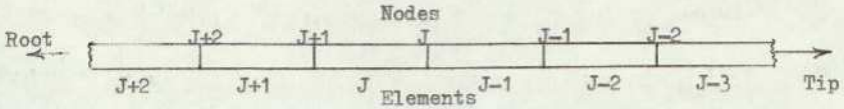

REPRESENTATION OF NODES AND ELEMENTS

FIGURE A2

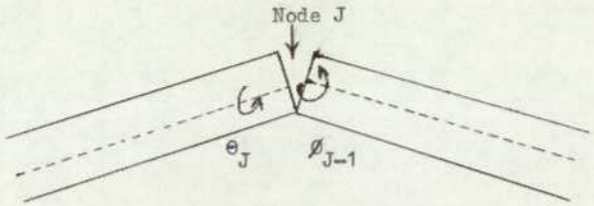

ϕ_{J-1} : Twisting deformation at the outboard end

θ_J : Twisting deformation at the inboard end

(When the sweep-back is absent $\phi_{J-1} = \theta_J$)

TORSIONAL DISPLACEMENTS OF A SWEEP-BACK ELEMENT

FIGURE A3

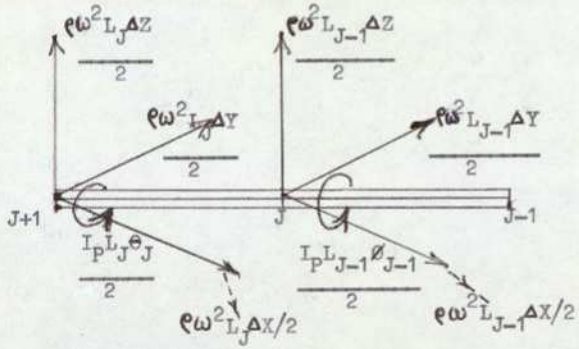

INERTIA FORCES CAUSED ON ELEMENTS J-1 AND J DUE TO DISPLACEMENTS AT NODE J

FIGURE A4

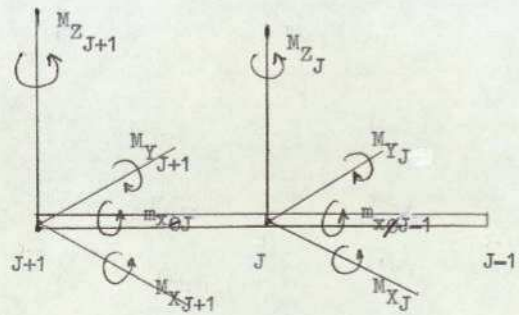

MOMENTS APPLIED TO INBOARD SECTION BY INERTIA FORCES ON THE ELEMENT

FIGURE A5

DERIVATION OF CENTRIFUGAL LOADS

The assumptions and definitions made in 3.1 are applicable. A rotary blade is assumed to revolve at an angular frequency of Ω radians about Z axis and a simple harmonic vibrational frequency is assumed. ρ is the mass density. The total mass of an element of length L is therefore given by ρL. Considering the centrifugal force in X direction only of an element whose X co-ordinates are X_1 and X_2. See figure A6. The co-ordinates X_1 and X_2 are assumed to undergo distorsions ΔX_1 and ΔX_2 above steady state geometry in X direction. The elongated X co-ordinates are now given by $X_1+\Delta X_1$ and $X_2+\Delta X_2$

$$\therefore \text{ the new length in X direction } = (X_1+\Delta X_1) - (X_2+\Delta X_2) \qquad \text{.....A77}$$

The mass per unit length in X direction $\rho_X = \rho_L \Big/ \left\{(X_1+\Delta X_1)-(X_2+\Delta X_2)\right\}$ A78

Centrifugal force at a distance X is given by $\rho_X X \Omega^2 \, dX$

$$\text{Total centrifugal force } = \rho_X \int_{(X_2+\Delta X_2)}^{(X_1+\Delta X_1)} X\Omega^2 \, dX \qquad \text{.....A79}$$

$$= \rho_X \Omega^2 \left[\frac{X^2}{2}\right]_{X_2+\Delta X_2}^{X_1+\Delta X_1}$$

$$= \Omega^2 \rho_X \left\{\frac{(X_1+\Delta X_1)^2 - (X_2+\Delta X_2)^2}{2}\right\} \qquad \text{.....A80}$$

Substituting the value for ρ_X from A78 in A80

$$= \rho_L \Omega^2 \left\{\frac{X_1^2+\Delta X_1^2 +2X_1\Delta X_1 - X_2^2 - \Delta X_2^2 - 2X_2\Delta X_2}{2(X_1-X_2+\Delta X_1-\Delta X_2)}\right\}$$

Ignoring the higher order terms

$$= \frac{\rho_L \Omega^2}{2(X_1-X_2)}\left[\left\{1 - \frac{(\Delta X_1-\Delta X_2)}{(X_1-X_2)}\right\}\left\{(X_1^2-X_2^2 +2X_1\Delta X_1-2X_2\Delta X_2)\right\}\right]$$

$$= \frac{\rho_L \Omega^2}{2(X_1 - X_2)} \left[\{X_1^2 - X_2^2\} - (X_1 + X_2)(\Delta X_1 - \Delta X_2) + 2X_1 \Delta X_1 - 2X_2 \Delta X_2 \right]$$

$$= \frac{\rho L \Omega^2}{2(X_1 - X_2)} \left\{ (X_1 - X_2)(X_1 + X_2) + (X_1 - X_2)(\Delta X_1 + \Delta X_2) \right\}$$

$$= \frac{\rho L \Omega^2}{2} \left\{ X_1 + X_2 + \Delta X_1 + \Delta X_2 \right\} \qquad \text{.....A81}$$

Similarly the total centrifugal force of an element in Y direction can be derived. Without going into the details of integration process the force is given by

$$= \frac{\rho L \Omega^2}{2} \left\{ Y_1 + Y_2 + \Delta Y_1 + \Delta Y_2 \right\} \qquad \text{.....A82}$$

It is to be noted that there won't be any centrifugal load component in Z direction.

Moments due to centrifugal forces:

The centrifugal forces of an element in X and Y directions are given by the equations A81 and A82. If an arbitrary element J is chosen the forces in X and Y directions may be written as follows:

$$P_X = \frac{\rho_J \Omega^2 L_J}{2} (X_J + \Delta X_J + X_{J+1} + \Delta X_{J+1}) \qquad \text{.....A83}$$

$$P_Y = \frac{\rho_J \Omega^2 L_J}{2} (Y_J + \Delta Y_J + Y_{J+1} + \Delta Y_{J+1}) \qquad \text{.....A84}$$

These loads are represented in figures A7 and A8. The moments are refered to the inboard end of element J which is denoted by J+1.

Figure 7 for e.g. could be represented as shown in figure A9.

Taking moments about Y axis (for P_X loads)

$$M_{Y_{J+1}} = \frac{\rho_J \Omega^2 L_J}{2} (X_J + \Delta X_J) \times \text{Moment arm in Z direction}$$

$$+ \frac{\rho_J \Omega^2 L_J}{2} (X_{J+1} + \Delta X_{J+1}) \times \text{Moment arm in Z direction} \qquad \text{.....A85}$$

The moment arms are given by $2/3(Z_J-Z_{J+1})$ and $1/3(Z_J-Z_{J+1})$

Substituting these moments in A85

$$M_{Y_{J+1}} = \frac{\rho_J \Omega^2 L_J}{2}(X_J+\Delta X_J)\ 2/3(Z_J-Z_{J+1}) +$$

$$\frac{\rho_J \Omega^2 L_J}{2}(X_{J+1}+\Delta X_{J+1})\ 1/3(Z_J-Z_{J+1}) \quad \text{.....A86}$$

Taking moments about Z axis

$$M_{Z_{J+1}} = -\frac{\rho_J \Omega^2 L_J}{2}\left\{(X_J+\Delta X_J)2/3(Y_J-Y_{J+1})+(X_{J+1}+\Delta X_{J+1})1/3 \cdot(Y_J-Y_{J+1})\right\} \quad \text{.....A87}$$

Similar moments can be given for loads in Y direction aswell

Moment about X axis:

$$M_{X_{J+1}} = -\frac{\rho_J \Omega^2 L_J}{2}\left\{(Y_J+\Delta Y_J)2/3(Z_J-Z_{J+1})+(Y_{J+1}+\Delta Y_{J+1})1/3 \cdot(Z_J-Z_{J+1})\right\} \quad \text{.....A88}$$

Moments about Z axis

$$M_{Z_{J+1}} = \frac{\rho_J \Omega^2 L_J}{2}\left\{(Y_J+\Delta Y_J)2/3(X_J-X_{J+1})+(Y_{J+1}+\Delta Y_{J+1})1/3 \cdot(X_J-X_{J+1})\right\} \quad \text{.....A89}$$

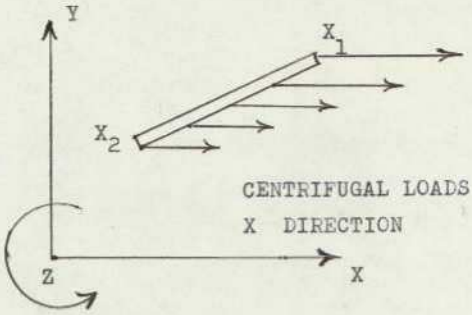

CENTRIFUGAL LOADS IN AN ELEMENT
X DIRECTION

FIGURE A6

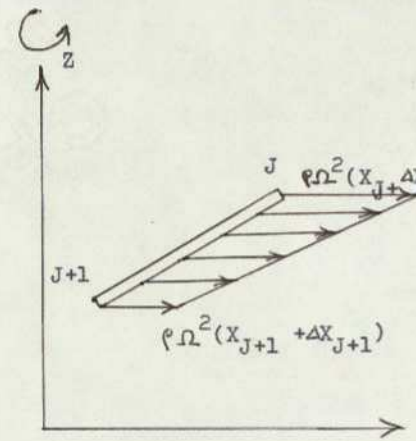

CENTRIFUGAL FORCES IN
X DIRECTION
OF AN ELEMENT J

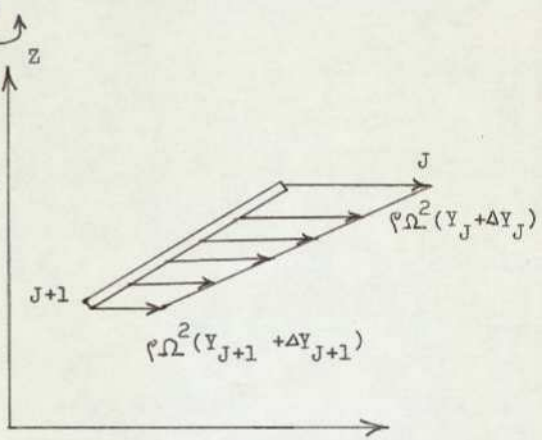

CENTRFUGAL FORCES IN
Y DIRECTION
OF AN ELEMENT J

FIGURE A7

FIGURE A8

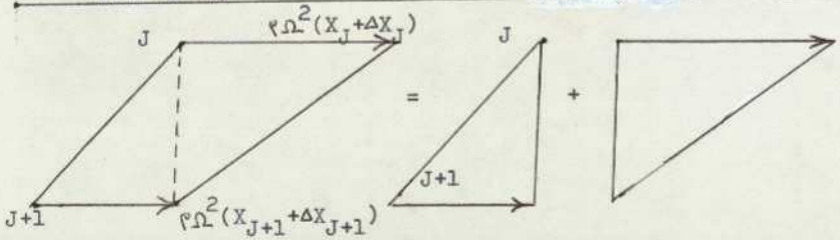

CENTRIFUGAL FORCES IN X DIRECTION OF AN ELEMENT J
DIVIDED INTO TWO COMPONENTS

FIGURE A9

APPENDIX 7
LISTING OF THE PROGRAMME VTRI

```
WORK(ED)
SEND TO(GEOSSEMICOMP)
SEMICOMPILED(SUBGROUPIANY,SUBRO %FIOLP)
LIST(LP)
LIBRARY(ED,SUBGROUPESCE)
PROGRAM(ROTK)
INPUT 1=CR0
OUTPUT 2=LP0
TRACE 0
END
```

```
C PROGRAMME STARTS
      MASTER EIGN
      REAL LG,IY,IZ,JSV,IP
      DIMENSION XS(11),YS(11),ZS(11),LG(10),
     1RHO(10),BETA(11),DRMT(3,3),CON(6,5),R5(8,5),
     1A(10),IY(10),IZ(10),JSV(10),B1(10),B2(10),B3(10),CNT(6,5),
     1EY(11),EZ(11),PLFL(8,5),PLFO(8,5),TRA(6,6),EC(6,6),STR(4,6),
     1FXMT(8,8),BETB(11),EIGA(50,50),BH(50),FRC(4,5),RES(6,5),
     1DC(3,3),DM(3,3),EIGB(50,50),R(8,5),P(6,6),S(6,6),TT(6,6),
     1TEMP(8,5),FLA(6,5),IP(10),R3(8,5),R4(8,5),RR(8,5),
     1CEN(6,5),TAMP(8,5),W(14),CFT(6,5),CJN(6,5),
     1AK(2500),FSMOD(2500),INT(48),ITS(50),FSR(50),
     1BAB(6,5),BUN(440),FSI(50),SVOD(2500),T(2850)
C DECLARATION OF COMMON STORAGE VARIABLES
      COMMON/DATA/XS,YS,ZS,LG,RHO,BETA,DRMT,EY,EZ,
     1DC,DM,CNT,OMEGA,EXMT,A,IY,IZ,JSV,B1,B2,B3,E,G,
     1BETB,EIGA,EIGB,R,TEMP,TRA,EC,STR,FRC,RES,FLA,IP,
     1BAB,BUN,TAMP,R3,R4,RR,CEN,CON,BH,CFT,CJN,R5,P,S,TT
C INPUT DATA-THESE ARE FED FROM SEPARATE DATA FILES
      READ(1,1101)N
 1101 FORMAT(I0)
      READ(1,1001)E,G,SIG,OMEGA
 1001 FORMAT(12F0.0)
      DO 5 I=1,N
    5 READ(1,1002)A(I),IY(I),IZ(I),JSV(I),EY(I),EZ(I),B1(I),
     1B2(I),B3(I),RHO(I),IP(I)
 1002 FORMAT(12F0.0)
      DO 6 I=1,N+1
    6 READ(1,1003)XS(I),YS(I),ZS(I),BETA(I),BETB(I)
 1003 FORMAT(12F0.0)
C INPUT DATA VIA DATA FILES COMPLETED
C START CLEARING ARRAYS
```

```
      DO 17 I=1,6
      DO 17 J=1,5
   17 BAB(I,J),FLA(I,J),RES(I,J),CON(I,J)=0
      BAB(1,1),BAB(2,2),BAB(3,3)=1.0
      DO 13 I=1,8
       DO 13 J=1,5
      PLFO(I,J),PLFL(I,J),TEMP(I,J)=0
   13 RR(I,J),TAMP(I,J)=0
      DO 14 I=1,6
       DO 14 J=1,6
   14  EC(I,J),TRA(I,J),P(I,J),S(I,J),TT(I,J)=0
      DO 16 I=1,6
   16 TRA(I,I)=1.0
      DO 18 I=1,4
      DO 18 J=1,5
   18 FRC(I,J)=0.0
      DO 25 I=1,4
      DO 25 J=1,6
   25 STR(I,J)=0.0
      DO 19 I=1,3
      DO 19 J=1,3
   19 DC(I,J),DN(I,J),DRMT(I,J)=0
      DO 20 I=1,8
      DO 20 J=1,8
   20 FXMT(I,J)=0
      DO 21 I=1,50
      DO 21 J=1,50
   21 EIGA(I,J),EIGB(I,J)=0
      DO 11 I=1,6
      DO 11 J=1,5
      CEN(I,J),CFT(I,J),CJN(I,J)=0.0
   11 CNT(I,J)=0
C ALL ARRAYS ARE INITIALISED
      DO 15 I=1,N
      BA=XS(I)-XS(I+1)
      BB=YS(I)-YS(I+1)
      BC=ZS(I)-ZS(I+1)
      LG(I)=SQRT(BA*BA+BB*BB+BC*BC)
   15 CONTINUE
C PRINT OUT ALL INPUT DATA
      WRITE(2,1102)N
 1102 FORMAT(///18HONUMBER OF MEMBERS/50(I0/))
      WRITE(2,1104)E,G,SIG
 1104 FORMAT(///46HOELASTICITY MOD   RIGIDITY MOD   POISONS RATIO/
     150(3E15.6/))
      DO 8 I=1,N
       WRITE(2,1106)(I,A(I),I=1,N)
 1106 FORMAT(///17HOAREAS OF MEMBERS/50(7(4(I4,E12.4)/)))
      WRITE(2,1107)(I,IY(I),I=1,N)
 1107 FORMAT(///25HOI1 MOMENT OF AREA Y AXIS/50(7(4(I4,E12.4)/)))
      WRITE(2,1108)(I,IZ(I),I=1,N)
 1108 FORMAT(///25HOI1 MOMENT OF AREA Z AXIS/50(7(4(I4,E12.4)/)))
      WRITE(2,1109)(I,JSV(I),I=1,N)
 1109 FORMAT(///26HOST VENANTS SECTION CONSTANTS/50(7(4(I4,E12.4)/)))
      WRITE(2,1111)(I,EY(I),I=1,N)
 1111 FORMAT(///32HOY AXIS CO-ORDINATE OF CS WRT CG/50(7(4(I4,E12.4)/)))
      WRITE(2,1110)(I,IP(I),I=1,N)
 1110 FORMAT(///18HOPITCHING INERTIAS/50(7(4(I4,E12.4)/)))
      WRITE(2,1112)(I,EZ(I),I=1,N)
 1112 FORMAT(///32HOZ AXIS CO-ORDINATE OF CS WRT CG/50(7(4(I4,E12.4)/)))
      WRITE(2,1115)(I,B1(I),I=1,N)
 1115 FORMAT(///25HOHIGHER MOMENTS OF AREA 1/50(7(4(I4,E12.4)/)))
      WRITE(2,1116)(I,B2(I),I=1,N)
 1116 FORMAT(///25HOHIGHER MOMENTS OF AREA 2/50(7(4(I4,E12.4)/)))
      WRITE(2,1117)(I,B3(I),I=1,N)
 1117 FORMAT(///25HOHIGHER MOMENTS OF AREA 3/50(7(4(I4,E12.4)/)))
```

```
      WRITE(2,1118)(I,RHO(I),I=1,N)
 1118 FORMAT(///27HOMASS DENSITIES OF SECTIONS/50(7(4(I4,E12.4)/)))
    8 CONTINUE
      DO 9 I=1,N+1
      WRITE(2,1120)(I,XS(I),I=1,N+1)
 1120 FORMAT(///29HOX CO ORDINATE OF CGS OVERALL/50(7(4(I4,E12.4)/)))
      WRITE(2,1121)(I,YS(I),I=1,N+1)
 1121 FORMAT(///29HOY CO ORDINATE OF CGS OVERALL/50(7(4(I4,E12.4)/)))
      WRITE(2,1122)(I,ZS(I),I=1,N+1)
 1122 FORMAT(///29HOZ CO ORDINATE OF CGS OVERALL/50(7(4(I4,E12.4)/)))
      WRITE(2,1123)(I,BETA(I),I=1,N+1)
 1123 FORMAT(///21HOBETA PRETWIST ANGLES/50(7(4(I4,E12.4)/)))
      WRITE(2,1124)(I,BETB(I),I=1,N+1)
 1124 FORMAT(///21HOBETB PRETWIST ANGLE1/50(7(4(I4,E12.4)/)))
    9 CONTINUE
      WRITE(2,1203)OMEGA
 1203 FORMAT(///28HOANGULAR VELOCITY IN RADIANS/50(E15.6/))
C PRINT OUT OF INPUT DATA COMPLETED
      WRITE(2,1205)(I,LG(I),I=1,N)
 1205 FORMAT(///18HOSECTIONAL LENGTHS/50(7(4(I4,E12.4)/)))
C ELEMENT JJ CALCULATIONS STARTS
      DO 50 JJ=1,N
      CALL FLEX(JJ)
      CALL COSN(JJ)
      CALL RESL(JJ)
      CALL STRU(JJ)
C UNIT LOAD CALCULATIONS STARTS
      DO 500 JS=1,JJ
      DO 501 I=1,8
      DO 501 M=1,5
  501 R(I,M)=0.0
      BAB(4,4)=(XS(JS)-XS(JS+1))/LG(JS)
      BAB(5,4)=(YS(JS)-YS(JS+1))/LG(JS)
      BAB(6,4)=(ZS(JS)-ZS(JS+1))/LG(JS)
      KK=0
      IF(JS.EQ.1)KK=1
      BAB(4,5)=(XS(JS-1+KK)-XS(JS+KK))/LG(JS-1+KK)
      BAB(5,5)=(YS(JS-1+KK)-YS(JS+KK))/LG(JS-1+KK)
      BAB(6,5)=(ZS(JS-1+KK)-ZS(JS+KK))/LG(JS-1+KK)
      DO 502 KK=1,2
      CALL TRAN(JS,JJ+KK-1)
      CALL MULT(TRA,BAB,CON,6,6,5)
      CALL MULT(EC,CON,RES,6,6,5)
      CALL MULT(STR,RES,FRC,4,6,5)
  502 CALL ASMB(JJ,KK-1)
      DO 503 I=1,8
      DO 503 M=1,5
  503 BUN(40*(JS-1)+8*(M-1)+I)=R(I,M)
  500 CONTINUE
C UNIT LOADS ARE STORED IN THE MATIX 'BUN'
C ELEMENT J CALCULATIONS STARTS
C CENTRIFUGAL LOAD CALCULATIONS STARTS
      DO 51 J=1,JJ+1
      DO 510 I=1,8
      DO 510 M=1,5
  510 R(I,M)=0.0
      IF(J.EQ.M+1) GO TO 51
      DO 145 I=1,6
      DO 145 M=1,5
  145 CEN(I,M)=0
      IF(J.EQ.JJ+1) GO TO 123
      IF(J.EQ.JJ) GO TO 113
      CALL CENT(JJ,J)
      CALL MULT(EC,CEN,RES,6,6,5)
      CALL MULT(STR,RES,FRC,4,6,5)
      CALL ASMB(JJ,0)
```

```
  113 CALL CENT(JJ+1,J)
      CALL MULT(EC,CEN,RES,6,6,5)
      CALL MULT(STR,RES,FRC,4,6,5)
      CALL ASMB(JJ,1)
      IF(J.EQ.1) GO TO 110
      CALL CENF(JJ,J-1)
      CALL MULT(EC,CEN,RES,6,6,5)
      CALL MULT(STR,RES,FRC,4,6,5)
      CALL ASMB(JJ,0)
  123 CALL CENF(JJ+1,J-1)
      CALL MULT(EC,CEN,RES,6,6,5)
      CALL MULT(STR,RES,FRC,4,6,5)
      CALL ASMB(JJ,1)
  110 IF(J.EQ.1.AND.JJ.EQ.1) GO TO 122
      IF(J.LT.JJ) GO TO 122
      IF(J.EQ.JJ+1) GO TO 125
      DO 116 I=1,6
      DO 116 M=1,5
  116 CFT(I,M)=0
      DO 117 JI=1,J-1
      CALL CEJJ(JI)
      DO 118 I=1,6
      DO 118 M=1,5
  118 CFT(I,M)=CFT(I,M)+CJN(I,M)
  117 CONTINUE
      CALL MULT(EC,CFT,RES,6,6,5)
      CALL MULT(STR,RES,FRC,4,6,5)
      CALL ASMB(JJ,0)
      IF(J.EQ.JJ) GO TO 122
  125 DO 119 I=1,6
      DO 119 M=1,5
  119 CFT(I,M)=0
      DO 120 JI=1,JJ
      CALL CEJJ(JI)
      DO 121 I=1,6
      DO 121 M=1,5
  121 CFT(I,M)=CFT(I,M)+CJN(I,M)
  120 CONTINUE
      CALL MULT(EC,CFT,RES,6,6,5)
      CALL MULT(STR,RES,FRC,4,6,5)
      CALL ASMB(JJ,1)
  122 DO 128 I=1,8
      DO 128 M=1,5
  128 RR(I,M)=R(I,M)
      DO 12 I=1,8
      DO 12 M=1,5
   12 R4(I,M),R5(I,M),R3(I,M),R(I,M)=0.0
C CENTRIFUGAL LOAD CALCULATIONS COMPLETED
C FLAPPING LOAD CALCULATIONS STARTS
      DO 55 K=1,2
      DO 57 M=4,6
   57 FLA(M,K+3)=0.0
      DO 56 KK=1,2
      IF(J+K.GT.JJ+2.OR.J+K.LT.3) GO TO 56
      IF(K.EQ.2) GO TO 60
      CALL FLAP(J,K)
      GO TO 61
   60 CALL FLAP(J,K)
   61 IF(J+K-1.GT.JJ+KK-1) GO TO 56

      CALL TRAN(J+K-1,JJ+KK-1)
      CALL MULT(TRA,FLA,CON,6,6,5)
      CALL MULT(EC,CON,RES,6,6,5)
      CALL MULT(STR,RES,FRC,4,6,5)
      CALL ASMB(JJ,KK-1)
   56 CONTINUE
```

```
   55  CONTINUE
C FLAPPING LOAD CALCULATIONS COMPLETED
C FORMATION OF EIGEN VALUE PROBLEM STARTS
      DO 79 I=1,8
      DO 79 M=1,5
      SUM=0
      SUN=0
      DO 80 K=1,8
      SUM=EXMT(I,K)*RR(K,M)+SUM
      SUN=EXMT(I,K)*RR(K,M)+SUN
   80 CONTINUE
      TEMP(I,M)=SUM
      TAMP(I,M)=SUN
   79 CONTINUE
C RECALL UNIT LOADS FROM STORAGE
      DO 53 JS=1,JJ
      DO 504 I=1,8
      DO 504 M=1,5
  504 PLFL(I,M)=BUN(40*(JS-1)+8*(M-1)+I)
      DO 83 M=1,5
      DO 81 MM=1,5
      K1=(JS-1)*5+M
      K2=(J-1)*5+MM
      SUM1=EIGA(K1,K2)
      SUM2=EIGB(K1,K2)
      DO 82 K=1,8
      SUM1=PLFL(K,M)*TEMP(K,MM)+SUM1
      SUM2=PLFL(K,M)*TAMP(K,MM)+SUM2
   82 CONTINUE
      EIGA(K1,K2)=SUM1
      EIGB(K1,K2)=SUM2
   81 CONTINUE
   83 CONTINUE
   53 CONTINUE
C EIGEN VALUE PROBLEM IS SET SUITABLE FOR LIBRARY
C SUBROUTINE CALLS
   51 CONTINUE
C ELEMENT J CALCULATIONS COMPLETED
   50 CONTINUE
C ELEMENT JJ CALCULATIONS COMPLETED
      WRITE(2,1200)
 1200 FORMAT(' POSITION CHECK1'/)
      N1=N*5
      DO 150 I=1,N1
  150 EIGB(I,I)=EIGB(I,I)+1
      DO 151 I=1,N1
      DO 151 J=1,N1
      AK(I+N1*(J-1))=EIGB(I,J)
  151 FSMOD(I+N1*(J-1))=EIGA(I,J)
      WRITE(2,1201)
 1201 FORMAT(' POSITION CHECK2'/)
C LIBRARY SUBROUTINES OPERATION STARTS
      CALL FPMGESOL(N1,N1,0.000001,AK(1),FSMOD(1),W(1),
     =DET,IRANK,NRB)
      WRITE(2,1125)NRB
 1125 FORMAT(///18HONUMBER OF RANKING/50(I0/))
      WRITE(2,1126)IRANK
 1126 FORMAT(///18HONUMBER OF RANKTWO/50(I0/))
      IVS=0
      CALL FPDIRHESSE(N1,FSMOD(1),INT(1))
      CALL FPQRHESSE(N1,FSMOD(1),ITS(1),FSR(1),FSI(1),SVOD(1),
     1IVS)
      WRITE(2,1202)
 1202 FORMAT(' POSITION CHECK3'/)
      CALL FPQRVS(N1,FSMOD(1),SVOD(1),FSR(1),FSI(1),T(1))
      CALL FPBACK(N1,FSMOD(1),SVOD(1),FSI(1),INT(1))
```

```
C CALCULATION-ANALYSIS OF FREQUENCIES AND MODE SHAPES
      DO 300 I=1,N1
  300 BH(I)=FSR(I)
      DO 301 I=1,N1
      K=1
      DO 302 J=2,N1
  302 IF(BH(J).GT.BH(K)) K=J
      ITS(I)=K
  301 BH(K)=-1000000
      DO 303 I=1,N1
      BH(I)=FSR(ITS(I))
      T(I)=FSI(ITS(I))
      DO 303 J=1,N1
  303 AK((I-1)*N1+J)=SVOD((ITS(I)-1)*N1+J)
      DO 304 I=1,N1
      FSR(I)=BH(I)
      FSI(I)=T(I)
      DO 304 J=1,N1
  304 SVOD((I-1)*N1+J)=AK((I-1)*N1+J)
      DO 200 I=1,N1
      IF(FSR(I).LE.0.0) GO TO 306
      F=0.1591549/SQRT(FSR(I))
      WRITE(2,1208) I,F
 1208 FORMAT(7HRESULT,I3,10HFREQUENCY,F13.6,11H CYCLES/SEC)
      I1=I*N1-(N1-1)
      DO 200 K=1,5
      IF(K.EQ.1) GO TO 350
      IF(K.EQ.2) GO TO 351
      IF(K.EQ.3) GO TO 352
      IF(K.EQ.4) GO TO 353
      IF(K.EQ.5) GO TO 354
  350 WRITE(2,1209) K
 1209 FORMAT(I5,23HMODE SHAPE LONGITUDINAL)
      GO TO 370
  351 WRITE(2,1210) K
 1210 FORMAT(I5,23HMODE SHAPE DRAG BENDING)
      GO TO 370
  352 WRITE(2,1211) K
 1211 FORMAT(I5,23HMODE SHAPE FLAP BENDING)
      GO TO 370
  353 WRITE(2,1212) K
 1212 FORMAT(I5,18HMODE SHAPE TORSION)
      GO TO 370
  354 WRITE(2,1213) K
 1213 FORMAT(I5,24HMODE SHAPE SWEEP TORSION)
  370 K1=K+I1-1
      WRITE(2,1214)(SVOD(K1+5*(J-1)),J=1,N)
 1214 FORMAT(10F12.8)
      GO TO 200
  306 IF(FSR(I).EQ.0.0) GO TO 307
      WRITE(2,1215) I
      FSR(I)=-1.0
 1215 FORMAT(6HRESULT,I5,13HNEGATIVE ROOT)
      GO TO 200
  307 WRITE(2,1216) I
 1216 FORMAT(6HRESULT,I5,9HZERO ROOT)
  200 CONTINUE
      WRITE(2,1207)(I,FSI(I),I=1,N1)
 1207 FORMAT(///16HOIMAGINARY ROOTS/50(10(5(I4,E15.4)/)))
      STOP
      END

GMENT, LENGTH  2480, NAME  EIGN
```

```
C END OF CALCULATIONS
C COSN SUBROUTINE -CALCULATION OF DIRECTION COSINES
      SUBROUTINE COSN(I)
      REAL LG,IY,IZ,JSV,IP
      DIMENSION XS(11),YS(11),ZS(11),LG(10),
     1RHO(10),BETA(11),DRMT(3,3),CON(6,5),R5(8,5),
     1A(10),IY(10),IZ(10),JSV(10),B1(10),B2(10),B3(10),CNT(6,5),
     1EY(11),EZ(11),PLFL(8,5),PLFO(8,5),TRA(6,6),EC(6,6),STR(4,6),
     1FXMT(8,8),BETB(11),EIGA(50,50),BH(50),FRC(4,5),RES(6,5),
     1DC(3,3),DM(3,3),EIGB(50,50),R(8,5),P(6,6),S(6,6),TT(6,6),
     1TEMP(8,5),FLA(6,5),IP(10),R3(8,5),R4(8,5),RR(8,5),
     1CEN(6,5),TAMP(8,5),U(14),CFT(6,5),CJN(6,5),
     1AK(2500),FSHOD(2500),INT(48),ITS(50),FSR(50),
     1BAB(6,5),BUN(440),FSI(50),SVOD(2500),T(2850)
      COMMON/DATA/XS,YS,ZS,LG,RHO,BETA,DRMT,EY,EZ,
     1DC,DM,CNT,OMEGA,FXMT,A,IY,IZ,JSV,B1,B2,B3,E,G,
     1BETB,EIGA,EIGB,R,TEMP,TRA,EC,STR,FRC,RES,FLA,IP,
     1BAB,BUN,TAMP,R3,R4,RR,CEN,CON,BH,CFT,CJN,R5,P,S,TT
      B4=SIN(BETA(I))
      B5=COS(BETA(I))
      DM(1,1)=1.0
      DM(2,2),DM(3,3)=B5
      DM(2,3)=B4
      DM(3,2)=-B4
      BBI1=XS(I)-XS(I+1)
      BBI2=YS(I)-YS(I+1)
      BBI3=ZS(I)-ZS(I+1)
      B6=BBI1/LG(I)
      B7=BBI2/LG(I)
      B8=BBI3/LG(I)
      DC(1,1)=B6
      DC(1,2)=B7
      DC(1,3)=B8
      B9=SQRT(B6**2+B7**2)
      B10=SQRT(B7**2+B8**2)
      B11=SQRT(B8**2+B6**2)
      IF (B8.GT.0.9999) GO TO 475
      DC(2,1) = -B7/B9
      DC(2,2) =  B6/B9
      DC(2,3) =  0
      DC(3,1) = -B8*B6/B9
      DC(3,2) = -B8*B7/B9
      DC(3,3) =  B9
      GO TO 480
  475 DC(1,1),DC(1,2)=0
      DC(1,3)         =1
      DC(2,1),DC(2,3)=0
      DC(2,2)         =1
      DC(3,1)         =-1
      DC(3,2),DC(3,3)=0
      WRITE(2,1312) JJ
 1312 FORMAT(I5,44HALTERNATIVE DIRECTION COSINE USED REF THESIS)
      GO TO 480
  480 CALL MULT(DM,DC,DRMT,3,3,3)
      RETURN
      END

GMENT. LENGTH   227, NAME  COSN
```

```
C FLEXIBILITY MATRIX CALCULATIONS
C SUBROUTINE FORMING FLEXIBILITY MATRIX
      SUBROUTINE FLEX(T)
      REAL LG,IY,IZ,JSV,IP
      DIMENSION XS(11),YS(11),ZS(11),LG(10),
     1RHO(10),BETA(11),DRMT(3,3),CON(6,5),R5(8,5),
     1A(10),IY(10),IZ(10),JSV(10),B1(10),B2(10),B3(10),CNT(6,5),
     1EY(11),EZ(11),PLFL(8,5),PLFO(8,5),TRA(6,6),EC(6,6),STR(4,6),
     1FXMT(8,8),BETB(11),EIGA(50,50),BH(50),FRC(4,5),RES(6,5),
     1DC(3,3),DM(3,3),EIGB(50,50),R(8,5),P(6,6),S(6,6),TT(6,6),
     1TEMP(8,5),FLA(6,5),IP(10),R3(8,5),R4(8,5),RR(8,5),
     1CEN(6,5),TAMP(8,5),U(14),CFT(6,5),CJN(6,5),
     1AK(2500),FSMOD(2500),INT(48),ITS(50),FSR(50),
     1BAB(6,5),BUN(440),FSI(50),SVOD(2500),T(2850)
      COMMON/DATA/XS,YS,ZS,LG,RHO,BETA,DRMT,EY,EZ,
     1DC,DM,CNT,OMEGA,FXMT,A,IY,IZ,JSV,B1,B2,B3,E,G,
     1BETB,EIGA,EIGB,R,TEMP,TRA,EC,STR,FRC,RES,FLA,IP,
     1BAB,BUN,TAMP,R3,R4,RR,CEN,CON,BH,CFT,CJN,R5,P,S,TT
      BTS=(BETB(I)-BETA(I))/LG(I)
          BET=BETB(I)-BETA(I)
      C1=B1(I)*BTS/A(I)
      C2=      BTS*(B3(I)-EZ(I)*B1(I))/IY(I)
      C3=      BTS*(B2(I)-EY(I)*B1(I))/IZ(I)
      SVJ=G*JSV(I)*(1+IZ(I)**2+BTS**2/(IY(I)*2*A(I)))
      A1 =LG(I)/SVJ
      A11=A1*C1**2
      A12=LG(I)/(E*A(I))
      A2=A12+A11
      A3=C1*A1
      A4=C2*A1
      A5=C3*A1
      A6=A3*C2
      A7=A3*C3
      A8=A4*C3
      A9=LG(I)/(E*IY(I))+C2**2*A1
      A10=LG(I)/(E*IZ(I))+C3**2*A1
      A11=A6*BET*BET
      A12=A7*BET*BET
      A13=A4*BET*BET
      A14=A5*BET*BET
      FXMT(1,1),FXMT(2,2)=A2/3
      FXMT(1,2)=A2/6
      FXMT(1,3),FXMT(2,4)=A3/3
      FXMT(1,4),FXMT(2,3)=A3/6
      FXMT(1,5)=A6/3-A7/12*BET-A11/60
      FXMT(1,6),FXMT(2,5)=A6/6-A7/12*BET-A11/40
      FXMT(1,7)=A7/3+A6/12*BET-A12/60
      FXMT(1,8),FXMT(2,7)=A7/6+A6/12*BET-A12/40
      FXMT(2,6)=A6/3-A7/4*BET-A11/10
      FXMT(2,8)=A7/3+A6/4*BET-A12/10
      FXMT(3,3),FXMT(4,4)=A1/3
      FXMT(3,4)=A1/6
      FXMT(3,5)=A4/3-A5/12*BET-A13/60
      FXMT(3,6),FXMT(4,5)=A4/6-A5/12*BET-A13/40
      FXMT(3,7)=A5/3+A4/12*BET-A14/60
      FXMT(3,8),FXMT(4,7)=A5/6+A4/12*BET-A14/40
      FXMT(4,6)=A4/3-A5/4*BET-A13/10
      FXMT(4,8)=A5/3+A4/4*BET-A14/10
      FXMT(5,5)=A9/3+(A10-A9)/30*BET**2-A8/6*BET
      FXMT(5,6)=A9/6+(A10-A9)/20*BET**2-A8/6*BET
      FXMT(5,7)=A9/12-BET-A10/12*BET-A8/3-A8/15*BET**2
      FXMT(5,8),FXMT(6,7)=A9/12*BET-A10/12*BET+A8/6*BET-A8/10*BET**2
      FXMT(6,6)=A9/3+(A10-A9)/5*BET**2-A8/2*BET
      FXMT(6,8)=A9/4*BET-A10/4*BET+A8/3-A8/2.5*BET**2
      FXMT(7,7)=A10/3+(A9-A10)/30*BET**2+A8/6*BET
```

```
      FXMT(7,8)=A10/6-(A9-A10)/20*BET**2+A8/6*BET
      FXMT(8,8)=A10/3-(A9-A10)/5*BET**2+A8/2*BET
      DO 3 K=2,8
      DO 3 J=1,K-1
      FXMT(K,J)=FXMT(J,K)
    3 CONTINUE
      RETURN
      END

.EGMENT, LENGTH   680, NAME  FLEX


      SUBROUTINE MULT(P,S,TT,NN,MM,KK)
      DIMENSION P(NN,MM),S(MM,KK),TT(NN,KK)
      DO 1 I=1,NN
      DO 1 II=1,KK
    1 TT(I,II)=0
      DO 2 I=1,NN
      DO 2 II=1,MM
      DO 2 K=1,KK
    2 TT(I,K)=TT(I,K)+P(I,II)*S(II,K)
      RETURN
      END

SEGMENT. LENGTH   110, NAME  MULT


      SUBROUTINE FLAP(I,K)
      REAL LG,IY,IZ,JSV,IP
      DIMENSION XS(11),YS(11),ZS(11),LG(10),
     1RHO(10),BETA(11),DRMT(3,3),CON(6,5),R5(8,5),
     2A(10),IY(10),IZ(10),JSV(10),B1(10),B2(10),B3(10),CNT(6,5),
     3EY(11),EZ(11),PLFL(8,5),PLFO(8,5),TRA(6,6),EC(6,6),STR(4,6),
     4FXMT(8,8),BETB(11),EIGA(50,50),BH(50),FRC(4,5),RES(6,5),
     5DC(3,3),DM(3,3),EIGB(50,50),R(8,5),P(6,6),S(6,6),TT(6,6),
     6TEMP(8,5),FLA(6,5),IP(10),R3(8,5),R4(8,5),RR(8,5),
     7CEN(6,5),TAMP(8,5),W(14),CFT(6,5),CJN(6,5),
     8AK(2500),FSMOD(2500),INT(48),ITS(50),FSR(50),
     9BAB(6,5),BUN(44),FST(50),SVOD(2500),T(2850)
      COMMON/DATA/XS,YS,ZS,LG,RHO,BETA,DRMT,EY,EZ,
     1DC,DM,CNT,OMEGA,FXMT,A,IY,IZ,JSV,B1,B2,B3,E,G,
     2BETB,EIGA,EIGB,R,TEMP,TRA,EC,STR,FRC,RES,FLA,IP,
     3BAB,BUN,TAMP,R3,R4,RR,CEN,CON,BH,CFT,CJN,R5,P,S,TT
      SUN=RHO(I-1)*LG(I-1)/2.0
      FLA(1,1),FLA(2,2),FLA(3,3)=SUN
      FLA(4,2)=-SUN*(ZS(I-1)-ZS(I))/3.0
      FLA(4,3)= SUN*(YS(I-1)-YS(I))/3.0
      FLA(4,5)= IP(I-1)*(XS(I-1)-XS(I))/2.0
      FLA(5,1)=-FLA(4,2)
      FLA(5,3)=-SUN*(XS(I-1)-XS(I))/3.0
      FLA(5,5)=  IP(I-1)*(YS(I-1)-YS(I))/2.0
      FLA(6,1)=-FLA(4,3)
      FLA(6,2)=-FLA(5,3)
      FLA(6,5)=IP(I-1)*(ZS(I-1)-ZS(I))/2.0
  420 RETURN
      END

SEGMENT. LENGTH   196, NAME  FLAP
```

```
      SUBROUTINE FLAB(I,K)
      REAL LG,IY,IZ,JSV,IP
      DIMENSION XS(11),YS(11),ZS(11),LG(10),
     1RHO(10),BETA(11),DRMT(3,3),CON(6,5),R5(8,5),
     1A(10),IY(10),IZ(10),JSV(10),B1(10),B2(10),B3(10),CNT(6,5),
     1EY(11),EZ(11),PLFL(8,5),PLFO(8,5),TRA(6,6),EC(6,6),STR(4,6),
     1FXMT(8,8),BETB(11),EIGA(50,50),BH(50),FRC(4,5),RES(6,5),
     1DC(3,3),DM(3,3),EIGB(50,50),R(8,5),P(6,6),S(6,6),TT(6,6),
     1TEMP(8,5),FLA(6,5),IP(10),R3(8,5),R4(8,5),RR(8,5),
     1CEN(6,5),TAMP(8,5),W(14),CFT(6,5),CJN(6,5),
     1AK(2500),FSMOD(2500),INT(48),ITS(50),FSR(50),
     1BAB(6,5),BUN(440),FSI(50),SVOD(2500),T(2850)
      COMMON/DATA/XS,YS,ZS,LG,RHO,BETA,DRMT,EY,EZ,
     1DC,DM,CNT,OMEGA,FXMT,A,IY,IZ,JSV,B1,B2,B3,E,G,
     1BETB,EIGA,EIGB,R,TEMP,TRA,EC,STR,FRC,RES,FLA,IP,
     1BAB,BUN,TAMP,R3,R4,RR,CEN,CON,BH,CFT,CJN,R5,P,S,TT
      SUN= RHO(I)*LG(I)/2.0
      FLA(1,1),FLA(2,2),FLA(3,3)=SUN
      FLA(4,2)=-SUN*(ZS(I)-ZS(I+1))*2.0/3.0
      FLA(4,3)= SUN*(YS(I)-YS(I+1))*2.0/3.0
      FLA(4,4)= IP(I)*(XS(I)-XS(I+1))/2.0
      FLA(5,1)=-FLA(4,2)
      FLA(5,3)=-SUN*(XS(I)-XS(I+1))*2.0/3.0
      FLA(5,4)= IP(I)*(YS(I)-YS(I+1))/2.0
      FLA(6,1)=-FLA(4,3)
      FLA(6,2)=-FLA(5,3)
      FLA(6,4)= IP(I)*(ZS(I)-ZS(I+1))/2.0
  425 RETURN
      END

EGMENT, LENGTH   158, NAME  FLAB


      SUBROUTINE TRAN(I,II)
      REAL LG,IY,IZ,JSV,IP
      DIMENSION XS(11),YS(11),ZS(11),LG(10),
     1RHO(10),BETA(11),DRMT(3,3),CON(6,5),R5(8,5),
     1A(10),IY(10),IZ(10),JSV(10),B1(10),B2(10),B3(10),CNT(6,5),
     1EY(11),EZ(11),PLFL(8,5),PLFO(8,5),TRA(6,6),EC(6,6),STR(4,6),
     1FXMT(8,8),BETB(11),EIGA(50,50),BH(50),FRC(4,5),RES(6,5),
     1DC(3,3),DM(3,3),EIGB(50,50),R(8,5),P(6,6),S(6,6),TT(6,6),
     1TEMP(8,5),FLA(6,5),IP(10),R3(8,5),R4(8,5),RR(8,5),
     1CEN(6,5),TAMP(8,5),W(14),CFT(6,5),CJN(6,5),
     1AK(2500),FSMOD(2500),INT(48),ITS(50),FSR(50),
     1BAB(6,5),BUN(440),FSI(50),SVOD(2500),T(2850)
      COMMON/DATA/XS,YS,ZS,LG,RHO,BETA,DRMT,EY,EZ,
     1DC,DM,CNT,OMEGA,FXMT,A,IY,IZ,JSV,B1,B2,B3,E,G,
     1BETB,EIGA,EIGB,R,TEMP,TRA,EC,STR,FRC,RES,FLA,IP,
     1BAB,BUN,TAMP,R3,R4,RR,CEN,CON,BH,CFT,CJN,R5,P,S,TT
      TRA(4,2)=-(ZS(I)-ZS(II))
      TRA(4,3)= YS(I)-YS(II)
      TRA(5,1)=-TRA(4,2)
      TRA(5,3)=-(XS(I)-XS(II))
      TRA(6,1)=-TRA(4,3)
      TRA(6,2)=-TRA(5,3)
      RETURN
      END

EGMENT, LENGTH    75, NAME  TRAN
```

```
      SUBROUTINE RESL(II)
      REAL LG,IY,IZ,JSV,IP
      DIMENSION XS(11),YS(11),ZS(11),LG(10),
     1RHO(10),BETA(11),DRMT(3,3),CON(6,5),R5(8,5),
     1A(10),IY(10),IZ(10),JSV(10),B1(10),B2(10),B3(10),CNT(6,5),
     1EY(11),EZ(11),PLFL(8,5),PLFO(8,5),TRA(6,6),EC(6,6),STR(4,6),
     1FXMT(8,8),BETB(11),EIGA(50,50),BH(50),FRC(4,5),RES(6,5),
     1DC(3,3),DM(3,3),EIGB(50,50),R(8,5),P(6,6),S(6,6),TT(6,6),
     1TEMP(8,5),FLA(6,5),IP(10),R3(8,5),R4(8,5),RR(8,5),
     1CEN(6,5),TAMP(8,5),W(14),CFT(6,5),CJN(6,5),
     1AK(2500),FSMOD(2500),INT(48),ITS(50),FSR(50),
     1BAB(6,5),BUN(440),FSI(50),SVOD(2500),T(2850)
      COMMON/DATA/XS,YS,ZS,LG,RHO,BETA,DRMT,EY,EZ,
     1DC,DM,CNT,OMEGA,FXMT,A,IY,IZ,JSV,B1,B2,B3,E,G,
     1BETB,EIGA,EIGB,R,TEMP,TRA,EC,STR,FRC,RES,FLA,IP,
     1BAB,BUN,TAMP,R3,R4,RR,CEN,CON,BH,CFT,CJN,R5,P,S,TT
      DO 405 M=1,3
      DO 405 MM=1,3
      EC(M,MM)=DRMT(M,MM)
      EC(M+3,MM+3)=DRMT(M,MM)
  405 CONTINUE
      RETURN
      END
```

SEGMENT, LENGTH 63, NAME RESL

```
      SUBROUTINE STRU(II)
      REAL LG,IY,IZ,JSV,IP
      DIMENSION XS(11),YS(11),ZS(11),LG(10),
     1RHO(10),BETA(11),DRMT(3,3),CON(6,5),R5(8,5),
     1A(10),IY(10),IZ(10),JSV(10),B1(10),B2(10),B3(10),CNT(6,5),
     1EY(11),EZ(11),PLFL(8,5),PLFO(8,5),TRA(6,6),EC(6,6),STR(4,6),
     1FXMT(8,8),BETB(11),EIGA(50,50),BH(50),FRC(4,5),RES(6,5),
     1DC(3,3),DM(3,3),EIGB(50,50),R(8,5),P(6,6),S(6,6),TT(6,6),
     1TEMP(8,5),FLA(6,5),IP(10),R3(8,5),R4(8,5),RR(8,5),
     1CEN(6,5),TAMP(8,5),W(14),CFT(6,5),CJN(6,5),
     1AK(2500),FSMOD(2500),INT(48),ITS(50),FSR(50),
     1BAB(6,5),BUN(440),FSI(50),SVOD(2500),T(2850)
      COMMON/DATA/XS,YS,ZS,LG,RHO,BETA,DRMT,EY,EZ,
     1DC,DM,CNT,OMEGA,FXMT,A,IY,IZ,JSV,B1,B2,B3,E,G,
     1BETB,EIGA,EIGB,R,TEMP,TRA,EC,STR,FRC,RES,FLA,IP,
     1BAB,BUN,TAMP,R3,R4,RR,CEN,CON,BH,CFT,CJN,R5,P,S,TT
      STR(1,1),STR(2,2),STR(3,5)=1.0
      STR(4,6)=-1.0
      STR(2,2)=EZ(II)
      STR(2,3)=-EY(II)
      RETURN
      END
```

SEGMENT, LENGTH 43, NAME STRU

```
      SUBROUTINE ASMB(II,K)
      REAL LG,IY,IZ,JSV,IP
      DIMENSION XS(11),YS(11),ZS(11),LG(10),
     1RHO(10),BETA(11),DRMT(3,3),CON(6,5),R5(8,5),
     1A(10),IY(10),IZ(10),JSV(10),B1(10),B2(10),B3(10),CNT(6,5),
     1EY(11),EZ(11),PLFL(8,5),PLFO(8,5),TRA(6,6),EC(6,6),STR(4,6),
     1FXMT(8,8),BETB(11),EIGA(50,50),BH(50),FRC(4,5),RES(6,5),
     1DC(3,3),DM(3,3),EIGB(50,50),R(8,5),P(6,6),S(6,6),TT(6,6),
     1TEMP(8,5),FLA(6,5),IP(10),R3(8,5),R4(8,5),RR(8,5),
     1CEN(6,5),TAMP(8,5),W(14),CFT(6,5),CJN(6,5),
     1AK(2500),FSMOD(2500),INT(48),ITS(50),FSR(50),
     1BAB(6,5),BUN(440),FST(50),SVOD(2500),T(2850)
      COMMON/DATA/XS,YS,ZS,LG,RHO,BETA,DRMT,EY,EZ,
     1DC,DM,CNT,OMEGA,FXMT,A,IY,IZ,JSV,B1,B2,B3,E,G,
     1BETB,EIGA,EIGB,R,TEMP,TRA,EC,STR,FRC,RES,FLA,IP,
     1BAB,BUN,TAMP,R3,R4,RR,CEN,CON,BH,CFT,CJN,R5,P,S,TT
      DO 410 M=1,5
      R(1+K,M)=R(1+K,M)*FRC(1,M)
      R(3+K,M)=R(3+K,M)*FRC(2,M)
      R(5+K,M)=R(5+K,M)*FRC(3,M)
      R(7+K,M)=R(7+K,M)*FRC(4,M)
  410 CONTINUE
      RETURN
      END

EGMENT, LENGTH   134, NAME  ASMB


      SUBROUTINE CENT(JJ,J)
      REAL LG,IY,IZ,JSV,IP
      DIMENSION XS(11),YS(11),ZS(11),LG(10),
     1RHO(10),BETA(11),DRMT(3,3),CON(6,5),R5(8,5),
     1A(10),IY(10),IZ(10),JSV(10),B1(10),B2(10),B3(10),CNT(6,5),
     1EY(11),EZ(11),PLFL(8,5),PLFO(8,5),TRA(6,6),EC(6,6),STR(4,6),
     1FXMT(8,8),BETB(11),EIGA(50,50),BH(50),FRC(4,5),RES(6,5),
     1DC(3,3),DM(3,3),EIGB(50,50),R(8,5),P(6,6),S(6,6),TT(6,6),
     1TEMP(8,5),FLA(6,5),IP(10),R3(8,5),R4(8,5),RR(8,5),
     1CEN(6,5),TAMP(8,5),W(14),CFT(6,5),CJN(6,5),
     1AK(2500),FSMOD(2500),INT(48),ITS(50),FSR(50),
     1BAB(6,5),BUN(440),FST(50),SVOD(2500),T(2850)
      COMMON/DATA/XS,YS,ZS,LG,RHO,BETA,DRMT,EY,EZ,
     1DC,DM,CNT,OMEGA,FXMT,A,IY,IZ,JSV,B1,B2,B3,E,G,
     1BETB,EIGA,EIGB,R,TEMP,TRA,EC,STR,FRC,RES,FLA,IP,
     1BAB,BUN,TAMP,R3,R4,RR,CEN,CON,BH,CFT,CJN,R5,P,S,TT
      CS=-RHO(J)*OMEGA*OMEGA*LG(J)/2
      CEN(1,1),CEN(2,2)=1.0*CS
      CEN(4,2)=(-2.0/3.0*ZS(J)-1.0/3.0*ZS(J+1)+ZS(JJ))*CS
      CEN(4,3)=(-2.0/3.0*YS(J)-1.0/3.0*YS(J+1))*CS
      CEN(5,1)=-CEN(4,2)
      CEN(5,3)=(2.0/3.0*XS(J)+1.0/3.0*XS(J+1))*CS
      CEN(6,1)=YS(JJ)*CS
      CEN(6,2)=-XS(JJ)*CS
      RETURN
      END

GMENT, LENGTH   146, NAME  CENT
```

```
      SUBROUTINE CENF(JJ,J)
      REAL LG,IY,IZ,JSV,IP
      DIMENSION XS(11),YS(11),ZS(11),LG(10),
     1RHO(10),BETA(11),DRMT(3,3),CON(6,5),R5(8,5),
     1A(10),IY(10),IZ(10),JSV(10),B1(10),B2(10),B3(10),CNT(6,5),
     1EY(11),EZ(11),PLFL(8,5),PLFO(8,5),TRA(6,6),EC(6,6),STR(4,6),
     1FXMT(8,8),BETB(11),EIGA(50,50),BH(50),FRC(4,5),RES(6,5),
     1DC(3,3),DM(3,3),EIGB(50,50),R(8,5),P(6,6),S(6,6),TT(6,6),
     1TEMP(8,5),FLA(6,5),IP(10),R3(8,5),R4(8,5),RR(8,5),
     1CEN(6,5),TAMP(8,5),W(14),CFT(6,5),CJN(6,5),
     1AK(2500),FSMOD(2500),INT(48),ITS(50),FSR(50),
     1BAB(6,5),BUN(44),FSI(50),SVOD(2500),T(2850)
      COMMON/DATA/XS,YS,ZS,LG,RHO,BETA,DRMT,EY,EZ,
     1DC,DM,CNT,OMEGA,FXMT,A,IY,IZ,JSV,B1,B2,B3,E,G,
     1BETB,EIGA,EIGB,R,TEMP,TRA,EC,STR,FRC,RES,FLA,IP,
     1BAB,BUN,TAMP,R3,R4,RR,CEN,CON,BH,CFT,CJN,R5,P,S,TT
      CS=-RHO(J)*OMEGA*OMEGA*LG(J)/2
      CEN(1,1),CEN(2,2)=1.0*CS
      CEN(4,2)=(-1.0/3.0*ZS(J)-2.0/3.0*ZS(J+1)+ZS(JJ))*CS
      CEN(4,3)=(-1.0/3.0*YS(J)-2.0/3.0*YS(J+1))*CS
      CEN(5,1)=-CEN(4,2)
      CEN(5,3)=(1.0/3.0*XS(J)+2.0/3.0*XS(J+1))*CS
      CEN(6,1)=YS(JJ)*CS
      CEN(6,2)=-XS(JJ)*CS
      RETURN
      END

SEGMENT, LENGTH    146, NAME  CENF
      SUBROUTINE CEJJ(J)
      REAL LG,IY,IZ,JSV,IP
      DIMENSION XS(11),YS(11),ZS(11),LG(10),
     1RHO(10),BETA(11),DRMT(3,3),CON(6,5),R5(8,5),
     1A(10),IY(10),IZ(10),JSV(10),B1(10),B2(10),B3(10),CNT(6,5),
     1EY(11),EZ(11),PLFL(8,5),PLFO(8,5),TRA(6,6),EC(6,6),STR(4,6),
     1FXMT(8,8),BETB(11),EIGA(50,50),BH(50),FRC(4,5),RES(6,5),
     1DC(3,3),DM(3,3),EIGB(50,50),R(8,5),P(6,6),S(6,6),TT(6,6),
     1TEMP(8,5),FLA(6,5),IP(10),R3(8,5),R4(8,5),RR(8,5),
     1CEN(6,5),TAMP(8,5),W(14),CFT(6,5),CJN(6,5),
     1AK(2500),FSMOD(2500),INT(48),ITS(50),FSR(50),
     1BAB(6,5),BUN(44),FSI(50),SVOD(2500),T(2850)
      COMMON/DATA/XS,YS,ZS,LG,RHO,BETA,DRMT,EY,EZ,
     1DC,DM,CNT,OMEGA,FXMT,A,IY,IZ,JSV,B1,B2,B3,E,G,
     1BETB,EIGA,EIGB,R,TEMP,TRA,EC,STR,FRC,RES,FLA,IP,
     1BAB,BUN,TAMP,R3,R4,RR,CEN,CON,BH,CFT,CJN,R5,P,S,TT
      CS=-RHO(J)*OMEGA*OMEGA*LG(J)/2
      CJN(4,3)=(YS(J)+YS(J+1))*CS
      CJN(5,3)=(-XS(J)-XS(J+1))*CS
      CJN(6,1)=-CJN(4,3)
      CJN(6,2)=-CJN(5,3)
      RETURN
      END

SEGMENT, LENGTH     77, NAME  CEJJ

      FINISH

COMPILATION -  NO ERRORS
```

PRINT OUT SHOWING 'GEO2' REQUEST

```
          GEO2
OP
GEO2 MARK 1A READY
TYPE MODE
←CARD
←JOB JNTO,AEP240,SUBRAMANIAN
←SECONDS 300
←LINES 3000
←CFORTRAN ,,,PD,50000
←RFORTRAN ,,290
←****
←DOC PROG
←%VTRI
←****
←DOC DATA
←%JNTO
←****
←FINISH
OK
17-32-01 ← LOGO
CONNECTED FOR      8 MINS
MILL TIME USED    12 SECS
SESSION COST     1.82
```

LOGIC OF PROGRAMME VTRI

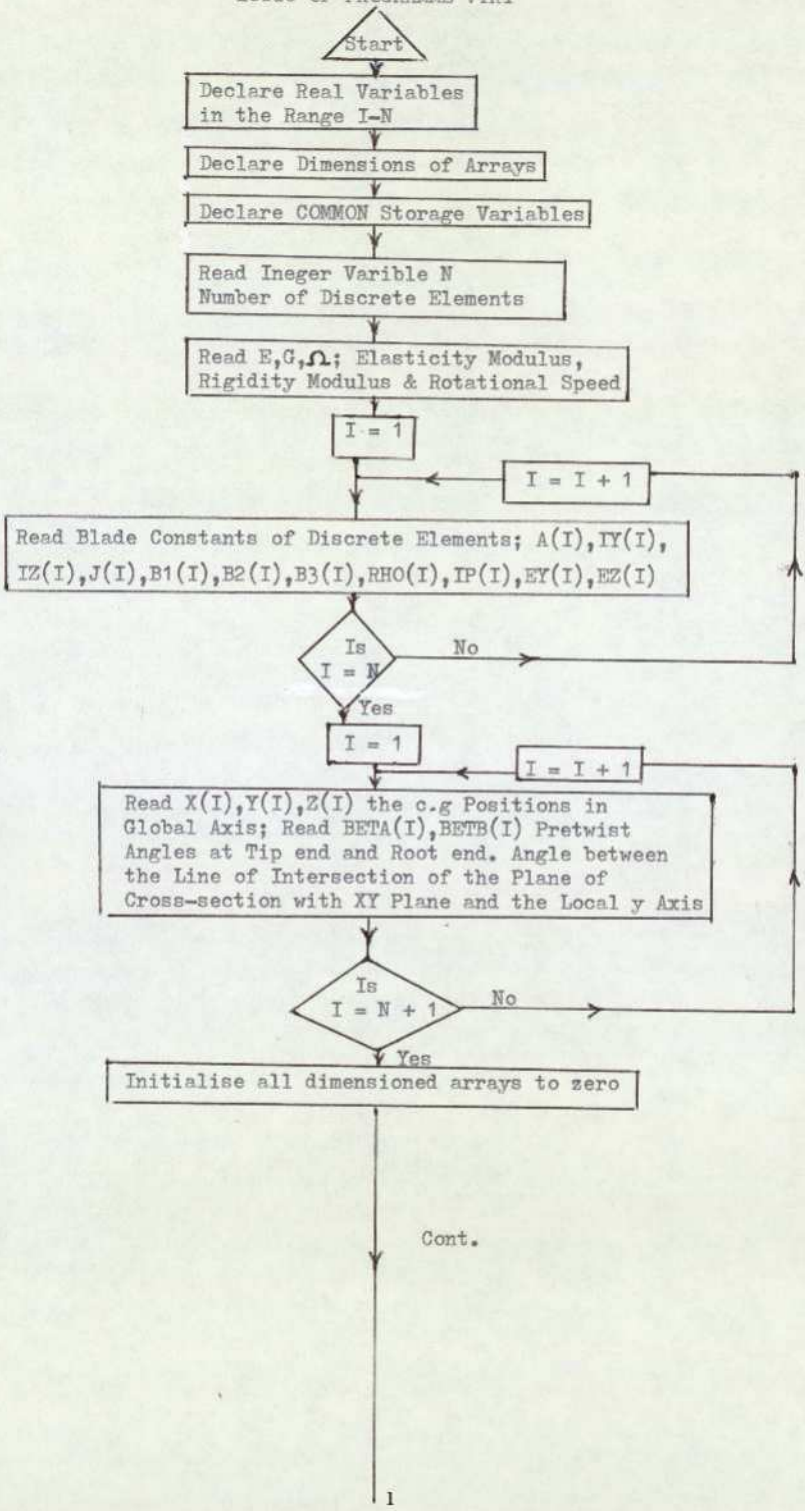

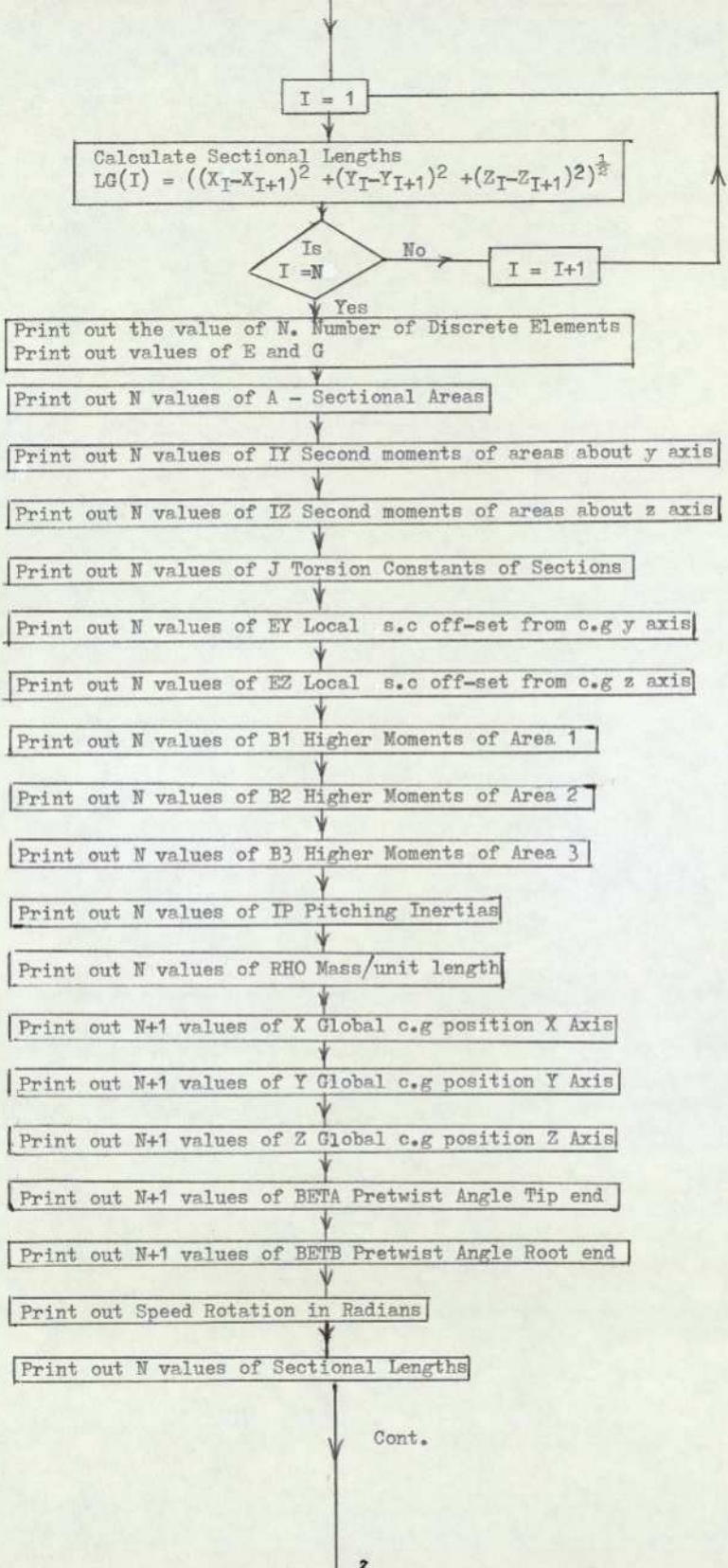
I = 1
Calculate Sectional Lengths
LG(I) = ((X_I-X_I+1)^2 +(Y_I-Y_I+1)^2 +(Z_I-Z_I+1)^2)^1/2
Is I =N
No
I = I+1
Yes
Print out the value of N. Number of Discrete Elements
Print out values of E and G
Print out N values of A - Sectional Areas
Print out N values of IY Second moments of areas about y axis
Print out N values of IZ Second moments of areas about z axis
Print out N values of J Torsion Constants of Sections
Print out N values of EY Local s.c off-set from c.g y axis
Print out N values of EZ Local s.c off-set from c.g z axis
Print out N values of B1 Higher Moments of Area 1
Print out N values of B2 Higher Moments of Area 2
Print out N values of B3 Higher Moments of Area 3
Print out N values of IP Pitching Inertias
Print out N values of RHO Mass/unit length
Print out N+1 values of X Global c.g position X Axis
Print out N+1 values of Y Global c.g position Y Axis
Print out N+1 values of Z Global c.g position Z Axis
Print out N+1 values of BETA Pretwist Angle Tip end
Print out N+1 values of BETB Pretwist Angle Root end
Print out Speed Rotation in Radians
Print out N values of Sectional Lengths
Cont.

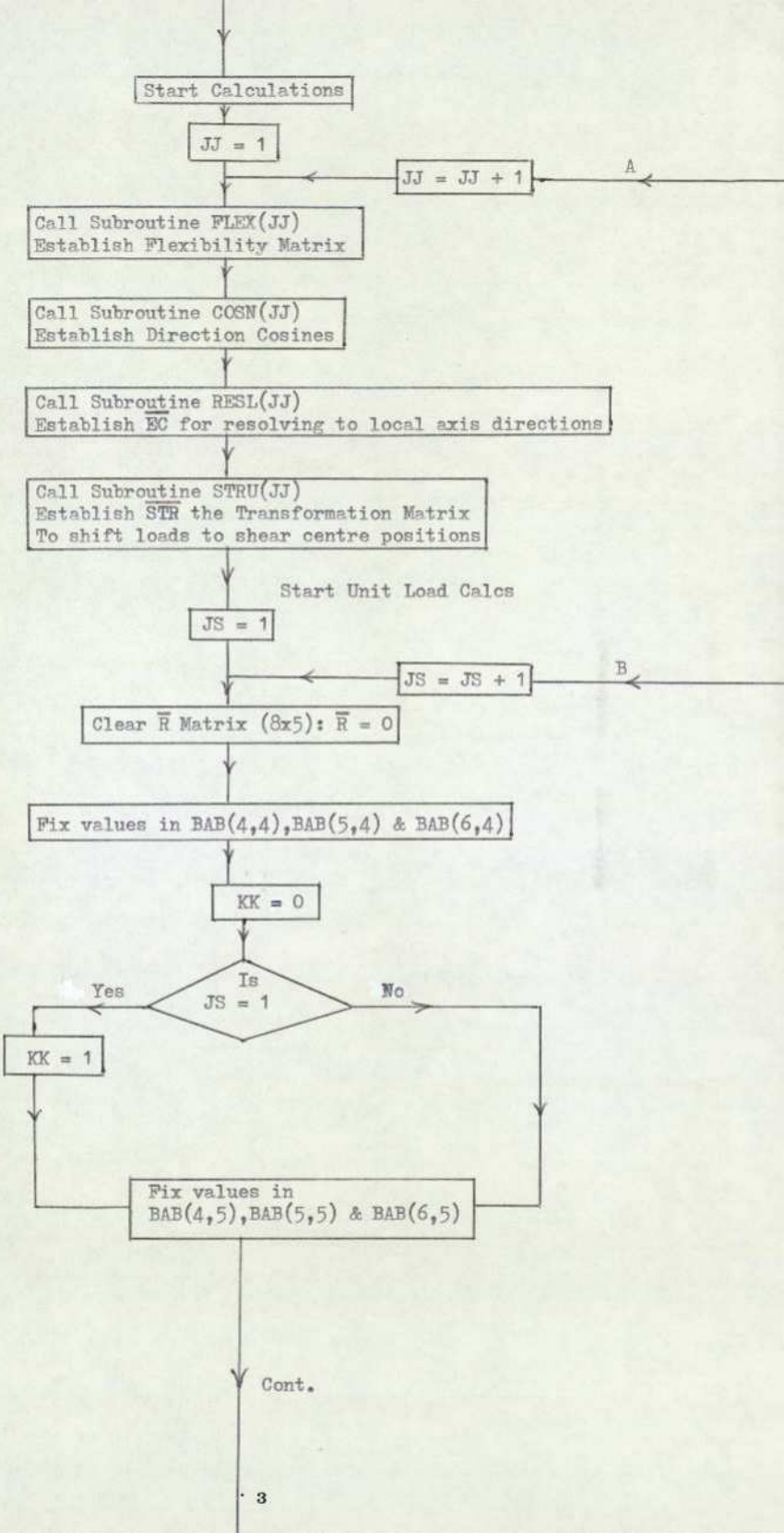
Start Calculations
JJ = 1
JJ = JJ + 1
A
Call Subroutine FLEX(JJ)
Establish Flexibility Matrix
Call Subroutine COSN(JJ)
Establish Direction Cosines
Call Subroutine RESL(JJ)
Establish EC for resolving to local axis directions
Call Subroutine STRU(JJ)
Establish STR the Transformation Matrix
To shift loads to shear centre positions
Start Unit Load Calcs
JS = 1
JS = JS + 1
B
Clear R Matrix (8x5): R = 0
Fix values in BAB(4,4),BAB(5,4) & BAB(6,4)
KK = 0
Is
JS = 1
Yes
No
KK = 1
Fix values in
BAB(4,5),BAB(5,5) & BAB(6,5)
Cont.

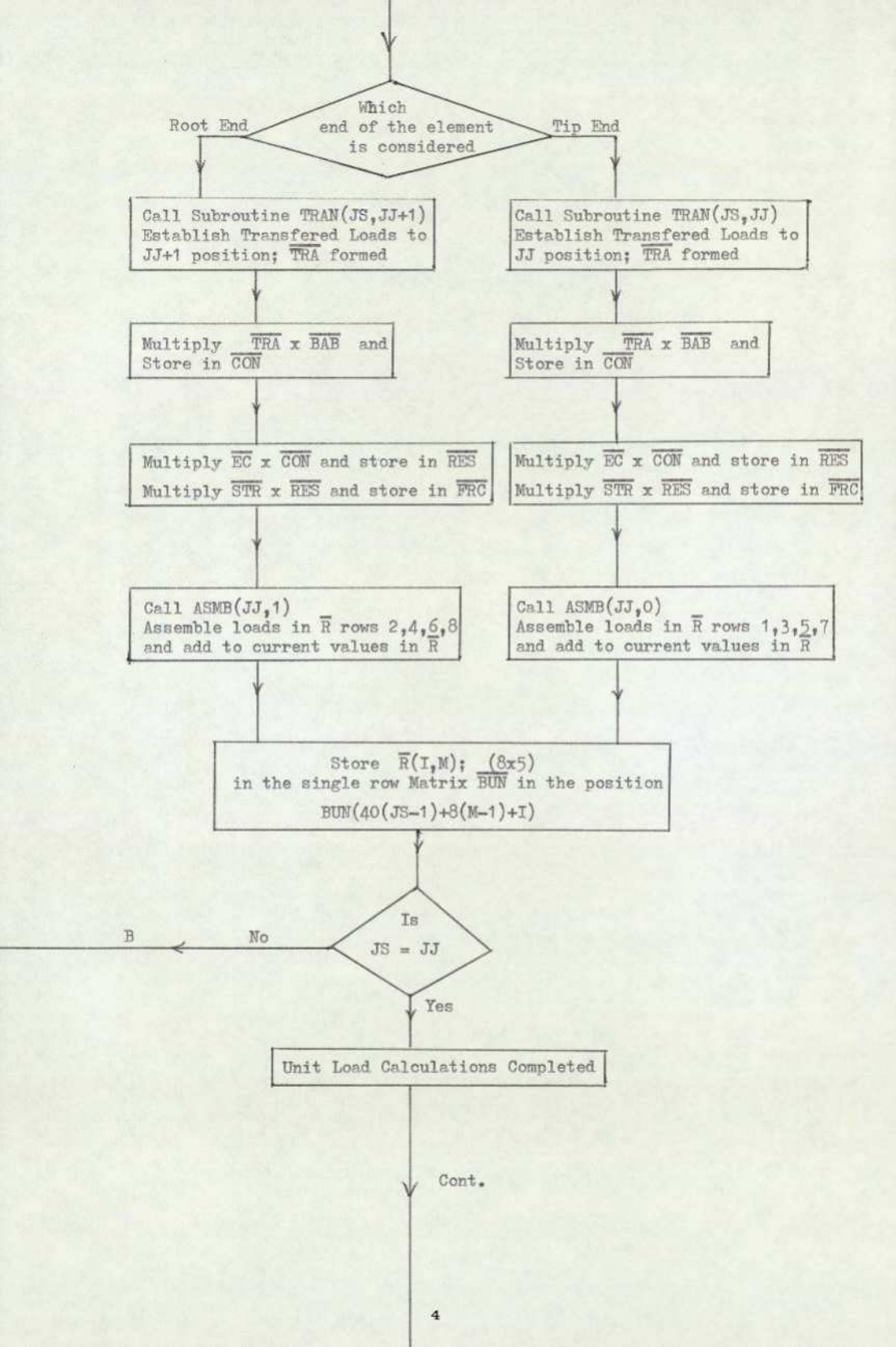
Which end of the element is considered
Root End
Tip End
Call Subroutine TRAN(JS,JJ+1) Establish Transfered Loads to JJ+1 position; TRA formed
Call Subroutine TRAN(JS,JJ) Establish Transfered Loads to JJ position; TRA formed
Multiply TRA x BAB and Store in CON
Multiply TRA x BAB and Store in CON
Multiply EC x CON and store in RES
Multiply STR x RES and store in FRC
Multiply EC x CON and store in RES
Multiply STR x RES and store in FRC
Call ASMB(JJ,1) Assemble loads in R rows 2,4,6,8 and add to current values in R
Call ASMB(JJ,0) Assemble loads in R rows 1,3,5,7 and add to current values in R
Store R(I,M); (8x5) in the single row Matrix BUN in the position BUN(40(JS-1)+8(M-1)+I)
Is JS = JJ
No
B
Yes
Unit Load Calculations Completed
Cont.

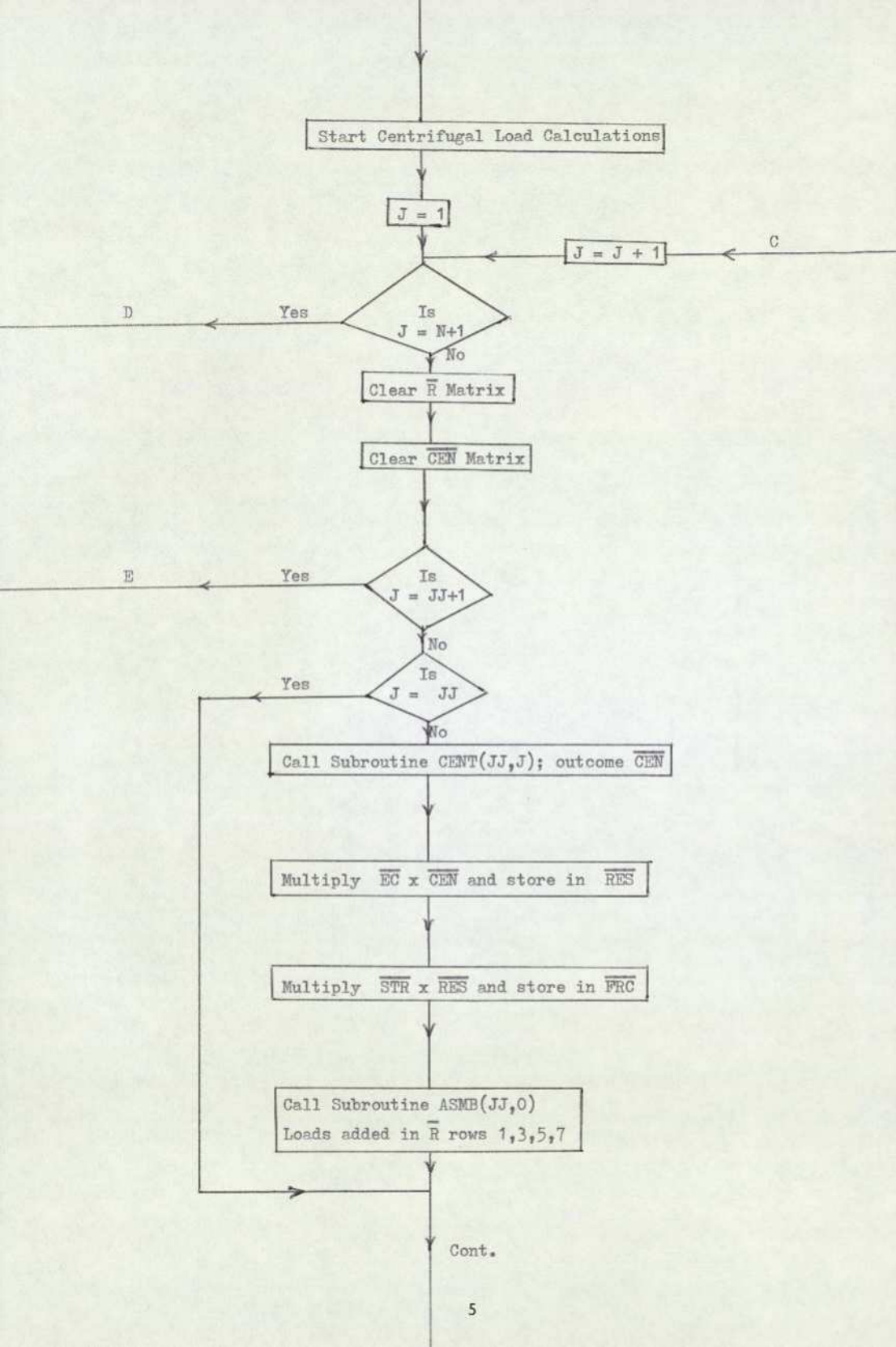
Start Centrifugal Load Calculations
J = 1
J = J + 1
C
Is J = N+1
Yes
D
No
Clear R̄ Matrix
Clear CEN̄ Matrix
Is J = JJ+1
Yes
E
No
Is J = JJ
Yes
No
Call Subroutine CENT(JJ,J); outcome CEN̄
Multiply EC̄ x CEN̄ and store in RES̄
Multiply STR̄ x RES̄ and store in FRC̄
Call Subroutine ASMB(JJ,0)
Loads added in R̄ rows 1,3,5,7
Cont.

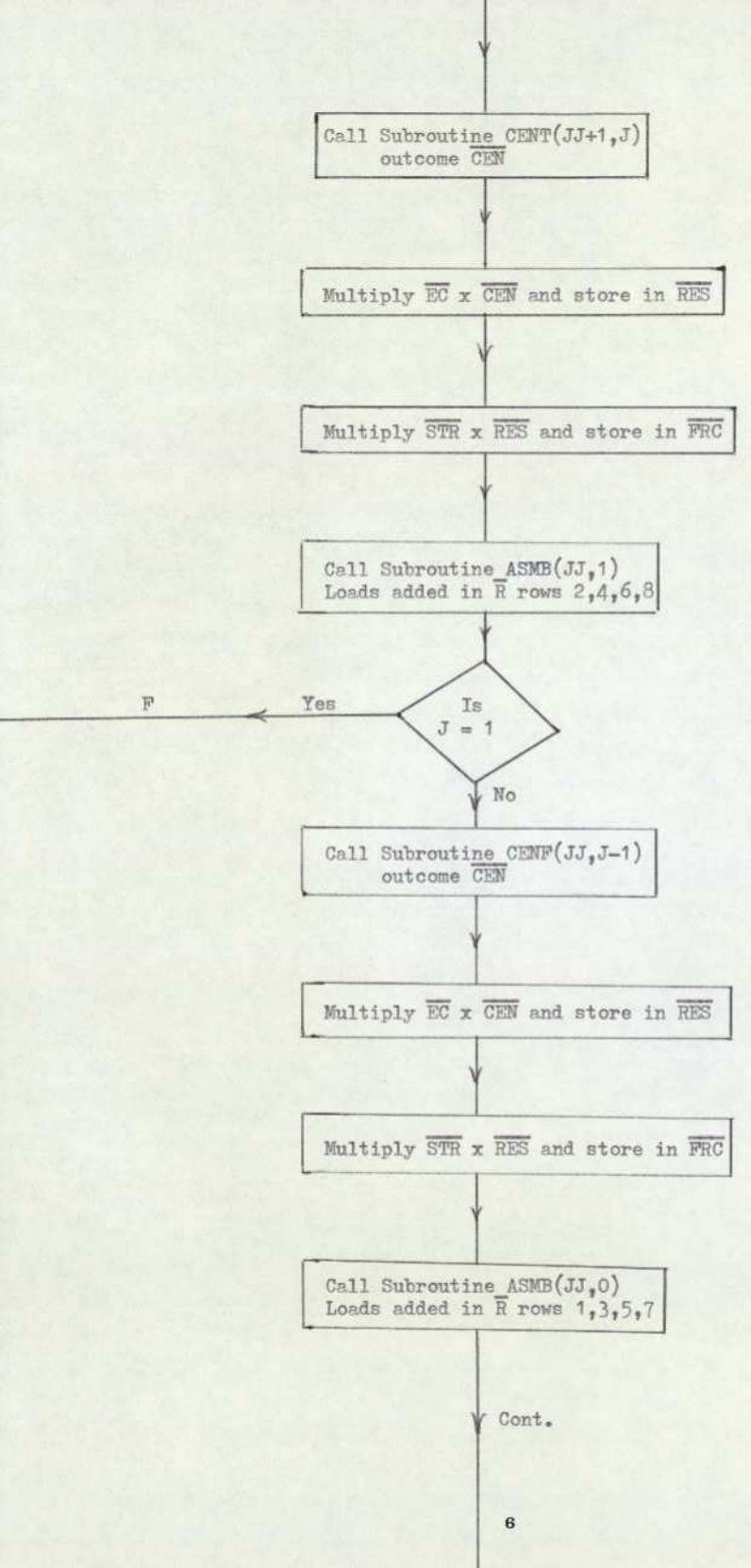
Call Subroutine CENT(JJ+1,J)
outcome $\overline{CEN}$
Multiply $\overline{EC}$ x $\overline{CEN}$ and store in $\overline{RES}$
Multiply $\overline{STR}$ x $\overline{RES}$ and store in $\overline{FRC}$
Call Subroutine ASMB(JJ,1)
Loads added in $\overline{R}$ rows 2,4,6,8
Is
J = 1
Yes
F
No
Call Subroutine CENF(JJ,J-1)
outcome $\overline{CEN}$
Multiply $\overline{EC}$ x $\overline{CEN}$ and store in $\overline{RES}$
Multiply $\overline{STR}$ x $\overline{RES}$ and store in $\overline{FRC}$
Call Subroutine ASMB(JJ,0)
Loads added in $\overline{R}$ rows 1,3,5,7
Cont.

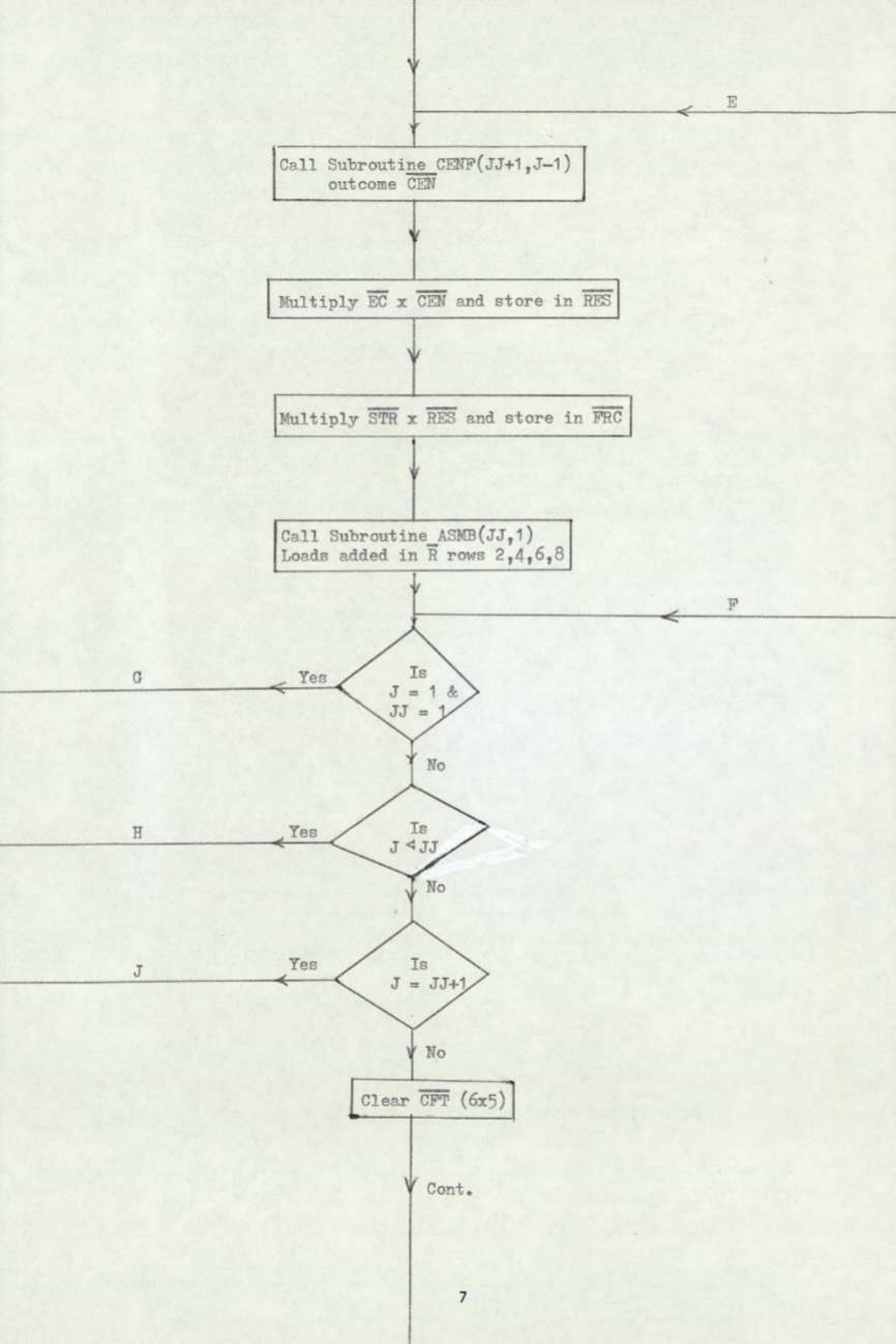
E
Call Subroutine CENF(JJ+1,J-1)
outcome CEN
Multiply EC x CEN and store in RES
Multiply STR x RES and store in FRC
Call Subroutine ASMB(JJ,1)
Loads added in R rows 2,4,6,8
F
Is
J = 1 &
JJ = 1
Yes
G
No
Is
J < JJ
Yes
H
No
Is
J = JJ+1
Yes
J
No
Clear CFT (6x5)
Cont.

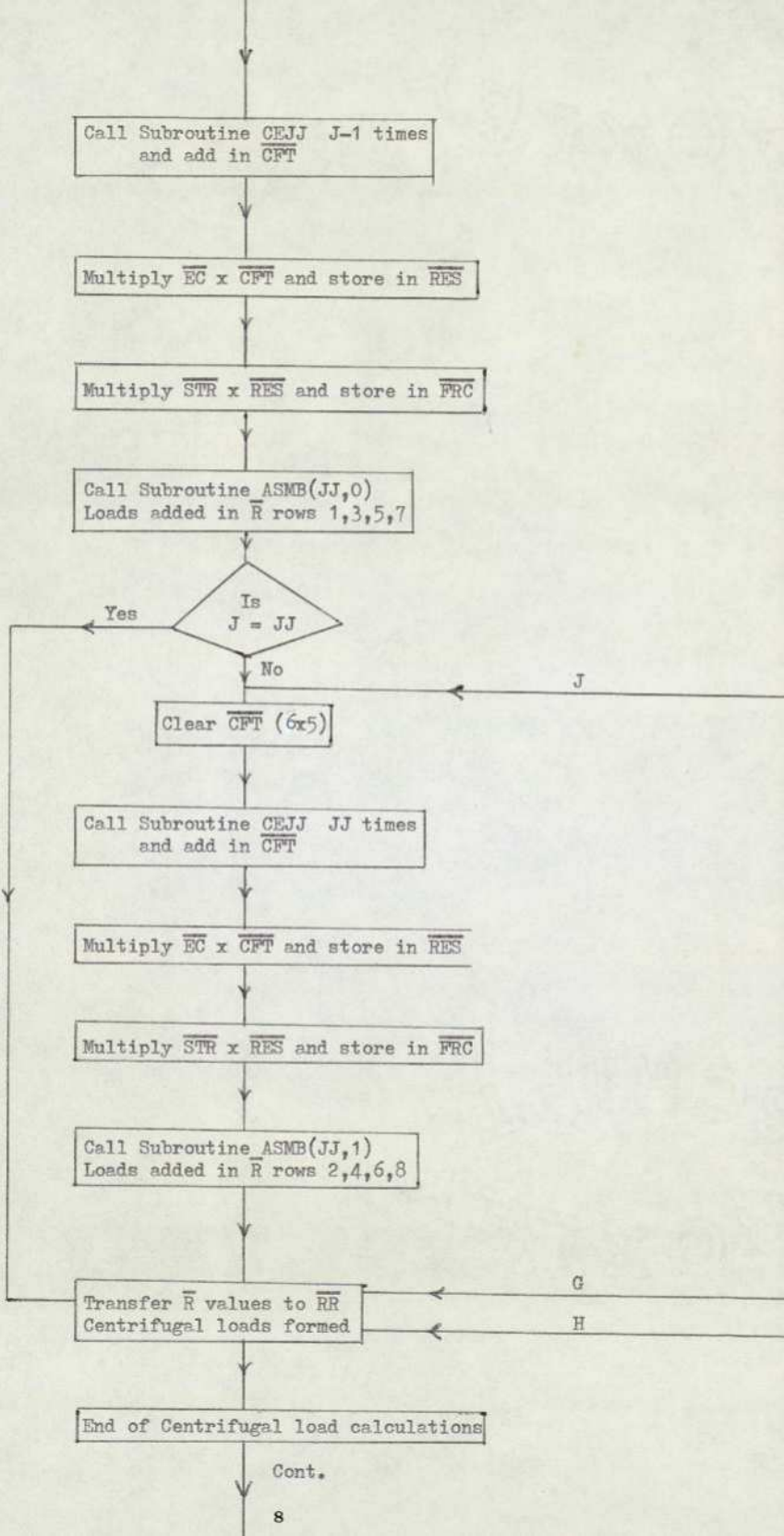
Call Subroutine CEJJ J-1 times and add in CFT
Multiply EC x CFT and store in RES
Multiply STR x RES and store in FRC
Call Subroutine ASMB(JJ,0) Loads added in R rows 1,3,5,7
Is J = JJ
Yes
No
J
Clear CFT (6x5)
Call Subroutine CEJJ JJ times and add in CFT
Multiply EC x CFT and store in RES
Multiply STR x RES and store in FRC
Call Subroutine ASMB(JJ,1) Loads added in R rows 2,4,6,8
G
H
Transfer R values to RR Centrifugal loads formed
End of Centrifugal load calculations
Cont.

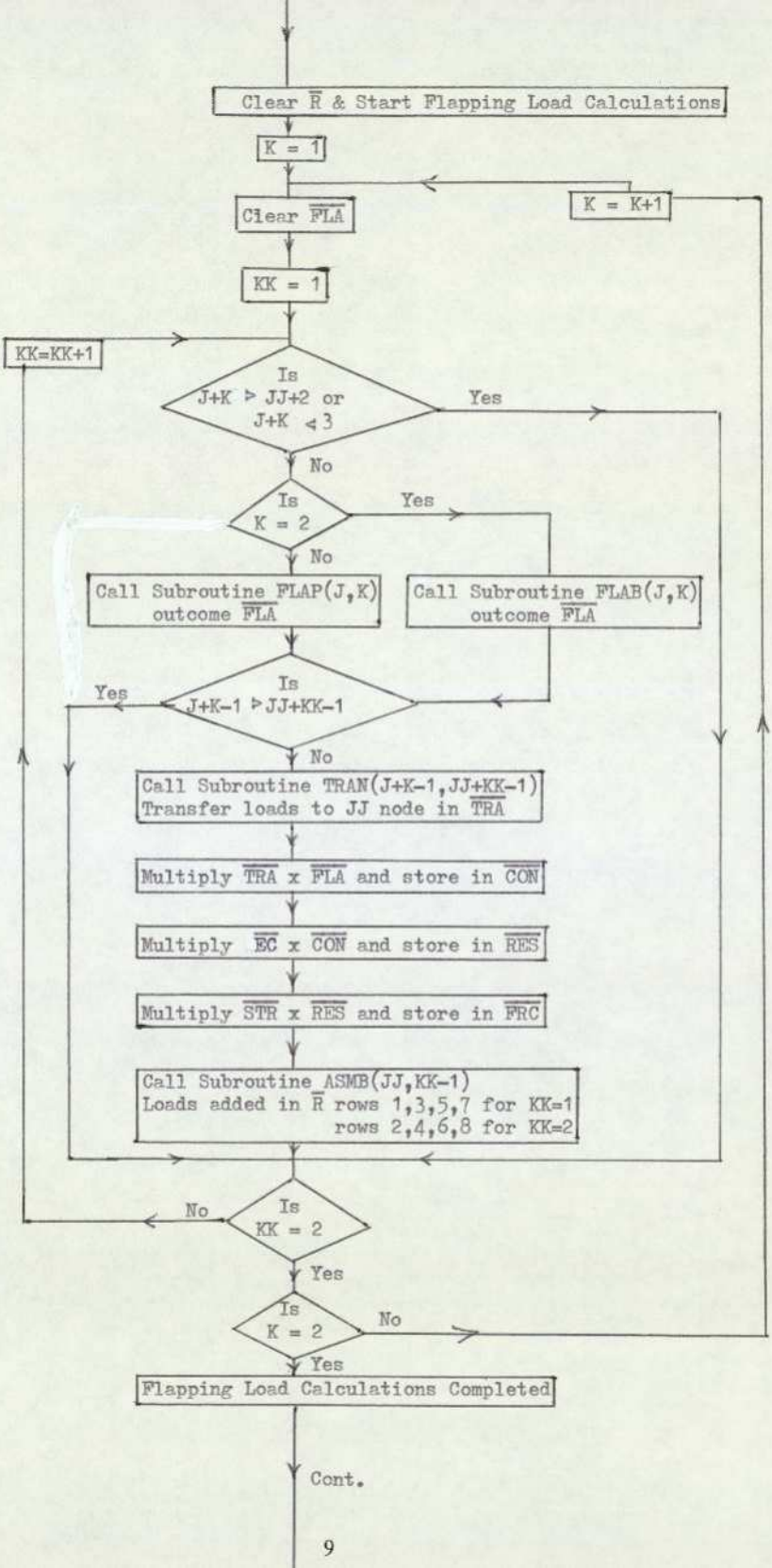
Clear R & Start Flapping Load Calculations
K = 1
K = K+1
Clear FLA
KK = 1
KK=KK+1
Is J+K ▷ JJ+2 or J+K ◁ 3
Yes
No
Is K = 2
Yes
No
Call Subroutine FLAP(J,K) outcome FLA
Call Subroutine FLAB(J,K) outcome FLA
Is J+K-1 ▷ JJ+KK-1
Yes
No
Call Subroutine TRAN(J+K-1,JJ+KK-1) Transfer loads to JJ node in TRA
Multiply TRA x FLA and store in CON
Multiply EC x CON and store in RES
Multiply STR x RES and store in FRC
Call Subroutine ASMB(JJ,KK-1) Loads added in R rows 1,3,5,7 for KK=1 rows 2,4,6,8 for KK=2
Is KK = 2
No
Yes
Is K = 2
No
Yes
Flapping Load Calculations Completed
Cont.

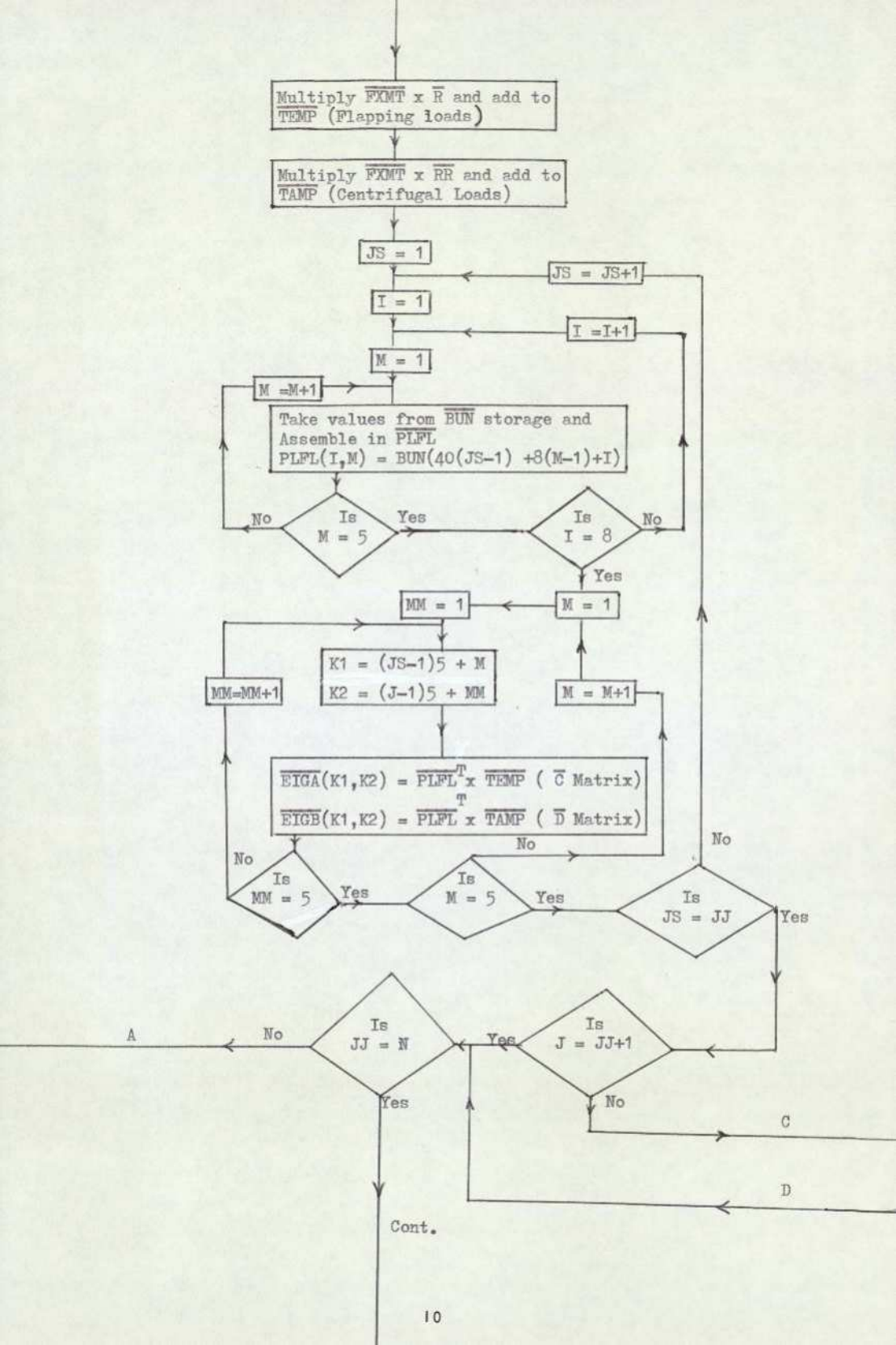
Multiply FXMT x R and add to TEMP (Flapping loads)
Multiply FXMT x RR and add to TAMP (Centrifugal Loads)
JS = 1
JS = JS+1
I = 1
I =I+1
M = 1
M =M+1
Take values from BUN storage and Assemble in PLFL
PLFL(I,M) = BUN(40(JS-1) +8(M-1)+I)
Is M = 5
No
Yes
Is I = 8
No
Yes
MM = 1
M = 1
K1 = (JS-1)5 + M
K2 = (J-1)5 + MM
MM=MM+1
M = M+1
EIGA(K1,K2) = PLFL^T x TEMP (C Matrix)
EIGB(K1,K2) = PLFL^T x TAMP (D Matrix)
Is MM = 5
Is M = 5
Is JS = JJ
Is JJ = N
Is J = JJ+1
A
C
D
Cont.

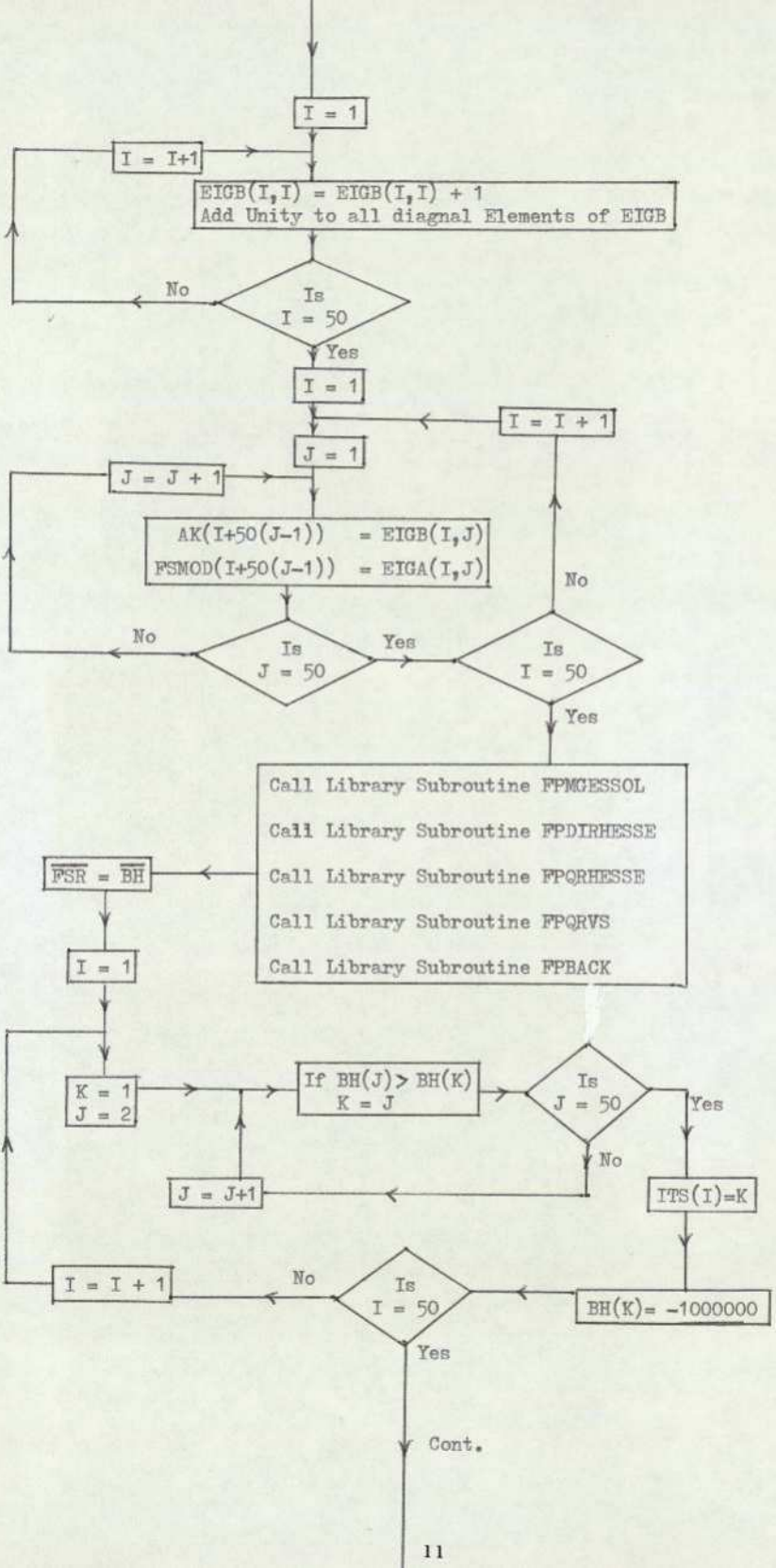
I = 1
I = I+1
EIGB(I,I) = EIGB(I,I) + 1
Add Unity to all diagnal Elements of EIGB
No
Is
I = 50
Yes
I = 1
I = I + 1
J = 1
J = J + 1
AK(I+50(J-1)) = EIGB(I,J)
FSMOD(I+50(J-1)) = EIGA(I,J)
No
Is
J = 50
Yes
Is
I = 50
No
Yes
Call Library Subroutine FPMGESSOL
Call Library Subroutine FPDIRHESSE
Call Library Subroutine FPQRHESSE
Call Library Subroutine FPQRVS
Call Library Subroutine FPBACK
FSR = BH
I = 1
K = 1
J = 2
If BH(J)> BH(K)
K = J
Is
J = 50
Yes
No
J = J+1
ITS(I)=K
I = I + 1
No
Is
I = 50
BH(K)= -1000000
Yes
Cont.

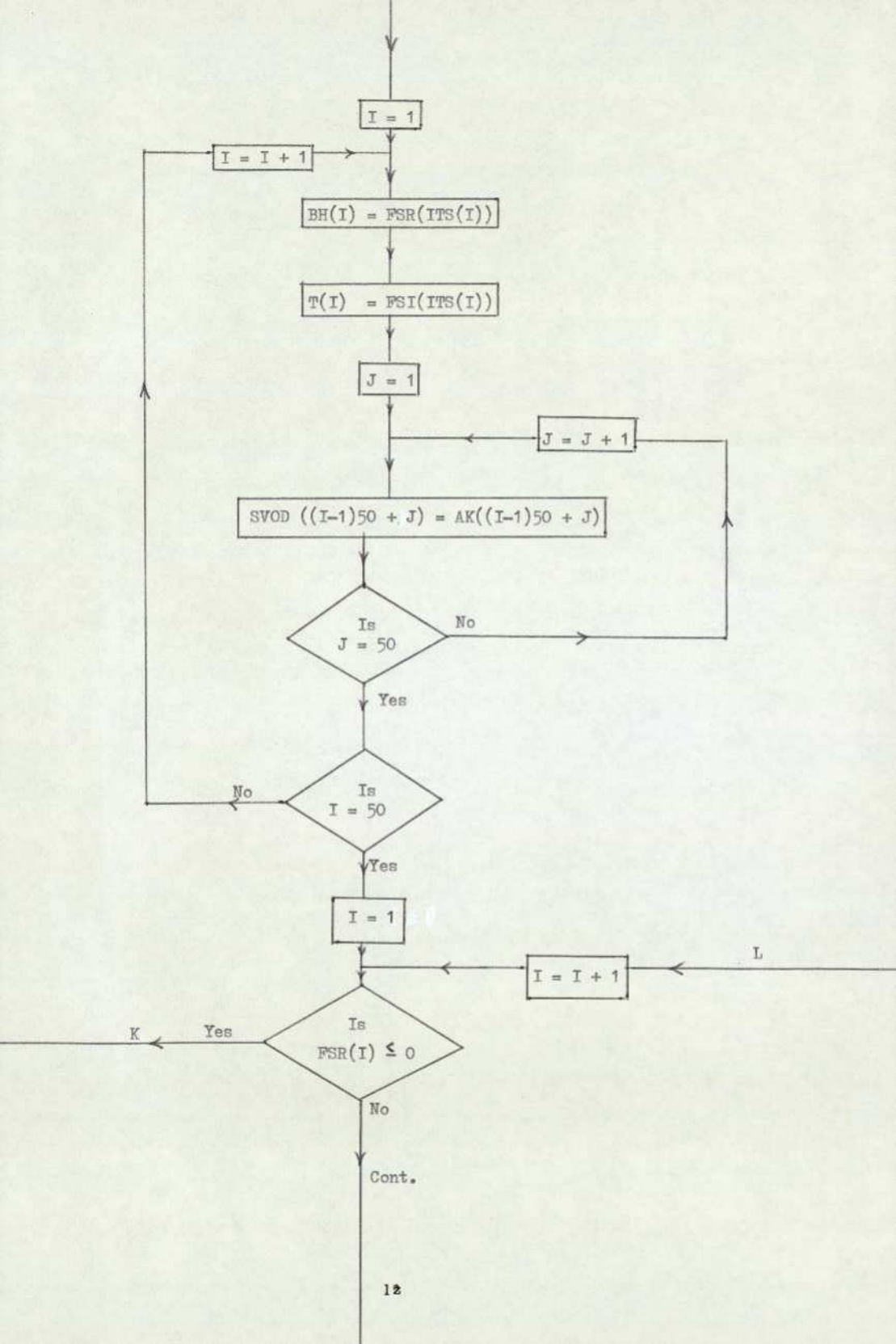
I = 1
I = I + 1
BH(I) = FSR(ITS(I))
T(I) = FSI(ITS(I))
J = 1
J = J + 1
SVOD ((I-1)50 + J) = AK((I-1)50 + J)
Is J = 50
No
Yes
Is I = 50
No
Yes
I = 1
L
I = I + 1
Is FSR(I) ≤ 0
K
Yes
No
Cont.

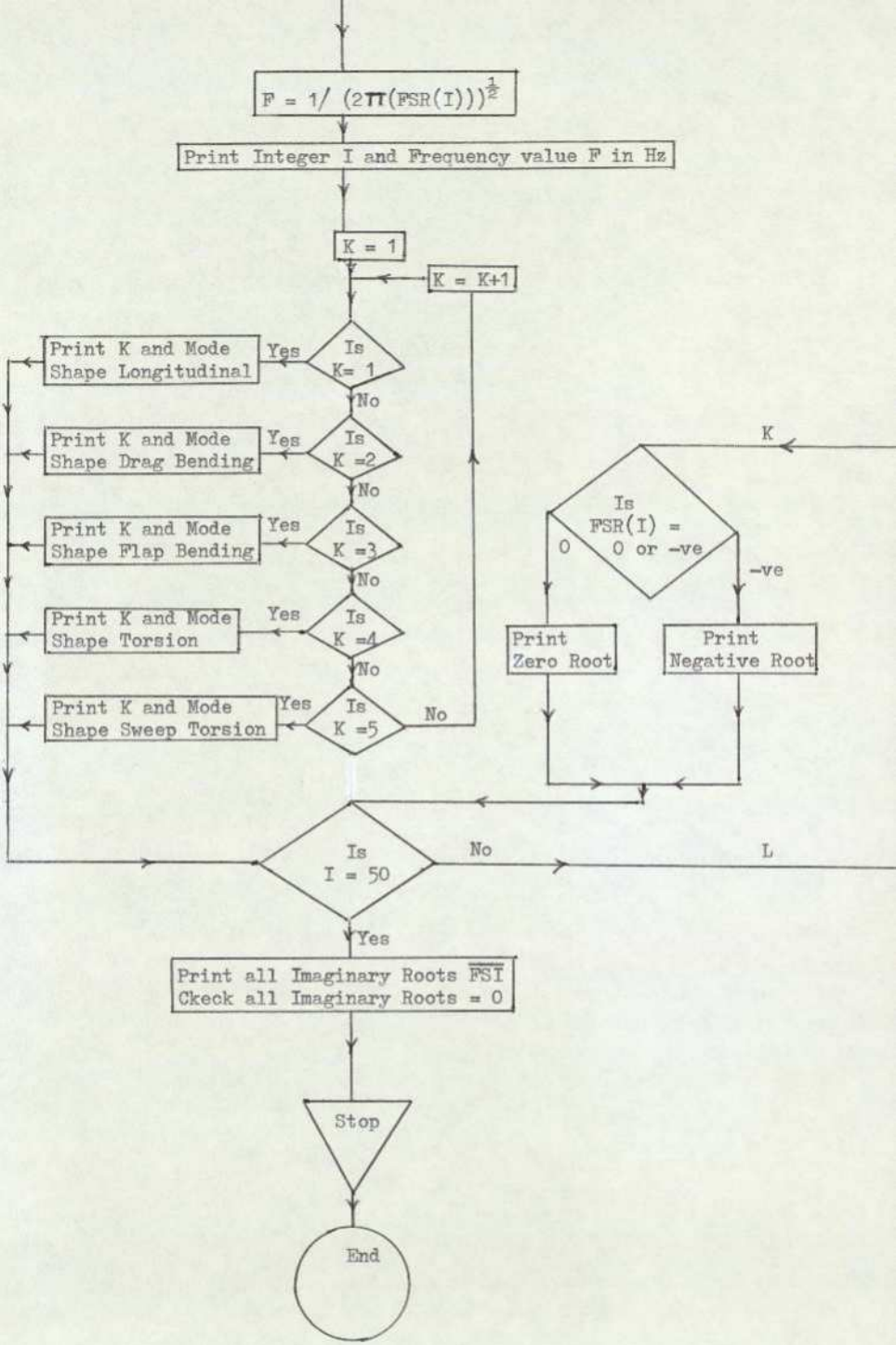
F = 1/ (2π(FSR(I)))^½
Print Integer I and Frequency value F in Hz
K = 1
K = K+1
Is K= 1
Yes
Print K and Mode Shape Longitudinal
No
Is K =2
Yes
Print K and Mode Shape Drag Bending
No
Is K =3
Yes
Print K and Mode Shape Flap Bending
No
Is K =4
Yes
Print K and Mode Shape Torsion
No
Is K =5
Yes
Print K and Mode Shape Sweep Torsion
No
K
Is FSR(I) = 0 or -ve
0
-ve
Print Zero Root
Print Negative Root
Is I = 50
No
L
Yes
Print all Imaginary Roots FSI
Ckeck all Imaginary Roots = 0
Stop
End

```
FORTRAN COMPILATION BY #XFAT UK 6A    DATE 03/08/77  TIME 13.22.57

0001                  WORK(ED)
0002                  SEND TO(GEO,SEMICOMP)
0003                  SEMICOMPILED(SUBGROUP(ANY,SUBRO XFIOLP)
0004                  NOLIST(LP)

DOCUMENT CARD         NORMICARD        : LP00 ON 03/08/77 AT 13.25

NUMBER OF MEMBERS
10

ELASTICITY MOD    RIGIDITY MOD    POISONS RATIO
 0.3.0000E 08     0.120000E 08    0.250000E 00

AREAS OF MEMBERS
 1  0.9140E-01   2  0.9140E-01   3  0.9140E-01   4  0.9140E-01
 5  0.9140E-01   6  0.9140E-01   7  0.9140E-01   8  0.9140E-01
 9  0.9140E-01  10  0.9140E-01

II MOMENT OF AREA Y AXIS
 1  0.1000E-03   2  0.1000E-03   3  0.1000E-03   4  0.1000E-03
 5  0.1000E-03   6  0.1000E-03   7  0.1000E-03   8  0.1000E-03
 9  0.1000E-03  10  0.1000E-03

II MOMENT OF AREA Z AXIS
 1  0.6710E-02   2  0.6710E-02   3  0.6710E-02   4  0.6710E-02
 5  0.6710E-02   6  0.6710E-02   7  0.6710E-02   8  0.6710E-02
 9  0.6710E-02  10  0.6710E-02
```

ST VENANTS SECTION CONSTANTS

1 0.2708E-03 2 0.2708E-03 3 0.2708E-03 4 0.2708E-03
5 0.2708E-03 6 0.2708E-03 7 0.2708E-03 8 0.2708E-03
9 0.2708E-03 10 0.2708E-03

Y AXIS CO-ORDINATE OF CS URT CG

1 0.0000E 00 2 0.0000E 00 3 0.0000E 00 4 0.0000E 00
5 0.0000E 00 6 0.0000E 00 7 0.0000E 00 8 0.0000E 00
9 0.0000E 00 10 0.0000E 00

PITCHING INERTIAS

1 0.5005E-05 2 0.5005E-05 3 0.5005E-05 4 0.5005E-05
5 0.5005E-05 6 0.5005E-05 7 0.5005E-05 8 0.5005E-05
9 0.5005E-05 10 0.5005E-05

Z AXIS CO-ORDINATE OF CS URT CG

1 0.0000E 00 2 0.0000E 00 3 0.0000E 00 4 0.0000E 00
5 0.0000E 00 6 0.0000E 00 7 0.0000E 00 8 0.0000E 00
9 0.0000E 00 10 0.0000E 00

HIGHER MOMENTS OF AREA 1

1 0.0000E 00 2 0.0000E 00 3 0.0000E 00 4 0.0000E 00
5 0.0000E 00 6 0.0000E 00 7 0.0000E 00 8 0.0000E 00
9 0.0000E 00 10 0.0000E 00

HIGHER MOMENTS OF AREA 2

1 0.0000E 00 2 0.0000E 00 3 0.0000E 00 4 0.0000E 00
5 0.0000E 00 6 0.0000E 00 7 0.0000E 00 8 0.0000E 00
9 0.0000E 00 10 0.0000E 00

HIGHER MOMENTS OF AREA 3

1 0.0000E 00 2 0.0000E 00 3 0.0000E 00 4 0.0000E 00
5 0.0000E 00 6 0.0000E 00 7 0.0000E 00 8 0.0000E 00
9 0.0000E 00 10 0.0000E 00

MASS DENSITIES OF SECTIONS

1 0.6718E-04 2 0.6718E-04 3 0.6718E-04 4 0.6718E-04
5 0.6718E-04 6 0.6718E-04 7 0.6718E-04 8 0.6718E-04
9 0.6718E-04 10 0.6718E-04

X CO ORDINATE OF CGS OVERALL

1 0.6000E 01 2 0.5400E 01 3 0.4800E 01 4 0.4200E 01
5 0.3600E 01 6 0.3000E 01 7 0.2400E 01 8 0.1800E 01
9 0.1200E 01 10 0.6000E 00 11 0.0000E 00

Y CO ORDINATE OF CGS OVERALL

1 0.0000E 00 2 0.0000E 00 3 0.0000E 00 4 0.0000E 00
5 0.0000E 00 6 0.0000E 00 7 0.0000E 00 8 0.0000E 00
9 0.0000E 00 10 0.0000E 00 11 0.0000E 00

Z CO ORDINATE OF CGS OVERALL

1 0.0000E 00 2 0.0000E 00 3 0.0000E 00 4 0.0000E 00
5 0.0000E 00 6 0.0000E 00 7 0.0000E 00 8 0.0000E 00
9 0.0000E 00 10 0.0000E 00 11 0.0000E 00

BETA PRETWIST ANGLES

1 0.0000E 00 2 0.0000E 00 3 0.0000E 00 4 0.0000E 00
5 0.0000E 00 6 0.0000E 00 7 0.0000E 00 8 0.0000E 00
9 0.0000E 00 10 0.0000E 00 11 0.0000E 00

BETA PRETWIST ANGLES

1 0.0000E 00 2 0.0000E 00 3 0.0000E 00 4 0.0000E 00
5 0.0000E 00 6 0.0000E 00 7 0.0000E 00 8 0.0000E 00
9 0.0000E 00 10 0.0000E 00 11 0.0000E 00

ANGULAR VELOCITY IN RADIANS

0.000000E 00

SECTIONAL LENGTHS

1 0.6000E 00 2 0.6000E 00 3 0.6000E 00 4 0.6000E 00
5 0.6000E 00 6 0.6000E 00 7 0.6000E 00 8 0.6000E 00
9 0.6000E 00 10 0.6000E 00

POSITION CHECK1

POSITION CHECK2

NUMBER OF RANKING

0

RESULT 1

FREQUENCY 105.51470 CYCLES/SEC

1MODE SHAPE LONGITUDINAL

0.00000000 0.00000000 0.00000000 0.00000000 0.00000000 0.00000000 0.00000000 0.00000000 0.00000000 0.00000000

2MODE SHAPE DRAG BENDING

0.00000000 0.00000000 0.00000000 0.00000000 0.00000000 0.00000000 0.00000000 0.00000000 0.00000000 0.00000000

3MODE SHAPE FLAP BENDING

1.00000000 0.86220676 0.72517981 0.59454437 0.46882189 0.33926483 0.22969791 0.13636959 0.06381855 0.01676040

4MODE SHAPE TORSION

0.00000000 0.00000000 0.00000000 0.00000000 0.00000000 0.00000000 0.00000000 0.00000000 0.00000000 0.00000000

5MODE SHAPE SWEEP TORSION

0.00000000 0.00000000 0.00000000 0.00000000 0.00000000 0.00000000 0.00000000 0.00000000 0.00000000 0.00000000

RESULT 2

FREQUENCY 668.216054 CYCLES/SEC

1MODE SHAPE LONGITUDINAL

-0.00000000 -0.00000000 -0.00000000 -0.00000000 -0.00000000 -0.00000000 -0.00000000 -0.00000000 -0.00000000 -0.00000000

2MODE SHAPE DRAG BENDING

-0.00000000 -0.00000000 -0.00000000 -0.00000000 -0.00000000 -0.00000000 -0.00000000 -0.00000000 -0.00000000 -0.00000000

3MODE SHAPE FLAP BENDING

1.00000000 0.51896726 0.06308883 -0.32456194 -0.59664759 -0.72004127 -0.68879545 -0.53017374 -0.30355004 -0.09351139

4MODE SHAPE TORSION

-0.00000000 -0.00000000 -0.00000000 -0.00000000 -0.00000000 -0.00000000 -0.00000000 -0.00000000 -0.00000000 -0.00000000

5MODE SHAPE SWEEP TORSION

-0.00000000 -0.00000000 -0.00000000 -0.00000000 -0.00000000 -0.00000000 -0.00000000 -0.00000000 -0.00000000 -0.00000000

RESULT 3

FREQUENCY 844.319392 CYCLES/SEC

1MODE SHAPE LONGITUDINAL

0.00000000 0.00000000 0.00000000 0.00000000 0.00000000 0.00000000 0.00000000 0.00000000 0.00000000 0.00000000

2MODE SHAPE DRAG BENDING

1.00000000 0.86220676 0.72517981 0.59454437 0.46882189 0.33926483 0.22969791 0.13636959 0.06381855 0.01676040

3MODE SHAPE FLAP BENDING

-0.00000000 -0.00000000 -0.00000000 0.00000000 0.00000000 0.00000000 0.00000000 0.00000000 0.00000000 0.00000000

4MODE SHAPE TORSION

0.00000000 0.00000000 0.00000000 0.00000000 0.00000000 0.00000000 0.00000000 0.00000000 0.00000000 0.00000000

5MODE SHAPE SWEEP TORSION

0.00000000 0.00000000 0.00000000 0.00000000 0.00000000 0.00000000 0.00000000 0.00000000 0.00000000 0.00000000

RESULT 4

FREQUENCY 1063.88785 CYCLES/SEC

1MODE SHAPE LONGITUDINAL

0.00000000 0.00000000 0.00000000 0.00000000 0.00000000 0.00000000 0.00000000 0.00000000 0.00000000 0.00000000

2MODE SHAPE DRAG BENDING

0.00000000 0.00000000 0.00000000 0.00000000 0.00000000 0.00000000 0.00000000 0.00000000 0.00000000 0.00000000

3MODE SHAPE FLAP BENDING

-0.00000000 -0.00000000 -0.00000000 -0.00000000 -0.00000000 0.00000000 0.00000000 0.00000000 0.00000000 0.00000000

4MODE SHAPE TORSION

1.00000000 0.98768834 0.95105652 0.89100652 0.80901699 0.70710678 0.58778525 0.45399050 0.30901699 0.15643447

5MODE SHAPE SWEEP TORSION

1.00000000 0.98768834 0.95105652 0.89100652 0.80901699 0.70710678 0.58778525 0.45399050 0.30901699 0.15643447

RESULT 5

FREQUENCY 1922.102307 CYCLES/SEC

1MODE SHAPE LONGITUDINAL

0.00000000 0.00000000 0.00000000 0.00000000 0.00000000 0.00000000 0.00000000 0.00000000 0.00000000 0.00000000 0.00000000

2MODE SHAPE DRAG BENDING

-0.00000000 -0.00000000 0.00000000 0.00000000 0.00000000 0.00000000 0.00000000 0.00000000 0.00000000 0.00000000 0.00000000

3MODE SHAPE FLAP BENDING

1.00000000 0.20447407 -0.42475203 -0.68261303 -0.48885937 0.01632081 0.53319406 0.77040445 0.61889846 0.23515086

4MODE SHAPE TORSION

-0.00000000 -0.00000000 -0.00000000 -0.00000000 0.00000000 0.00000000 0.00000000 0.00000000 0.00000000 0.00000000 0.00000000

5MODE SHAPE SWEEP TORSION

-0.00000000 -0.00000000 -0.00000000 0.00000000 0.00000000 0.00000000 0.00000000 0.00000000 0.00000000 0.00000000 0.00000000

RESULT 6

FREQUENCY 3245.378916 CYCLES/SEC

1MODE SHAPE LONGITUDINAL

-0.00000000 -0.00000000 -0.00000000 -0.00000000 -0.00000000 -0.00000000 -0.00000000 -0.00000000 -0.00000000 -0.00000000 -0.00000000

2MODE SHAPE DRAG BENDING

0.00000000 0.00000000 0.00000000 -0.00000000 -0.00000000 -0.00000000 -0.00000000 -0.00000000 -0.00000000 -0.00000000

3MODE SHAPE FLAP BENDING

-0.00000000 -0.00000000 0.00000000 0.00000000 0.00000000 -0.00000000 -0.00000000 0.00000000 0.00000000 -0.00000000

4MODE SHAPE TORSION

1.00000000 0.89100652 0.58778525 0.15643446 -0.30901699 -0.70710678 -0.95105652 -0.98768834 -0.80901699 -0.45399050

5MODE SHAPE SWEEP TORSION

1.00000000 0.89100652 0.58778525 0.15643446 -0.30901699 -0.70710678 -0.95105652 -0.98768834 -0.80901699 -0.45399050

RESULT 7

FREQUENCY 3922.54282 CYCLES/SEC

1MODE SHAPE LONGITUDINAL

0.00000000 0.00000000 0.00000000 0.00000000 0.00000000 0.00000000 0.00000000 0.00000000 0.00000000 0.00000000

2MODE SHAPE DRAG BENDING

-0.00000000 -0.00000000 -0.00000000 0.00000000 0.00000000 0.00000000 0.00000000 0.00000000 0.00000000 0.00000000

3MODE SHAPE FLAP BENDING

1.00000000 -0.11409726 -0.69935027 -0.41403039 0.35084358 0.74905013 0.34329806 -0.43988479 -0.78718034 -0.41054175

4MODE SHAPE TORSION

-0.00000000 -0.00000000 -0.00000000 -0.00000000 -0.00000000 0.00000000 0.00000000 0.00000000 0.00000000 0.00000000

5MODE SHAPE SWEEP TORSION

-0.00000000 -0.00000000 -0.00000000 -0.00000000 0.00000000 0.00000000 0.00000000 0.00000000 0.00000000 0.00000000

RESULT 8

FREQUENCY 5479.308423 CYCLES/SEC

1MODE SHAPE LONGITUDINAL

-0.00000000 -0.00000000 -0.00000000 -0.00000000 -0.00000000 -0.00000000 -0.00000000 -0.00000000 -0.00000000 -0.00000000

2MODE SHAPE DRAG BENDING

1.00000000 0.51896726 0.06308837 -0.32456194 -0.59664759 -0.72[illegible]4127 -0.68379545 -0.53017374 -0.30355004 -0.09351439

3MODE SHAPE FLAP BENDING

-0.00000000 -0.00000000 0.00000000 0.00000000 -0.00000000 -0.00000000 -0.00000000 -0.00000000 -0.00000000 -0.00000000

4MODE SHAPE TORSION

-0.00000000 -0.00000000 -0.00000000 0.00000000 0.00000000 0.00000000 0.00000000 -0.00000000 -0.00000000 -0.00000000

5MODE SHAPE SWEEP TORSION

-0.00000000 [illegible]

BIBLIOGRAPHY

1 Argyris J H
"On the analysis of complex elastic structures"
Applied Mechanics Reviews; Vol II, No 7, July 1958

2 Bogdanoff J L and Horner J T
"Torsional vibration of rotating twisted bars"
Journal of the Aeronautical Sciences - April 1956

3 Borg S F and Gennaro J J
"Modern Structural Analysis"
Van Nostrand Reinhold Company 1969

4 Bramwell A R S
"Helicopter Dynamics"
Edward Arnold - 1976

5 Calderbank V J
"A course on Programming in Fortran IV"
Chapman and Hall Ltd 1972

6 Carnegie W
"Vibration of Pretwisted Cantilver Blading"
Proceedings of the I Mech E Vol 173 No 12, 1959

7 Carnegie W
"Static Bending of Pretwisted Cantilever Blading"
Proceedings of the I Mech E Vol 171 No 32, 1957

8 Carnegie W
"Experimental Determination of the centre of flexure and centre of torsion coordinates of an assymmetrical aerofoil cross section"
Journal of Mech Engineering Science, Vol I No 3, 1959

9 Carnegie W, Dawson B and Thomas J
"Vibration characteristics of cantilever blading"
Applied Mechanics Convention, I Mech E, 1966

10 Dawson B
"Vibration characteristics of cantilever beams of uniform cross section"
PhD Thesis, University of London, 1967

11 Dawson B
"Vibration of a straight assymmetrical aerofoil cross-section blade"
MSc Thesis - University of Birmingham 1959

12 Diprima R C and Handleman G H
"Vibration of twisted beams"
Quarterly Applied Mathematics - 1954

13 Doolin B F
"The application of matrix methods to coordinate transformations occurring in systems studies involving large motions of aircraft"
NACA. Technical Note 3968 March 1957

14 Dunholter R J
"Static displacements and coupled frequencies of a twisted bar"
Journal of the Aeronautical Sciences - April 1946

15 Duncan W J, Ellis D L, and Scruton C
"The flexural centre and the centre of twist of an elastic cylinder"
Phil Magazine 57, Vol 16, No 104, August 1933

16 Elms D G
"Linear Elastic Analysis"
B T Batsford Ltd 1970

17 Hopkin H R
"A scheme of notation and nomenclature for aircraft dynamics and associated aerodynamics"
Royal Aircraft Establishment - Technical Report 66200 - 1966

18 Houbolt J C and Brooks G W
"Differential equations of motion for combined flapwise bending, chordwise bending and torsion of twisted non-uniform rotor blades"
NACA Report 1346 - October 1956

19 ICL Student Edition
"Extended Fortran"
International Computers Ltd 1974

20 Isakson G and Eisley J C
"Natural frequencies in bending of twisted rotating and non-rotating blades" NASA Technical Note D-371 April 1959

21 Isakson G and Eisley J G
"Natural frequencies in coupled bending and torsion of twisted rotating and non-rotating blades"
NASA - CR65. 1964

22 Jarrett G W and Werner P C
"The vibration of rotating, tapered, twisted beams"
Journal of Applied Mechanics September 1953

23 Langhaar H L
"Energy methods in applied mechanics"
John Wiley and Sons Inc 1962

24 Leckie F A and Lindberg G M
"The effect of lumped parameters on beam frequencies"
The Aeronautical Quarterly August 1963

25 Levy S
"Computerisation of Influence Coefficients for aircraft structures with discontinuities and sweep back"
Journal of the Aeronautical Sciences Vol 14 No 10, October 1947

26 Lindberg G M
"Vibration of non uniform beams"
The Aeronautical Quarterly, November 1963

27 Martin H C
"Introduction to matrix methods of structural analysis"
McGraw-Hill Book Company, 1966

28 Meek J L
"Matrix structural analysis"
McGraw-Hill Book Company 1971

29 Mendelson A and Gendler S
"Analytical and experimental investigation of effect of twist of vibrations of cantilever beams"
NACA Technical Note 2300 - October 1950

30 Montoya
"Coupled bending and torsional vibrations in a twisted rotating blade"
Brown Boveri Review Vol 53. March 1966

31 Morrison D
"Determination of shear and torsion centres"
DER. 111/J239 - Associated Electrical Industries. September 1967

32 Myklestad N O
"A simple tabular method of calculating deflections and influence coefficients of beams"
Journal of the Aeronautical Sciences - January 1946

33 Niblett T
"Normal bending modes of a rotating beam"
Royal Aircraft Establishment Tech Memo - struct 657. January 1966

34 Ormiston R A and Hodges D H
"Linear flap-lag dynamics of hingeless helicopter rotor blades in hover"
Journal of the American Helicopter Society, April 1972

35 Osgood W R
"The shear centre again"
ASME. December 1942

36 Pipes L A and Hovanessian S A
"Matrix computer methods in engineering"
John Wiley and Sons Inc 1969

37 Prohl M A
"A method for calculating vibration frequency and stress of a banded group of turbine buckets"
Transactions of the ASME - January 1958

38 Przemieniecki J S
"Theory of matrix structural analysis"
McGraw-Hill Book Company 1968

39 Rosard D D
"Natural frequencies of twisted cantilever beams"
Journal of applied mechanics - June 1953

40 Schulman Y
"Stability of a flexible helicopter rotor blade in forward flight"
Journal of the Aeronautical Sciences - July 1956

41 Sobey A J
"Dynamical analysis of the shaft fixed helicopter blade"
Royal Aircraft Establishment TR 73175 March 1974

42 Subramanian S K
"Second order effects on blade vibration"
MPhil Thesis, University of Surrey, 1972

43 Targoff W P
"The associated matrices of bending and coupled bending torsion vibration"
Journal of the Aeronautical Sciences - October 1947

44 Timoshenko S P and Gere J M
"Mechanics of material"
Van Nostrand Reinhold Company 1973

45 Thompson W T
"Matrix solution for the vibration of non uniform beams"
Journal of Applied Mechanics - September 1953

46 WADC. Technical Report 56-27. 1956

47 Weaver F L and Prohl M A
"High frequency vibration of steam turbine buckets"
Transactions of the ASME - January 1958

48 Wilde E
"A method of determining the normal modes and frequencies of a helicopter rotor blade"
Royal Aircraft Establishment. Tech Note 62, June 1964

49 Williams R F
"The normal modes of vibration of a rotating beam"
Research Memorandum Aero 72/7. The City University. November 1972

50 Zahorski A T
"Free vibrations of swept back wing"
Journal of the Aeronautical Sciences - December 1947

51 City University Computer Unit
"Library Subroutines"